Late Cretaceous to Early Eocene sedimentation in the Sinop-Boyabat Basin, north-central Turkey:

facies analysis of turbiditic to shallow-marine deposits

Beate L.S. Leren

Thesis for the Candidatus Scientiarum Degree
in Petroleum Geology/Sedimentology

Department of Earth Science
University of Bergen
Bergen, Norway
2003

ABSTRACT

The Sinop-Boyabat Basin is a SE-trending, elongate basin in the Sakarya Zone of Central Pontides, northern Turkey, filled with a succession of Early Cretaceous to Middle Eocene deposits, nearly 7 km thick. The basin evolved from a forearc graben controlled by the process of Western Black Sea rifting into a foreland trough increasingly influenced and eventually inverted by compressional deformation associated with the Pontide/Tauride orogeny.

This thesis summarized the results of a detailed sedimentological study of the Late Cretaceous to Early Eocene part of the basin-fill succession, ca. 2 km thick, which comprises three formations (Gürsökü Fm., Akveren Fm. and Atbaşı Fm.). The aim of the study was to reconstruct the basin's palaeogeographical and tectonic history on the basis of sedimentary facies analysis, supplemented with petrographical, micropalaeontological and ichnological data. Special emphasis was on the depositional processes involved and on the basin's responses to active tectonics and relative sea-level changes. The basin-fill succession studied has been described and its sedimentation processes interpreted in terms of eight component sedimentary facies, ranging from hemipelagites and turbidites to tempestites and shallow-marine calcarenites/limestones. These facies constitute four facies associations, stacked conformably upon one another with gradational boundaries: predominantly siliciclastic turbidites (FA 1), calcareous turbidites (FA 2), turbiditic to tempestitic carbonate-ramp deposits (FA 3) and ramp-drowning, predominantly hemipelagic deposits (FA 4).

The Campanian-Maastrichtian Gürsökü Formation (up to 1200 m thick) consists of sheet-like turbidites interbedded with calcareous mudstones and marlstones (FA 1). These deposits represent the medial to distal reaches of a deep-marine turbiditic system that was supplied with siliciclastic and increasingly abundant bioclastic sediment from the basin's uplifted southwestern margin and was formed by unconfined, low- to high-density turbidity currents flowing eastwards along the basin axis. A sinuous turbiditic palaeochannel occurs in the lowermost part of the formation, but the system was subject to gradual headward backstepping and it is thus unknown if its proximal part involved many more channels. The Campanian uplift correlates with the accretion of Kirşehir microcontinent to the Sakarya margin of Eurasia, and this first pulse of compression, superimposed on the rifting-driven subsidence, marked the onset of a foreland regime in the basin.

The overlying Maastrichtian-Palaeocene Akveren Formation (up to 600 m thick) consists of sheet-like calcarenitic turbidites interbedded with marlstones and calcareous mudstones (FA 2), passing upwards into a tempestite-dominated succession overlain by shoreface calcarenites and shallow-marine reefal limestones (FA 3). These deposits represent a turbiditic carbonate slope apron evolving into a carbonate ramp increasingly influenced by storms and covered by a basinward-expanding reefal platform. The rapid upward shallowing, from bathyal to littoral conditions, indicates a decline in subsidence, probably accompanied by mild compressional uplift of the basin floor. This pulse of compressional deformation correlates with the trench closure and the onset of continental collision in the adjacent Tauride-Anatolide Zone to the south.

The Late Palaeocene-Early Eocene Atbaşı Formation (up to 200 m thick) consists of variegated calcareous mudstones interspersed with thin calcarenitic tempestites and turbidites (FA 4). These deposits represent a rapid rise in relative sea level that caused shoreline backstepping, cessation of sand supply, reduced sedimentation rate and extensive seafloor oxidation in the sediment-starved basin. This change indicates a strong pulse of rifting, with a rapid wholesale sinking of the basin and its footwall margin. The overlying Early-Middle Eocene Kusuri Formation (up to 1400 m thick), not covered in detail by the present study, is a siliciclastic turbiditic succession recording the last stages of the basin development, until its closure by tectonic inversion that correlates with the culmination of the Tauride-Anatolide orogeny.

ACKNOWLEDGEMENTS

This thesis is a part of my studies for the Canditatus Scientiarum degree in petroleum geology and sedimentology at the Department of Earth Sciences, University of Bergen. First of all I would like to thank my supervisor, Prof. Dr. Wojtek Nemec (Univ. of Bergen), for vital guiding during my field work as well as insightful and critical reading of the manuscript. I am also grateful to my co-workers at the larger project of which my thesis is a part of; Dr. Scient. student Nils Erik Janbu (Univ. of Bergen), M.Sc Łukasz Gągała (Wrocław Univ.), and M.Sc Ediz Kırman (Ankara Univ.). My thesis would not have turned out this way without our fruitful discussions and close collaboration. Nils Erik Janbu is especially thanked for constructive critics of my ideas and interpretations; Ediz Kırman is particularly acknowledged for vital help with drawing figures and for all those hours he spent behind the wheels during our fieldwork.

Prof. Dr. Alferd Uchman (Jagiellonian Univ.) is thanked for identifications of trace fossils in the field; Dr. Çihat Alçiçek (Denizli Univ.) and Dr. Ayhan Ilgar (MTA, Ankara) for helpful assistance during our fieldwork; Dr. Erücment Sirel (Ankara Univ.) and Dr. Enis Kemal Sagular (Isparta Univ.) for microfossil datings and microfaunal environmental work, and Dr. John Howell (Univ. of Bergen) for editing the English grammar in the manuscript. Dr. Ole J. Martinsen at Norsk Hydro Research Centre is thanked for the funding of this thesis.

I would also like to express my gratitude to my fellow geology students and friends at the Department of Earth Sciences, in particular Siv Tanja Moe, Camilla Thrana and Tanja Aune for reliable support and for reading and commenting selected parts of the manuscript. Last, but not the least I am grateful to my parents for their interest and support, especially financially, during my period as a Cand. Scient. student.

Beate L. S. Leren

Bergen, June 2003.

CONTENTS

CHAPTER 1:

INTRODUCTION

1. 1. The aim and methods

This thesis reports on the results of a sedimentological study of the Late Cretaceous to Early Eocene marine sedimentary succession in the Sinop-Boyabat Basin of north-central Turkey. The studied succession comprises three formations (Gürsökü Fm., Akveren Fm. and Atbaşı Fm.), which consist of siliciclastic to calcareous deposits and represent a transition from deep- to shallow-marine sedimentation in a large, east-trending and tectonically active basin. The trough-like basin, >350 km long and initially ca. 150 km wide, formed in the Early Cretaceous time as a extensional graben within the Black Sea rift system of the southern margin of Eurasia and evolved into a foreland basin increasingly affected by the Pontide orogeny of northern Anatolia. The orogeny, driven by the northward subduction of Neothethys oceanic plate, culminated in the collision of the Anatolide-Tauride microcontinental blocks with the Eurasian margin and resulted in a progressive closure of the basin by tectonic inversion. The Late Cretaceous-Early Eocene basin-fill succession represents the first major part of the basin history, whereas the second and final part, represented by the Eocene succession, is addressed by a parallel doctoral study by Nils Erik Janbu (Univ. of Bergen).

The principal aim of the present study was to recognize the depositional processes and sedimentary environments of the thick (ca. 2000 m) and lithologically varied Late Cretaceous-Early Eocene succession on the basis of detailed lithostratigraphic logging and facies analysis. Special attention has been given to the record of contemporaneous tectonic activity and relative sea-level changes, and the sedimentological field study has been supplemented with a microscopic analysis of rock-sample thin sections and with micropalaeontological and ichnological data.

Log number	Formation part	Thickness logged
1a	Lower Gürsökü	38 m
1b	Lower Gürsökü	27 m
2	Middle Gürsökü	40 m
3	Upper Gürsökü	21 m
4	Upper Gürsökü	17 m
5	Lower Akveren	50 m
6	Lower-middle Akveren	76 m
7	Middle Akveren	51 m
8	Middle Akveren	49 m
9	Middle Akveren	34 m
10	Middle Akveren	156 m
11	Middle-upper Akveren	15 m
12	Middle-upper Akveren	13 m
13	Middle-upper Akveren	27 m
14	Middle-upper Akveren	8 m
15	Upper Akveren	44 m
16	Upper Akveren	14 m
17	Upper Akveren	55 m
18	Lower Atbaşı	25 m
19	Lower Atbaşı	17 m
20	Middle Atbaşı	7 m

Table 1.1. Overview of the sedimentary logs measured in this study. Logs 1a and 1b are from two parts of the same outcrop section, where faults rendered correlation difficult. For location see Figure 1.1.

The field data have been collected during 8 weeks of fieldwork, with three field sessions held in the autumn of 2001 and the spring and autumn of 2002. The logging included macroscopical identification of primary sedimentary structures and determination of mean grain size, using a magnification (10x) glass and a grain-size comparator. The descriptive terminology used is after Harms *et al.* (1975, 1982) and Collinson and Thompson (1982). In total, 20 logs (Table 1.1) with a combined thickness of nearly 800 m have been derived from the three formations and their different parts (Fig. 1.1), and these detailed data are given in Appendix 1. Rock thin sections have been studied with a standard polarizing microscope, and their petrographic descriptions are given in Appendix 2. Siliciclastic rocks are classified according to Pettijohn *et al.* (1987) and calcareous rocks according to Dunham (1962). Palaeocurrent measurements have been corrected for tectonic tilt and are presented as rose diagrams, plotted with the computer program Rose 1.0 (Thompson and Thompson, 1993). Micropalaeontological dating of sediment samples and recognition of trace fossils have been done for this project by other researchers (see below).

The field study was conducted as a part of a larger project that involved two other

principal researchers, Nils Erik Janbu (Dr.Scient. student in sedimentology, focusing on the overlying Eocene succession) and Łukasz Gągała (M.Sc. student in structural geology); as well as Ediz Kırman, Dr. Çihat Alçiçek, and Dr. Ayhan Ilgar as field assistants and co-workers; and Prof. Dr. Alfred Uchman (Jagiellonian Univ.) as a collaborating specialist on trace fossils. Micropalaeontological analyses of rock samples were done by Dr. Ercüment Sirel (Ankara Univ.), and Dr. Enis Kemal Sagular (Isparta Univ.). The project was supervised by Prof. Dr. W. Nemec, who also actively participated in the field work. The whole project was sponsored by the Norsk Hydro Research Centre as a contribution to a broader research programme on deep-marine systems, led by Dr. Ole J. Martinsen.

1.2. The study area

The Sinop-Boyabat Basin is located in the Central Pontides of northern Turkey (Fig. 1.1). The Pontide mountain belt marks the boundary between the compound Anatolian craton to the south and the Black Sea region to the north. The basin was tectonically inverted by the Pontide orogeny, and hence shows a series of E-trending anticlines and synclines, as well as major southward thrusts and northward backthrusts (Fig. 1.1).

The study area is ca. 4500 km^2, with isolated large outcrops of good quality. The Ekinveren Thrust Zone, the Balıfaki Fault and the Erikli Fault (Fig. 1.1) have elevated large parts of the basin up to 1500 m above the sea level. The folded rock succession has a varied and commonly steep inclination of bedding. Good outcrops and the high dip angle allowed large parts of the formations to be logged in roadcut and river valley sections, with a trend commonly almost perpendicular to the bedding strike. There are also several good outcrop sections in the coastal cliffs along the Black Sea shoreline. Sedimentary structures are generally easy to recognize, although carbonate cementation have locally obliterated the primary features. The inclined bedding renders lateral control limited, hence several logs have been taken where possible (Table 1.1).

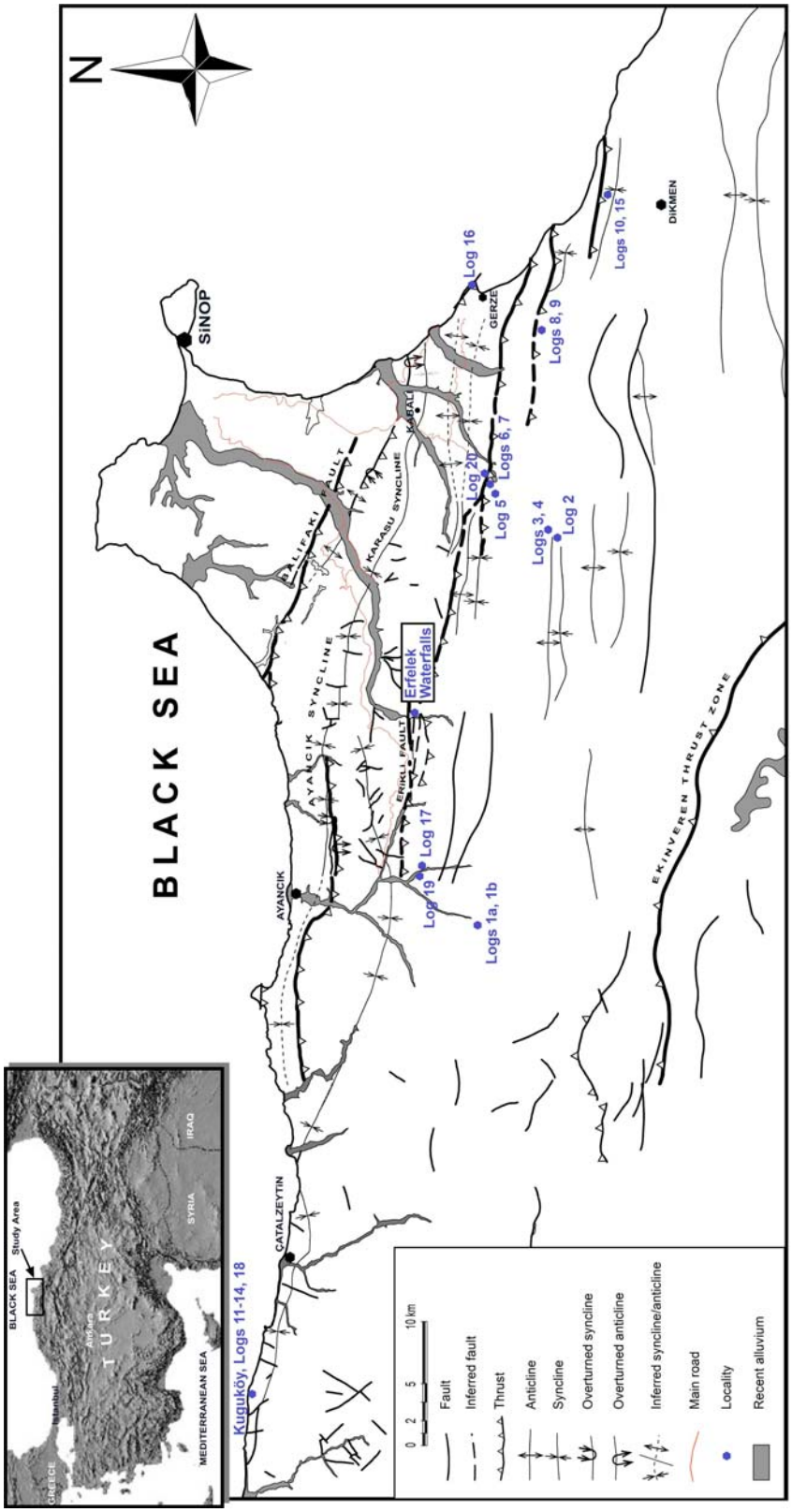

Figure 1.1. Structural map of the Sinop-Boyabat Basin, north-central Turkey (modified from Barka et al., (1985) and Aydın et al. (1995a)).The main outcrop localities and the location of logs are indicated in blue.

1.3. Previous studies

The Cretaceous-Palaeogene sedimentary succession of the Central Pontides has been mapped and its stratigraphy, tectonic structure and regional plate-tectonic context have studied over the last few decades (Badgley, 1959; Ketin and Gümüş, 1963; Göksu *et al.*, 1974; Gedik and Korkmaz, 1984; Sonel *et al.*, 1989; Tüysüz, 1990; Aydın *et al.*, 1995a; Robinson *et al.*, 1995; Görür, 1997; Görür and Tüysüz, 1997; Okay and Şahintürk, 1997; Ustaömer and Robertson, 1997; Tüysüz, 1999). However, few sedimentological studies have been done (Gedik and Korkmaz, 1984; Sonel *et al.*, 1989; Aydın *et al.*, 1995a), no one of them detailed and all published in local Turkish journals.

The majority of the previous research was meant chiefly to assess the region's potential for containing petroleum resources – which seemed to be a reasonable possibility in the broader context of the Black Sea petroleum province. Seismic profiles were acquired and several exploration wells drilled by the Turkish Petroleum Company (Aydın *et al.*, 1995a), but no significant discoveries have thus far been made. Most of these exploration studies are summarized in unpublished internal reports, mainly confidential and written in Turkish. In the original mapping of the Sinop-Boyabat Basin by Badgley (1959) and by Ketin and Gümüş (1963), the main lithostratigraphic units were distinguished and named after the local villages. However, the type sections of the individual formations are seldom defined, whereas there is commonly more than one village bearing the same name (e.g., there are at least three villages named Gürsökü in the study area). Both the original maps and their newer versions (Görür and Tüysüz, 1997; Tüysüz, 1999) are insufficient as a basis for detailed stratigraphic correlation. Apart from evident local errors due to an unresolved complexity of tectonic structure, the maps are often confusing when confronted with the outcrop sections. Some local improvements of the geological map have been done by Janbu *et al.* (this project) in the course of the field study, but no attempt has been made to revise the map sheets in a systematic manner. The formation names and boundaries used in the present study are chiefly after Aydın *et al.* (1995a) and Tüysüz (1999).

CHAPTER 2:

REGIONAL GEOLOGY AND STRATIGRAPHY

2.1. Tectonic setting

In broad terms, the Anatolian craton of Turkey (Fig. 2.1) was assembled through the Alpine orogeny in Jurassic to Oligocene time, by the accretion of Africa-derived microcontinents to the southern margin of Eurasia as a result of the opening and northward subduction of Neotethys. The E-trending Pontide and Tauride orogenic zones of Anatolia (Fig. 2.1) represent the two main successive stages of this plate-tectonic process of accretion, which terminated with the frontal collision of the Arabian platform of Africa with the Eurasian

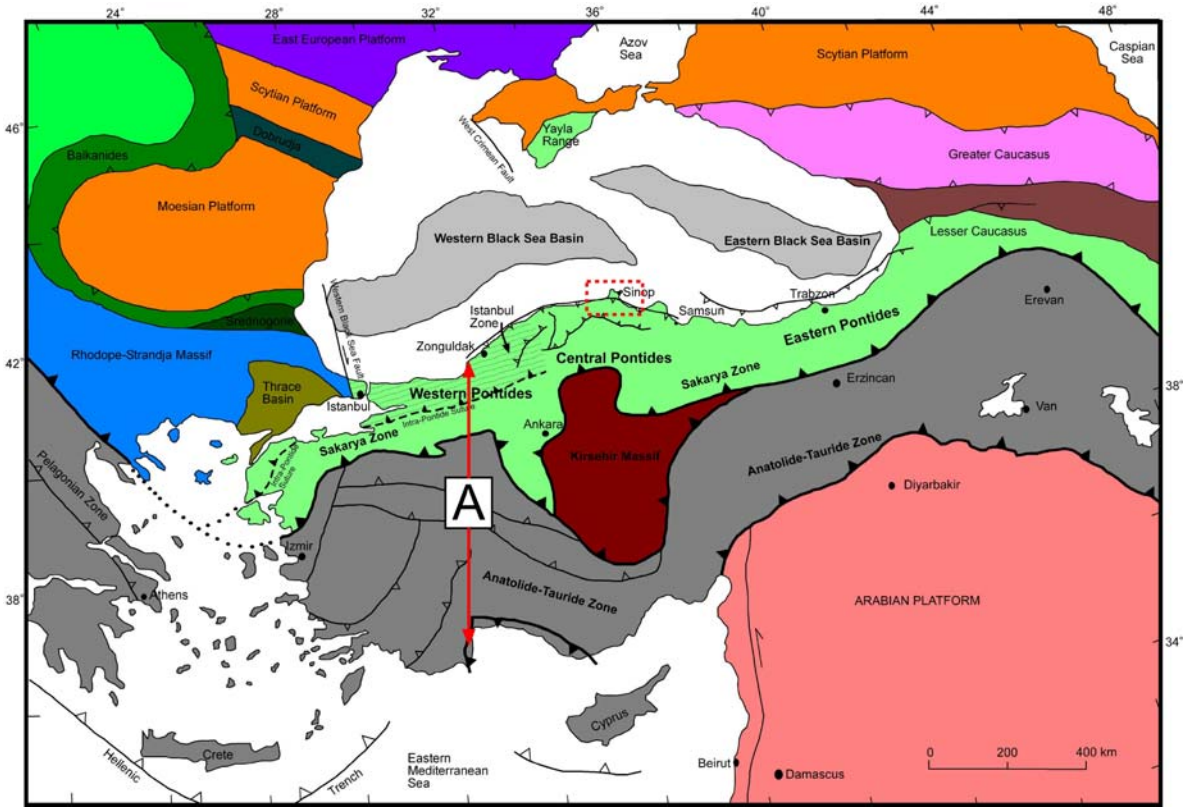

Figure 2.1. Tectonic map of Anatolia (A) and surrounding regions. Note the Pontide orogenic belt and the present study area (red rectangle). Modified from Robinson et al. (1996), Tüysüz (1999), Okay et al. (2001) and Nikishin et al. (2003).

margin. The accretion process itself was diachronous, spatially non-uniform, and the microcontinents underwent deformation, rotation and partial disintegration when accreted to the margin, and thus largely lost their identity. The largest and least deformed is the crystalline Kirşehir Massif (Fig. 2.1).

The Pontide orogenic zone of northern Turkey (Fig. 2.1) formed through several phases of non-uniform compression and had a highly differential development in its western, central and eastern segments (Okay and Şahintürk, 1997; Ustaömer and Robertson, 1997). The fold and thrust belt of the Pontide orogenic suture includes the contemporaneously deformed accretionary zone, referred to as the Sakarya Zone (Fig. 2.1). The Sinop-Boyabat Basin (Fig. 2.2), with its thick succession (≤ 6 km) of Late Cretaceous-Eocene deposits, may be regarded as an important recorder of the tectonic history of the Central Pontides. The E-trending basin, originally >350 km long and ~150 km wide, was situated on the Eurasian margin and formed as a result of its rifting, accompanied by volcanism, but was progressively affected by pulses of the growing orogenic compression, which eventually closed and inverted the basin (Tüysüz, 1999).

The main tectonic factors and phases of regional development and the history of the Sinop-Boyabat Basin (Fig. 2.3) are outlined below.

The onset of rifting – The Eurasian margin became subject to active tectonic extension and rifting in the Early Cretaceous time, when the northward subduction of the Neotethys oceanic plate initiated the development of the Black Sea Rift (Okay *et al.*, 1994; Robinson *et al.*, 1996; Ustaömer and Robertson, 1997). The rifting processes led probably to the formation of mantle convection cells, and caused crustal break-up in the western part of the Black Sea Rift that persisted until Cenozoic time (Cloetingh *et al.*, 2003), long after the Pontide suture formed and the subduction shifted southwards to the Tauride-Hellenide zone and further to the Cyprean and Cretan arcs. The Sinop-Boyabat Basin formed in Barremian time on the southern flank of the SE-extended Western Black Sea Rift (Cloetingh *et al.*, 2003). The basin was an asymmetrical graben, whose northern margin initially shed volcaniclastic sediment and lavaflows, but was soon submerged due to extensional collapse (Fig. 2.3; Aydın *et al.*, 1995a; Tüysüz, 1999).

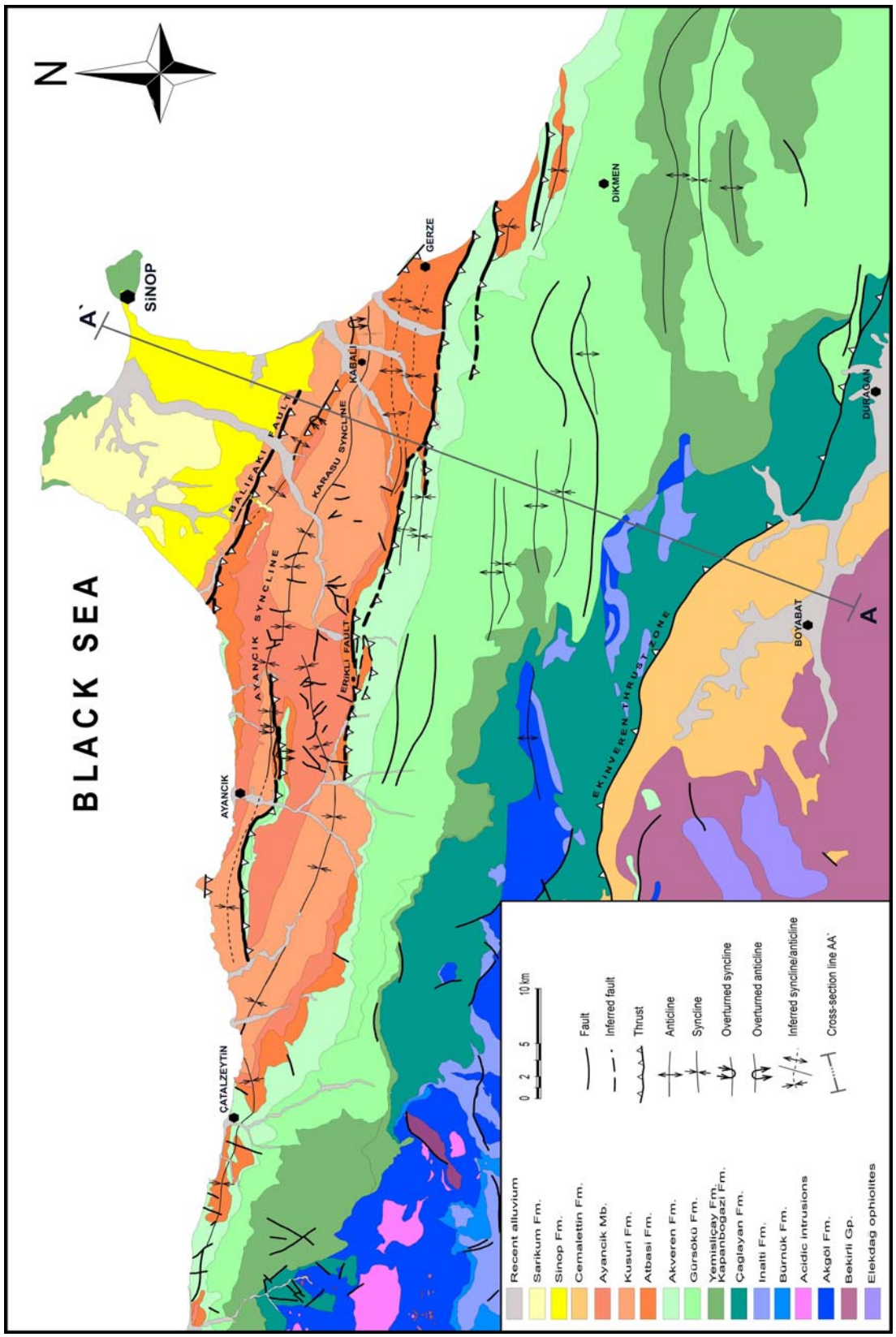

Figure 2.2. Geological map of the Sinop-Boyabat Basin, north-central Turkey. The cross-section line A-A' corresponds to the interpretive cartoon shown in Fig. 2.3. Figure modified from Barka et al., (1985) and Aydın et al. (1995a).

Island-arc volcanism – The subduction of Neotethys oceanic plate under the Eurasian margin resulted in a volcanic arc extending along the Black Sea region from Georgia in the east to Bulgaria in the west in the Cenomanian to Maastrichtian time (Tüysüz, 1990; Okay *et al.*, 1994; Robinson *et al.*, 1996; Okay and Şahintürk, 1997; Ustaömer and Robertson, 1997; Yılmaz *et al.*, 1997; Tüysüz, 1999; Okay *et al.*, 2001; Nikishin *et al.*, 2003). In the study area, the volcanic zone was located directly north of the Sinop-Boyabat Basin, with submarine volcanic rocks, tephra and hyaloclastic breccias presently exposed at the northern tip of the Sinop Peninsula and probably also occurring further offshore (Robinson *et al.*, 1995). Backarc extension led to the formation of the Black Sea Rift, with the eastern segment offset relative to the western segment by a SE-trending transfer zone ridge (Fig. 2.1). The Western Black Sea Rift is widely considered to have opened in Cenomanian-Coniacian time (Robinson *et al.,* 1995, 1996; Okay and Şahintürk, 1997; Meredith and Egan, 2002; Rangin *et al.*, 2002; Cloetingh *et al.,* 2003; Nikishin *et al.*, 2003), whereas the Eastern Black Sea Rift may have opened at the same time (Nikishin *et al.*, 2003) or considerably later, in the Maastrichtian (Okay and Şahintürk, 1997) or possibly even Palaeocene time (Robinson *et al.*, 1995, 1996). The volcanic activity in the Central Pontides occurred until the middle Campanian time (Tüysüz, 1999; Okay *et al.*, 2001). The cessation of volcanism is attributed to the decline of subduction and the collision of the Kirşehir Massif and Sakarya blocks with the Eurasian margin (Fig. 2.1), which according to Okay and Tüysüz, (1999) commenced in Maastrichtian time.

Continental collision – Orogenic compression began to affect the Sinop-Boyabat Basin near the end of Cretaceous, and the continental collisions continued until the Palaeocene time (Okay and Tüysüz, 1999). According to Tüysüz *et al.* (1995), the suturing of Kirşehir Massif with Sakarya Zone occurred from Cenomanian to Late Maastrichtian time. However, a new collisional regime commenced in Western Pontides in the earliest Palaeocene and in the Eastern Pontides in the Late Palaeocene, when the Sakarya Zone with the Kirşehir Massif and the Anatolide-Tauride Zone collided (Fig. 2.1; Okay and Tüysüz, 1999; Gürer and Aldanmaz, 2002). Pulses of compression occurred until the suturing of southern Anatolian blocks and the formation of Tauride orogen came chiefly to an end in the Oligocene time. The contraction led to thin-skinned thrusting, although much

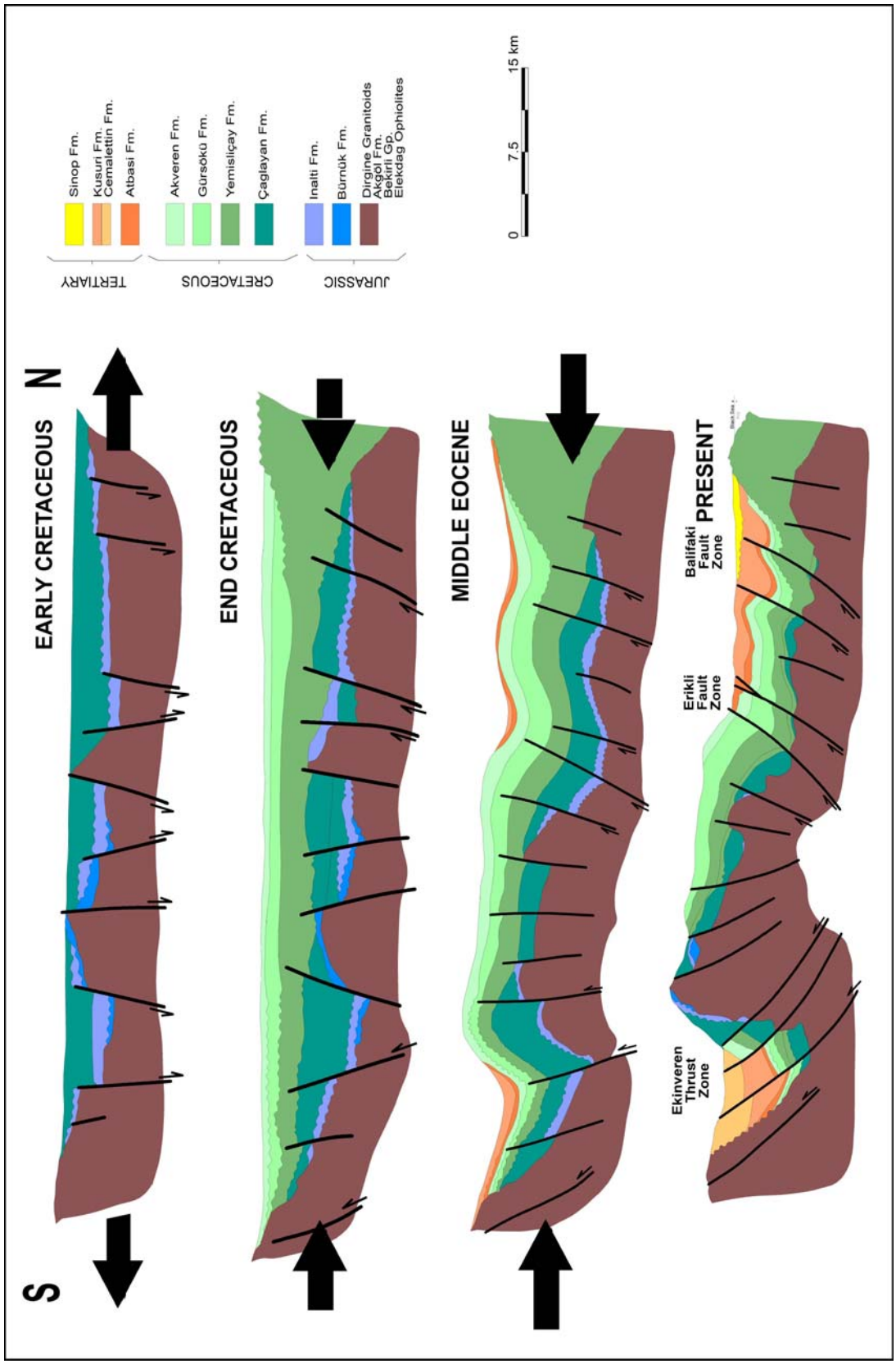

Figure 2.3. Tectonic development of the Sinop-Boyabat Basin shown as a series of vertical cross-sections (modified from Aydin et al., 1995a). The location of the section line is shown in Figure 2.2.

of the compressional deformation was accommodated by the reversal of pre-existing normal faults (Fig. 2.3; Aydın *et al.*, 1995a). Since at least the Early Eocene, the Erikli Thrust Zone and associated backthrusts formed a pop-up ridge that divided the Sinop-Boyabat Basin longitudinally into two parallel troughs (Fig. 2.3): the northern Sinop Basin and the southern Boyabat Basin. Compression gradually closed the two basins between the Middle Eocene and Early Miocene (Okay and Şahintürk, 1997), when most of the present-day tectonic structure was formed (Fig. 2.3).

2.2. Stratigraphy of the Sinop-Boyabat Basin

This section is a short review of the basin-fill succession (Fig. 2.4). The crystalline basement consists of granitoids and a range of metamorphic rocks, including igneous intrusions and slivers of obducted ophiolites (Figs. 2.2 and 2.3).

Bedrock – The Late Cretaceous deep-water deposits are underlain by pre-rift platform carbonates of Late Jurassic to Early Cretaceous age, deposited mainly in the Western and Central Pontides (Ustaömer and Robertson, 1997; Tüysüz, 1999). These shallow-marine carbonate rocks, including the local Bürnük Formation and the more extensive Inaltı Formation (Figs. 2.2 and 2.3), are considered to be the bedrock in the present study.

Çağlayan Formation – The carbonate bedrock is overlain unconformably by the Çağlayan Formation of Barremian to Albian age (Gedik and Korkmaz, 1984; Tüysüz, 1990; Aydın *et al.*, 1995a). This formation has an estimated thickness of 50 to 2000 m, comprises alternating turbiditic sandstones and shales, sandy limestones, conglomerates and olistostromes deposited in a horst and graben topography, and is thought to represent the onset of backarc rifting on the Eurasian margin (Görür and Tüysüz, 1997; Tüysüz, 1999).

Kapanboğazı Formation – The red-coloured *ammonitico rosso* pelagic limestones and marls of the Kapanboğazı Formation (Fig. 2.4) overlie conformably the older deposits (Aydın *et al.*, 1995a; Tüysüz, 1999). This carbonate formation is of Cenomanian to Turonian/Coniacian age (Aydın *et al.*, 1995a; Ustaömer and Robertson, 1997; Tüysüz,

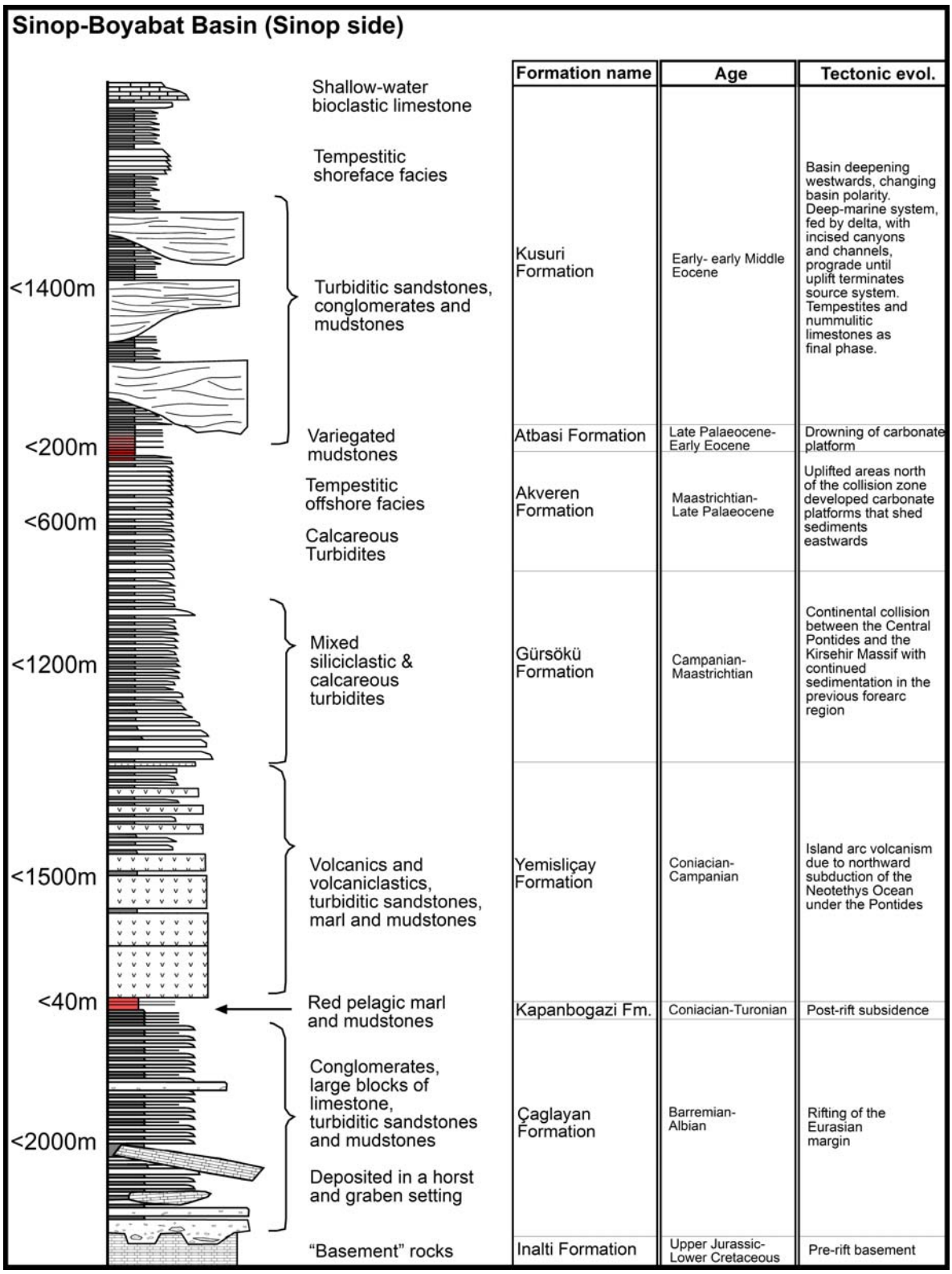

Figure 2.4. Stratigraphy of the Sinop Basin (i.e., the northern half of the Sinop-Boyabat Basin).

1999) and has a thickness of 10-40 m (Görür and Tüysüz, 1997; Tüysüz, 1999).

Yemisliçay Formation – The Coniacian to Campanian Yemisliçay Formation overlies conformably the Kapanboğazı Formation (Fig. 2.3) and consists of pyroclastic-flow tephra (lithic tuffs) and lavaflow basalts and andesites, alternating with sandstone turbidites (mainly T*bc*), massflow conglomerates, mudstones and minor marlstones (Gedik and Korkmaz, 1984; Aydın *et al.*, 1995a; Tüysüz, 1999). The formation is 200 to 1500 m thick, generally thinning southwards (Aydın *et al.*, 1995a; Görür and Tüysüz, 1997; Tüysüz, 1999). The volcaniclastic sediment and lavaflows were derived from the basin's northern margin (Aydın *et al.*, 1995a) and show an upward change in chemical composition that probably reflects evolution of the volcanic arc and a change from a rift-related to a subduction-related magmatic source (Gedik *et al.*, 1984).

Gürsökü Formation – The Gürsökü Formation has a gradational contact with the underlying Yemisliçay Formation and consists of non-volcanogenic, predominantly siliciclastic turbiditic sandstones interbedded with mudstones, calcareous mudstones and marlstones. The turbidites are gradually more calcareous upwards in the formation. According to Aydın *et al.* (1995a), the main difference between the Yemisliçay Formation and the Gürsökü Formation is that the latter contains no tephra interbeds. Micropalaeontological analyses of samples for the present study indicate a Campanian to Maastrichtian age of the Gürsökü Formation (E. Sirel, personal comm., 2001-2002), which confirms previous datings (Aydın *et al.*, 1995a; Görür and Tüysüz, 1997; Tüysüz, 1999). The thickness of this formation has been estimated variously to be 1200 m in wells and seismic sections (Aydın *et al.*, 1995a), but up to 2500 m (Tüysüz, 1999) or possibly 3000 m (Görür and Tüysüz, 1997) on the basis of geological maps.

Akveren Formation – The Akveren Formation has a gradational contact with the underlying Gürsökü Formation and consists of alternating calcarenites, calcareous mudstones, marlstone and massive bioclastic limestones. The calcarenite beds are turbidites, although the topmost part of the formation is recognized to be a succession of calcarenitic tempestites. The Akveren Formation is much richer in calcareous sediment than the Gürsökü Formation, but their boundary is transitional and difficult to define clearly in

the field. The thickness of the Akveren Formation has been variously estimated at 200-500 m (Tüysüz, 1999), up to 600 m (Aydın *et al.*, 1995a) or 500-1000 m (Görür and Tüysüz, 1997). The age of this formation was reported to be Maastrichtian by Görür (1997) and Görür and Tüysüz (1997), but Maastrichtian to Middle Palaeocene by Aydın *et al.* (1995a). Micropalaeontological analyses of samples taken for the present study indicate a Maastrichtian to Late Palaeocene age (E. Sirel, personal comm., 2001-2002).

Atbaşı Formation – The Atbaşı Formation overlies conformably the Akveren Formation (Aydın *et al.*, 1995a) and consists of variegated mudstones, which renders it a basinal marker unit. The calcareous mudstones are intercalated with thin marls and calcarenitic turbidites. Micropalaeontological analyses indicate a Late Palaeocene to possibly earliest Eocene age (E. Sirel, personal comm., 2001-2002), which confirms the earlier dating by Tüysüz, (1999), but does not quite agree with the Middle Palaeocene to Early Eocene age suggested by Aydın *et al.* (1995a). The thickness of the Atbaşı Formation was estimated to be around 400 m by Aydın *et al.* (1995a), 30-500 m by Görür (1997) and 40-100 m by Tüysüz (1999). The divergency is mainly due to the difficulty in defining the upper boundary of the formation, because the deposits in its upper part are grey and lighter in colour, transitional to the overlying Kusuri Formation.

Kusuri Formation – The occurrence of this formation is limited mainly to the Sinop Basin (Fig. 2.4), that is, to the northern half of the Sinop-Boyabat Basin, after it was tectonically split into the northern Sinop trough and the southern Boyabat trough (Fig. 2.3). The Kusuri Formation has a gradational lower boundary and is predominantly siliciclastic, composed of turbiditic sandstones, mudstones and minor thin marlstones (Aydın *et al.*, 1995a). Micropalaeontological analyses indicate an Early to Middle Eocene age (E. Sirel, personal comm., 2001-2002), and the formation thickness is estimated to be 800-1200 m (Görür and Tüysüz, 1997), possibly up to 1400 m (Aydın *et al.*, 1995a). The lower part of the Kusuri Formation abounds in thick palaeochannel sandstones and conglomerates, and has been referred to as the Ayancık Sandstone Member, whereas the topmost part consists of shallow-marine limestones, referred to as the Istafan Cape Limestone Member (Leren *et al.*, 2002; Janbu *et al*., 2003).

The coeval Early to Middle Eocene deposits in the adjacent Boyabat Basin (Fig. 2.2) are siliciclastic turbiditic sandstones interbedded with mudstones and minor marlstones, comparably to the Kusuri Formation (Sonel *et al.*, 1989; Janbu *et al*., 2003). The overlying Cemalettın Formation (Aydın *et al.*, 1995a), several hundred metres thick, consists of coarse-grained, shallow-water deltaic deposits overlain by conglomeratic braided-river alluvium. The age of these poorly dated deposits is thought to be Late Eocene and possibly Oligocene (Janbu *et al*., 2003).

Unconformable cover – The Late Cretaceous to Eocene basin-fill succession in the Sinop Basin is overlain unconformably by Pliocene(?) shallow-marine calcarenites and fluvial deposits in the area of Sinop Peninsula (see Sinop Fm. and Sarikum Fm. in Fig. 2.2).

CHAPTER 3:

SEDIMENTARY FACIES

3.1. Basic nomenclature and definitions

Descriptive classification is the first step in the distinction of sedimentary facies and interpretation of their origin (Boggs, 1995; Reading and Levell, 1996). Facies are the basic "building blocks" of a sedimentary succession, distinguished on the basis of the bulk of deposit characteristics, including mineral composition, texture, primary structures, colour, fossil content and bedding geometry (Harms *et al.*, 1975). Different facies are considered to be of different origins, and hence to represent different depositional processes or basin conditions. Some facies are environmentally diagnostic, but others are not, and it is usually an association of facies that is most informative in this respect. Facies association is defined as an assemblage of spatially and genetically related facies representing a particular sedimentary environment or subenvironment.

The sandstones in the present study are mainly of a mixed siliciclastic and calcareous composition, and hence not easy to classify in descriptive terms. In the textural and compositional classification proposed by Mount (1985), three end-members are considered: siliciclastic sand, non-calcareous mud and allochems (carbonate grains), together with carbonate mud (or micrite). According to this classification, the sandstones in the present case would be categorized as allochemic/micritic sandstones, or sandy allochemic limestones. However, a nomenclature of this kind is seldom used in the sedimentological literature. It is more convenient to classify sandstones into two compositional categories, siliciclastic and calcarenitic, even though the limiting proportion of carbonate and siliciclastic detritus for these categories is not specified in the literature and has to be rather arbitrary. Pettijohn *et al*. (1987) and Tucker (2001) defined calcarenite as a clastic limestone with components of similar grain sizes as terrigenous sand, with or without carbonate cement. Bryhni (1999) defined calcarenite as a detrital limestone containing less than 50 vol.% siliciclastic grains of sand size, or a sandstone composed predominantly of carbonate grains. On the basis of these definitions, calcarenites in this study are defined as sandstones with more than 50 vol.%

carbonate detritus (chiefly bioclastic material in the present case), whereas calcrudites are similarly conglomerates dominated by carbonate detritus.

On the basis of detailed field observations collected by sedimentological logging (see logs in Appendix 1) and thin-section analysis (Appendix 2), eight main sedimentary facies have been distinguished in the studied succession (Table 3.1). In the present chapter, the individual facies are described and interpreted in terms of their possible depositional processes.

Table 3.1. Guide to the sedimentary facies distinguished in the present study.

FACIES		***Subfacies***	
F1	Calcrudites of granule to pebble grade	**F1a**	Clast-supported pebble calcrudite
		F1b	Clast- to matrix-supported, bioclastic, granule calcrudites
F2	Thick- to medium-bedded siliciclastic sandstones and calcarenites with planar parallel stratification and/or current-ripple cross-lamination	**F2a**	Very coarse- to very fine-grained siliciclastic sandstones
		F2b	Fine-grained to silty calcarenites
F3	Stratified calcarenites with wave-formed and combined-flow sedimentary structures		
F4	Massive calcarenites		
F5	Thin-bedded siliciclastic sandstones and calcarenites with mainly current-ripple cross-lamination	**F5a**	Very coarse- to very fine-grained or silty siliciclastic sandstones
		F5b	Very fine-grained to silty calcarenites
F6	Massive bioclastic limestones	**F6a**	Bedded limestones
		F6b	Non-bedded limestone
F7	Marlstones		
F8	Calcareous mudstones	**F8a**	Grey to greenish-grey calcareous mudstones
		F8b	Variegated calcareous mudstones

3.2. Facies F1: calcrudites of granule to pebble grade

The calcrudite deposits have been divided into two subfacies, F1a and F1b (Table 3.1) to account for variation in their grain size and composition. These subfacies are first described and then jointly interpreted as one facies.

Subfacies F1a: clast-supported pebble-grade calcrudite – This deposit (Fig. 3.1), occurs as a solitary lenticular bed in the upper part of the Akveren Formation (see Log 17 in Appendix 1). The calcrudite overlies erosionally a reddish calcareous mudstone of facies F8b and has an uneven top covered by a coarse-grained calcarenite of facies F3. The lenticular bed has a lateral extent of 340 cm and is up to 25 cm thick, with a basal

erosioal relief of up to 20 cm. The gravel is subrounded to well rounded, but moderately sorted. The mean clast size varies between 1 to 5 cm, and the maximum size measured is 16 cm (floating outsized cobbles, see Fig. 3.1). Clasts are mainly spherical and discoidal fragments of limestone and marlstone. Scattered bioclasts include fragments of echinoids, bryozoans and various sponges. The calcrudite bed shows weak normal grading in the upper part, marked chiefly by the lack of cobbles and scarcity of large pebbles at the top. Matrix is reddish-brown, fine-grained calcareous sand.

Figure 3.1. Calcrudite of facies F1a in the upper part of the Akveren Formation (see Log 17 in Appendix 1); note the erosional base (red line). The hammer is 30 cm.

Subfacies F1b: clast- to matrix-supported, bioclastic, granule-grade calcrudites - These deposits occur in the middle to upper part of the Akveren Formation in the Kuğuköy outcrop section (see Log 11 in Appendix 1). Their beds have uneven bases and are broadly lenticular, up to 100 m in lateral extent and 14 cm in thickness. They overlie erosionally marlstones of facies F7 and are commonly covered by marlstone or a massive calcarenite of facies F4. Basal erosional relief is up to 2 cm, with common load casts up to 5 cm deep. The gravel is subangular to subrounded, but poorly to moderately sorted, and the beds generally lack grading. Texture varies from clast- to matrix-supported, even within one bed, and the matrix is medium to very coarse calcareous sand. The gravel fraction contains more than 80 vol.% carbonate detritus of granule grade, with an admixture of pebbles derived from limestone and greenish tuff, mainly no larger than 3 cm in size. No bioclasts have been identified on macroscopical basis,

probably because of the relatively small size and fragmented nature of the debris. The calcrudite beds of this facies seem to be somewhat weaker cemented, and more readily affected by outcrop weathering.

Interpretation – The calcrudites of facies F1 resemble deposits of non-cohesive debris flows derived from the slopes of basin-margin carbonate platforms (e.g., Coniglio and Dix, 1992), generated by gravitational failures, possibly in combination with storms or tsunami events (Drzewiecki and Simó, 2002). Subfacies F1a and F1b are thought to have been emplaced by similar processes, but derived from somewhat different parts of a gravelly beach zone of carbonate platform margin. The resedimentation of wave-worked gravel by non-cohesive debris flows might imply a close proximity to the source (Stow *et al*., 1996).

Debris flows are sediment gravity flows characterized by plastic rheological behaviour (Johnson, 1970; Lowe, 1982), which means that the sediment shear strength must be exceeded by shear stress, or the slope-parallel component of gravity force, for the flow to occur and that the flowing sediment will then "freeze" *en masse* when the shear stress decreases below the shear-strength limit. Lowe (1982) divided debris flows into two categories: cohesive debris flows (or mudflows) and grainflows. In a mudflow, it is the cohesion of clay-bearing, fine-grained matrix that supports larger clasts (Johnson, 1970; Hampton, 1975), whereas in a grainflow, it is the intense shear, grain collisions and dispersive pressure that allow large clasts to support themselves (Bagnold, 1954; Lowe, 1976). A slope in excess of 35^{o} is required for a grainflow to be mobile (Lowe, 1976, 1979; Middleton and Southard, 1984), and a characteristic feature of grainflow deposit is inverse grading (Bagnold, 1954; Lowe, 1976). Notably, no such grading is recognizable in the deposits of facies F1 in the present case.

However, not every non-cohesive debris flow must necessarily be a grainflow, as Lowe's (1982) classification implies. Non-cohesive sediment can flow without significant collisions, with the grains rubbing past one another (Drake, 1990); or with the sediment mass gliding on a thin layer of intensely shearing grains (Campbell, 1989). Therefore, Nemec and Steel (1984) classified debris flows into cohesive and cohesionless (or frictional), according to the predominant component of Coulomb shear strength, with the classical mudflow and grainflow as end-members of a flow spectrum. The deposits of facies F1 are thought to represent the cohesionless part of this spectrum, but not necessarily grainflows by definition. When destabilized and avalanching down

the steep slope of carbonate platform, the rounded gravel may have initially been dispersed or perhaps briefly suspended by an accompanying current, which would reduce the internal friction of the coarse sediment and hence increase its mobility and runout distance (Nemec, 1990). The weak normal grading in the deposits of facies F1 suggests, in fact, that the gravel may have been dumped from a bypassing turbidity current and turned into a mobile debris flow at some distance from the source (Lowe, 1982; Ghibaudo, 1992; Vrolijk and Southard, 1997).

Alternatively, the conglomerates of facies F1 may be deposits of storm-generated rip currents – the topographically controlled, erosional and pulsating nearshore jets of seaward returning water (Bowen and Inman, 1969; Dalrymple, 1975). The bottom velocities of rip currents are up to 2-3 m/s, whereas megarips can reach speeds of 5-10 m/s. These currents can carry gravel over a seaward distance of several kilometres, where the sediment will be dumped and deposited in a non-tractional manner, or it may turn briefly into a cohesionless debris flow (Gruszczyński *et al.*, 1993). Notably, subfacies F1a is directly associated with sandstones interpreted to be tempestites (facies F3), and also subfacies F1b occurs in the middle to upper part of the Akveren Formation, below its tempestitic culmination, where storm-generated rip currents could episodically alternate with turbidity currents. Rip currents would be capable of sweeping beach gravel by themselves, whereas an independent triggering factor might be needed to generate a sediment gravity flow. Among the possible mechanisms for the generation of debris flows on carbonate platform slopes are (Drzewiecki and Simó, 2002): slope instability caused by seismic shaking and/or tsunami backsurges; spontaneous slope failures due to depositional oversteepening; and slope collapsing due to undercutting by storm waves, a relative sea-level fall or differential compaction. In addition was the Sinop-Boyabat Basin tectonically active and any of those factors could have episodically been involved in the deposition of the calcrudites of facies F1.

3.3. Facies F2: thick- to medium-bedded siliciclastic sandstones and calcarenites with planar parallel stratification and/or current-ripple cross-lamination

The sandstones of this facies are medium- to thick-bedded (*sensu* Boggs, 1995), that is, forming beds thicker than 10 cm. The deposits are divided into two subfacies on the

basis of their grain size and mineral composition (thin-section analyses in Appendix 2). The subfacies are first described and then jointly interpreted as one facies.

Subfacies F2a: very coarse- to very fine-grained siliciclastic sandstones – These are medium- to thick-bedded sandstones, common in the Gürsökü Formation (see Logs 1a-b to 4 in Appendix 1). The sandstones are light-grey to grey in colour, but are dark-grey to brownish-grey in weathered outcrop walls. The majority of beds are tabular, but some are visibly thinning or pinching out laterally. Bed thicknesses are from 10 to 200 cm, predominantly 15-45 cm. The beds have sharp bases with an erosional relief of 0.5 to 12 cm, sporadically up to 135 cm (e.g., see Log 1b (~4m depth) in Appendix 1), and generally have planar tops with a gradational transition to the overlying marlstone or mudstone. Beds are commonly stacked directly upon one another and to variable extent amalgamated (Fig. 3.2).

Figure 3.2. Sandstones of subfacies F2a, stacked directly upon one another and to various degree amalgamated (example from the lower part of Gürsökü Formation; see Log 1a in Appendix 1). The stratigraphic thickness of the exposure is ca. 6 m, and the way up is to the upper right.

In some of such packages, the erosional bed boundaries are inclined laterally (see further discussion in section 4.2). The coarser sandstone beds locally contain scattered small pebbles and/or granules at the base, and the gravel component is occasionally abundant enough to be categorized as a sand-supported granule conglomerate. The

majority of beds are normally graded, commonly capped by marlstone (facies F7) or calcareous mudstone (subfacies F8a). They show planar parallel stratification overlain by current-ripple cross-lamination, with parallel lamination in the thin, silty topmost part. Ripple cross-lamination predominates. Planar parallel stratification occurs in some of the thicker and coarse-grained beds, and not always shows visible upward fining but graded planar parallel stratification. Some beds have a massive (non-stratified) basal division, and the thicker ones locally show trough cross-stratification with trough thicknesses of up to 8 cm. At least one bed shows basal scour-and-fill features with sigmoidal cross-stratification, similar as described from laboratory experiments by Jopling (1965), where the scours probably represent large flutes.

The grading in some of the sandstone beds is inconsistent, with abrupt grain-size changes (e.g., a very coarse-grained lower part, 1-2.5 cm thick, is overlain a fine/medium or very fine-grained upper part). Mudclasts, 0.5 to 16 cm long, occur aligned with the planar parallel strata and/or scattered in ripple cross-laminated division. In a few thick sandstone beds, mudclasts are concentrated in one or more bands. Shell fragments occur scattered in the massive and planar parallel-stratified divisions, and occasionally are concentrated in distinct zones.

Plant detritus occurs sporadically as thin films or short lenses (<1 cm in length) between parallel laminae, or scattered in ripple cross-laminated divisions. Solemarks such as groove and flute casts are common at the bases of sandstone beds, and so are also load casts, some up to 10 cm in height. Water-escape features and convolute ripple cross-lamination are common in the finer-grained, medium-bedded sandstones, with a few beds showing distinct dish structures. Burrows are common, best recognizable as sand-filled subvertical pipes at the bed soles.

On the basis of thin sections (Fig. 3.3), the sandstones in subfacies F2a are classified as carbonate-cemented litharenites (*sensu* Pettijohn *et al*., 1987), moderately sorted. They consist of subrounded to mainly angular grains of quartz (7-50 vol.%); various rock fragments (30-90 vol.%), including fine-grained volcanic rocks (probably volcanic glass or ash fragments); plagioclase (3-5 vol.%); and some unspecified dark minerals (>5 vol.%), including opaques. Sporadic components include fragments of mica and bioclasts (foraminifera, bryozoans, brachiopods and echinoderm plates) (Fig. 3.3A). The most common cement is micritic calcite, although equant sparitic calcite cement is also locally present (Fig. 3.3B).

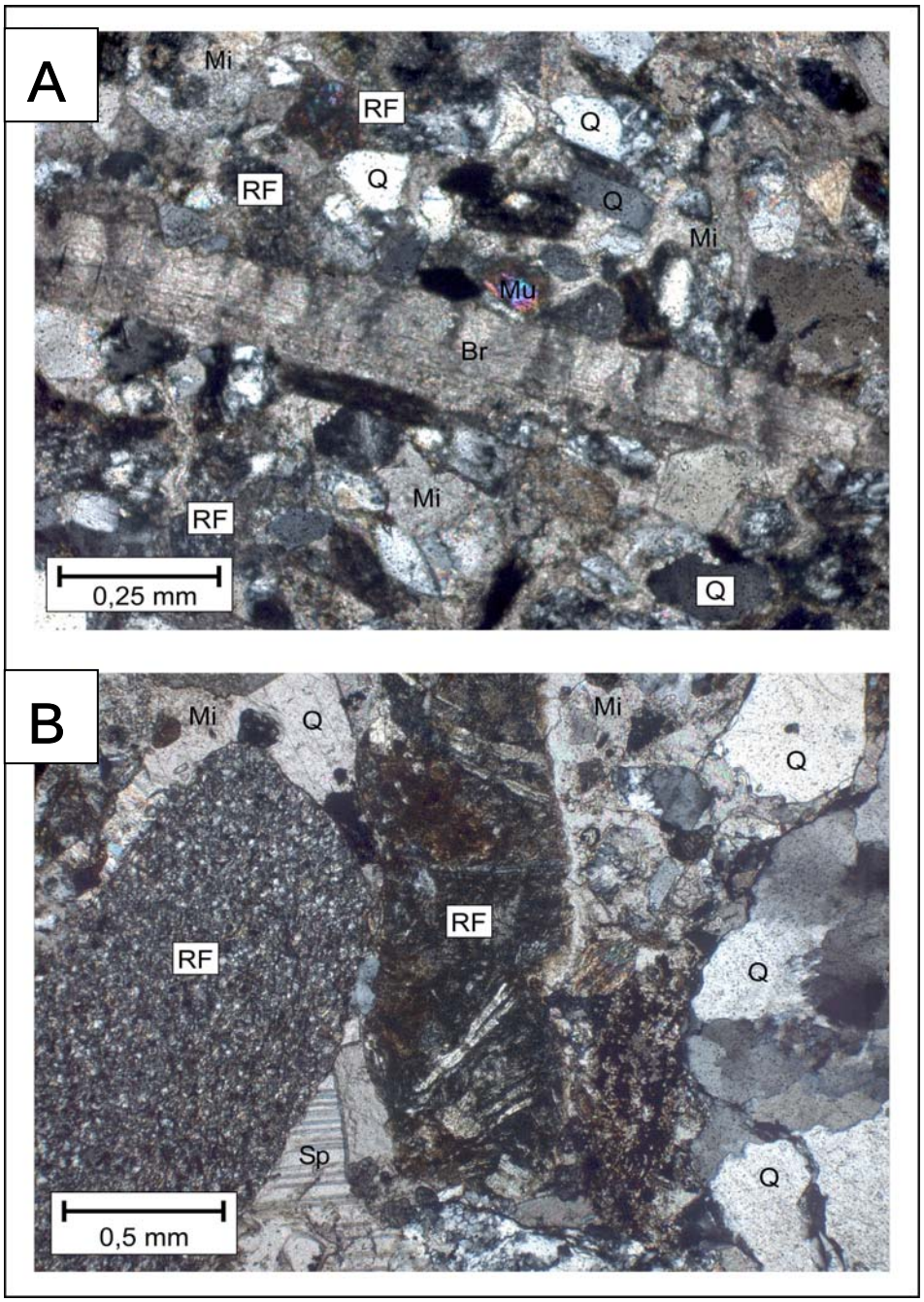

Figure 3.3. Thin-section microphotographs (XPL) of the siliciclastic sandstones of facies F2a in the Gürsökü Formation. Letter symbols: Br – brachiopod fragment, Mi – micrite cement, Mu – muscovite, Q – quartz, RF – volcanic rock fragment, Sp – sparite cement. (A) Sample from Log 1a; note the partly dissolved volcanic rock fragment replaced by mica with high interference colours. (B) Sample from Log 2.

Subfacies F2b: fine-grained to silty calcarenites – These are medium- to thick-bedded calcarenites, common in the Akveren Formation (see Logs 5-10 and 15 in Appendix 1) and present as subordinate component in the Atbaşı Formation (see Log 20 in Appendix 1). The calcarenites are light yellowish-grey, with a whitish- to brownish-grey weathering colour. Their beds are tabular, 10-78 cm thick, with sharp, even bases

and gradational or sharp tops, while the basal erosional relief of the F2b beds is insignificant. The medium-thick beds are very fine-grained to silty. The thicker ones are fine-grained and commonly amalgamated (Fig. 3.4). A few beds are exceptionally coarse, composed of very coarse bioclastic sand in their lower parts and scattered granules and mudclasts, some to 40 cm in length (Fig. 3.5; Log 15 (depth 21m) in Appendix 1).

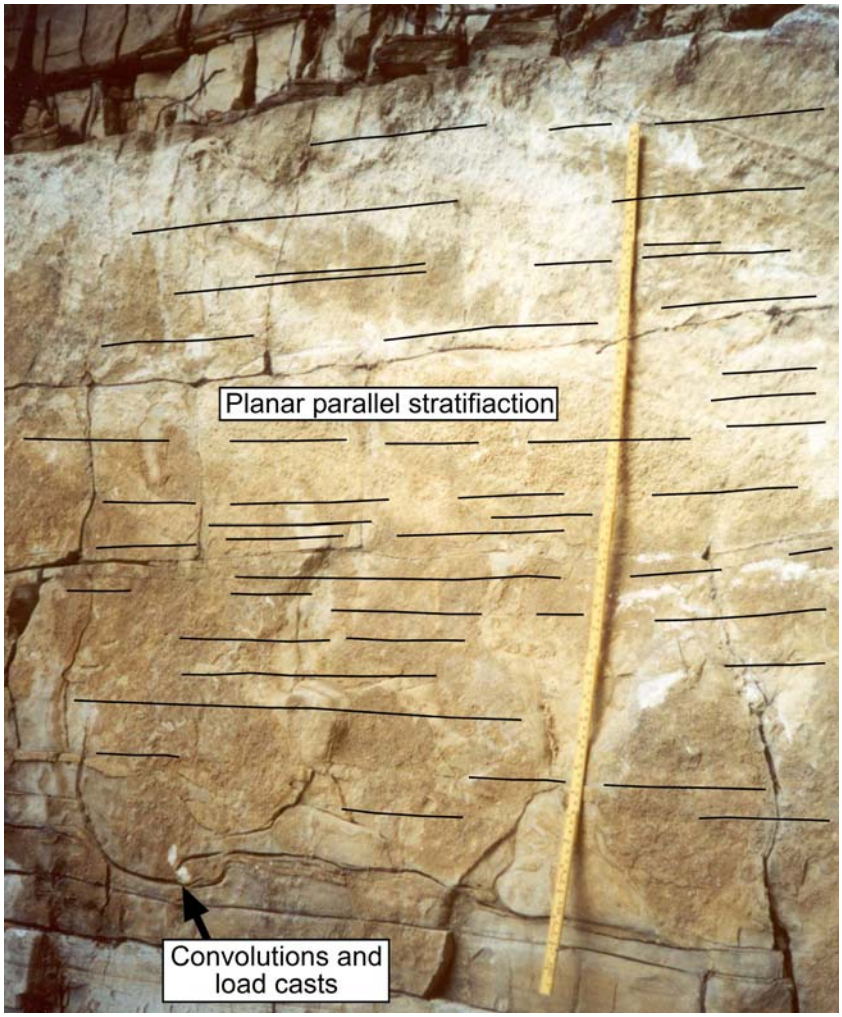

Figure 3.4. Example of subfacies F2b in the middle part of Akveren Formation (detail from Log 9 in Appendix 1). Note the amalgamated beds with planar parallel stratification. The measuring stick is 1 m.

The calcarenite beds are normally graded, with planar parallel stratification overlain by current-ripple cross-lamination, occasionally of climbing-ripple type, and with an interval of thin parallel lamination in the silty top part (Figs. 3.6 and 3.7). The beds are typically capped by a marlstone (facies F7) or a calcareous mudstone (subfacies F8a). Trough cross-stratification occurs in some of the thicker beds, with trough thicknesses of up to 17.5 cm. Convolute ripple cross-lamination and/or bed-top parallel lamination are common. The calcarenites contain chert (amorphous silica) concretions, up to 9 cm in thickness, locally forming semi-continuous bands up to 100 cm long, typically at the

boundary between planar parallel stratification and ripple cross-lamination. Flute casts are common at bed bases (Fig. 3.8), as are also load casts, occasionally with small mud flames and sand tongues. Burrows are found mainly at the bed bases, recognizable as sand-filled tubes up to 1 cm in diameter.

Figure 3.5. Example of a thick, coarse-grained calcarenite bed of subfacies F2b in the upper part of the Akveren Formation (detail from Log 15 in Appendix 1). Note the cavities after mudclasts, up to 40 cm long, in the middle massive part of the bed. The measuring stick is 1 m.

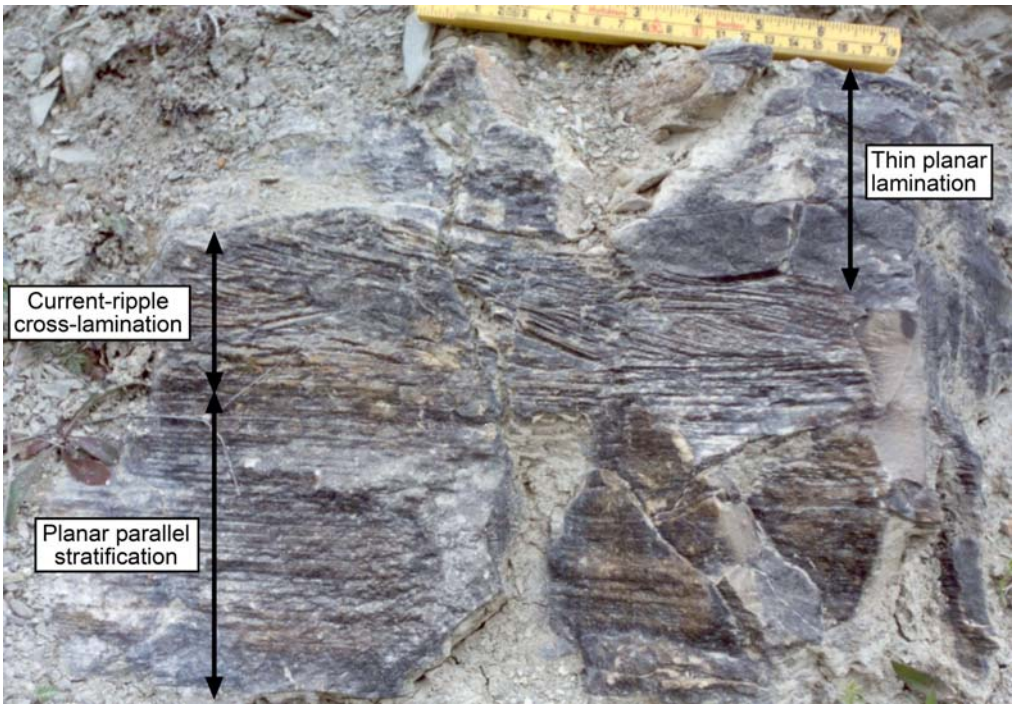

Figure 3.6. An example calcarenite bed of subfacies F2b in the lower-middle part of the Akveren Formation (detail from Log 6 in Appendix 1). The measuring stick is 20 cm.

Figure 3.7. Calcarenite bed of subfacies F2b, with well-developed climbing-ripple cross-lamination; detail from the middle part of Akveren Formation. The lens cap is 6 cm.

Figure 3.8. The sole of a calcarenite bed of subfacies F2b, showing flute casts; detail from the lower- middle part of Akveren Formation (Log 10 in Appendix 1).

Thin sections show the calcarenites to be well sorted and composed predominantly of bioclasts, with scattered angular to subrounded grains (<5 vol.%) of quartz, mica and various rock fragments, including volcanic tuff and glass. The calcarenites are mainly grainstones (*sensu* Dunham, 1962) with micritic calcite cement. Bioclasts have thick micritic envelopes and are typically fragmented forams, bryozoans, echinoderms, molluscs and red coralline algae (mainly crustose corallines *Corallinaceae Melobesieae*) (Fig. 3.9). They represent the *foramol* facies of Lees and Buller (1972).

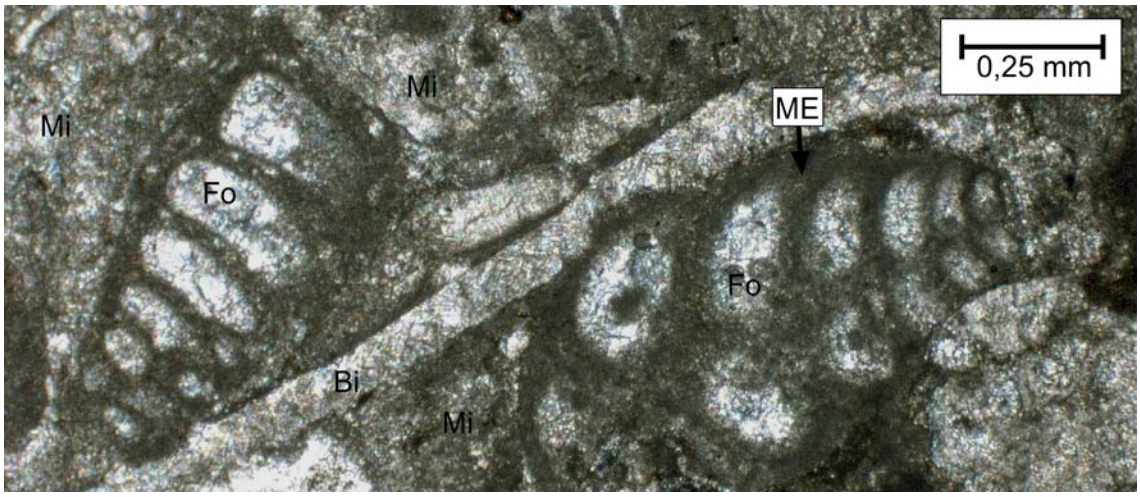

Figure 3.9. Microphotograph of a calcarenite of subfacies F2b (sample from the middle part of Akveren Formation, Log 9 in Appendix 1). Letter symbols: Bi – bivalve fragment, Fo – foram test, ME – micritic envelope, and Mi – micrite cement. Note the thick micritic envelopes on the two foram fragments and the cement in which several small bioclasts have been totally micritized and are impossible to identify.

Interpretation – The sandstone beds of facies F2 are interpreted to be deposits of low-density and occasional high-density turbidity currents. This interpretation is based mainly on the tabular geometry and sedimentary structures of the beds, which resemble classical Bouma-type turbidites (Fig. 3.10). The coarse grain-size and angularity of siliciclastic grains in subfacies F2a suggests sediment supply from a basin-margin fluvial source, probably a delta, rather than a beach and shoreface zone. The change from the siliciclastic turbidites of subfacies F2a to the calcareous turbidites of subfacies F2b in the stratigraphic succession is gradual, attributed to a progressive switch in sediment supply, with the siliciclastic terrigenous source abandoned in favour of a temperate, shallow-marine carbonate platform (Lees and Buller, 1972). The micritic carbonate cement and admixture of bioclasts in the sandstones of subfacies F2a indicate a mixed source. Chert concretions, common in the bioclastic subfacies F2b, indicate precipitation of silica during diagenesis in burrow fills or around fossils (Tucker, 2001). Particles of biogenic silica, such as radiolarian and diatom shells and sponge spicules, undergo dissolution, and this silica often tends to precipitate nearby as chert (Hesse, 1987; Tucker, 2001).

A turbidity current is a turbulent, fluidal type of subaqueous sediment-gravity flow in which buoyancy, hindered settling and the upward component of turbulent eddies are supporting the sediment grains (Middleton, 1970; Middleton and Hampton, 1976). The sediment is carried in turbulent suspension, and is gradually settling into bedload

traction as the flow power decreases. Turbidity currents are commonly assumed to have a Newtonian rheology (Lowe, 1979, 1982; Mutti, 1992; Stow *et al*., 1996; Kneller and Buckee, 2000), although there is no reason to assume that the flow viscosity remain constant. As pointed out by Nemec (1990, 1995), the viscosity of a flowing sediment-water mixture depends strongly on the sediment concentration, and because the latter is vertically non-uniform and varies with the intensity of turbulence – so does necessarily also the turbidity current's viscosity. In short, turbidity currents, and particularly their high-density varieties, can behave almost as non-Newtonian fluids (i.e., fluids whose viscosity depends on the shear strain rate). With this assumption in mind, it is easy to understand the development of rheological interfaces within a turbidity current, and the current's own ability to accelerate (waxing) or decelerate (waning) along such interfaces (Lowe, 1982; Postma *et al*., 1988; Kneller and Branney, 1995; Vrolijk and Southard, 1997). For example, the abrupt textural changes, graded planar parallel stratifiaction and other apparent internal discontinuities in some of the sandstone beds of facies F2 can be attributed to such intra-flow bypass (waxing) phases.

In terms of the Bouma model (Fig. 3.10), the majority (>88 %) of subfacies F2a beds can be classified as turbidites T_{bcd} and the rest (<12%) as turbidites T_{abc}, T_c and T_{cd}. The beds of subfacies F2b are almost exclusively (<99%) turbidites T_{bc} and T_{cd} (Figs. 3.4, 3.6 and 3.7). The turbiditic division A represents rapid, non-tractional deposition of sediment load dumped directly from turbulent suspension (Middleton, 1970; Lowe, 1988; Allen, 1991). The turbidites containing division A are considered to be deposits of high-density turbidity currents (*sensu* Lowe, 1982). Division B represents tractional transport of sand as bedload sheets, in the upper flow regime (Harms *et al.*, 1975, 1982). Division C represents tractional transport of sand in the form of migrating ripples, which means the lower part of lower flow regime (Harms *et al*., 1975, 1982). Climbing ripples indicate traction accompanied by relatively intense fallout of sand grains from suspension (Allen, 1982); in these conditions, the sediment lost by erosion of the ripple stoss side is less than the addition of sediment from suspension fallout on the lee side (Collinson and Thompson, 1982; Boggs, 1995).

The apparent hydraulic discontinuity corresponding to the change from plane-bed to ripple configuration (see above) is normally a consequence of the "depletive" behaviour of turbidity current (*sensu* Kneller and Branney, 1995), with the flow boundary layer becoming too thin for dunes to form. However, dunes can form when the boundary

layer is sufficiently thick, as it often happens in channelized currents (Allen, 1982) or in an unconfined turbidity current characterized by an "accumulative" behaviour (*sensu* Kneller and Branney, 1995). This type of behaviour probably characterized some of the non-channalized currents in the present case, because the sandstone beds of facies F2 occasionally show trough cross-stratification. The cross-set thickness indicate small dunes, <18 cm in height.

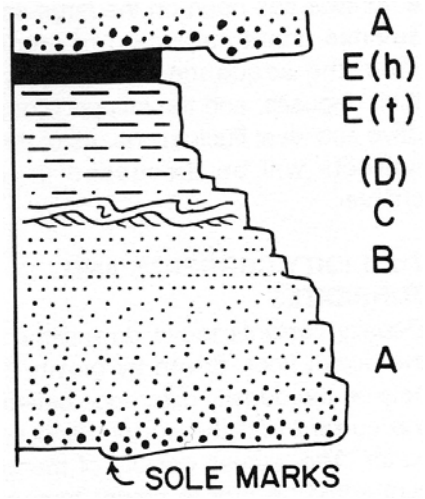

Figure 3.10. The vertical organization of sedimentary structures in a classical, Bouma-type turbidite (from Walker, 1992). The letter symbols A to E denote turbidite divisions defined by Bouma (1962).

The turbiditic division D, typically comprising silt or silty mud, is the least understood part of a turbidite. It is widely considered to represent the tail, or final phase, of the waning turbidity current, when the deposition of abundant fine sediment from suspension combines with a weak and possibly pulsating traction (Middleton, 1970; Allen, 1982; Lowe, 1982; Ghibaudo 1992; Stow *et al*., 1996). With reference to the existing results of laboratory studies, Nemec (1995) suggested that division D may be deposited solely from suspension, because the fallout process of a rich, turbulent cloud of fine sediment tends to occur in a rhythmic manner and these pulses may result in thin, delicate and partly diffuse laminae.

The solemarks and convolutions observed in facies F2 are among typical features of turbidites. Flute marks are products of turbulent scour, formed by eddies moving along the flow during the passage of the turbidity current's head (Stow *et al*., 1996). Load casts form when non-compacted fine sediment, such as mud, is overlain by a coarser sediment layer, such that an inverse density gradient is established; the interface can readily be disturbed by slight stress, such as a seismic shock or the shear force of overpassing current (Collinson and Thompson, 1982; Boggs, 1995). Convolute

lamination is a result of hydroplastic deformation, whereas dish structures are products of rapid dewatering (Stow and Shanmugam, 1980; Allen, 1982; Collinson and Thompson, 1982; Boggs, 1995).

Similarly, rip-up mudclasts are common in turbidites (Ghibaudo 1992; Stow *et al.*, 1996), owing to the erosional character of turbidity currents and the cohesive nature of their substrate. The rip-up clasts are typically derived by the current's head and incorporated in the basal part of turbidite, but may also be derived by the scouring action of the current's body, especially when waxing. The progressive rising of the depositional surface (Vrolijk and Southard, 1997) may render the mudclasts, as well as shell fragments or plant debris (if available), to be deposited at a relatively high level in the turbidite, possibly in more than one horizon (Postma *et al.*, 1988; see examples in Fig. 3.5 and in Log 1b, Appendix 1).

It is likely that at least the thickest turbidites of subfacies F2b, such as the very coarse-grained calcarenite beds with scattered outsized clasts and evidence of high-density turbidity current (Fig. 3.5 and Log 15 (depth 21 m) in Appendix 1), are "seismoturbidites" related to strong earthquakes. Furthermore, it is possible that the mineral composition of sediment (calcareous *versus* siliciclastic) had some effect on the flow characteristics of turbidity currents. Bioclastic sediment in temperate conditions would seldom be subject to early cementation (James and Bone, 1991), and would thus be prone to gravitational failures much like a terrigenous siliciclastic sediment (Braga *et al.,* 2001). However, bioclasts are more porous, of lower density, more easily rounded by abrasion; and though possessing a large variety of shapes, they are easily coated by algae and lose their angularity (Molina *et al.*, 1997; Tucker, 2001). As a result, bioclastic sediment is more easily lifted and supported by turbulence, and has lower intergranular friction. Accordingly, one might speculate that the bioclastic turbidity currents may have been capable of carrying sediment further away from the basin-margin source, out in the basin, while being less powerful and also less erosive, compared to analogous siliciclastic currents in similar basin-floor conditions. These assumptions are corroborated by the little basal erosional relief of the calcarenite beds in subfacies F2b.

3.4. Facies F3: calcarenites with wave-formed and combined-flow stratifications

Description – These calcarenites predominate in the uppermost part of the Akveren Formation (see Logs 15, 16, 17, and 19, Appendix 1). Their beds are generally tabular and vary from thin to thick, with a maximum measured thickness of 81 cm. Bed bases are sharp, with no or little erosional relief (<3 cm), whereas the tops are sharp, occasionally gradational, and vary from planar to undulatory (with asymmetrical to symmetrical wavy undulations, mainly 2-8 cm in relief**).** The calcarenite beds commonly overlie directly one another, or are capped by marlstone (facies F7) or calcareous mudstone (facies F8).

The calcarenites are whitish- to yellowish-grey, but have a light grey to brownish-grey weathering colour. In wide outcrops (>100 m), some of the packages of amalgamated beds are seem to be thinning laterally. The mean grain size varies from very coarse to very fine sand. The thicker beds are generally coarse-grained, commonly containing limestone granules and occasionally outsized clasts of marl (<37 cm long) and/or calcarenite (<13 cm) at the bases.

The internal sedimentary structures include planar parallel stratification, with parting lineation recognizable on bedding planes (Fig. 3.11); undulatory stratification resembling closely hummocky and/or swaley cross-stratification, with wavelengths of 50-220 cm (Figs. 3.12 and 3.13); wave-ripple cross-lamination attributed to symmetrical and asymmetrical 3-D vortex ripples (Figs. 3.14 and 3.15A, C), similar as described by Harms *et al.* (1982); and cross-lamination attributed to asymmetrical combined-flow ripples, with broad rounded crests and narrow troughs (Fig. 3.15B), similar as reported from laboratory experiments by Yokokawa *et al.* (1995). The scale of hummocky cross-sets commonly decreases upwards within a bed (Fig. 3.12). Small-scale hummocky cross-sets (3-D vortex ripples) have wavelengths of 10-25 cm and locally show convolutions attributed to water escape (Fig. 3.14). Some beds have massive, normally graded basal parts and rare beds show low-angled cross stratification.

Mudclasts, up to 4 cm in size, occur scattered along planar parallel strata. Diagenetic chert concretions locally form semi-continuous bands, up to 9 cm thick, parallel to the bed boundaries. Bed bases show vertical and horizontal burrows (sand-filled pipes 0.5-1 cm in diameter), and one *Ophiomorpha nodosa* trace has been recognized at the base of

a thick package of amalgamated calcarenite beds of facies F3 near the top of the Akveren Formation (see Log 16 (depth ~9m) in Appendix 1).

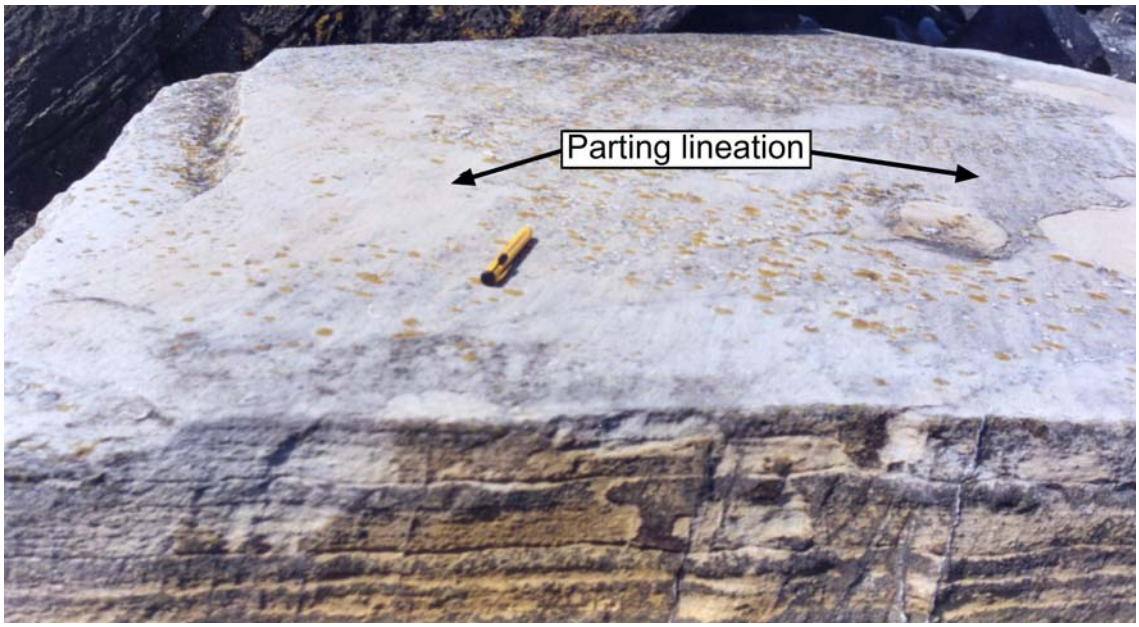

Figure 3.11. Calcarenite bed of facies F3, with planar parallel stratification and clear evidence of parting lineation (parallel to the pen) on the bedding plane. Detail from the uppermost part of the Akveren Formation (Log 16 in Appendix 1). The pen is 13 cm.

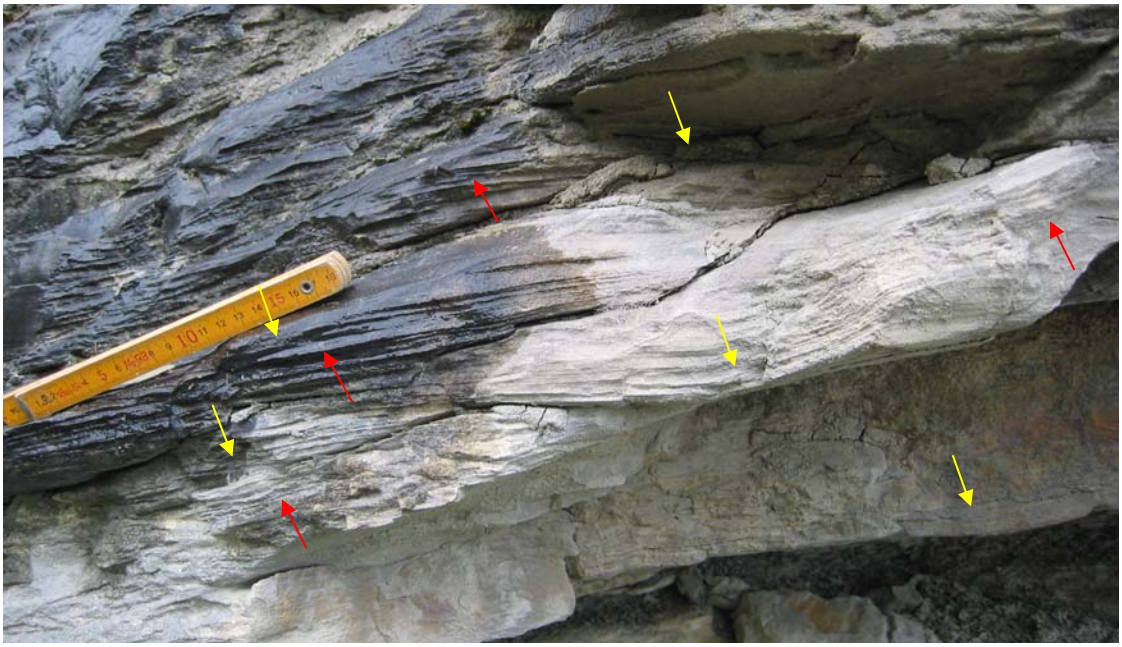

Figure 3.12. Example of a calcarenite bed of facies F3 in the uppermost part of Akveren Formation (detail from Log 17 in Appendix 1). The undulatory stratification with concave-upward (yellow arrows) and convex-upward geometry (red arrows) is interpreted to be hummocky cross-stratification. The measuring stick is 20 cm.

Figure 3.13. Example of hummocky cross-stratification in a calcarenite bed of facies F3 (block fallen from the outcrop of the uppermost part of Akveren Formation, near the Erfelek Waterfalls locality; for location, see Figure 1.1). The blues lines are strata traces drawn with a marker pen. Note the vertical exaggeration.The measuring stick is 1 m.

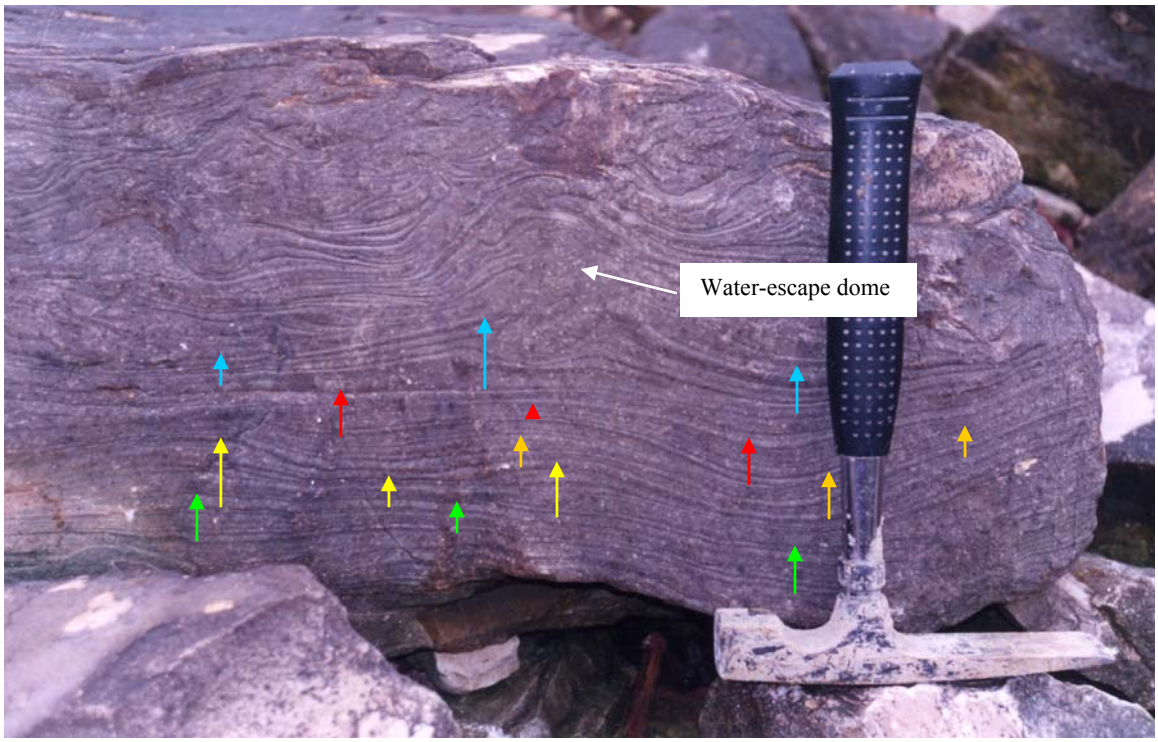

Figure 3.14. Small-scale hummocky stratification (3-D vortex wave-ripple cross-lamination), convoluted in the upper part due to dewatering. The colour arrows indicate some of the undulatory packages of laminae; note the thickening of laminae within hummocks. Example from a calcarenite bed of facies F3 in the uppermost part of Akveren Formation. The hammer is 30 cm.

Thin sections of the calcarenites of facies F3 (see Appendix 2) show bioclastic sediment with rare scattered siliciclastic grains (<1 vol.%), including quartz, opaque grains and fragments of volcanic rocks. All calcarenite samples belong to the grainstone category (*sensu* Dunham, 1962). The fragmented bioclasts represent molluscs, forams, bryozoans, brachiopods, red coralline algae (crustose corallines *Corallinaceae Melobesieae*) and echinoderm plates (Fig. 3.16). The sediment is classified as the *foramol* facies of Lees and Buller (1972). Cement is mainly micritic calcite, although sparitic cement occurs also locally as syntaxial overgrowths of calcite crystals around bioclasts. Bioclasts typically have a blurry appearance due to diagenetic changes and thick micritic envelopes.

Interpretation – The calcarenites of facies F3 are interpreted to be tempestites, deposited by storm-generated combined-flow currents in the offshore transition to shoreface zone (sublittoral to littoral environment). The sedimentary structures support

Figure 3.15. Examples of different varieties of wave-ripple cross-lamination in the calcarentites of facies F3 (details from the upper part of Akveren Formation). The lens cap is 6 cm. (A) Planar parallel stratification overlain by cross-lamination attributed to asymmetrical 3-D vortex and post-vortex ripples. (B) Cross-lamination attributed to combined-flow ripples. (C) Cross-lamination attributed to reversing crests ripples.

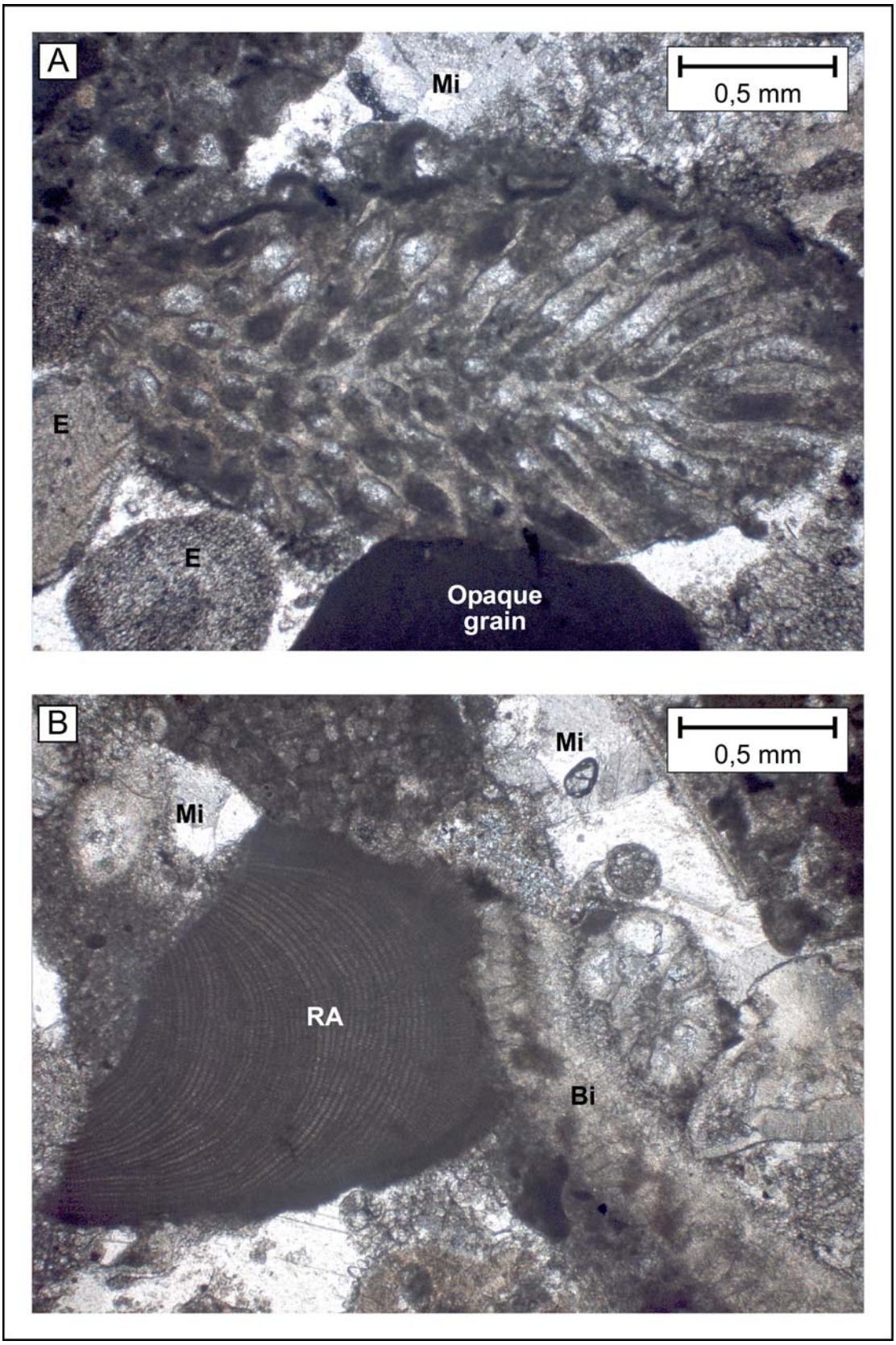

Figure 3.16. Microphotographs (XPL) of the calcarenites of facies F3; samples from Log 17, uppermost Akveren Formation. Letter symbols: Bi – bivalve, E – echinoderm, Mi – micrite cement, and RA – red coralline algae. (A) Subtransverse section of a fragment of bryozoan colony, surrounded by echinoderms and an opaque grain. (B) Fragment of red coralline algal colony (Corallinaceae Melobesieae) to the left and a bivalve fragment to the right.

this interpretation, whereas the bioclastic *foramol*-type sediment indicates derivation from a temperate-climate, shallow-water carbonate platform of the basin margin, similar as inferred for the calcareous sediment of facies F2. Hummocky and swaley stratifications (Fig. 3.17) are widely regarded to be diagnostic features of storm deposits (Harms *et al.*, 1982; Leckie and Walker, 1982; Nøttvedt and Kreisa, 1987; Duke, 1990; Southard *et al.*, 1990; Duke *et al.*, 1991; DeCelles and Cavazza, 1992; Walker and Plint, 1992; Johnson and Baldwin, 1996; Seguret *et al.*, 2001). Similarly, the wide range of wave-formed, oscillatory and combined-flow ripple cross-laminations (Figs. 3.14 and 3.15) is fully compatible with storm deposits (Allen, 1982; Harms *et al.*, 1982; Myrow and Southard, 1996).

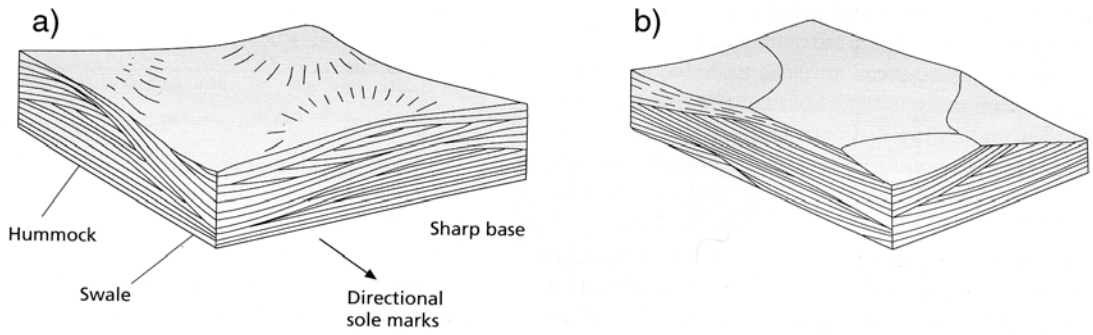

Figure 3.17. Diagrams showing hummocky cross-stratification (a) and swaley cross-stratification (b). From Tucker (2001).

On the other hand, the sharp-based tabular sandstone beds may seem to resemble turbidites T*(a)bc*, especially since some rare cases of undulatory stratification ("small-scale HCS") have been reported from turbidites and attributed to antidunes generated by standing waves along the interface between a denser, thin underflow and the thicker, low-density overpassing flow (Prave and Duke, 1990). However, the calcarenite beds in the present case have fairly sharp tops and their internal similarity to tempestites (e.g. Molina *et al.*, 1997, their Fig. 3; Vera and Molina, 1998, their facies 5) is ubiquitous, rather than sporadic or rare. Therefore, a storm origin is preferred for the deposits of facies F3, even though some of these beds may well be subordinate turbidites or turbidites with wave-reworked tops (Myrow *et al.*, 2002).

3.5. Facies F4: massive calcarenites

Description – These are massive calcarenites that occur as bed packages in the middle and upper part of the Akveren Formation (see Logs 11-14 and Log 18 in Appendix 1). The calcarenites have a whitish to pinkish light-grey colour, but their weathering colour is brownish to reddish grey. The beds are up to 41 cm thick and roughly tabular (Fig. 3.18). Bed boundaries are sharp and uneven, commonly undulating, with a basal erosional relief of up to 5 cm. Internally, the beds show multiple scour-and fill features, typically little more than 60 cm wide and 10-15 cm thick. These lenticular internal features are less distinct in facies F4 deposits near the top of the Akveren Formation, close to its transition to the overlying Atbaşı Formation (e.g., see Log 18). The beds of facies F4 are capped by calcareous mudstone (facies F8), marlstones (facies F7) and/or bedded bioclastic limestone (subfacies F6a). Some beds are stacked directly upon one another and largely amalgamated. The packages of facies F4 beds are locally truncated by broad and shallow scours (Fig. 3.18), up to 1-2 m in relief, which are discussed separately in section 4.3.

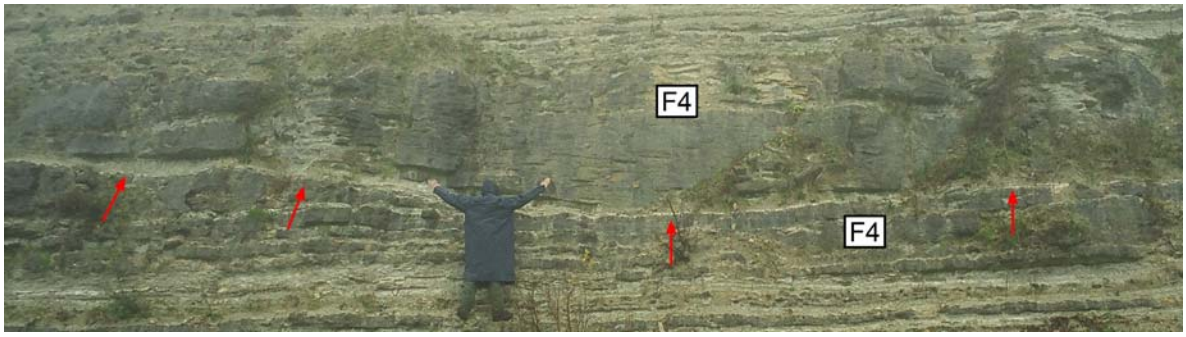

Figure 3.18. Package of facies F4 beds in the middle-upper part of Akveren Formation (detail from Log 11 in Appendix 1). Note that the two packages of calcarenite beds are separated by a broad and shallow, channel-like scour (red arrows).

The mean grain-size is highly variable from bed to bed, ranging from very coarse sand with sparse granules to very fine sand. Only one thin section has been analyzed (sample from a coarse-grained calcarenite in Log 18; see data in Appendix 2). The sediment is bioclastic (Fig. 3.19), of *foramol* type, with scattered, subrounded outsized fragments of marlstone (<5 cm in size), mudstone (<4 cm), calcarenite (<4 cm) and coarse-grained

greenish tephra (<7 cm). Sporadic sand-sized siliciclastic grains (<5 vol.%) are angular to subrounded fragments of plagioclase, quartz, volcanic glass and tuff. Bioclasts are mainly foraminifera, up to medium sand in size, but include also bryozoans, brachiopods, bivalves, red coralline algae (mostly crustose corallines *Corallinaceae Melobesieae*) and echinoderm plates. Micritic coatings on bioclasts are common, and the grainstone's cement is exclusively micrite. Because their abundant cement and low siliciclastic content, these calcarenites are often difficult to distinguish from the bedded limestones of subfacies F6a.

Most of the calcarenite beds are normally graded, although the grading is not particularly pronounced, no matter if the bed is coarse- or fine-grained. Solemarks are rare, and so are also load casts (see in Logs 11 and 13, Appendix 1). Dewatering injection features (sand dykes <10 cm thick, injected into the overlying bed) are occasionally found (e.g., in Log 11; 4 m depth). Apart from the concave-upward internal scours, the calcarenite bed structure is mainly massive. Vague planar parallel stratification is locally recognizable, and a few beds show diffuse ripple cross-lamination at the top. Burrows are common, both vertical and horizontal, in the form of mud-filled pipes up to 1.5 cm in diameter.

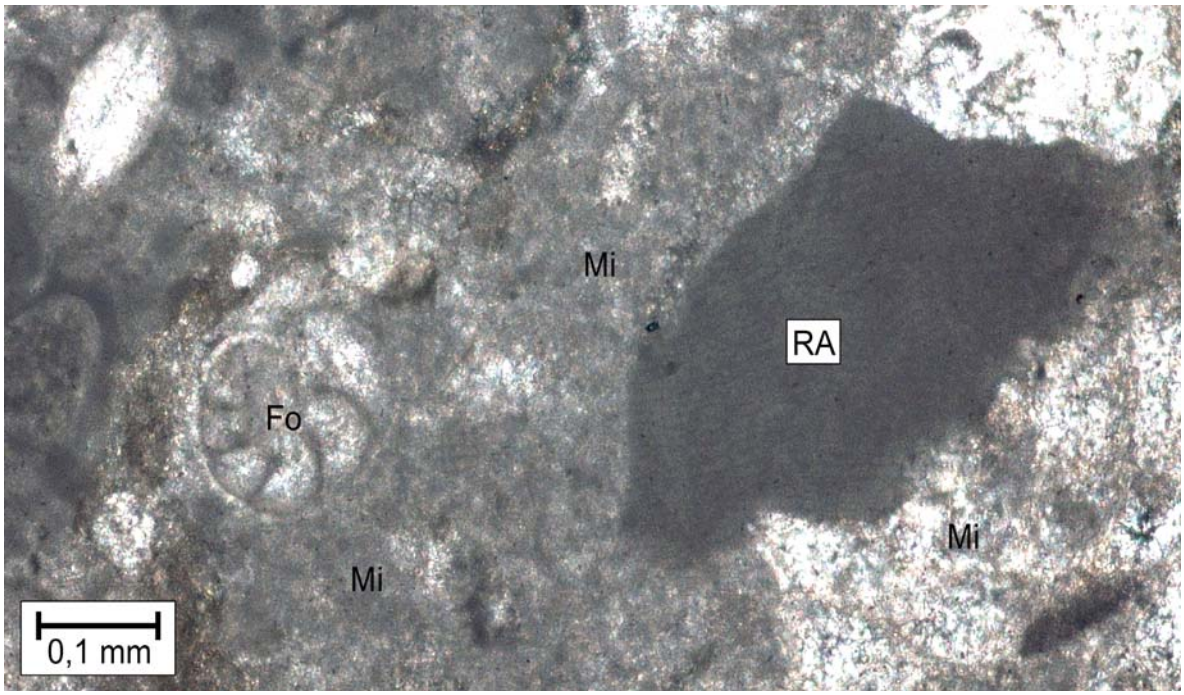

Figure 3.19. Microphotograph (XPL) of a calcarenite of facies F4; sample from the upper part of Akveren Formation (Log 18 in Appendix 1). Letter symbols: Fo – foram fragment, Mi – micritic cement, and RA – red coralline algae.

Interpretation – The scarcity of sedimentary structures makes the interpretation of facies F4 difficult. The massive appearance of the beds is probably due to their calcareous composition (nearly pure bioclastic sediment) and high degree of cementation, which may have obliterated primary stratification (e.g. Coniglio and Dix, 1992). The association with facies F1b, F6, F7 and F8 points to two possible depositional processes: storm-generated compensation currents or turbidity currents. This latter interpretation seems to be more likely. The calcarenites of facies F4 are thought to be deposits of unsteady, pulsating (i.e., alternatingly waning and waxing), high-density turbidity currents (*sensu* Lowe, 1982). Each surging pulse would scour unevenly the substrate (previous deposit) and form a new turbiditic unit T*a(b)*; and the amalgamation of these successive units would commonly terminate with the formation of current ripples by the waning current (unit T*abc*). The beds of facies F4 are thus considered to be composite calciturbidites of T*a(b)a(b)a(b)…a(b)c* type and singular calciturbidites T*a(b)*.

The turbidity currents were derived from a temperate shallow-marine carbonate platform (cf. Mullins and Cook, 1986) and generated by storms, possibly in combination with seismic events (Harris, 1994; Drzewiecki and Simó, 2002). Harris (1994) described similar deposits and attributed them – with reference to several other studies – to turbidity currents generated by storms eroding a shallower-water carbonate platform. The depositional setting in the present case would be one of a fore-reef seafloor gentle-inclined slope, and the pulsating behaviour of the turbidity currents might be attributed to the fluctuating energy of storm events. However, it cannot be precluded that some of the calcarenitic beds of facies F4 are tempestites or deposits of rip currents, whose behaviour and deposits might resemble closely those of turbidity currents (Myrow and Southard, 1996).

3.6. Facies F5: thinly bedded siliciclastic sandstones and calcarenites with mainly current-ripple cross-lamination

The sandstone beds of this facies are the thinner (<10 cm) equivalents of facies F2, and have thus similarly been divided into the two varieties: siliciclastic sandstones and

calcarenites. The two subfacies are first described and then jointly interpreted below.

Subfacies F5a: very coarse- to very fine-grained or silty siliciclastic sandstones – These are light to dark grey in colour, with a brownish-grey weathering colour. They are mineralogically similar to the sandstones of subfacies F2a and occur in the Gürsökü Formation (see Logs 1a-b to 4 in Appendix 1). Their beds are predominantly tabular, sporadically pinching out laterally, and are capped by marlstone (facies F7) or calcareous mudstone (subfacies F8a). The beds have gradational tops and sharp bases with little erosional relief (<2.5 cm). Granules and small pebbles (<0.7 cm) are occasionally scattered along the bases of coarse-grained beds (e.g., see in Log 1a, Appendix 1).

Figure 3.20. Siliciclastic sandstone beds of subfacies F5a, with current-ripple cross-lamination underlain by planar parallel stratification and capped by marlstone (facies F7). Detail from the middle part of Gürsökü Formation (Log 2 in Appendix 1). The ruler scale is in centimetres.

Internally, the beds show mainly current-ripple cross-lamination, locally underlain by a thin division of planar parallel stratification (Fig. 3.20) or trough cross-stratification. The

thinnest and finest-grained beds (<1.5 cm) are cross-laminated throughout, with the ripple cross-sets reflected in uneven top surfaces and commonly occurring as semi-detached lenses (starved sand/silt ripples). Scattered flat-lying mudclasts (occasionally up to 4 cm in size), convolute lamination and both flute and load cast are fairly common. Plant detritus is found scattered in some beds, and many beds are also bioturbated, showing vertical and horizontal burrows.

Subfacies F5b: very fine-grained to silty calcarenites – These are analogous to the thicker-bedded subfacies F2b and similarly common in the Atbaşı and Akveren formations (see Log 5-10, 15 and 20 in Appendix 1). The calcarenites are yellowish-grey in colour, with light bluish- to brownish-grey weathering colours. A thin section from Log 20 (Atbaşı Formation, see Appendix 2) shows a micrite-cemented grainstone composed of bioclastic sediment of *foramol* type, with less than 10 vol.% of angular quartz grains, some coated by hematite. Bioclasts are predominantly forams, with a minor admixture of fragmented bivalves and echinoid spicules and scattered plant detritus.

The beds have sharp bases and gradational tops and are mainly tabular, but some have uneven upper boundaries. There is little or no basal erosional relief (<2 cm), and the irregular tops are mainly due to preserved ripple forms, though commonly bioturbated. Bed amalgamation is relatively rare.

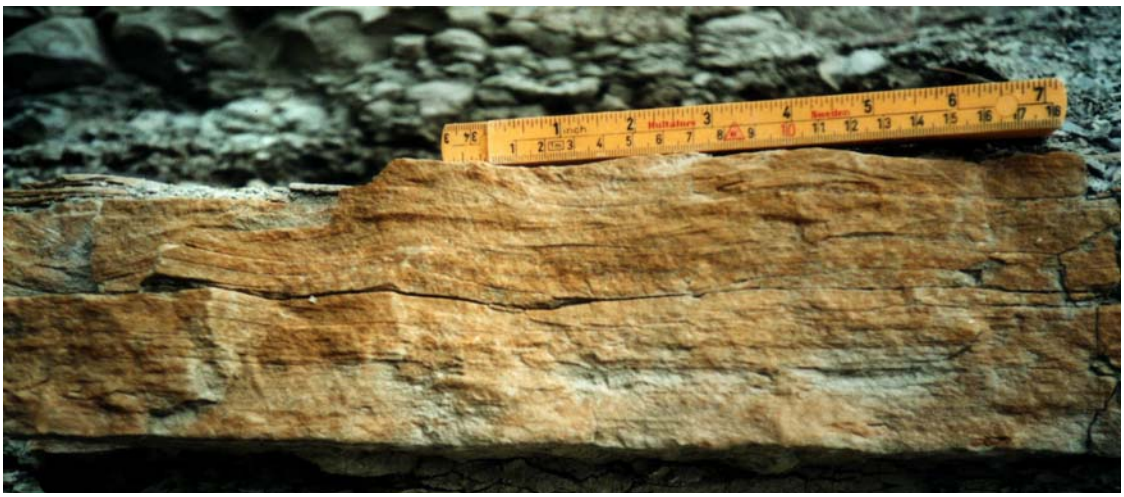

Figure 3.21. An example calcarenite bed of subfacies F5b; detail from the lower-middle part of Akveren Formation (Log 10 in Appendix 1). Note the planar parallel stratification overlain by current-ripple cross-lamination. The ruler is 20 cm.

These calcarenites beds are normally graded, with sporadic flute and load casts at the bases. The main sedimentary structure is current-ripple cross-lamination, commonly convoluted and occasionally underlain by planar parallel stratification (Fig. 3.21) and/or overlain by a thin silty division of delicate parallel lamination, locally containing plant detritus. Beds thinner than 1.5 cm typically consist of semi-detached, solitary lenticular cross-sets (starved ripples). The beds of subfacies F5b are commonly overlain by marlstone (facies F7) or calcareous mudstone (facies F8). Chert concretions in subfacies F5b are less common than in the corresponding subfacies F2b. Bed bases show vertical and horizontal burrows (sand-filled tubes, mainly <0.5 cm in diameter).

Interpretation – The sheet-like geometry and internal sedimentary structures of facies F5 beds render them similar to Bouma-type turbidites T*(b)c(d)* (Fig. 3.10), which means deposits of low-density turbidity currents (*sensu* Lowe, 1982). Low-density turbidity currents can originate either as a residual flow of fine-grained sediment suspension after the deposition of coarse-grained load, or as an independent current of low sediment concentration (Lowe, 1982; Ghibaudo, 1992; Mutti, 1992; Kneller and Buckee, 2000). The deposits of facies F5 are associated with, and compositionally similarity to, those of facies F2, which supports the notion of the former being the distal equivalents of the latter. The high-density turbidity currents generated at the basin margin must have varied in volume and run-out distance, and hence their deposits (F2) are alternating with those of low-density residual currents (F5) in the basin-fill succession.

The sandstones of facies F5 are products of a fully tractional deposition from unidirectional currents, which might possibly make them comparable to contourites (Stow and Piper, 1984; Coniglio and Dix, 1992; Faugères and Stow, 1993; Stow *et al.*, 1996). However, contour currents do not operate as episodic brief surges, and it is also doubtful that the trough-like Sinop-Boyabat Basin may have had such bottom currents.

3.7. Facies F6: massive bioclastic limestones

These massive bioclastic limestones occur in the upper part of the Akveren Formation, in outcrops near Kuğuköy west of Çatalzeytın (Fig. 1.1; Logs 11, 14 and 18 in Appendix 1). Based on the presence or absence of bedding, the limestones have been divided into two subfacies, which are first described and then interpreted jointly below.

Subfacies F6a: bedded limestones – These beds are 10-50 cm thick and ranging from predominantly lenticular, up to 3 m in lateral extent (Logs 11 and 14), to mainly tabular (Log 18). Bed boundaries are distinct, if not sharp, but commonly uneven, although no significant basal erosional relief is recognizable. The deposits are similar to the massive calcarenites in facies F4, but the bioclastic sediment here appears to be more crystalline, macroscopically homogeneous and stronger cemented. The limestone colour is whitish to pinkish grey, with reddish grey to brownish grey weathering colours. Subfacies F6a overlies subfacies F6b (see Logs 11 and 14 in Appendix 1), although a few beds of the former limestones have been found also below the latter. Limestone beds of F6a underlie and are overlain by calcarenites (facies F4), marlstones (facies F7) or calcareous mudstones (facies F8).

On a freshly broken surface, grains are hardly visible even with the aid of magnification glass. Recognizable are scattered bioclasts and greenish-grey volcanic rock fragments, 0.1-0.4 cm in size. Otherwise, the rocks appears to consist of finely crystalline calcite. Marlstone clasts up to 1.5 cm long and bedding-parallel mudclasts up to 2 cm in size are locally found. Some beds contain chert concretions, which locally form semi-continuous bands up to 1.5 cm thick. Horizontal and vertical tube-shaped burrows, up to 1 cm in diameter, are common.

Subfacies F6b: non-bedded limestone – This is forming a monotonous succession at the top of Log 14 (Appendix 1). The limestone succession at the Kuğuköy locality (Fig. 3.22) is white to brownish-grey in colour, 10-15 m thick and several kilometres in lateral extent. Freshly broken surfaces are whitish- to pinkish-grey. Although the monotonous succession apparently consists of amalgamated beds, particularly in the uppermost part, the

bedding is hardly recognizable and generally obscured by dense fractures (Fig. 3.23). The limestone succession overlies conformably a calcareous mudstone of subfacies F8b (see Log 14 and Fig. 3.23), with a few horizontal burrows at the base, and is conformably overlain by a package of alternating calcarenites (facies F4), bedded limestones (subfacies F6a), marlstones (facies F7) and calcareous mudstones (facies F8).

Figure 3.22. Limestones of subfacies F6b in a SE-striking outcrop of the upper part of Akveren Formation (Kuğuköy locality). Note the overall massive appearance of the limestone succession. Person (encircled) for scale.

The rock is a finely crystalline, homogeneous limestone with scattered coarse bioclasts and greenish volcanic rock fragments up to 0.1 cm in size. Rare scattered mudclasts, up to 1 cm long, occur at the base. A thin section (see Appendix 2 and Fig. 3.24) shows bioclasts of very fine to very coarse sand grade, microcrystalline, with thin micritic coatings and relatively few (<2 vol.%) associated siliciclastic grains and marlstone fragments. The bioclasts range from angular to subangular and include fragments of red coralline algae (mostly crustose corallines *Corallinaceae Melobesieae*), delicately branched cyclostome bryozoans, bivalves, forams, brachiopods, and echinoderm plates (Fig. 3.24). Siliciclastic

grains include subangular to rounded fragments of quartz, microcline, plagioclase and volcanic glass/tuff. Cement is micro- to macro-crystalline sparitic calcite, locally micritic, with sporadic evidence of syntaxial overgrowths around echinoderm clasts. The massive limestone is classified as a grainstone with crystalline zones (*sensu* Dunham, 1962).

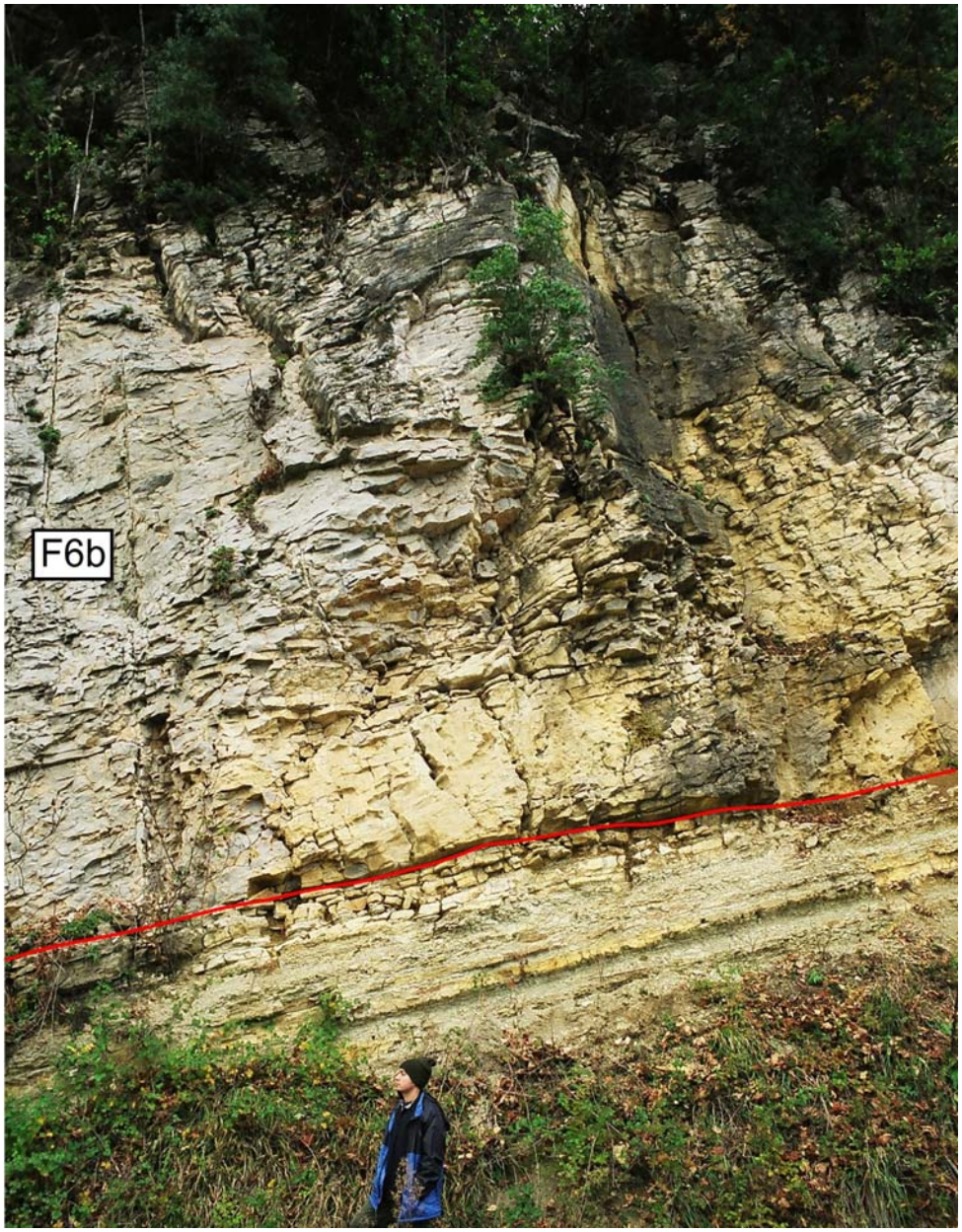

Figure 3.23. A succession of subfacies F6b limestones overlying conformably the deposits of facies F4, F6a and F8b in the upper part of Akveren Formation (see Log 14 in Appendix 1). Note the dense fracturing of the limestone. Standing person for scale.

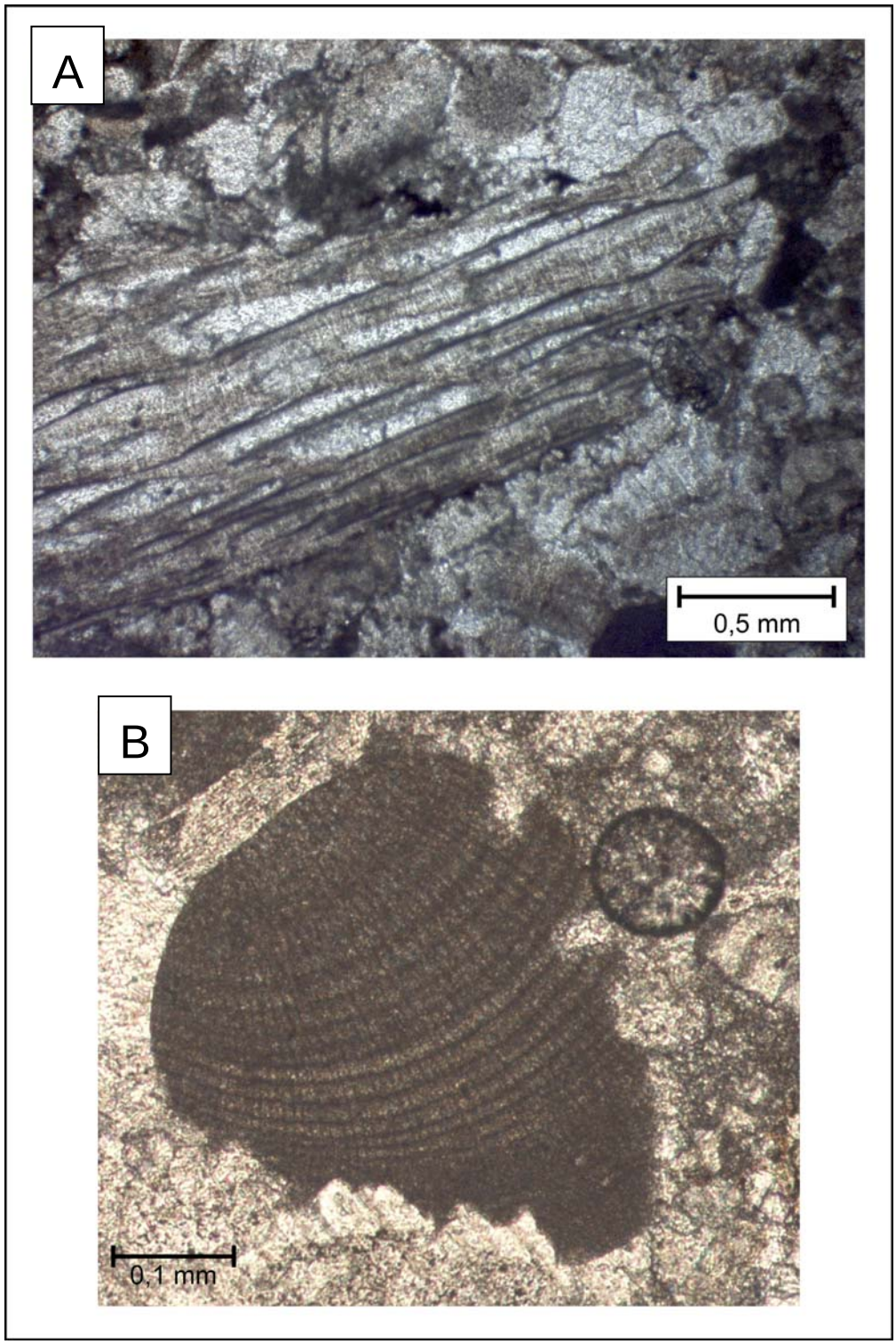

Figure 3.24. Microphotograph of a massive limestone of subfacies F6b in the upper part of Akveren Formation; sample from Log 14 in Appendix 1. (A) Delicate branching structure of cyclostome bryozoan fragment; XPL view. (B) Clast of red coralline algae (Corallinaceae Melobesieae) surrounded by micritic calcite cement; PPL view.

Interpretation – The composition of bioclastic sediment indicates a *foramol*-type source, similar as recognized for facies F2b, F5b, F3 and F4. The deposits of subfacies F6a are thought to represent sandy fore-reef sedimentation on a gentle-inclined slope, probably in continuity with the crest of the reef zone (Wright and Bruchette, 1996). Subfacies F6b may thus represent the expanding reef-complex, with the core and crestal zone dominated by red coralline algae and bryozoan corals. The reef platform has a *foramol* signature and would appear to have formed in temperate-climate waters of less than 20ºC (Lees and Buller, 1972; Wright and Burchette, 1996) and less than 25 m deep (Wray, 1978; Lønøy, 1996). The non-bedded character of subfacies F6b and the evidence of branching cyclostome bryozoans preclude a high-energy environment for the reef formation (James and Bone, 1991).

Bryozoans are small colonial organisms with little tolerance for strong waves, commonly in shallow to moderately deep seawater of normal salinity (Lønøy, 1996; Tucker, 2001). The delicately branching cyclostome bryozoan (Fig. 3.24A) may indicate water depth in excess of 70 m (James and Bone, 1991). Red coralline algae (Fig. 3.25B) are encrusting, coating, cementing and binding organisms common in high-energy, shoal-water reefal or bank-edge settings (Fig. 3.25; Wray, 1978; Adams *et al*., 1984; Adams and MacKenzie, 1998; Tucker, 2001); they prefer clear, low-turbidity and generally shallow (<25 m) water (Wray, 1978; Lønøy, 1996). The red coralline algae, by encrusting and binding/cementing the bryozoan colonies, were probably increasing the latter's tolerance of wave action and allowed the bryozoans to live in a relatively shallower water.

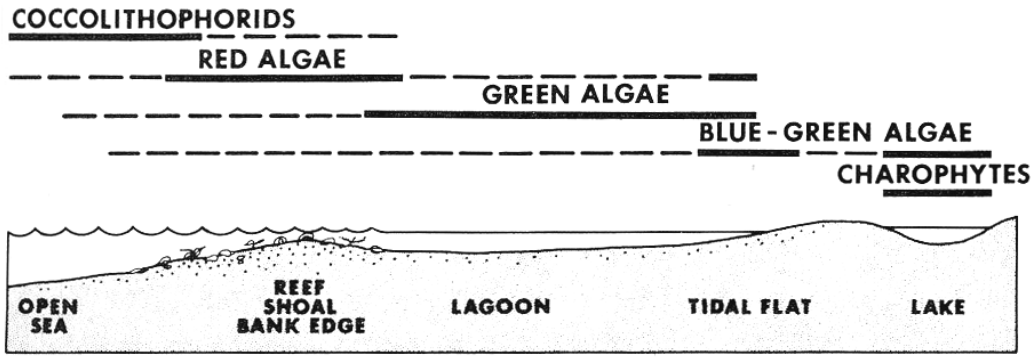

Figure 3.25. Generalized pattern of the environmental distribution of Cenozoic calcareous algae (after Wray, 1978).

Carbonate diagenesis can begin on the seafloor, already at the time of the deposition. The first phase of diagenesis, including grain degradation (Tucker, 2001), produces micritic envelopes that result from endolithic bacteria boring into the skeletal fragments (Boggs, 1995). The resultant microborings are later filled with micrite, and the repetitive boring and filling result in a micritic coating around the skeletal clasts. In the thin-section of subfacies F6b limestone, bioclasts with micritic envelopes are found only sporadically and the envelopes themselves are thin, which indicates that the skeletal debris was subject to only limited degradation and resedimentation. The thin section (Fig. 3.24) shows both micro- and macro-crystalline sparitic cement, the latter most abundant in the more crystalline parts of the sample. These cement types can originate in conditions varying from near-surficial to deep-burial phase (e.g., see Tucker, 2001), and it is likely that a deep-burial cementation would replace cement formed in shallow settings. In the present case, the occurrence of equant sparry calcite and the syntaxial overgrowths composed of larger calcite crystals are indicative of a deep-burial cementation.

The grainstone character of the deposit and the evidence of red coralline algae suggest sediment accumulation as a reef-complex or a sand bank in high-energy nearshore zone (Fig. 3.25). A criterion most commonly used to distinguish carbonate reefs from resedimented carbonate deposits, such as sand banks/ridges, is whether the bioclasts have formed and accumulated *in situ* or is a result of major transport. The thin section shows fragmented skeletal material, but the bioclasts themselves indicate limited degradation and resedimentation. The sparse micritic envelopes and the lack of strong abrasion (e.g. the delicate branching bryozoan colony; Fig. 3.24A), together with the apparent lack of large-scale cross-stratification, point to a short transport of bioclastic sediment in a shallow-marine environment of moderate hydraulic energy. The sedimentary environment of facies F6 is thus envisaged to have been a reefal shoal zone above the fairweather wave base, where texturally submature bioclastic fore-reef sand was produced, distributed and accumulated under the action of waves and tidal currents (James and Bone, 1991; Jones and Desrochers, 1992; Wright and Bruchette, 1996). The edge of the carbonate platform was likely a reflective shoreline with a foreshore slope, where the impact of storm waves would be dissipated in the beach zone and where sand-laden rip currents could form and possibly

turn into turbidity currents when plunging beneath the effective wave base. The extensive reefal platform probably had a varied topography, with low-relief ridges which would contribute to the dissipation of wave energy and minimize clast abrasion.

The stratigraphic position of the bedded fore-reef limestones (subfacies F6a) below the thick and extensive reefal platform (subfacies F6b) indicates reef-complex expansion and a major phase of basin shallowing. The lack of conglomeratic deposits and fore-reef breccias implies a ramp setting, with the fore-reef slope developed in continuity with the reefal platform (Wright and Bruchette, 1996). There was apparently no reef-edge escarpment, and the wave action over the platform was moderate and semi-continuous, grinding the fragile biogenic skeletal material into submature sand, rather than sporadically breaking the reefal rock mass into large chunks and forming gravel – as is the case in many classical coral reefs (Wright and Bruchette, 1996). The stratigraphic occurrence of fore-reef facies above the reefal limestones (Log 18 in Appendix 1) indicates that the reef-complex underwent a rapid retreat after the phase of its basinward advance (see further discussion in section 4.5).

3.8. Facies F7: marlstones

Description – Marlstone beds abound in the Akveren Formation (Logs 5-17) and are common also in the other formations logged (Logs 1-4 and logs 18-20 in Appendix 1). These deposits are easily distinguishable from the calcareous mudstones of facies F8, because they are harder, less fissile and less weathered in the outcrop sections. The rock colour ranges from whitish or light greenish grey (most common), to dark grey and pale olive green, and occasionally to reddish brown. An alternation of reddish and greenish marlstone layers is common at the transition of the Akveren Formation to the overlying Atbaşı Formation (e.g., in Log 18) and in the Atbaşı Formation (e.g., Logs 19 and 20 in Appendix 1).

The marlstone beds are tabular and 0.5 -129 cm thick, but mainly 10-30 cm (Fig. 3.26), with gradational tops and gradational to fairly sharp bases. A marlstone bed typically shows

grading from a silty marlstone at the base to a calcareous mudstone capping. The latter transition is commonly accompanied by a colour change from pale olive green to light or dark grey. The bases and tops of marlstone beds lack significant relief, but are occasionally slightly undulating.

The marlstones typically occur as direct cappings of the calcarenite beds of facies F2b, F3, F4 and F5b (Fig. 3.27) and as solitary beds capped and separated by the calcareous mudstones of subfacies F8a (Fig. 3.26).

Figure 3.26. Marlstone beds of facies F7 in the middle part of the Akveren Formation (detail from Log 8 in Appendix 1). The weathered marlstone beds have a reddish brown colour, but are standing out in relief and are clearly more resistant to physical weathering than their calcareous mudstone (subfacies F8a) cappings. The measuring stick is 1 m.

The majority of marlstone beds are massive ("structureless"), and only the basal silty marlstone occasionally shows ripple cross-lamination or delicate parallel lamination. The internal structure is massive even where the marlstone bed has a "wavy" geometry, with undulating base and/or top, as observed locally in the upper part of the Akveren Formation (e.g., Fig. 3.28 and Log 15 in Appendix 1). Scattered mudclasts up to 0.5 cm in size, coarse to very coarse sand grains and small (<0.5 cm) bioclasts or volcanic rock fragments are sporadically found, and a few beds contain dispersed plant detritus. Burrows are common, in the form of mud- or silt-filled pipes up to 2 cm in diameter, most often vertical or subvertical and isolated, but present throughout the bed.

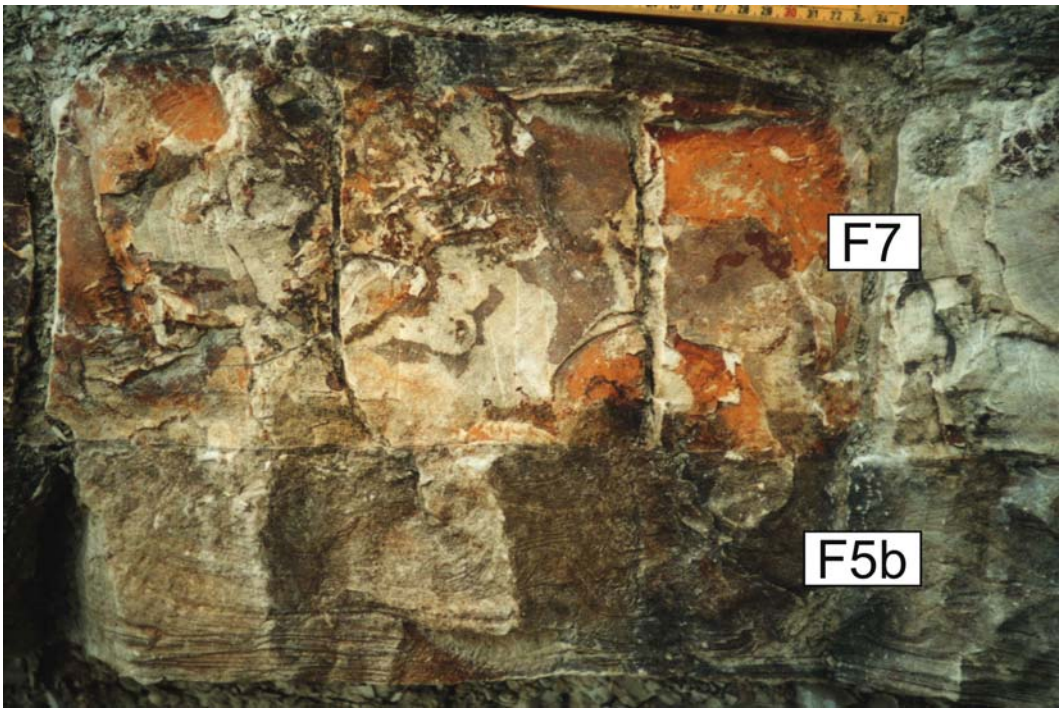

Figure 3.27. Marlstone bed of facies F7 overlying directly a calcarenites bed of subfacies F5b; detail from the middle part of Akveren Formation (Log 7 in Appendix 1). The rule scale (top) is in centimetres.

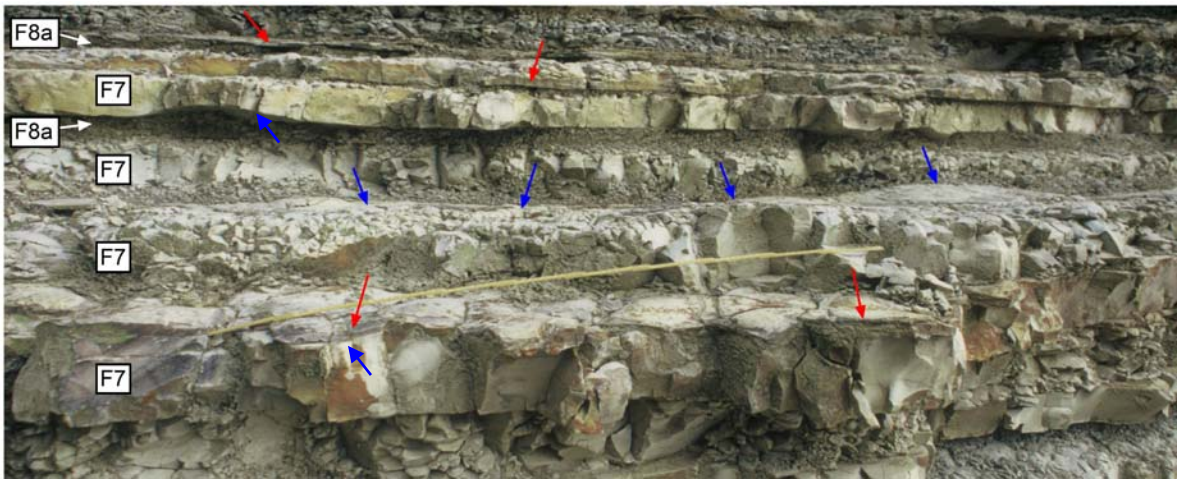

Figure 3.28. Marlstones of facies F7 alternating with the calcareous mudstones of subfacies F8a and thin calcarenites of subfacies F2b (red arrows) in the upper part of the Akveren Formation; detail from Log 15 in Appendix 1. Note the "wavy" geometry (undulating boundaries) of some of the marlstone beds (blue arrows). The measuring stick is 1 m.

Thin sections of marlstone samples from the studied succession (Appendix 2) show a variable amount of small, silt-sized bioclasts scattered in a micritic matrix. The bioclasts

are mainly foram fragments, commonly altered into micro-crystalline sparitic calcite by diagenesis. Depending on the volumetric concentration of bioclastic material, the marlstone might be classified as a wackestone (>10 vol.% bioclastics) or a calcareous mudstone (<10 vol.%) (*sensu* Dunham, 1962) on the basis of a single sample.

Marlstone is variously defined by different authors: as a calcareous mudstone (Kearey, 1996), a mudstone with subequal amounts of micrite and clay mineral particles (Lapidus and Winstanley, 1990), or a rock composed of sand, silt and clay size fractions with a 35-65 vol.% content of carbonate particles (Bryhni, 1999). In the ternary classification diagram of Hay *et al.* (1984), marlstone is defined as a hemipelagic to pelagic deposit composed of calcareous and siliceous biogenic particles as well as non-biogenic particles (Fig. 3.29). In this terminological framework, the marlstones of facies F7 can be classified as calcareous ooze deposits, because they practically lack non-biogenic detritus or show also no siliceous bioclastic component in the thin sections studied.

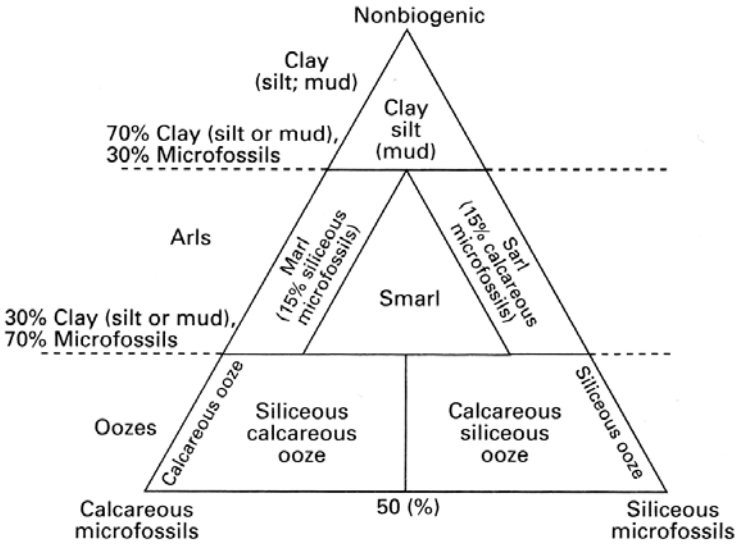

Figure 3.29. Ternary classification diagram for hemipelagic and pelagic sediments. After Hay et al., (1984).

Interpretation – The marlstones of facies F7 are massive and were apparently deposited from suspension fallout, although it cannot be entirely precluded that some internal features have been obliterated by diagenesis. The marlstone beds that are capping calcarenitic turbidites T*(a)bc* or cross-laminated carbonaceous siltstone layers (T*c*), are thus interpreted to be the D-divisions of Bouma-type turbidites, while marlstones capping calcarenitic

tempestites (facies F3) are attributed to deposits of dilute storm compensation currents. This interpretation is consistent with the carbonate source of the turbidites and tempestites (see earlier text) and implies that the turbidity and storm currents were charged with an abundant suspended load of carbonate mud, probably swept from the reefal platform by storms. The upward transition of marlstone into calcareous mudstone (facies F8) indicates that the "background" hemipelagic suspension in the basin was normally richer in siliciclastic sediment particles, and it was chiefly the frequent incursions of turbidity currents that led to the episodic deposition of marl (cf. James, 1997). In other words, the turbidites in the present case would appear to have a marly "hemipelagic" D-division and a muddy "pelagic" E-division, calcareous but more siliciclastic (see classical Bouma-type turbidite in Fig. 3.10). The fine grain size and low specific density of bioclastic detritus would explain the lack of tractional sedimentary structures in the marlstone beds, which all were apparently deposited solely from suspension fallout. A dilute calciturbiditic suspension is expected to settle more slowly through the water column than a similar siliciclastic suspension (Stow *et al*., 1984; Calvet and Tucker, 1988).

The boundaries of the "wavy" marlstone beds (Fig. 3.28) show out-of-phase base/top undulations and commonly have one of the boundaries flat, which means that the undulations are probably storm-wave scours. The sporadic seafloor erosion by waves would appear to have preceded and/or interrupted the deposition of the hemipelagic calcareous ooze (marl). This interpretation is consistent with the occurrence of these beds in the upper part of the Akveren Formation, where a marked shallowing of the basin is recognizable, culminating in calcarenitic shoreface facies (see further discussion in section 4.4).

Deposits similar to the T*cd* beds of facies F7, with cross-laminated silty basal parts, have been described by Calvet and Tucker (1988) and attributed to dilute density currents that were generated by weak to moderate storms and emplaced below the mean storm-wave base in the outer zone of a carbonate ramp.

The fine-grained bioclastic calciturbidites described by Stow and Piper (1984) consist of micrite and show a systematic pattern of vertical divisions (Fig. 3.30). This pattern is comparable to the characteristics of siliciclastic muddy turbidites, with the following two exceptions: the silt laminae (Bouma division D) are less distinct and the transition to

hemipelagic mud is commonly much more gradual. The indistinct lamination is attributed to the poorer separation of silt- and clay-sized particles in the case of biogenic sediment, because of the lesser floc strength in carbonate suspension in comparison with a siliciclastic one (Stow and Piper, 1984). Lamination can also be obliterated by bioturbation and the more pronounced diagenetic changes in calcareous sediment (Stow *et al*., 1984).

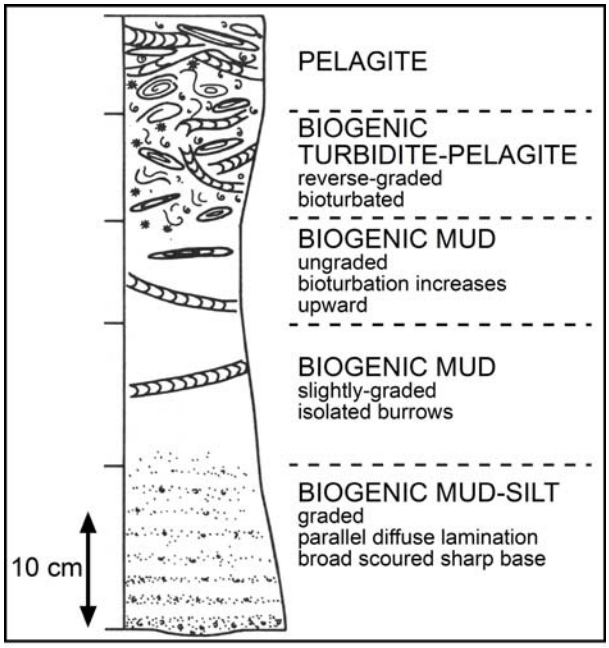

Figure 3.30. A model for fined-grained bioclastic turbidites. Modified from Stow and Piper (1984).

3.9. Facies F8: calcareous mudstones

Calcareous mudstones occur as interbeds in the entire stratigraphic succession, and virtually predominate in the Atbaşı Formation (see logs in Appendix 1). On the basis of their colour, the calcareous mudstones have been divided into two subfacies: grey to greenish-grey mudstones and variegated mudstones. They are described separately below and subsequently interpreted jointly as one facies.

Subfacies F8a: grey to greenish-grey calcareous mudstones – These mudstones form interbeds in the whole profile of the Akveren and Gürsökü formations (see Logs 1 to 17 in Appendix 1). Bed thicknesses vary from 0.5 to 44 cm, and the rock colour is occasionally

whitish grey, dark grey or blackish grey (Fig. 3.31). An upward change of colour from pale greenish grey to dark grey typifies the transitions from marlstone to calcareous mudstone (see previous section), common in the Gürsökü Formation and in the lower-middle part of Akveren Formation. The mudstones are fissile, which may or may not reflect primary lamination. Delicate parallel lamination is rarely recognizable, by the presence of silty streaks or laminea rich in plant detritus, and the mudstones seems to be strongly bioturbated. Vertical and horizontal burrows in the form of silt- or sand-filled tubes, up to 1 cm in diameter, are common.

Figure 3.31. Calcareous mudstones of subfacies F8a in the upper part of the Akveren Formation (detail from Log 16 in Appendix 1). Note the gradual colour changes from grey to blackish grey. The hammer is 30 cm.

Subfacies F8b: variegated calcareous mudstones – This subfacies of massive mudstones (Fig. 3.32) constitutes the bulk of the Atbaşı Formation, where it is interspersed with thin and relatively rare interbeds of facies F2b and F5b (see Logs 19 and 20 in Appendix 1). The rock colour varies from greenish grey and olive green to reddish brown and purple red, in alternating bands that are mainly 0.5 -30 cm thick, but occasionally up to

95 cm. Many bands are grey and some thin ones are blackish grey. The colouration bands have uneven and commonly transitional boundaries, but are generally parallel to bedding. The mudstone is locally mottled due to the occurrence of burrows, with mainly mud-filled horizontal and vertical tubes up to 2 cm in diameter, including *Ophiomorpha annulata* (Fig. 3.32). A sample from Log 19 shows a calcareous mud with less than 50 vol.% of bioclastic sediment, mainly fragments of algae and foram tests. The benthic and planktonic forams indicate a deep-water, subneritic environment (E. Sirel, personal comm. 2002).

Figure 3.32. Mottled reddish-brown mudstone of subfacies F8b in the lower part of Atbaşı Formation. Note the vertical trace of Ophiomorpha annulata. The measuring stick is 20 cm.

Interpretation – The calcareous mudstones are interpreted to be hemipelagic deposits representing the basinal "background" sedimentation of turbiditic mud, probably interlayered with storm-derived mud. Hemipelagic sedimentation occurs by the fallout of

very fine-grained suspension, with the grains settling through the water column as solitary particles or aggregates (Boggs, 1995). The calcareous bioclastic component implies a mixture of pelagic particles (planktonic algae, planktonic and benthic forams) and terrigeneous clay derived from the basin margins (James, 1997). Although the hemipelagic muddy suspension in the present case is considered to have been supplied chiefly by storms and turbidity currents, it is possibly that some other minor factors were involved (Fig. 3.33; Stow, 1985). The colour banding may reflect incursions of turbiditic mud, and hence an intercalation of the Bouma divisions E_t and E_h (Fig. 3.10). The reddish brown and purple red mudstones indicate a sediment-starved environment and seafloor oxidation, whereas the grey and greenish mudstones imply suboxic to anoxic conditions (Stow *et al*., 1996; Tucker, 2001).

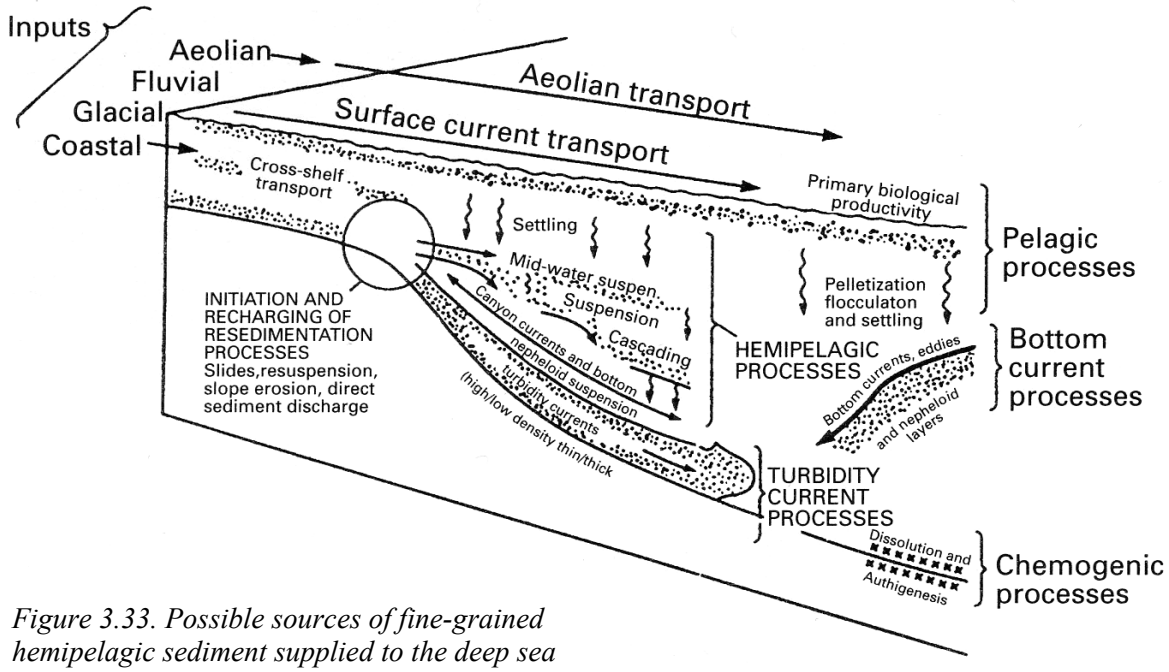

Figure 3.33. Possible sources of fine-grained hemipelagic sediment supplied to the deep sea (from Stow, 1985).

The differences in the colour of seafloor mud may be due to changes in sediment geochemistry, oxidation state of the bottom waters, amount of organic matter and pyrite content (Pickering *et al.*, 1986; Tucker, 2001). A high content of organic carbon or pyrite gives dark grey to black colouration, which thus reflect deposition below the storm wave base in a setting with high preservation of organic matter, such as conditions of poorly

oxygenated bottom water, or in a setting with high organic-matter supply (Stow *et al*., 1996). The reddish colours of deep-water mud are usually a result of finely disseminated hematitic (Fe_2O_3) pigment, which forms coatings and intergrowths on clay particles (Tucker, 2001). The red colour reflects early diagenesis of sediment in an oxidizing and sand-starved marine environment, where the hematitic pigment originates through an aging (dehydration) process of hydrated iron-oxide precursors, formed by the intrastratal weathering of iron-bearing minerals (such as biotite, certain clay minerals, pyrite, amphibole, hornblende and others). A spectrum of colours from pale reddish brown to purple red may reflect the variable amount of hematite pigment (Tucker, 2001).

The green colour of deep-water mud is typically due to ferrous (Fe^{+2}) iron, with no hematite or organic matter present. This colour may be the original early-diagenetic characteristic of sediment deposited in suboxic to anoxic conditions, or may form by a diagenetic alteration of original red colours, through the reduction of hematite ($Fe^{+3} \rightarrow Fe^{+2}$) by migrating groundwater (Tucker, 2001). A mottled colouration is usually due to bioturbational mottling, which means mixing of sediment by burrowing animals (Walker, 1992), or also may reflect localized iron reduction due to the presence of scattered organic particles (Tucker, 2001).

CHAPTER 4:

FACIES ASSOCIATIONS

4.1. The distinction of facies associations

A facies association is considered to be a genetically coherent assemblage of spatially related sedimentary facies (Boggs, 1995), which should ideally represent a particular sedimentary environment – or a particular set of physical, chemical and biological conditions (Reading and Levell, 1996). In the present case, facies associations have been distinguished on the basis of the stratigraphical grouping of sedimentary facies, with supplementary information on their ichnofauna and microfauna characteristics. Four main facies associations have been distinguished in the analyzed stratigraphic succession of Gürsökü, Akveren and Atbaşı formations (Table 4.1). Their spatial relationships are shown in Figure 4.1, and the relative contribution of the individual facies to each association is summarized in Table 4.2, while Table 4.3 gives an overview of the sedimentary facies that have been distinguished in this study (see chapter 3).

The distinction of sedimentary facies associations has been combined with the recognition of their ichnofacies, which means trace fossil assemblages that may be diagnostic of particular marine environments or bathymetric/salinity conditions (Crimes and Harper, 1970; Howard *et al*., 1971; Frey, 1975; Pemberton *et al*., 1992). For this purpose, the trace fossils identified in the outcrop sections have been compared with the principal associations of marine trace fossils that have been widely recognized and defined in the literature (Fig. 4.2).

In the present chapter, the four associations of sedimentary facies (Table 4.1) are described and interpreted to provide the sedimentological basis for a palaeoenvironmental and palaeogeographical interpretation of the studied basin-fill succession.

Table 4.1. Facies associations, their component sedimentary facies and stratigraphic occurrence.

Facies associations		***Subassociations***		***Component facies***	***Outcrop log***	***Formation***
FA 1	Predominantly siliciclastic turbidites	FA 1a	Sheet-like turbidites with mud/marl cappings	F2a, F5a, minor F7, F8a	1a, lowest 1b, 2, 3, 4	Gürsökü Fm.
		FA 1b	Isolated turbiditic palaeochannel	F2a, F5a, minor F7 and F8a	Middle to upper 1b	Lower part of Gürsökü Fm.
FA 2	Calcareous turbidites	FA 2a	Packages of sand-dominated turbidites with chutes	F1b, F4, F6a, F7	11, 12, 13, lower-middle 14	Middle part of Akveren Fm.
		FA 2b	Packages of hemipelagites with thin sandy turbidites	F4, F6a, F7, F8a	11, 12, 13, lower-middle 14	Middle part of Akveren Fm.
		FA 2c	Basin-plain assemblage of alternating sheet-like turbidites and hemipelagites	F2b, F5b, F7, F8a	5 to 10	Lower-middle part of Akveren Fm.
FA 3	Carbonate ramp deposits	FA 3a	Shallow-marine reefal complex	F6b	Uppermost 14	Upper part of Akveren Fm.
		FA 3b	Storm-influenced offshore transition to wave-dominated shoreface deposits	F1a, F3, F7, F8a, and minor F2b, F5b and F8b	15, 16, 17	Upper part of Akveren Fm.
FA 4	Carbonate ramp-drowning deposits	FA 4a	Hemipelagites with tempestites/turbidites and massive limestones	F3/F4, F6a, F7, F8a, minor F8b	18	Lower part of Atbaşı Fm.
		FA 4b	Hemipelagites with tempestites	F3, F7, F8b	19	Lower part of Atbaşı Fm.
		FA 4c	Hemipelagites with thin turbidites	F2b, F5b and F8b	20	Atbaşı Fm..

Table 4.2. Relative volume (thickness per cent) of sedimentary facies in their associations.

Facies		***Facies associations and subassociations***								
		FA 1	***FA 2a***	***FA 2b***	***FA 2c***	***FA 3a***	***FA 3b***	***FA 4a***	***FA 4b***	***FA 4c***
F1	**a**	0	0	0	0	0	0.25	0	0	0
	b	0	0.75	0	0	0	0	0	0	0
F2	**a**	36.5	0	0	0	0	0	0	0	0
	b	0	0	0	23	0	2	0	0	1.5
F3		0	0	0	0	0	39	0	38	0
F4		0	64.5	7.5	0	0	0	17	0	0
F5	**a**	18	0	0	0	0	0	0	0	0
	b	0	0	0	11	0	2	0	0	17.5
F6	**a**	0	1.25	1.5	0	0	0	51	0	0
	b	0	0	0	0	100	0	0	0	0
F7		31	30.25	67.5	41	0	27	11	13	18
F8	**a**	14.5	3.25	23.5	25	0	29.5	18	0	0
	b	0	0	0	0	0	0.25	3	49	63

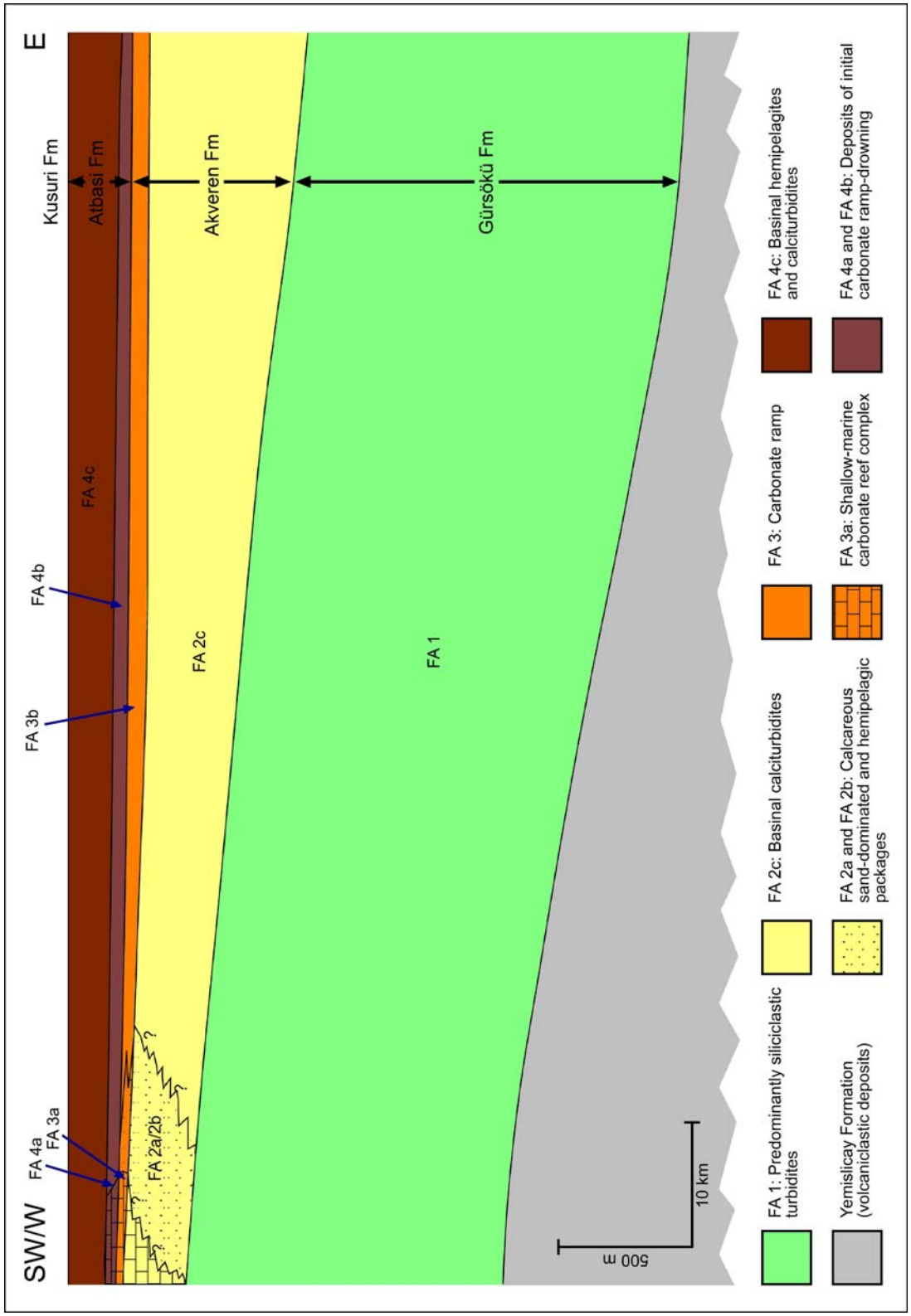

Figure 4.1. Basinal profile showing the interpreted spatial distribution of sedimentary facies associations distinguished in this study. The schematic cross-section is roughly parallel to the basin axis. Note the exaggerated vertical scale.

Table 4.3. Summary of the sedimentary facies distinguished in this study.

Facies		***Subfacies***		***Bed geometry and thickness***	***Texture and structures***	***Interpretation***
F1	Calcrudites of granule to pebble grade	F1a	Clast-supported, pebble calcrudite	Lenticular, <25 cm thick and <340 cm in lateral extent	Crudely normal grading, moderate sorting, subrounded to well rounded clasts of limestone and marl, sandy matrix	Non-tractional deposits of a bypassing turbidity current or strong rip current
		F1b	Clast- to matrix-supported, bioclastic granule calcrudites	Uneven beds <14 cm, thick, laterally discontinuous, <100m in extent	Massive, non-graded, poorly to moderately sorted, >80 vol.% bioclastic detritus, sandy matrix	
F2	Thick- to medium-bedded siliciclastic sandstones and calcarenites with planar parallel stratification and/or current-ripple cross-lamination	F2a	Very coarse- to very fine-grained siliciclastic sandstones	Tabular beds < 200 cm thick, some pinching out laterally	Normal grading, turbidites T*bc* (>88%) and T*abc* (<12%)	Low-density and subordinate high-density turbidity currents; the difference in composition reflects gradual change in the sediment source
		F2b	Fine- grained to silty calcarenites	Tabular beds <78 cm thick	Normal grading, calciturbidites T*bc* (<99%), minor T*abc,* common silica concretions	
F3	Stratified calcarenites with wave-formed and combined-flow structures			Tabular to wedge-shaped beds <81 cm thick, isolated to amalgamated	Very coarse- to very fine-grained, various types of wave-ripple cross-lamination, planar and hummocky/swaley stratification	Deposits of storm-generated combined-flow currents in offshore transition to shoreface zone (sublittoral to littoral)
F4	Massive calcarenites			Tabular beds <44 cm thick, with uneven boundaries, some amalgamated	Very coarse- to very fine-grained with scattered pebbles; mainly massive, with multiple internal scours, weak parallel stratification and cross-laminated tops	Composite calciturbidites T*abab…abc* and turbidites T*ab* deposited by pulsating high-density currents
F5	Thin-bedded siliciclastic sandstones and calcarenites with mainly current-ripple cross-lamination	F5a	Very coarse- to very fine-grained or silty siliciclastic sandstones	Tabular to uneven beds <10 cm thick	Normal grading; turbidites T*c(d)* and T*d*	Deposits of low-density turbidity currents; the difference in composition reflects gradual change in the sediment source
		F5b	Very fine-grained to silty calcarenites	Tabular to uneven beds <10 cm thick	Normal grading; calciturbidites T*c(d)* and T*d*, silica concretions	
F6	Massive bioclastic limestones	F6a	Bedded limestones	Uneven beds <50 cm thick, mainly amalgamated, commonly lenticular	Medium-grained grainstone, internally massive, bioclasts: red coralline algae, bryozoans, bivalves, forams, brachiopods and echinoderms	Shallow-inclined reef-complex (F6b) and fore-reef deposits (F6a)
		F6b	Non-bedded limestone	One thick unit (10-15 m), several kilometres in lateral extent		
F7	Marlstones			Mainly tabular <129 cm thick, occasionally with gently undulating bases and/or tops	Massive; occasionally with cross-laminated and/or weakly parallel laminated silty basal parts	Hemipelagic cappings (E-division) of turbidites and tempestites, and deposits of highly dilute turbidity and storm currents (T*de* and T*(c)de*)
F8	Calcareous mudstones	F8a	Grey to greenish-grey mudstones	Beds <44 cm thick	Massive, bioturbated; mainly grey to greenish, but also blackish or whitish grey	Hemipelagic "background" deposits, F8b indicates sediment-starved and oxidizing seafloor conditions
		F8b	Variegated mudstones	A whole formation unit, with variable colour bands <95 cm thick	Massive, bioturbated; olive green to brownish or purple red	

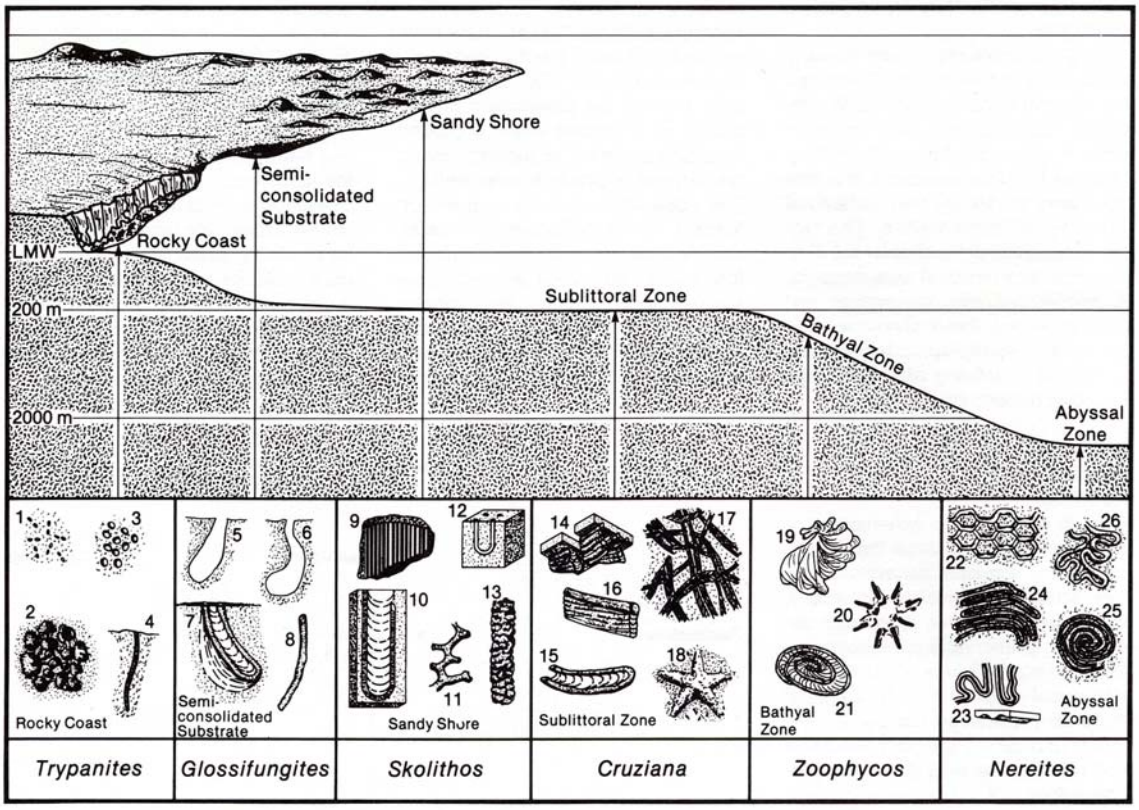

Figure 4.2. Marine ichnofacies placed in a representative environmental setting. Typical ichnofossils include: 1) Caulostrepsis, 2) Entobia, 3) echnoid borings, 4) Trypanites, 5,6) Gastrochaenolites, 7) Diplocraterion, 8) Psilonichnus, 9) Skolithos, 10) Diplocraterion, 11) Thalassinoides, 12) Arenicolites, 13) Ophiomorpha, 14) Phycodes, 15) Rhizocorallium, 16) Teichichnus, 17) Crossopodia, 18) Asteriacites, 19) Zoophycus, 20) Loernzinia, 21) Zoophycus, 22) Paleodictyon, 23) Tapherhelminthopsis, 24) Helmenthoida, 25) Spirorhaphe, 26) Cosmorhaphe. From Pemberton et al. (1992).

4.2. Facies association FA 1: predominantly siliciclastic turbidites

This facies association consists of the siliciclastic turbidites of facies F2a and F5a, capped by calcareous mudstones (F8a) and marlstones (F7) (Table 4.3), and constitutes the Gürsökü Formation (Table 4.4). It overlies gradationally the assemblage of volcanic rocks, volcaniclastic turbidites, marlstone and mudstones of the Yemisliçay Formation (Fig. 4.1), and also passes gradationally upwards into the calcarenitic turbidite assemblage of the lower-middle Akveren Formation (facies association FA 2). Where logged in the central and eastern parts of the study area, facies association FA 1 is nearly 1200 m thick, but is probably thinning towards the W and SW.

Table 4.4. Characteristics of facies association FA 1 in the logs of Gürsökü Formation. The logs are numbered in their stratigraphical order. The per cent values are thickness percentages.

LOG:	***1a***	***1b***	***2***	***3***	***4***
Part of Gürsökü Fm.:	lower part	lower part	middle part	upper part	upper part
Palaeocurrents:	sector N–E	sector NE–NW	mainly E	mainly E	mainly E
Biozone age:	Late Senonian	Late Senonian	Late Campanian	no fossils	no fossils
Facies subassociation:	FA 1a	mainly FA 1b	FA 1a	FA 1a	FA 1a
Facies F2a	57%	77%	14%	18%	16%
Facies F5a	10%	8.5%	31%	19%	22%
Facies F7	24%	6%	39%	42%	44%
Facies F8a	8%	8%	16%	21%	19%
Turbidite division A	12%	6%	1%	1%	0%
Turbidite division B	36%	64%	8%	5%	6%
Turbidite division C	19%	15%	35%	30%	31%
Turbidite division D*	25%	7%	40%	43%	44%
Divisions E_t + E_h	8%	8%	16%	21%	19%
Ichnofacies	Typical deep-marine *Nereites* ichnofacies (see Table 4.5)				

*****Including marlstones (facies F7).

Microfauna samples from Logs 1a and 1b indicate a Late Senonian age of the deposits, whereas samples from Log 2 indicate a Late Campanian age (E. Sirel, personal comm., 2002). The ichnofauna content of facies association FA 1 (Table 4.5) indicates a deep-marine *Nereites* ichnofacies (A. Uchman, personal comm., 2002). On the basis of its varied depositional architecture, the siliciclastic turbidite assemblage has been divided into two subassociations (Table 4.1): (a) sheet-like turbidites with mudstone/marlstone cappings and (b) amalgamated turbidites of an isolated submarine palaeochannel.

Ichnotaxa
Chondrites targionii
Chondrites intricatus
Ophiomorpha rudis
Trichichnus isp.
Arthrophycus tenius
Thalassionoides isp.
Nereites isp.
Ubina isp.
Paleodictyon majus

Table 4.5. Trace fossils identified in the outcrops of facies association FA 1, Gürsökü Formation (A. Uchman, personal comm., 2002).

Subassociation FA 1a – This facies subassociation comprises sheet-like siliciclastic turbidites of subfacies F2a and F5a capped with calcareous mudstones (subfacies F8a) and/or marlstones (facies F7) (Table 4.3, Figs. 4.3 and 4.4). The evidence from Logs 1a and 2-4 (Table 4.4) indicates that the turbidites are pinching out laterally more commonly in the lower part of the succession; and that they show a gradual upward increase in the content of calcareous grains and a decrease in the abundance of subfacies F2a and Bouma divisions A and B. This overall fining-upward trend is not accompanied by any obvious upward thinning or thickening of turbidites in the outcrops of facies subassociation FA 1a (see Logs 1a and 2-4 in Appendix 1). Measurements of palaeocurrents furthermore indicate a non-systematic upward change of palaeocurrent directions from northward to eastward upwards in this subassociations (Table 4.4), but a palaeocurrent trend towards east dominates in the turbidites of FA 1a (Fig. 4.5).

Figure 4.3. Deposits of facies subassociation FA 1a in the middle part of Gürsökü Formation in the central part of the basin (portion of succession in Log 2, Appendix 1). Note the alternation of sheet-like sandstones (subfacies F2a and F5a), mudstones (F8a) and marlstones (F7). The stratigraphical way up is upwards to the top right.

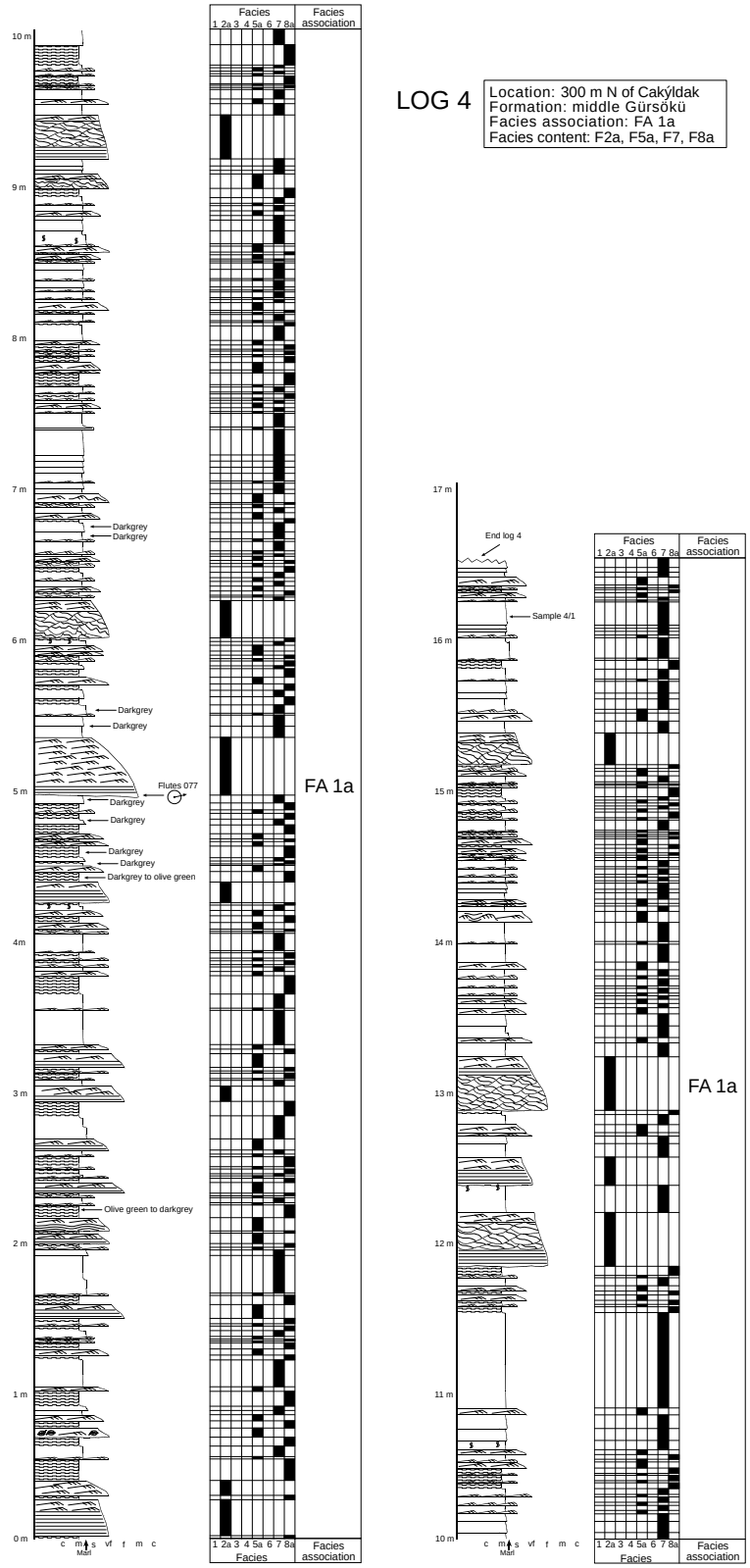

Figure 4.4 Log-example of FA 1a with facies distribution (Log 4; see also Appendix 1). From the upper Gürsökü Formation in the central part of the basin.

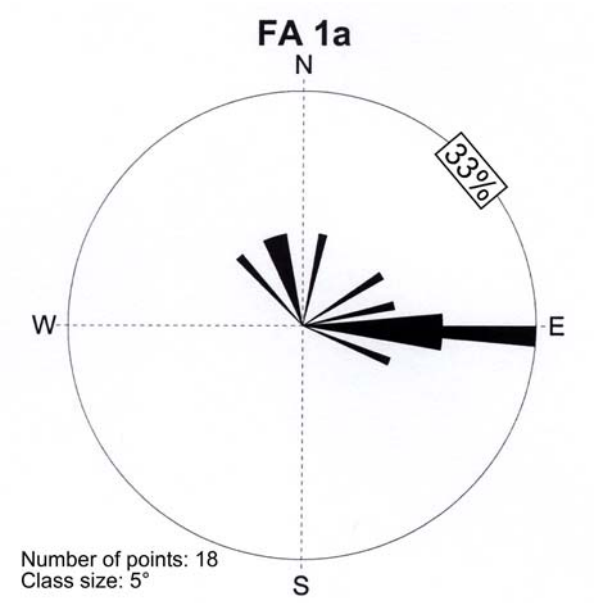

Figure 4.5. Rose diagram summarizing the palaeocurrent directional data from turbidite deposits of facies subassociation FA 1a.

Subassociation FA 1b – This facies assemblage comprises amalgamated siliciclastic turbidites that constitute the infill of an isolated submarine palaeochannel in the lower part of the Gürsökü Formation (see Log 1b; Appendix 1) in the central part of the basin (Figs. 4.6 and 4.7). The turbidites here are not only amalgamated, but also thicker-bedded, with thick Bouma divisions A and B and with highly uneven erosional boundaries. The palaeochannel is 22 m thick and its base is an erosional surface with local-scale relief of 135 cm (Fig. 4.7). The thick to medium turbidites of subfacies F2a predominate, with subordinate thin turbidites of subfacies F5a and minor interbeds of calcareous mudstone (subfacies F8a) and marlstone (facies F7), which dominate at the top part of the succession (Table 4.3 and Fig. 4.7). Packages of gently inclined beds, broadly sigmoidal in shape and separated by scours, form epsilon cross-bedding indicative of lateral accretion (Fig 4.6A). Two successive packages are dipping in opposite directions (NW and SE) and are separated by a zone of multiple scours, which implies vertically stacked lateral bars that were accreted to the channel's opposite banks. The uneven and amalgamated beds bear few palaeocurrent indices, but the directions of trough-shaped scour marks vary between NE and SE, which is consistent with the epsilon cross-bedding and indicates a north-eastward trend of the palaeochannel. The channel-fill turbidites are thinning and fining upwards, and also less amalgamated in the upper part (Fig. 4.7).

Interpretation of FA 1 (FA 1a and FA 1b) – The turbiditic subassociation FA 1a is interpreted to be deposits of unconfined turbidity currents of high to low density, derived from a siliciclastic source with an increasing contribution of calcareous sediment. The turbidity currents were apparently unconfined, but not basin-wide, as is indicated by the lateral pinch-out of many beds in central area of the basin. The succession of sheet-like, non-amalgamated turbidites indicates a basin-plain turbiditic system (Pickering and Hiscott, 1985), comparable to the type I setting of Mutti (1992) and the basin-floor system of the lower Ross Formation in western Ireland (Lien *et al*., 2003).

The turbiditic subassociation FA 1b in the lower part of the Gürsökü Formation is the infill of an isolated submarine channel, 22 m deep (Fig. 4.6B). The channel width exceeds the outcrop limits, but is estimated to be ca. 220 m, based on the mean depth/width ratio of 1/10 calculated for modern and ancient turbiditic channels (Kneller, 2002). The channel-fill architecture indicates an east-trending sinuous channel with point bars (Fig. 4.6B). The alternating thin sandstones (subfacies F5a) within calcareous mudstones cappings (subfacies F8a) at the top of the channel-fill succession represent the abandonment phase of the channel (Fig. 4.7). The channel was abandoned as a result of decreasing flow magnitude (Peakall *et al.,* 2000) or avulsion, although no other palaeochannels have been found in the Gürsökü Formation to support this latter notion.

The lower turbidite package, with erosional surfaces inclined towards the NW and the turbidites thickening in the same direction, is interpreted to be a left-bank point bar. The opposite, mirror-image architecture of the SE-inclined upper package indicates a right-bank point bar superimposed laterally onto the left-bank one (Fig. 4.6). The point bars are thought to be a result of the turbidity currents eroding the cut-bank side of the sinuous channel and depositing sediment against the opposite bank (e.g., Lien *et al.*, 2003). The transition between the left-bank and right-bank point bars in the present case is marked by a zone of irregular multiple scours and gravel-bearing, amalgamated turbidites ascribed to the channel thalweg zone. The stacking of the right-bank bar onto the left-bank bar is attributed to their downflow translation (Figs. 4.6B and 4.8), which means a progressive transformation of channel plan-form involving a lateral "swing" component and a downstream "sweep" component (*sensu* Peakall *et al.*, 2000). The channel-bend translation

Figure 4.6. (A) The exposure of FA 1b, of the lower Gürsökü Formation in the central part of the basin, shown in log 1b (Fig. 4.7). Channel axis is towards NE (obliquly towards the viewer). Note that layers in leftbank and rightbank point bar are thickening towards NW and SE, respectively. (B) Interpretive sketch of the channel-fill succession with the line of log 1b (Fig. 4.7) and diagrams explaining point-bar translation.

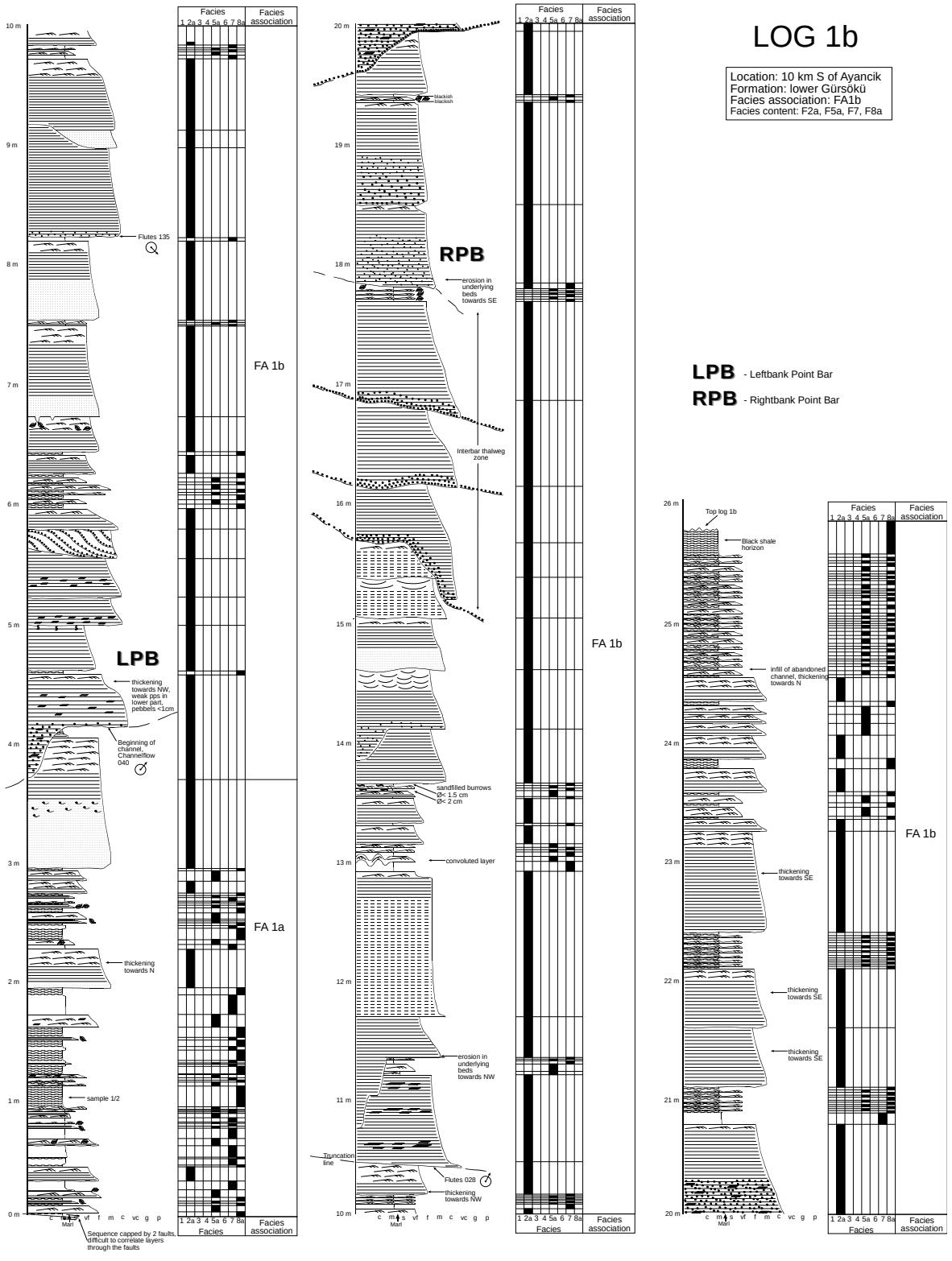

Figure 4.7. Log 1b with contribution of facies, shown as an example of FA 1b and interpreted as a submarine channel-infill. From lower Gürsökü Formation in the central part of the basin.

occurred concurrently with the channel aggradation, whereby the left-bank bar was not only stacked against the right-bank bar, but progressively covered the former, as a second storey, while the rising thalweg zone had gradually shifted from one side of the channel to the other. The channel-fill architecture seems to be comparable to the three-stage model of Peakall *et al.* (2000), involving lateral accretion, aggradation and abandonment.

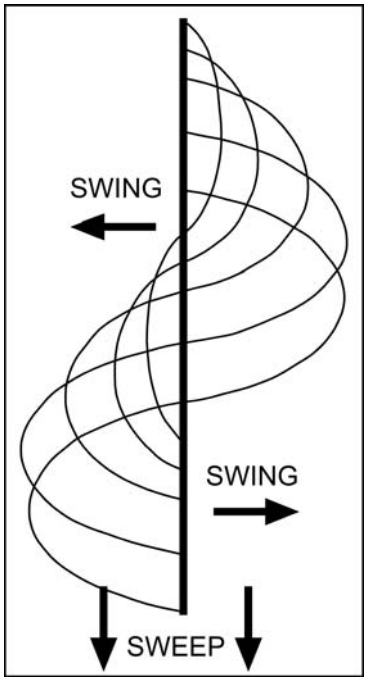

Figure 4.8. Schematical model for the development of a sinuous channel accompanied by channel-bend translation. The progressive change of the channel plan-form involves lateral "swing" and downstream "sweep" components. Slightly modified from Peakall et al. (2000).

Facies association FA 1 as whole is thought represent the medial to distal part of a turbiditic system that was sourced from the basin margin (Fig. 4.9), with an increasing contribution of contemporaneous bioclastic sediment. The turbiditic system is considered to have been a linear-source or multiple-source siliciclastic ramp (*sensu* Reading and Richards, 1994), with the source area hosting an incipient, expanding reefal platform. The depositional system was subject to aggradation and retreat (back-stepping), as is indicated by the upward fining trend and decline in high-density turbidity currents. The sediment was supplied from the western part of the basin and probably also from its southern margin, as the turbiditic system of the Gürsökü Formation replaced the volcaniclastic one of the Yemisliçay Formation, sourced mainly from the northern margin. The northern source seems to have been deactivated by a tectonic collapse and submergence of the margin.

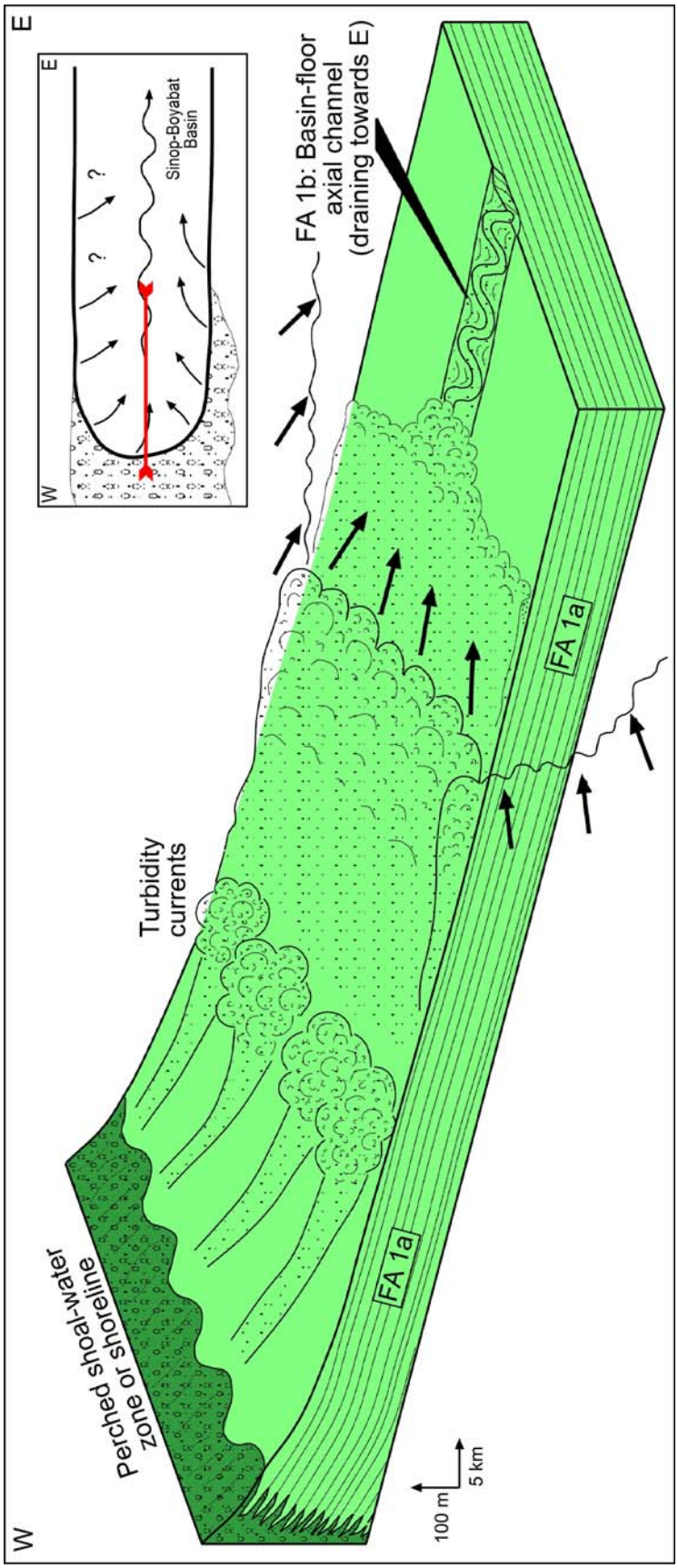

Figure 4.9. Schematic depositional model for facies association FA 1 (Gürsökü Formation) with inlet showing map view of the basin (red line indicates approximate location of the sketch): the siliciclastic sediment of volcanic provenance was supplied from the basin's western and south-western margins; the majority of turbidity currents descending the basin-margin slopes were unconfined, flowing northwards across the basin and/or eastwards along the basin axis; an axial channel was formed episodically, when a large number of currents merged into a sustained, powerful axial flow.

The significance of the solitary sinuous palaeochannel at the base of the Gürsökü Formation is unclear. The turbiditic system may have had one or more perennial channels in its proximal part, and the shifting channel may have occasionally extended to the medial reaches; or – alternatively – the system may have had a non-perennial channel forming episodically along the basin axis during the maxima of turbidity current activity. The turbiditic system might resemble that in the present-day Labrador Sea (Hesse, 1989; Hesse and Rakofsky, 1992), where a linear source composed of an array of slope ravines and small canyons is generating a large number of currents that merge along the basin axis to form a large sinuous channel. Chan and Dott (1983) inferred a similar depositional setting for the Eocene turbidites in the Tyee Basin, western Oregon. The elongate forearc trough had a linear source in the form a narrow shelf, with sediment derived from volcanic rocks. Although Chan and Dott (1983) considered the depositional system to include slope, submarine fan and basin-plain deposits, Reading and Richards (1994) re-classified it as a multiple-sourced, sand-rich siliciclastic ramp.

Similar conditions are envisaged for the depositional setting of the Gürsökü Formation (Fig. 4.9), prior to the development of the carbonate ramp system of the Akveren Formation. The majority of turbidity currents descending from the basin-margin slopes were unconfined, flowing north-eastwards to south-west from the basin western margins and spreading eastwards along the basin axis (Fig. 4.5). An axial channel was probably formed episodically, when a large number of turbidity currents descended simultaneously the basin-margin slopes and merged into a sustained, powerful flow along the basin axis. Arguably, only a sustained (long-duration) turbidity current is capable of forming a sinuous channel, although the channel may further evolve and be filled by common surge-type currents.

4.3. Facies association FA 2: calcareous turbidites

This facies association overlies gradationally the siliciclastic turbidites of facies association FA 1 (Fig. 4.1; Gürsökü Fm.) and constitutes the lower to middle part of the Akveren Formation (Logs 5 to 14 in Appendix 1). Its transitional lower part has been studied in selected outcrops in different parts of the entire study area. Based on micropalaeontological data, its outcrops in the Kuğuköy area in the western part of the basin (Logs 11-14) are considered to represent the upper-middle part of the Akveren Formation. This facies association has a wedge-shaped geometry, as it is thickest (up to 550 m) in the eastern part of the basin and thins towards the west, where is slightly thicker than 100 m (Fig. 4.1). The calcareous deposits of facies association FA 2 have been divided into three facies subassociations (Table 4.2): (a) packages of sand-dominated turbidites with chutes; (b) packages of hemipelagites with thin sandy turbidites; and (c) basin-plain assemblage of alternating sheet-like turbidites and hemipelagites. The first two assemblages alternate with each other in the stratigraphic succession and hence are discussed jointly below.

Subassociations FA 2a and FA 2b – These assemblages occur in the western part of the basin (Fig. 4.1), where they have been logged in the Kuğuköy area (Logs 11-13 and the lower-middle part of Log 14 in Appendix 1). The sand-rich and mud-rich assemblages alternate with each other in the stratigraphic succession (Figs. 4.10 and 4.11), whose base is unexposed, but the total thickness is interpreted to be maximum 100 m. Assemblage FA 2a is dominated by massive calcarenites (facies F4, 65 vol.%) interbedded with massive limestones (subfacies F6a), marlstones (facies F7) and minor thin layers of calcrudite (subfacies F1b) (Fig. 4.12, Tables 4.2 and 4.3). Similar facies occur as interbeds in assemblage FA 2b (Table 4.2), which is dominated by marlstones (facies F7, 67.5 vol.%) and calcareous mudstones (subfacies F8a).

Some of the FA2a units show an internal downlapping pattern of bedding (Fig. 4.11), which suggests deposition on a sloping surface. At least one of the units shows an internal trough-shaped scour, broad and shallow, up to 1 m in relief (Fig. 3.18). Incised in a package of alternating calcarenites (F4) and marlstones (F7), the concave-upward scour is filled by similar facies with a lateral onlap on its relief.

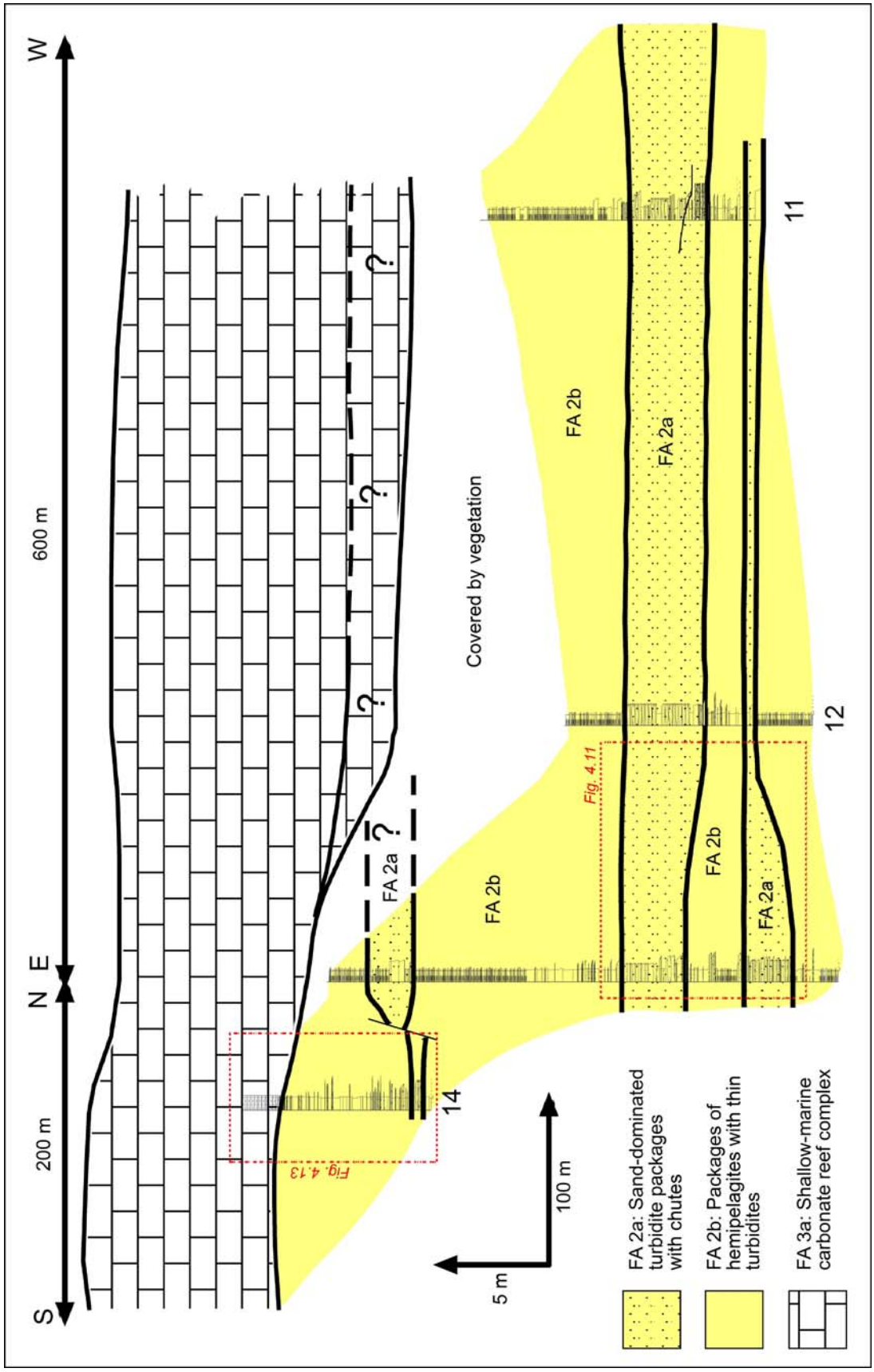

Figure 4.10. Correlation panel of Logs 11 to 14 in the middle-upper Akveren Formation, showing an alternation of facies associations FA 2a and FA 2b, with the limestone assemblage FA 3a at the top. From outcrop section in Kuğuköy area in the westernmost part of the basin.

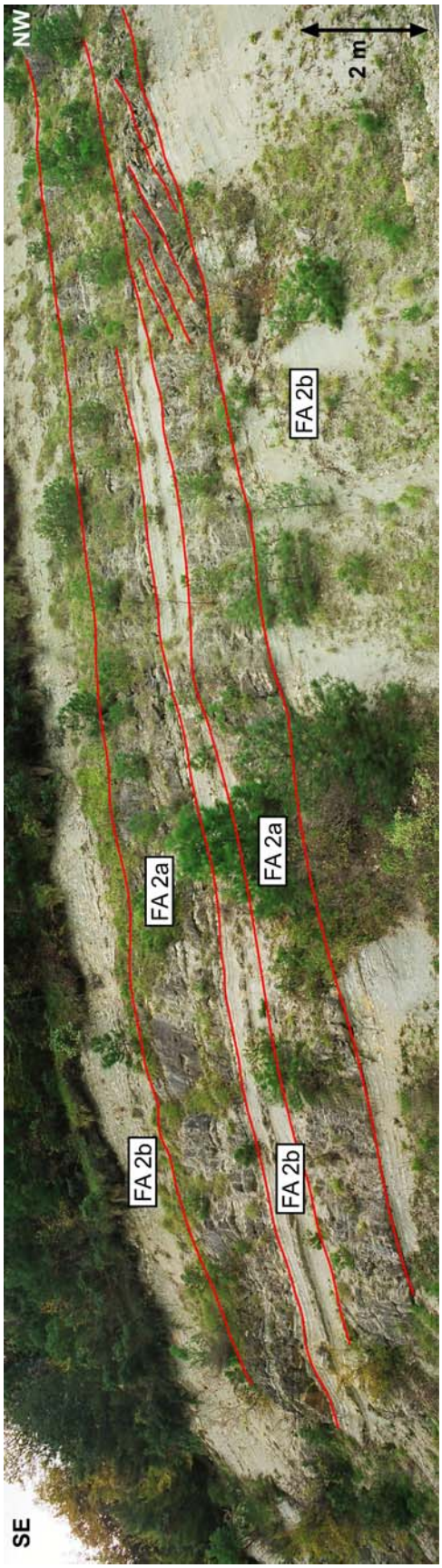

Figure 4.11. Exposure of the alternating packages of calcarenite-dominated packages FA 2a and marl-dominated packages FA 2b in the middle part of Akveren Formation in the western part of the study area. Note the downlapping geometry of bedding in FA 2a in the upper right corner of the photograph. See also the log correlation panel in Figure 4.10.

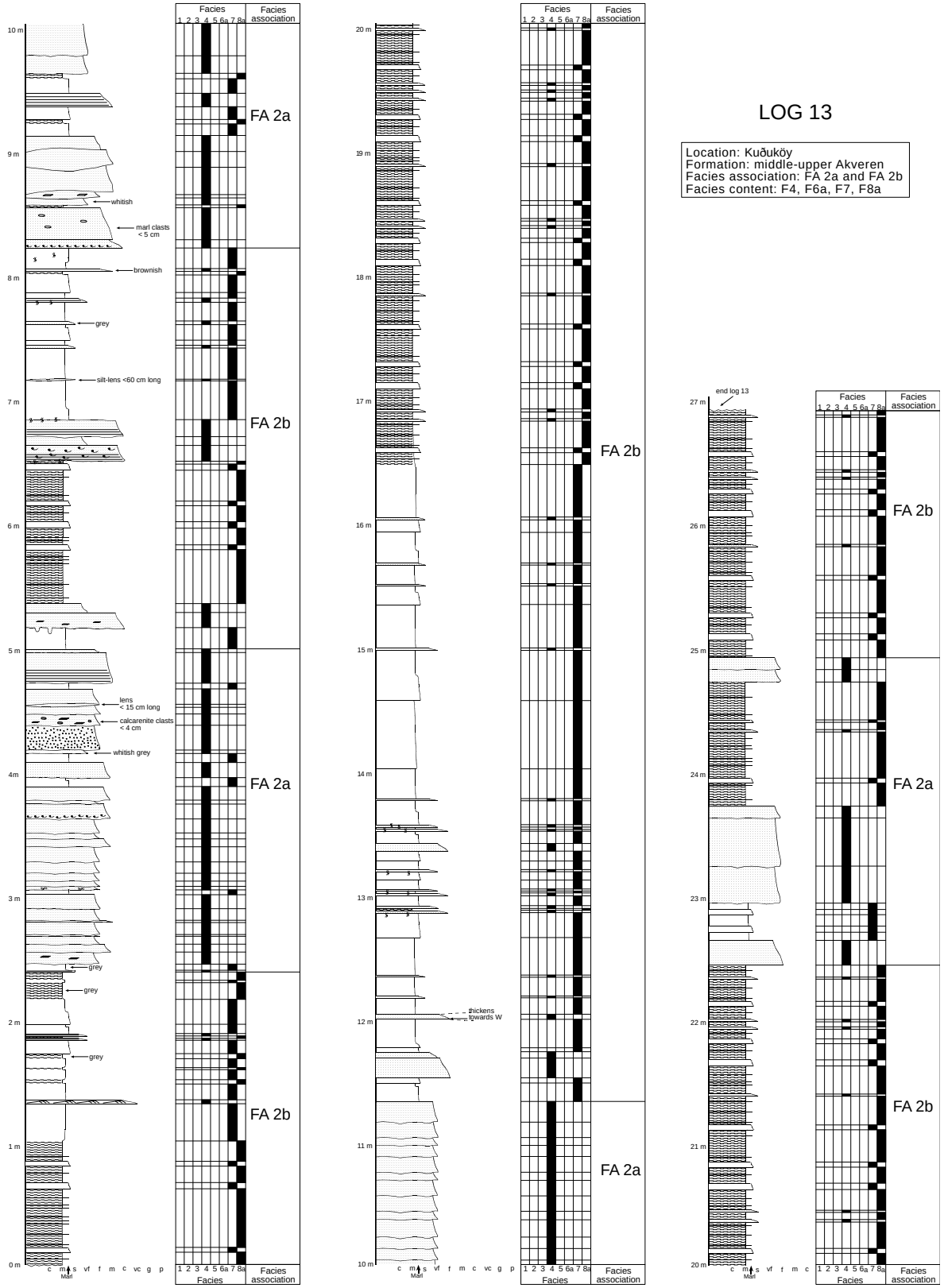

Figure 4.12. Log 13 from upper-middle Akveren Formation with associated facies distribution, showing alternating packages of FA 2a and FA 2b. From the Kuğuköy locality in the westernmost part of the basin.

Scour marks at the bases of some of the calcarenite beds in assemblages FA 2a and FA 2b indicate palaeocurrent directions towards the NNE and NE. Micropalaeontological data from the lowermost part of the outcrop (Figs. 4.10 and 4.11) indicate a Maastrichtian age and water depth of probably no more than 100 m (E. Sirel, personal comm., 2002). Few burrows have been recognized in the outcrop and hence ichnofacies is uncertain. In Logs 13 and 14, the uppermost package FA 2b shows a slight upward fining and is overlain conformably by the reefal assemblage FA 3a (Figs. 4.10 and 4.13).

Interpretation of FA 2a and FA 2b - The alternating packages FA 2a and FA 2b are thought to be low-angle clinothems of a sandy carbonate slope apron associated with the basin-margin reefal platform that prograded towards the NE/E (Fig. 4.10). Similar carbonate slope deposits have been described by Mullins and Cook (1986), Coniglio and Dix (1992) and Harris (1994) among others. The calcarenite-dominated packages FA 2a represent an increased basinward flux of sand and are attributed to normal (progradational) regressions, an interpretation supported by the local evidence of slope downlap. The marl-dominated packages FA 2b indicate an abrupt cessation of sand flux and are attributed to the basin margin inundation, probably caused by tectonics. The FA 2a-2b couplets can thus be regarded as parasequences reflecting the episodes of drowning and renewed gradual progradation of the basin-margin reefal platform

The basin-margin platform acted as a linear source, shedding sediment chiefly in response to storm backsurges and possibly earthquakes. The gently slope promoted non-channelized turbidity currents (cf. Mullins and Cook, 1986), and the storm events tended to generate pulsating, waning-waxing flows of relatively long duration (hours or days), as indicated by the characteristics of facies F4 (see earlier text). When abnormally enhanced by flow coalescence or a strong rip current, turbidity currents would occasionally bypass the slope by scouring it, rather than covering with sediment. The rare isolated palaeochannels, or slope chutes, are wide and shallow (Fig. 3.18), little more than 1 m in relief, and are filled with similar deposits as the scoured ones, which indicates bypassing erosional currents. Similar broad and shallow channels have been described from carbonate slope aprons by Mullins and Cook (1986).

The marl-rich packages FA 2b are probably pinching out towards the basin margin and

represent periods dominated by hemipelagic sedimentation. The decline in sand supply occurred after the relative sea-level rise made the breaker zone shift to the landward side of the carbonate platform, with only the infrequent strongest storms still capable of generating turbidity currents and spreading sand across the fore-reef slope. Shallow-water carbonate platforms are known to respond to a relative sea-level rise by rapid retrogradation, which is normally followed by the platform recovery and renewed progradation (Coniglio and Dix, 1992). In the present case, active tectonic extension may have episodically lowered the shallow-marine reefal platform, thus drowning the system and causing an episode of reduced sand supply. The neritic to subneritic carbonate slope, composed of facies associations FA 2a and FA 2b, acted as a transitional zone between the littoral reefal platform (facies subassociation FA 3a) of the basin margin and the bathyal basin-plain environment represented by facies subassociation FA 2c. Their stratigraphic relationship indicates an overall progradation and basinward expansion of the reefal platform (Fig. 4.13), accompanied by basin-floor aggradation and general shallowing (Fig. 4.1).

Facies subassociation FA 2c – This facies assemblage (Table 4.6 and Fig. 4.14), composed of the alternating calcarenite sheets (facies F2b and F5b) and calcareous hemipelagic deposits (facies F7 and F8a) (Table 4.3), constitutes the lower to middle part of the Akveren Formation in the central to eastern part of the basin (Fig. 4.15; see Logs 5 to 10 in Appendix 1). This is the thickest part (ca. 550 m) of the eastward-thicknening Akveren Formation. Facies subassociation FA 2c has transitional boundaries with the underlying siliciclastic assemblage FA 1 of the Gürsökü Formation and the overlying facies assemblage FA 3b (Fig. 4.1). The sedimentary succession is well-bedded, but the beds show no obvious upward thickening or thinning on an outcrop scale (see Logs 5-10 in Appendix 1 and Fig. 4.16). However, a comparison of the local logs indicates that the thickness percentage of marlstones (F7) increases upwards, whereas the thickness proportion of Bouma divisions B and C decreases (Table 4.6), which implies an overall upward fining of the thick assemblage FA 2c. Flute marks and ripple trough axes indicate palaeocurrent directions mainly towards the east (Fig. 4.17). Micropalaeontological data from Logs 7, 8 and 10 (Table 4.6) indicate a Late Maastrichtian age and warm-water, open marine conditions (E. Sirel, personal comm., 2002). Trace fossils (Table 4.7) indicate deep-marine *Nereites* ichnofacies (A. Uchman, personal comm., 2002).

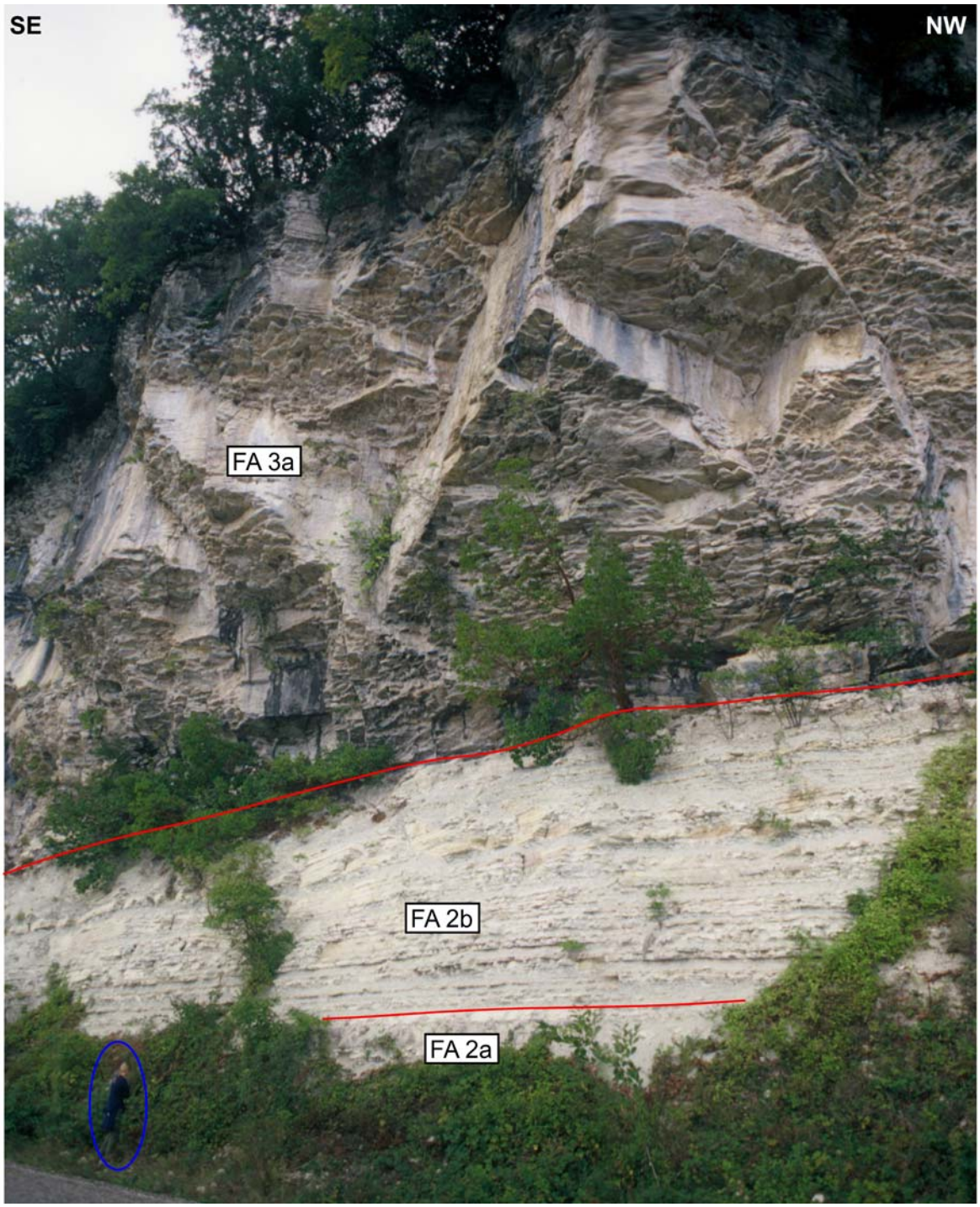

Figure 4.13. Facies assemblages FA 2a and FA 2b (upper-middle Akveren Formation) overlain conformably by the reefal assemblage FA 3a (upper Akveren Formation) in an outcrop in the Kuğuköy area in the western part of the basin. Note the retrogradational, fining-upward trend in facies assemblage FA 2b; see also in the log correlation panel from this area in Fig. 4.10. The standing person (encircled) for scale.

Table 4.6. Facies composition of the individual logs of facies association FA 2c in the lower to middle part of the Akveren Formation. The per cent values are thickness percentage.

LOG:	***5***	***6***	***7***	***8***	***9***	***10***
Part of Akveren Formation:	lower part	middle part	middle part	middle part	middle part	lower to middle part
Palaeocurrent directions:	E	E	NNE – E	E	E	NE
Biozone (age):	Late Campanian	No fossils	Late Maastrichtian	Late Maastrichtian	No fossils	Late Maastrichtian
Bathymetry:	uncertain		subneritic	subneritic		subneritic
Subfacies F2b:	17%	42%	18%	20%	29%	10%
Subfacies F5b:	19%	8.5%	13%	10%	10%	8%
Facies 7:	45%	23%	31%	43%	49%	53%
Subfacies F8a:	19%	27%	38%	27%	11%	29%
Division A:	0%	0%	1%	0%	0%	0%
Division B:	10%	19%	13%	7%	14%	5%
Division C:	25%	29%	17%	21%	24%	11%
Division D*:	46%	25%	31%	45%	51%	55%
Division E_t + E_h:	19%	27%	38%	27%	11%	29%
Ichnofacies:	Typical deep-marine *Nereites* ichnofacies (see Table 4.7)					

*****Bouma D including marlstones of facies F7.

Ichnotaxa	**Logs 6 and 7**	**Log 10**
Planarolites isp		x
Trichichnus isp.		x
Chondrites intricatus	x	x
Chondrites targionii	x	x
Thalassinoides isp.	x	x
Ophiomorpha annulata		x
Halimedites annulata		x
Zoophycos isp.	x	x
Phycosiphon incertum		x
Phymatoderma isp.		x
Scolicia strozzii	x	x
Cosmorhaphe isp.		x
Megagrapton irregulare	x	
Paleodictyon minimum		x

Table 4.7. Trace fossils recognized in the outcrops of facies subassociation FA 2c (lower to middle part of Akveren Formation); A. Uchman, personal.comm. (2002).

x – present

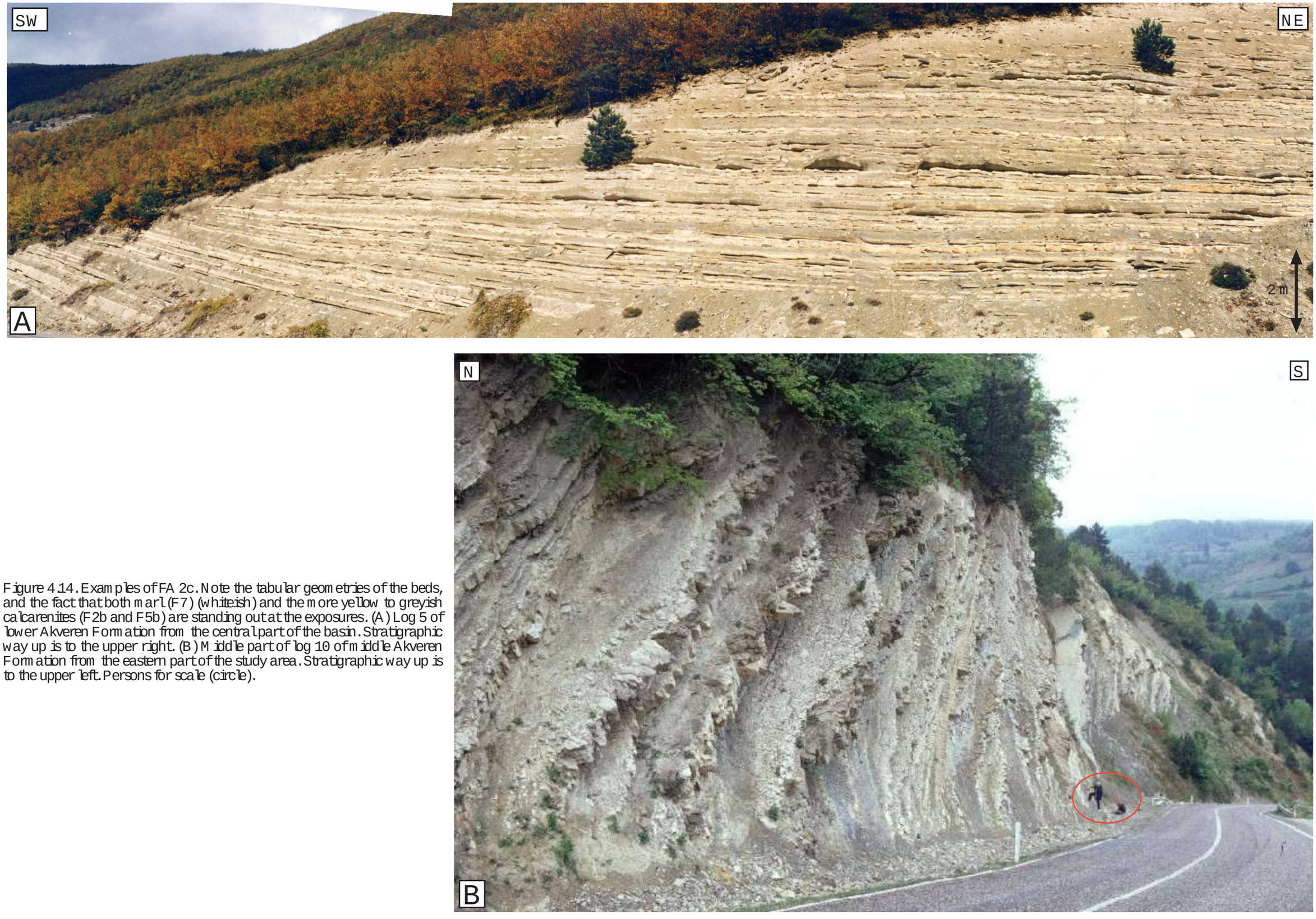

Figure 4.14. Examples of FA 2c. Note the tabular geometries of the beds, and the fact that both marl (F7) (whiteish) and the more yellow to greyish calcarenites (F2b and F5b) are standing out at the exposures. (A) Log 5 of lower Akveren Formation from the central part of the basin. Stratigraphic way up is to the upper right. (B) Middle part of log 10 of middle Akveren Formation from the eastern part of the study area. Stratigraphic way up is to the upper left. Persons for scale (circle).

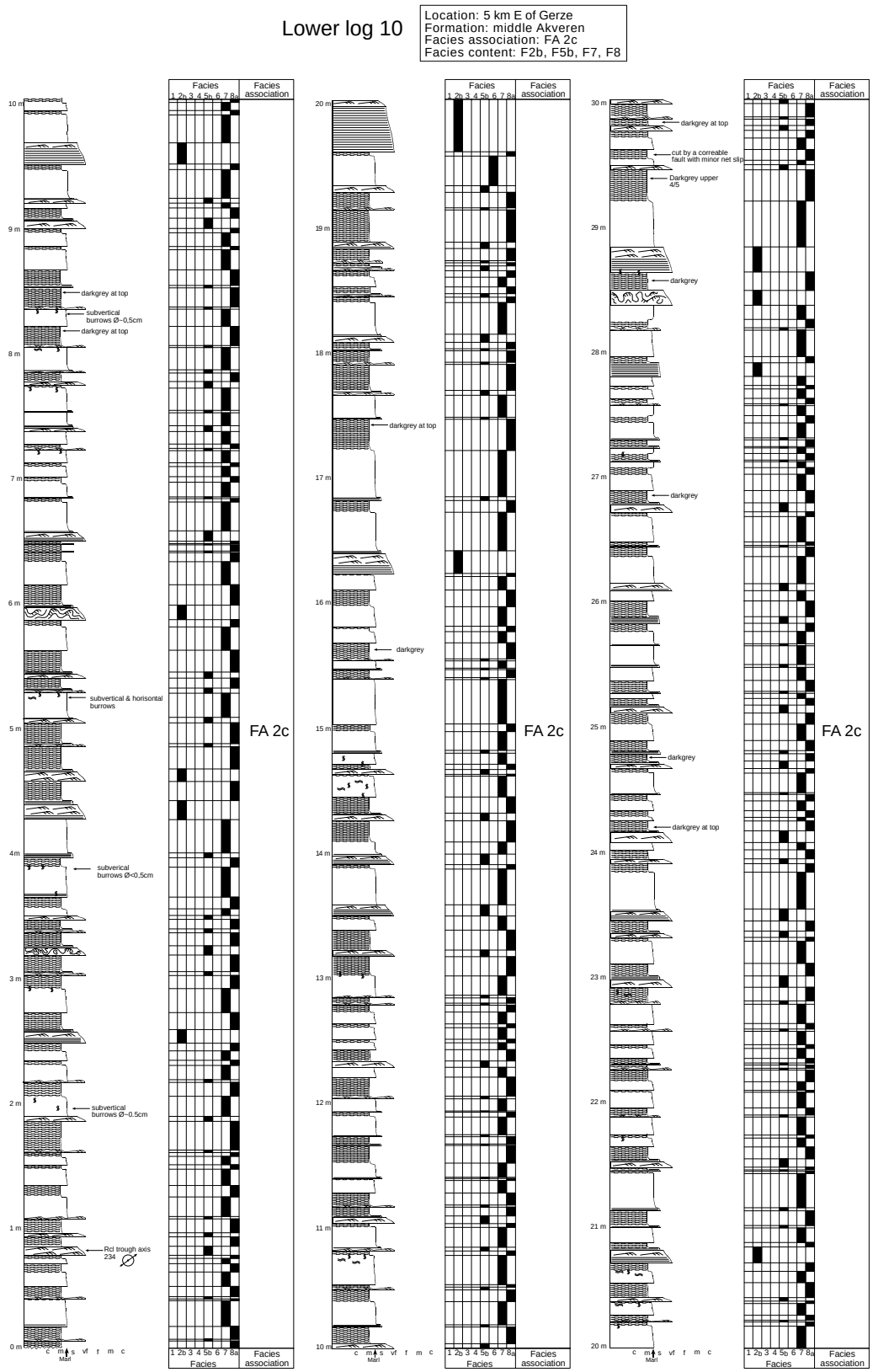

Figure 4.15. Lower part of Log 10 (total thickness 156 m; Appendix 1) showing FA 2c with relative distribution of facies. From middle Akveren Formation in the eastern part of the study area.

Interpretation of FA 2c - Facies subassociation FA 2c is thought to comprise the basin-plain deposits of calcareous, unconfined turbidity currents derived from the fore-reef slope formed by subassociations FA 2a and FA 2b (Fig. 4.18). Similar assemblages of calciturbidites, deposited from unconfined and chiefly low-density currents, are reported to be common in the lower slope, base-of-slope and basin-plain environments of carbonate ramps (Drzewiecki and Simó, 2002, their Table 1). The lack of upward thinning or thickening trends, as in the case of Log 10 (Fig. 4.16), is considered by Coniglio and Dix (1992) to be characteristic of carbonate platform-derived turbidites and hemipelagic deposits. The overall subtle upward fining of the succession of FA 2c deposits is attributed to the basin-floor aggradation and the resulting gradual decrease of the carbonate slope gradient, which must have reduced the ignition capacity of storm-derived sediment suspension plumes (see Parker, 1982). This notion is supported by the lack of significant erosional relief at the bases of the calciturbidite beds of facies F2b and F5b.

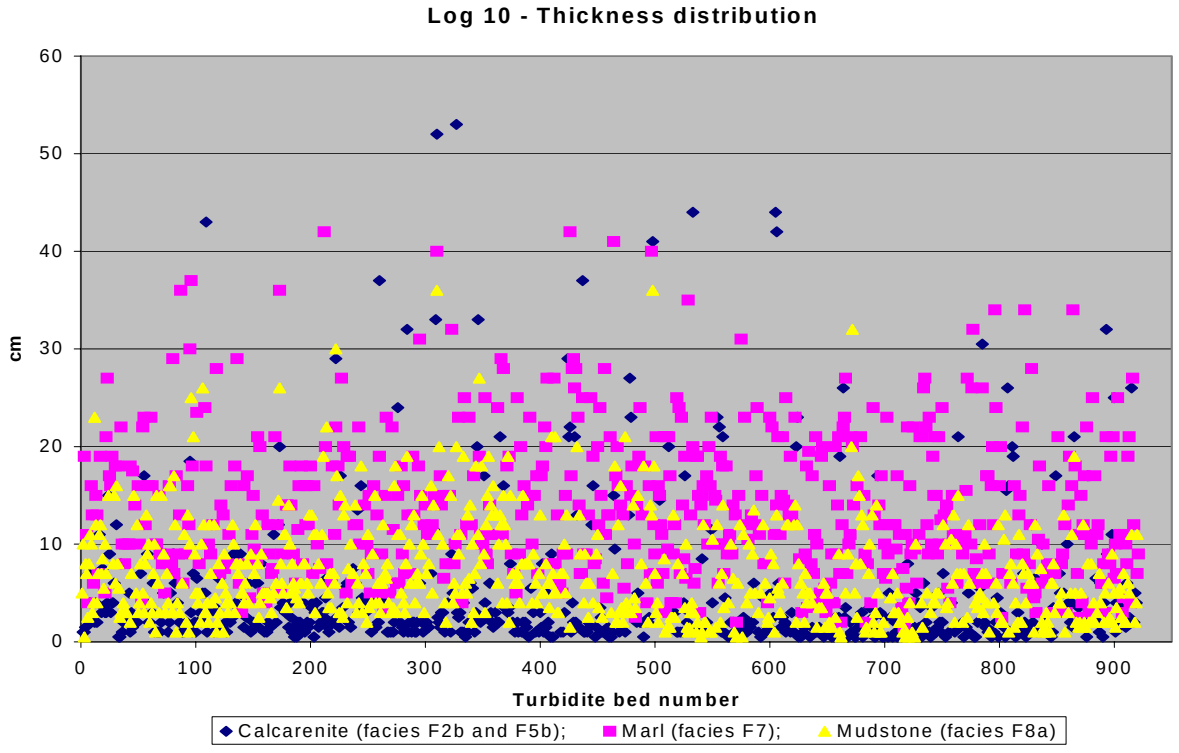

Figure 4.16. The stratigraphic distribution of bed thicknesses in facies subassociation FA 2c (Log 10 of the middle part of Akveren Formation, 156 m thick), eastern part of the study area. The turbidite beds have been plotted as their calcarenitic parts and marlstone/mudstone cappings. The horizontal scale indicates the stratigraphical order of beds; note the lack of any systematic trend (upward thickening or thinning) in this succession.

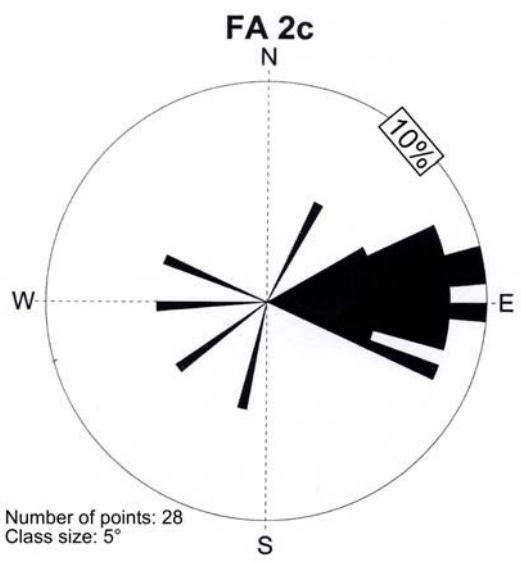

Figure 4.17. Rose diagram summarizing the palaeoflow direction measurements from facies subassociation FA 2c.

The evidence of westward palaeocurrent directions (Fig. 4.17) is probably the first sign of the basin floor's losing its eastward inclination, because of the prolonged differential accumulation of sediment (thicker to the east) and possibly also due to a more pronounced subsidence to the west (stronger tectonic extension). Some of the margin-derived turbidity currents were apparently turning westwards, instead of flowing along the basin axis towards the east. The subsequent deposition of the uppermost Akveren Formation and the Atbası Formation indicates, indeed, a rifting pulse and markedly increased subsidence rate, whereas the overlying Kusuri Formation shows a reversal in the pattern of sediment supply and direction of turbidity currents (Leren *et al*., 2002; Janbu *et al*., 2003).

4.4. Facies association FA 3: carbonate ramp deposits

This calcareous facies assemblage constitutes the upper part of the Akveren Formation, as has been recognized in the eastern (Logs 15 and 16), central (Log 17) and western part of the basin (Log 14). It has a transitional boundary with the underlying facies association FA 2 and a gradational to sharp conformable boundary with the overlying facies association FA 4 (Fig. 4.1), and is thickening eastwards from little more than 15 m to ca. 50 m. It has been divided into two subassociations (Table 4.1): (a) shallow-marine reefal complex and (b) storm-influenced offshore transition to wave-influenced shoreface deposits.

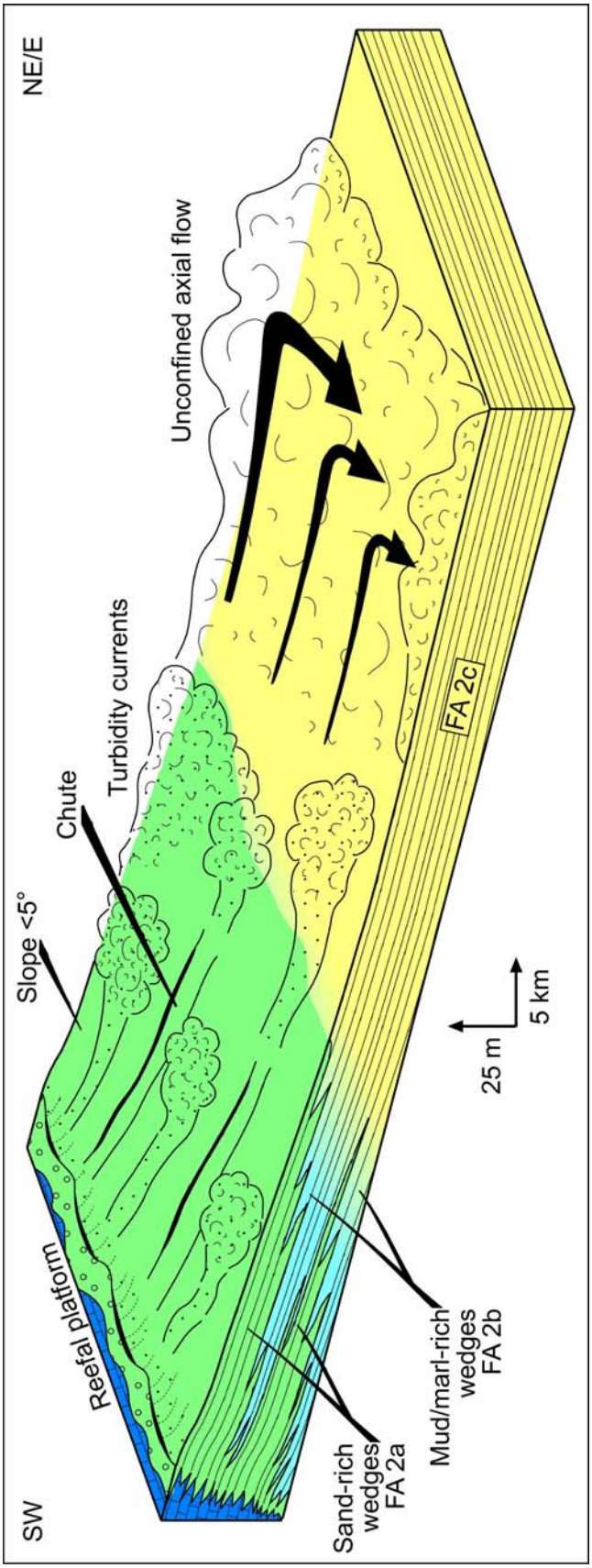

Figure 4.18. Schematic model for the deposition of facies association FA 2: a low-angle, neritic to subneritic carbonate slope apron, with sporadic shallow chutes, formed as the transitional zone between the basin-margin littoral reefal platform and the basin-plain bathyal environment. The alteration of subassociations FA 2a and FA 2b in the apron is attributed to relative sea-level changes (see further discussion in the text).

Facies subassociation FA 3a – This is a mono-facies assemblage composed of the massive, non-bedded limestones of subfacies F6b (Fig. 3.22 and Table 4.3), which occur in the Kuğoköy area in the westernmost part of the basin (Fig. 4.1; see also the upper part of Log 14 in Appendix 1). The limestones are up to 15 m thick and at least several kilometres in lateral extent, overlain by the variegated mudstones of the Atbaşı Formation (facies subassociation FA 4). As described earlier in the text, the *foramol*-type bioclastic component in the limestones of subfacies F6b indicates a shallow-marine environment of normal salinity and temperate climatic conditions. Few recognizable burrows have been found, probably because of the strong early-diagenetic alteration of the calcareous sediment and its heavy cementation.

The limestone unit is interpreted to be a basinward-expanded reefal complex, reflecting an overall shallowing of the basin. The massive reefal limestones were deposited at water depths of less than 25 m, and the underlying fore-reef deposits (bedded limestones of subfacies F6a) were probably deposited at water depths between 25 and 100 m. The red coralline algae recognized in subfacies F6b (Fig. 3.24A) are particularly common in the Cenozoic reefs and associated environments (Adams *et al*., 1984; Tucker, 2001), because large reef-building corals were scarce after the mass extinction that marked the Mesozoic-Cenozoic boundary (Burchette and Wright, 1992; James and Bourque, 1992; Wright and Burchette, 1996). The reefal platform was formed of small bryozoans encrusted by red coralline algae, that was ground into sand and silt particles by the perennial wave action and episodic storms.

Facies association FA 3b – This facies subassociation occurs as a lateral equivalent of the previous one in the central and eastern part of the basin (Fig. 4.1), where it is up to 50 m thick (for details, see Logs 15-17 in Appendix 1 and Table 4.8). It has gradational contacts with the underlying facies association FA 2c and the overlying facies association FA 4b (variegated mudstones). Subassociation FA 3b (Table 4.2) is composed mainly of the alternating beds of calcareous tempestites (facies F3), marlstones (facies F7) and grey to greenish-grey calcareous mudstone (subfacies F8a), with minor subordinate calcrudite (subfacies F1a) and calciturbidites (subfacies F2b and F5b) interbedded with variegated calcareous mudstones (subfacies F8b) at the top (Table 4.3 and Fig. 4.19). The outcrops of

subassociation FA 3b show a distinct upward increase in the proportion of sandstone beds, which are increasingly amalgamated (Fig. 4.20).

Calciturbidites (subfacies F2b and F5b) occur in the easternmost outcrops of subassociation FA 3b (Fig. 4.21), where palaeocurrent directions are towards the east (Fig. 4.22). The micropalaeontological data from facies subassociation FA 3b (Table 4.8) indicate consistently a Late Palaeocene age and point to water depths of less than 100 m (Log 16) or less than 40 m (Log 15) (E. Sirel, personal comm., 2002). On the other hand, trace fossils (Table 4.9) indicate deep-marine *Nereites* ichnofacies (A. Uchman, personal comm., 2002). The *Nereites* ichnofauna has been identified in the lower to middle part of this facies assemblage, whereas an *Ophiomorpha nodosa* trace has been found at the base of the upper part dominated by amalgamated calcarenite beds. The bathyal *Nereites* ichnofauna is inconsistent with the evidence from microfauna and sedimentary facies, which both indicate a neritic to littoral range of palaeoenvironments for subassociation FA 3b.

Table 4.8. Characteristics of facies subassociation FA 3b (upper part of Akveren Formation).

LOG:	***15***	***16***	***17***
Palaeocurrent directions:	E	no solemarks	no solemarks
Biozone (age):	Late Palaeocene	Thanetian or Selandian	Late Palaeocene
Palaeobathymetry:	<40 m	< 100 m	??
Subfacies F1b:	0%	0%	0.5%
Subfacies F2b:	6%	0%	0%
Facies F3:	5%	41%	62.5%
Subfacies F5b:	6%	0%	0%
Facies F7:	13%	37%	25%
Facies F8:	49%	22%	12%
Ichnofacies (see Table 4.9)	Burrows indicating deep-marine *Nereites* ichnofacies	Deep-marine *Nereites* ichnofacies; at least one *Ophiomorpha nodosa* indicative of littoral environment	Typical deep-sea *Nereites* ichnofacies

LOG 17

Location: Yenikonak, E of river
Formation: upper Akveren
Facies association: FA 3b
Facies content: F1a, F3, F7, F8

Figure 4.19. Log 17 from upper Akveren Formation, central part of basin, with associated facies distribution, shown as an example of FA 3b.

Facies subassociation FA 3b is interpreted to be carbonate deposits of a storm-influenced offshore transition zone to wave-worked shoreface zone representing the outer to middle part of an advancing carbonate ramp (Fig. 4.20). The upward change from the turbiditic deposits of association FA 2 to the wave-worked deposits of association FA 3 indicates a marked shallowing of the basin. Similar shallowing-upward successions from turbidites to tempestites and shoreface sandstones, siliciclastic and calcareous, have been described by a number of authors (e.g., Aigner and Reineck, 1982; Leckie and Walker, 1982; Monaco, 1992; Johnson and Baldwin, 1996; Vera and Molina, 1998).

Figure 4.20. Facies association FA 3b (upper part of Akveren Formation) at the Erfelek Waterfalls locality (Fig. 1.1) in the central part of the study area. Note the upward increase in the proportion and amalgamation of sandstone beds, attributed to the change from offshore transition (outer ramp) to shoreface environment (mid ramp) of the prograding carbonate ramp.

The high percentage of hemipelagic deposits and the association of calcarenitic turbidites (subfacies F2b and F5b) and tempestites (facies F3 in Log 15; Table 4.8), in the easternmost outcrop section, indicate a relatively "distal" environment slightly below the mean storm-wave base, where sediment was spread by both storm-generated turbidity currents and some of the strongest geostrophic currents (e.g., Vera and Molina, 1998, their Fig. 9; Bádenas and Aurell, 2001). The notion of an outer-ramp environment, deep neritic or subneritic, is supported by the palaeocurrent directions (Fig. 4.22) and deep-marine ichnofauna (Table 4.8). The concept of storm-generated turbidity currents has been somewhat controversial. Among its proponents are Hamblin and Walker (1979), Leckie and Walker (1982), Myrow and Southard (1996) and Myrow *et al.* (2002), who postulated a whole spectrum of flows – from purely gravitational to wave-modified turbidity currents, to density-modified and pure combined-flow geostrophic currents. Opponents include Duke (1990) and Duke *et al.* (1991), who have argued that the sole marks in storm-generated deposits reflect instantaneous flow conditions, rather than the longer-term mean flow conditions, and hence are not a compelling evidence of purely unidirectional currents; a combined flow can produce unidirectional flutes at the maximum phase of its seaward acceleration. The eastward palaeocurrent directions in the present case (Fig. 4.22) are inconclusive, because they may reflect both a topographically-controlled turbidity current flowing along the basin axis and a pressure-controlled geostrophic current flowing under the influence of Coriolis force (which would divert currents eastwards in the northern hemisphere). It is possible that a spectrum of storm-generated currents were involved in the deposition of sand in the outer ramp zone in the present case, as is suggested by the component calcarenitic facies (Table 4.8).

The evidence of deep-marine *Nereites* ichnofauna is incompatible with the offshore transition environment of facies subassociation FA 3b indicated by microfauna and the occurrence of tempestites, which both imply neritic conditions. The sandstone-rich upper part of assemblage FA 3b is poorly accessible (Fig. 4.20) and seems to contain few trace fossils, but the recognition of at least one *Ophiomorpha nodosa* supports the notion of a littoral zone indicated by storm-dominated shoreface facies (see Log 16 in Appendix 1; cf. DeCelles and Cavazza, 1992).

LOG 15

Location: 5 km E of Gerze
Formation: upper Akveren
Facies association: FA 3b
Facies content: F2b, F3, F5b, F7, F8a

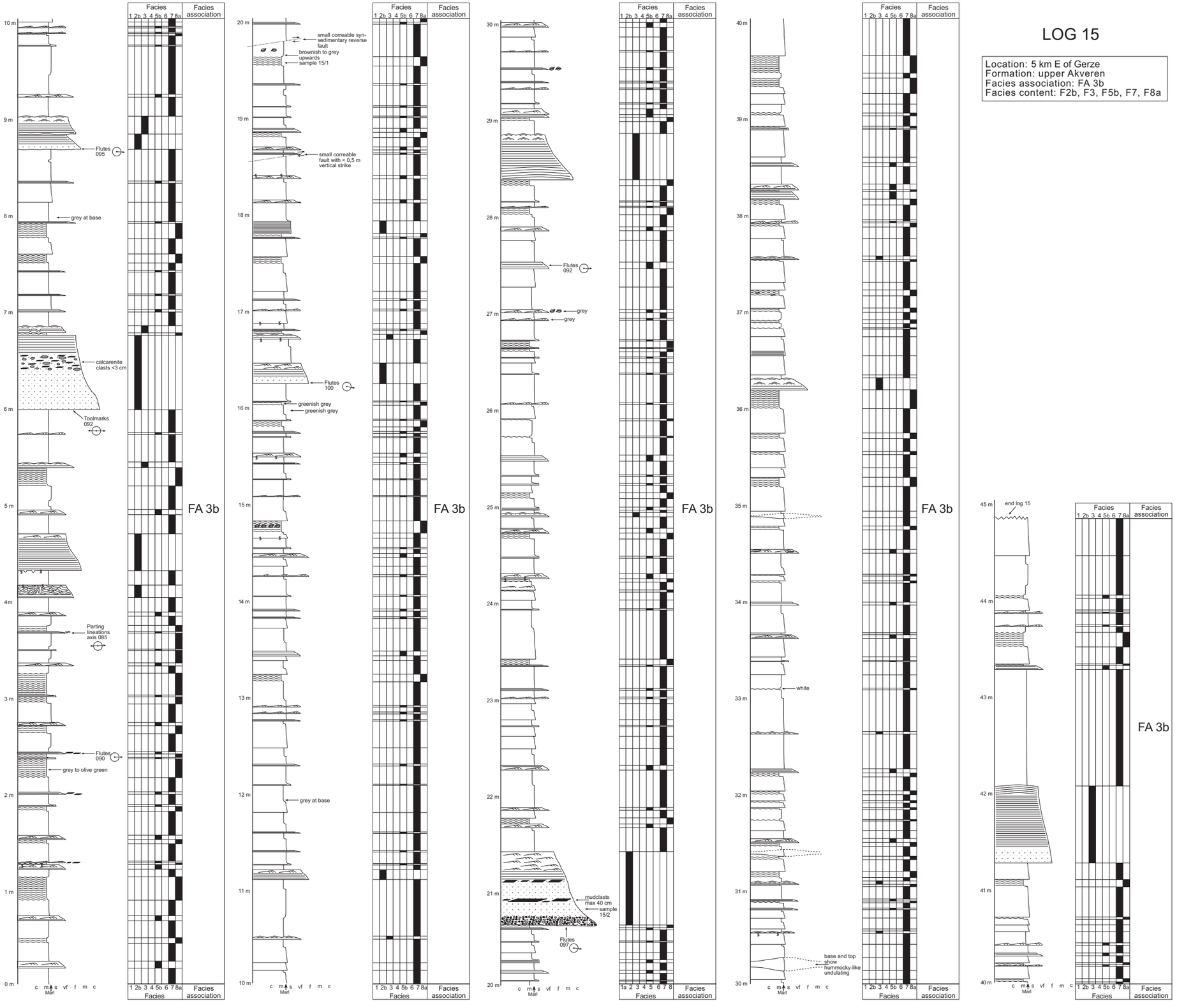

Figure 4.21. Log 15 from upper Akveren Formation with associated facies distribution, shown as an example of the distal parts of FA 3b, from eastern part of the study area.

Ichnotaxa	Log 16	Log 17	Erfelek Waterfalls
Planarolites isp.	x	x	x
Trichichnus isp.			x
Halopoa isp.			x
Chondrites intricatus		x	x
Chondrites targionii	x		
Thalassinoides isp.			x
Ophiomorpha annulata			x
Ophiomorpha ?*nodosa*	x		
Zoophycos isp.	x	x	
Lophoctenium isp.			x
Protovirgularia isp.			x
Scolicia strozzii			x
Nereites isp.			x
Urohelminthoida dertonensis			x
Megagrapton submontanum			x
Megagrapton irregulare		x	

Table 4.9. Trace fossils identified in facies subassociation FA 3b (the upper part of Akveren Formation). A. Uchman, personal comm. (2002).

x – present

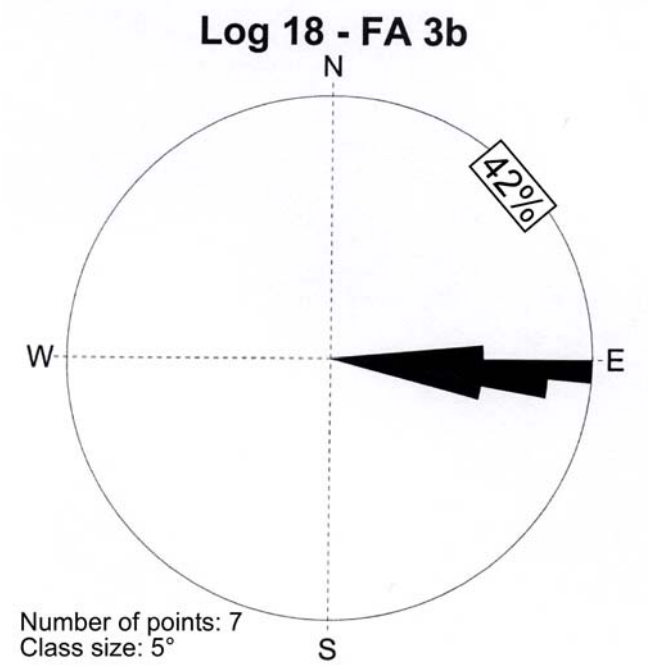

Figure 4.22. Rose diagram summarizing the palaeoflow measurements from Log 15 in the easternmost outcrop of subassociation FA 3b

A similar case of the occurrence of bathyal *Nereites* ichnofauna in a tempestitic offshore-transition facies succession with neritic microfauna has been reported from a Late Cretaceous shelf in Africa (Gierlowski-Kordesch and Ernst, 1987; Ernst and Zander, 1993). The presence of *Nereites* ichnofacies there was attributed to the existence of protected troughs in the shelf area, which were only occasionally affected by large storms and hence

had hydrodynamic conditions somewhat similar to those of a turbidite system.

The basin in the present case was subject to shallowing, perhaps initially accelerated by a pulse of tectonic compression, and one can thus speculate that the bathyal fauna may have survived the gradual change to neritic conditions because the episodic pattern of sedimentation remained much the same. The bathyal basin-plain environment over a long time was subject to hemipelagic sedimentation punctuated by storm-generated turbidity currents, and the basinal fauna was apparently well-adopted to these conditions (as is indicated by the consistent *Nereites* ichnofauna of the Gürsökü and Akveren formations). When the seafloor aggradation eventually led to neritic conditions, neither the bioclastic sediment source nor the frequency and magnitude of the discrete sand incursions would have changed, with the storm-generated geostrophic currents (FA 3) gradually replacing the storm-triggered turbidity currents (FA 2).

As pointed out by Pemberton *et al*. (1992), the main factors affecting ichnofauna community are not so much the water depth, distance from shore or particular tectonic setting, but rather the substrate type, hydraulic energy, sediment deposition rates, water turbidity, oxygen and salinity levels, and the quality and quantity of food supply. In the present case, a critical change in ecological conditions would thus be expected to have occurred with the onset of littoral sedimentation, and the shoreface calcarenites do indeed show evidence of no other traces that an *Ophiomorpha nodosa* burrow. The "inherited" *Nereites* community would thus appear to have been replaced at that stage by a rapidly expanding littoral *Glossifungites/Scolithos* community (Fig 4.2).

Interpretation of FA 3 - The depositional setting envisaged for facies association FA 3 (Fig. 4.23) is similar to the homoclinal carbonate-ramp model of Burchette and Wright (1992). The calciturbiditic bathyal system of facies association FA 2, sourced from a basin-margin reefal platform, is thought to have evolved into a calcarenitic ramp system as a result of the basin-floor aggradation accompanied by a progressive decrease of the basin-margin slope gradient. The shallowing of the basin may have been accelerated by uplift caused by a pulse of tectonic compression. The inner ramp consisted of a rapidly advancing, shallow-water reefal platform (subassociation FA 3a), whereas the medial ramp was a wave-dominated shoreface zone and the outer ramp was a storm-influenced neritic

zone (subassociation FA 3b). The ramp inclination had probably decreased from ca. 5° to less than 0.1° with time, which contributed to the gradual decline of the activity of storm-generated turbidity currents in favour of the storm-driven, direct compensational combined-flow currents.

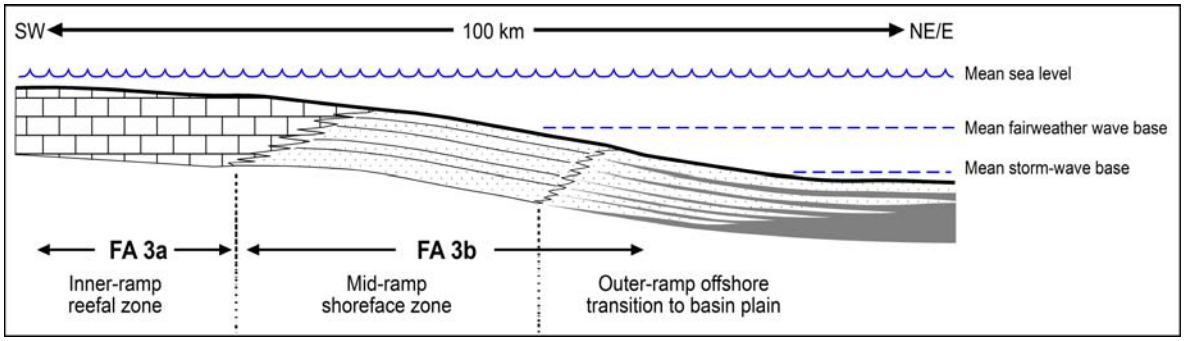

Figure 4.23. A carbonate ramp model suggested for the deposition of facies association FA 3. Based on Burchette and Wright (1992).

The occurrence of tempestites is the most diagnostic criterion for distinguishing gently-sloping ramps from steep-fronted carbonate platforms (Vera and Molina, 1998, their Table 1). Reef-building corals were scarce in the early Cenozoic time (Burchette and Wright, 1992; Wright and Burchette, 1996), which promoted the development of sandy bioclastic shoals with gently seaward slopes, instead of classical reefs with talus-spawning frontal escarpments. The evidence from thin sections strongly supports the notion that both the calciturbidites of facies F2 and the calcitempestites in facies F3 were derived from the same reefal source represented by the *foramol*-type limestones of subfacies F6b and facies subassociation FA 3a (Figs. 3.16 and 3.24).

4.5. Facies association FA 4: carbonate ramp-drowning deposits

This facies association constitutes the uppermost part of the Akveren Formation and the overlying Atbaşı Formation (Fig. 4.1), and its facies composition is represented by Logs 18-20 (Appendix 1), summarized in Table 4.10. Each of the logs represents one of the three following subassociations: (a) hemipelagites interbedded with tempestites/turbidites and massive limestones (Table 4.1); (b) hemipelagites interbedded with tempestites; and (c) hemipelagites interbedded with thin turbidites.

Table 4.10. Characteristics of facies association FA 4 in Logs 18-20, representing the uppermost part of Akveren Formation and the overlying Atbaşı Formation.

LOG:	***18***	***19***	***20***
Facies subassociation:	FA 4a	FA 4b	FA 4c
Formation:	uppermost Akveren Fm. and lower Atbaşı Fm.	lower Atbaşı Fm.	middle Atbaşı Fm.
Palaeocurrent directions:	no solemarks found	NE (one measurement)	E
Biozone (age):	no samples analyzed	Early Eocene	Early Eocene
Palaeobathymetry:		>100 m	>100 m
Subfacies F2b:	0%	0%	1.5%
Facies F3:	0%	38%	0%
Facies F4:	17%*	0%	0%
Subfacies F5b:	0%	0%	17.5%
Subfacies F6a:	51%	0%	0%
Facies F7:	11%	13%	18%
Subfacies F8a:	18%	0%	0%
Subfacies F8b:	3%	49%	63%
Ichnofacies:	No traces identified	Impoverished deep-marine *Nereites* ichnofacies	Impoverished deep-marine *Nereites* ichnofacies

*Possibly including some beds of facies F3.

The upward transition from facies association FA3 to association FA 4 is marked by the appearance of red-coloured/variegated calcareous mudstones of subfacies F8b in the succession. Facies association FA 4 is up to 200 m thick (Fig. 4.1). Its basal part, 20-25 m

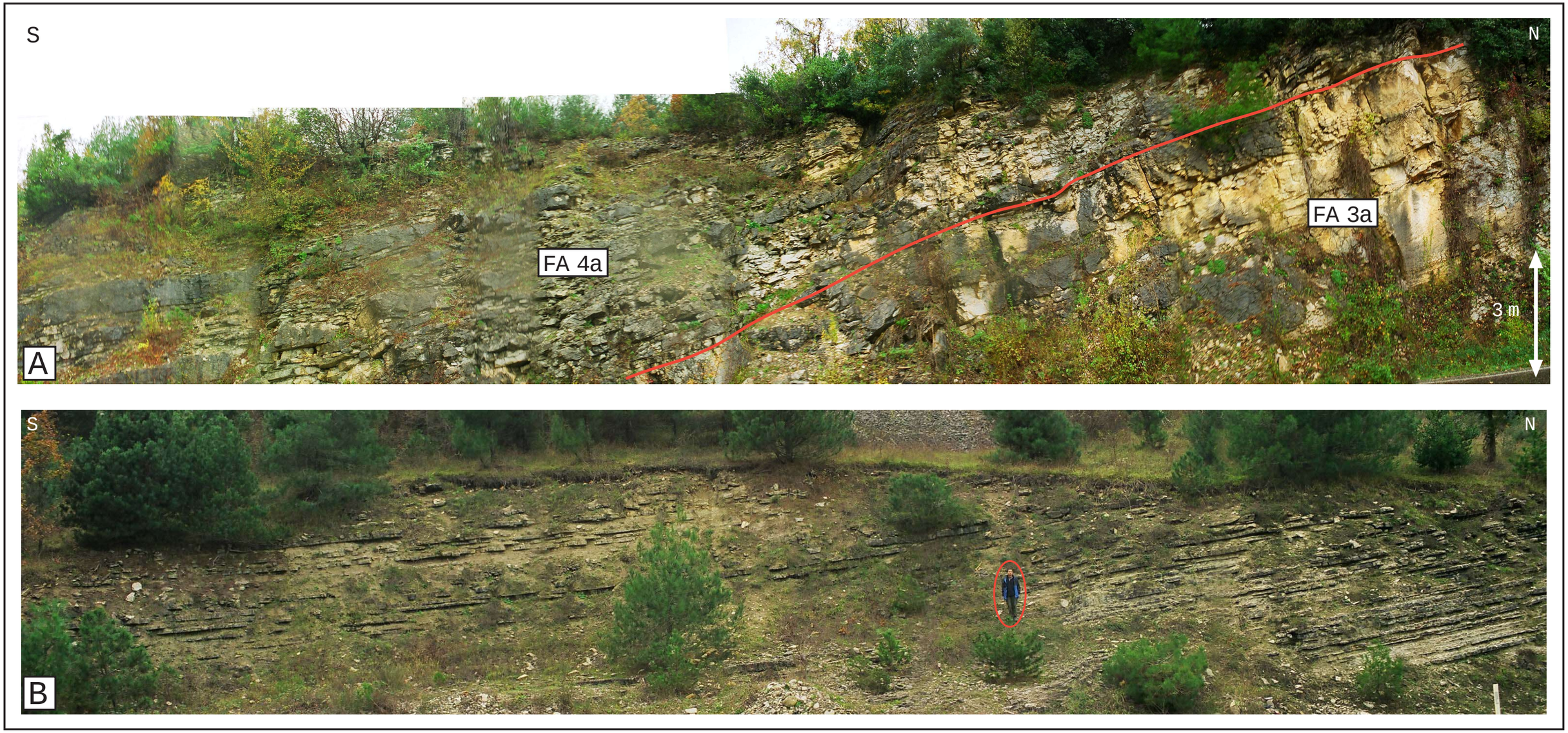

Figure 4.24. Exposures of FA 4a, uppermost Akveren and Atbasi formations from the westernmost part of the study area. Stratigraphic way up is to the upper right. (A) Example of the conformable transition from FA 3a to FA 4a. The lowermost part of log 18 was measured at this outcrop. (B) Outcrop equivalent to middle to upper log 18 showing alternations of tabular calcarenites (F3/F4), bedded massive limestone (F6a), marls (F7) and calcareous mudstones (F8). Person for scale (circle).

thick, consists of facies subassociation FA 4a in the western part of the basin and of subassociation FA 4b in the central and eastern part (Fig. 4.1). The whole middle and upper part (ca. 175 m thick) consist of subassociation FA 4c. The boundary with the overlying Kusuri Formation is gradational, marked by an increase in the amount of siliciclastic sediment and the frequency of turbidite sandstone beds.

Facies subassociation FA 4a – This facies assemblage (Fig. 4.24), exposed in the Kuğuköy area (Log 18 in Appendix 1 and Fig. 4.25), is a succession of hemipelagic calcareous mudstones, grey to greenish-grey (facies F8a) to variegated at the top (facies F8b), intercalated with isolated beds of calcarenitic tempestites (facies F3) and turbidites (facies F4) as well as massive limestones (facies F6a) and marlstones (facies F7) (Table 4.3). The succession is ca. 20 m thick and has a gradational boundary with the underlying facies subassociation FA 3a and a gradational upward transition into the variegated hemipelagic mudstones of subassociation FA 4c. The succession shows a thinning- and fining-upward trend, marked by a decreasing proportion of limestone beds and increasing content of mudstone and marlstone beds. No samples were taken for micropalaeontological analysis, but the stratigraphic position of this facies assemblage renders it a "proximal" equivalent of facies subassociation FA 4b (Fig. 4.1). No identification of ichnofacies was done in the outcrops, but the trace fossils seem to be similar as in the latter subassociation.

Facies subassociation FA 4a represents sedimentation in the inner to medial part of the carbonate ramp that was subject to drowning (i.e., relative sea-level rise). The reefal platform had retreated by back-stepping (cf. Wright and Burchette, 1996), while the basinward flux of calcareous sand gradually declined.

Facies subassociation FA 4b – This facies subassociation, ca. 25 m thick, forms the lower part of the Atbaşı Formation in the central part of the basin (Log 19 in Appendix 1). The lower contact with facies subassociation FA 3b is gradational, and so is also the upward transition to the variegated hemipelagites of subassociation FA 4c (Fig. 4.1). The deposits are grey to greenish-grey calcareous mudstones (facies F8b), increasingly variegated upwards, intercalated with thin calcitempestites (facies F3) and marlstones (facies F7) (Tables 4.3 and Fig. 4.26). No obvious upward thinning or thickening of calcarenite beds is recognizable in Log 19, but a clear upward thinning and fining can be

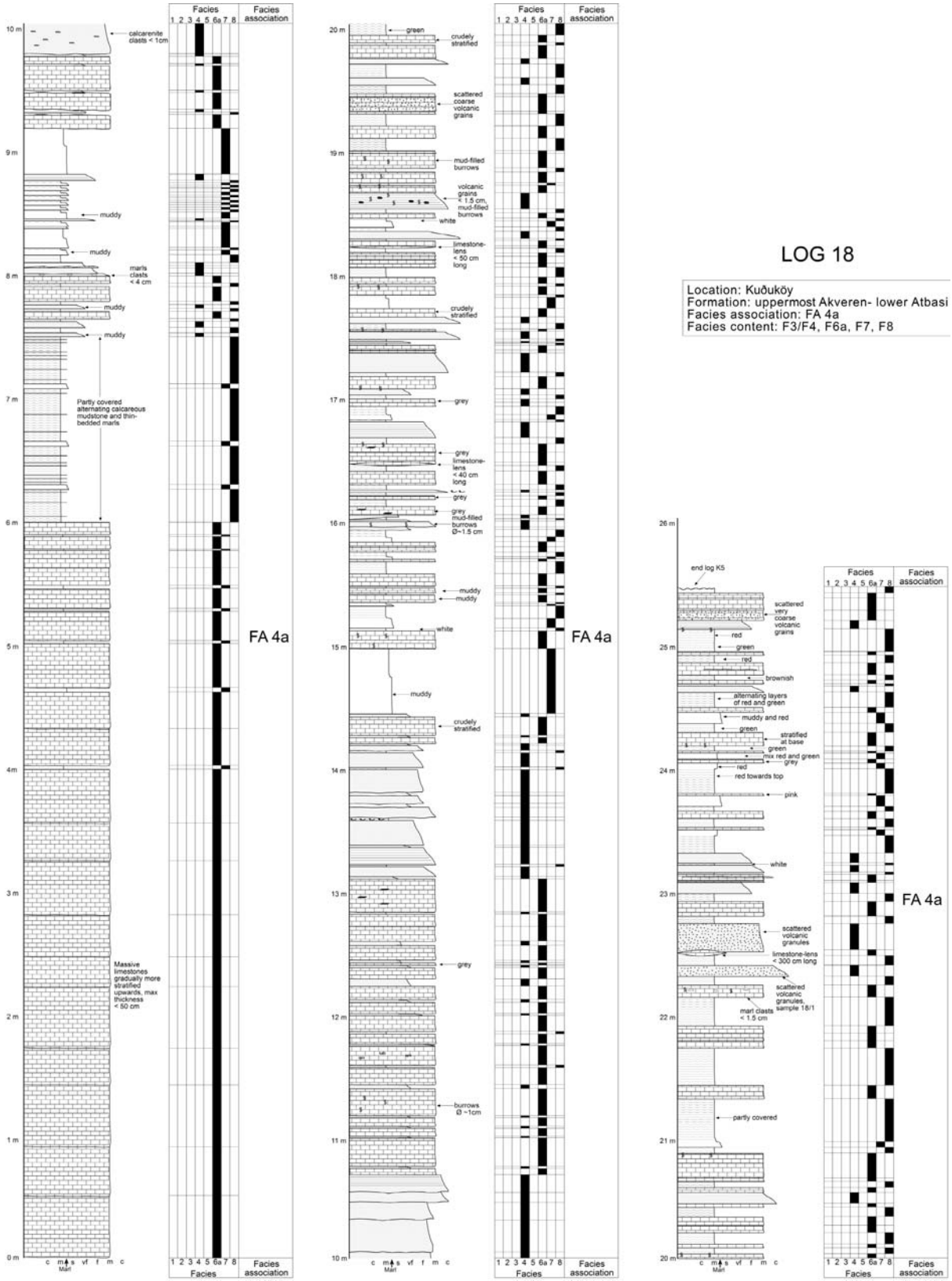

Figure 4.25. Log 18 of the uppermost Akveren and lower Atbaşı formation with associated facies distribution of FA 4a. From the westernmost part of the study area.

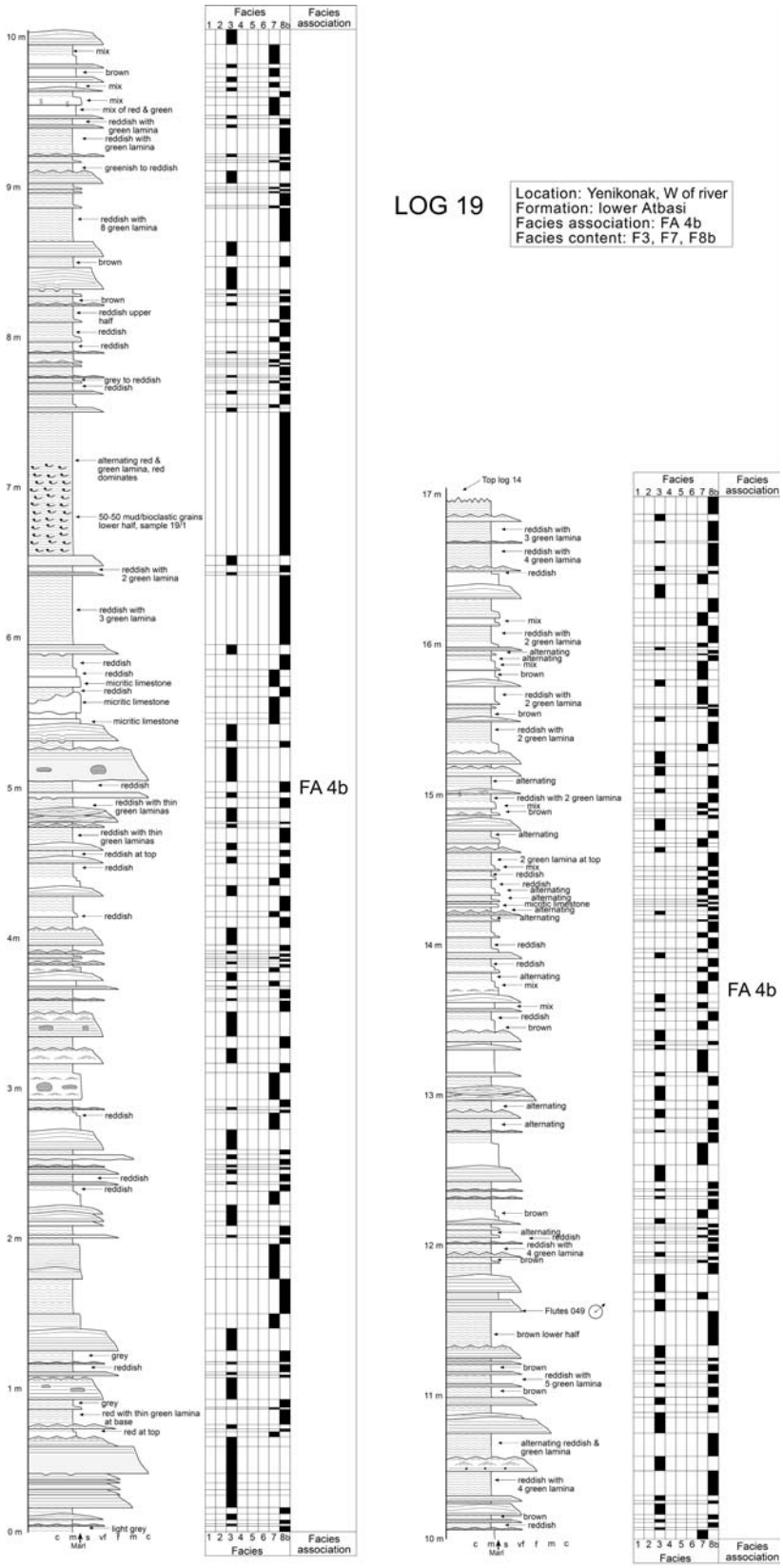

Figure 4.26. FA 4b shown by Log 19 with contribution of interpreted facies. From lower Atbaşı Formation in the central parts of the basin.

seen in other, unmeasured exposures of this facies subassociation. Micropalaeontological data indicate an Early Eocene age (E. Sirel, personal comm., 2002). Trace fossils include *Ophiomorpha annulata, Phycodes* isp., and *Belorhaphe* isp., which indicate an impoverished deep-marine *Nereites* ichnofacies (A. Uchmann, personal comm., 2002). The deep-marine ichnofauna is incompatible with the inferred tempestitic origin of the calcarenite interbeds, which implies that either the environment was no more than deep neritic and influenced by storms (see discussion of subassociation of FA 3b in the previous section), or the thin calcarenite beds are simply turbidites (i.e, facies F4 would appear to have been misinterpreted as facies F3). This second possibility seems quite likely here, because subassociation FA 4b is the "distal", deeper-water equivalent of subassociation FA 4a, in which both tempestites and turbidites have been recognized – and these latter would likely extend farther offshore than the former.

The deposits of subassociation FA 4b, like those of subassociation FA 4a, represent a phase of relative sea-level rise, when the reefal platform was drowned and the associated carbonate ramp had retreated by back-stepping. The deposits of FA 4b represent thus the outer carbonate ramp. The appearance of red-coloured mudstones in this stratigraphic unit signals the approaching phase of sediment-starved conditions and the beginning of seafloor oxidation.

Facies subassociation FA 4c – This facies assemblage, up to 175 m thick, has been logged in the middle part of the Atbaşı Formation in the central part of the basin (Figs. 4.27 and 4.28). Log 20 (Table 4.10) shows the lower part of facies subassociation FA 4c, which overlies gradationally subassociations FA 4a and FA 4b and constitutes the remaining part of the Atbaşı Formation (Fig. 4.1). The deposits are predominantly variegated mudstones (facies F8b) intercalated with thin variegated marls (F7) and thin calcarenitic turbidites (facies F2b and F5b) (Table 4.3, Figs. 4.27 and 4.28). The mudstones have a purple red colour with olive-green bands, but are reddish-brown and grey in the upper part, where they eventually pass into the dark grey mudstones of the overlying Kusuri Formation.

No obvious upward thinning or thickening of calcarenite beds is recognizable in Log 20 (Fig. 4.27), but unmeasured other sections show an overall upward fining and thinning, particularly on an outcrop-to-outcrop basis towards the east. Identified trace fossils include

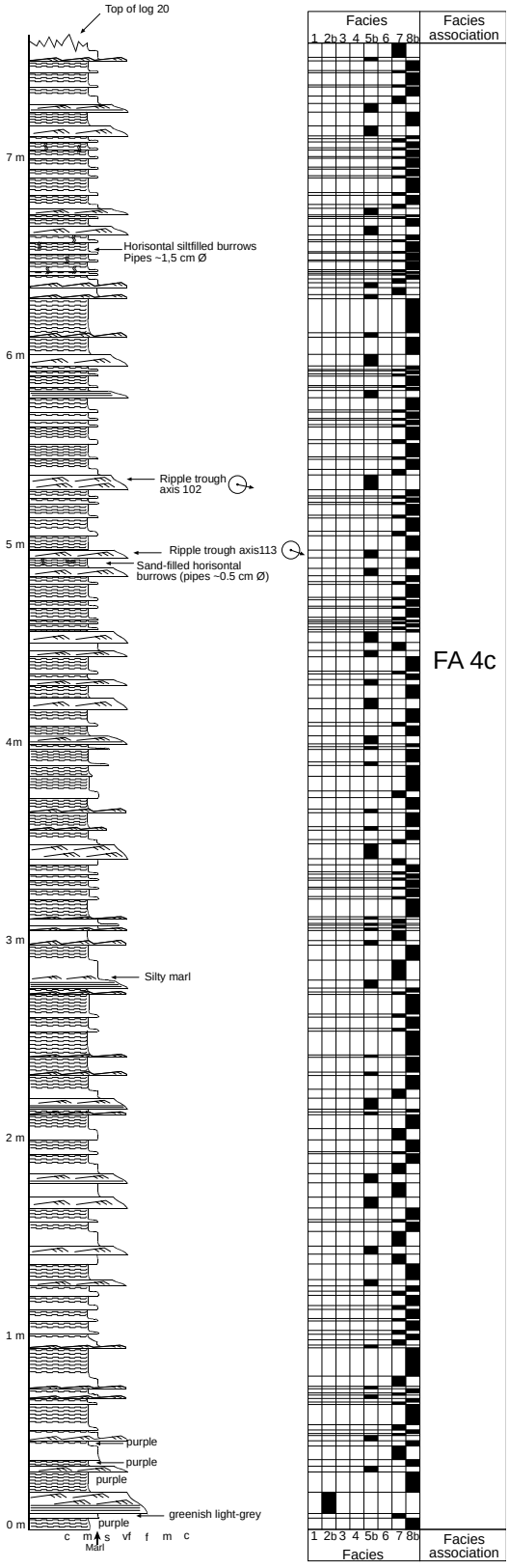

Figure 4.27. Log example (Log 20; Appendix 1) with associated facies distribution showing FA 4c. From the middle Atbaşı Formation in central part of the basin.

Planolites isp. and *Scolcia strozzii*, which indicate an impoverished *Nereites* ichnofacies (A. Uchman, personal comm., 2002). Micropalaeontological evidence indicates a latest Palaeocene(?) to Early Eocene age of the deposits and a water depth in excess of 100 m (E. Sirel, personal comm., 2002). Few measurable palaeocurrent indices have been found, but the directions of the sporadic turbiditic currents were apparently towards the east (Table 4.10).

The deposits of facies subassociation FA 4c represent a prolonged phase of hemipelagic sedimentation in a shelf environment after the major rise of relative sea level, when the supply of sand to the basin had dramatically declined and intense seafloor oxidation occurred on a large scale. It is possibly that the transgression was accompanied by a change in basinal water circulation and perhaps also by a climatic change, which might have contributed to the rapid decay of the reefal organic community. The isolated thin calcarenites represent episodic incursions of low-density turbidity currents, apparently rare and probably triggered by some of the strongest storms.

Interpretation of FA 4 - Facies association FA 4 as a whole is considered to be the record of a relatively rapid deactivation of the basin-margin bioclastic source, attributed to a relative sea-level rise that drowned the reefal platform and caused retreat of the carbonate ramp (Fig. 4.29; cf. Burchette and Wright, 1992). The termination of the reefal system occurred as the rate of sea level rise outpaced the vertical accumulation of carbonate sediment that provided the substrate for the reef-forming organisms (Jones and Desrochers, 1992). The stratigraphic change from littoral deposits (FA 3) to neritic/bathyal deposits (FA 4) strongly supports the notion of a major rise in relative sea level, attributed to a pulse of rifting and rapid subsidence of the basin.

The deposition of the overlying Kusuri Formation marked a renewal of sediment supply and increase in sedimentation rate. However, the sediment at that stage was siliciclastic, derived from the eastern end of the basin and dispersed by westward-flowing turbidity currents, commonly powerful enough to form large submarine channels (Leren *et al*., 2002; Janbu *et al.,* 2003).

Figure 4.28. Facies subassociation FA 4c in the middle part of Atbaşı Formation in the central area of the basin (locality of Log 20, Appendix 1 and Fig. 4.27).

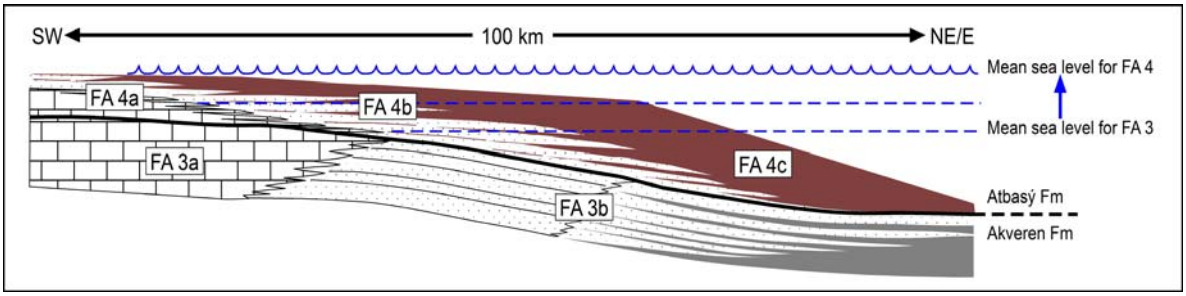

Figure 4.29. Interpretive sketch showing the transition from facies association FA 3 to association FA 4. A relative sea-level rise caused drowning of the basin-margin reefal platform, which was accompanied by a back-stepping retreat of the sandy carbonate ramp. The landward expansion of facies subassociation FA 4c marked the maximum of marine flooding.

CHAPTER 5:

SUMMARY AND DISCUSSION

In this chapter, the results of the facies analysis are summarized and discussed with reference to the regional geological context (possible source areas) and a comparison with coeval sedimentary successions in adjacent basins. On this basis, the Late Cretaceous to Early Eocene tectonic and palaeogeographic development of the basin is tentatively reconstructed.

5.1. The Late Cretaceous–Early Eocene sedimentation in the Sinop-Boyabat Basin

The Sinop-Boyabat Basin evolved as an asymmetrical, SE-trending extensional graben increasingly affected by the compressional regime of the Pontide orogeny and accumulated up to 6-7 km of clastic deposits during the Early Cretaceous to Middle Eocene time (Figs. 2.2, 2.3 and 2.4). The Early Cretaceous basin-fill consists of volcaniclastic turbidites and lava-flow deposits derived chiefly from the basin's northern margin (Aydın *et al.*, 1995a), which soon became submerged by hanging-wall subsidence and ceased to act as a significant source area. The subsequent supply of sediment was mainly from the basin's western end and southern (footwall) margin. The Late Cretaceous to Early Eocene basin-fill succession, increasingly calcareous and up to 2 km thick, comprises the Gürsökü, Akveren and Atbaşı formations (Fig. 2.4), which have been the topic of the present study. These formations consist of different facies associations, whose spatial relationships and inferred sediment sources are summarized in the interpretive longitudinal cross-section parallel to the basin axis shown in Figure 5.1. Each facies association represents a different sedimentary environment, or different conditions of sediment accumulation in the basin.

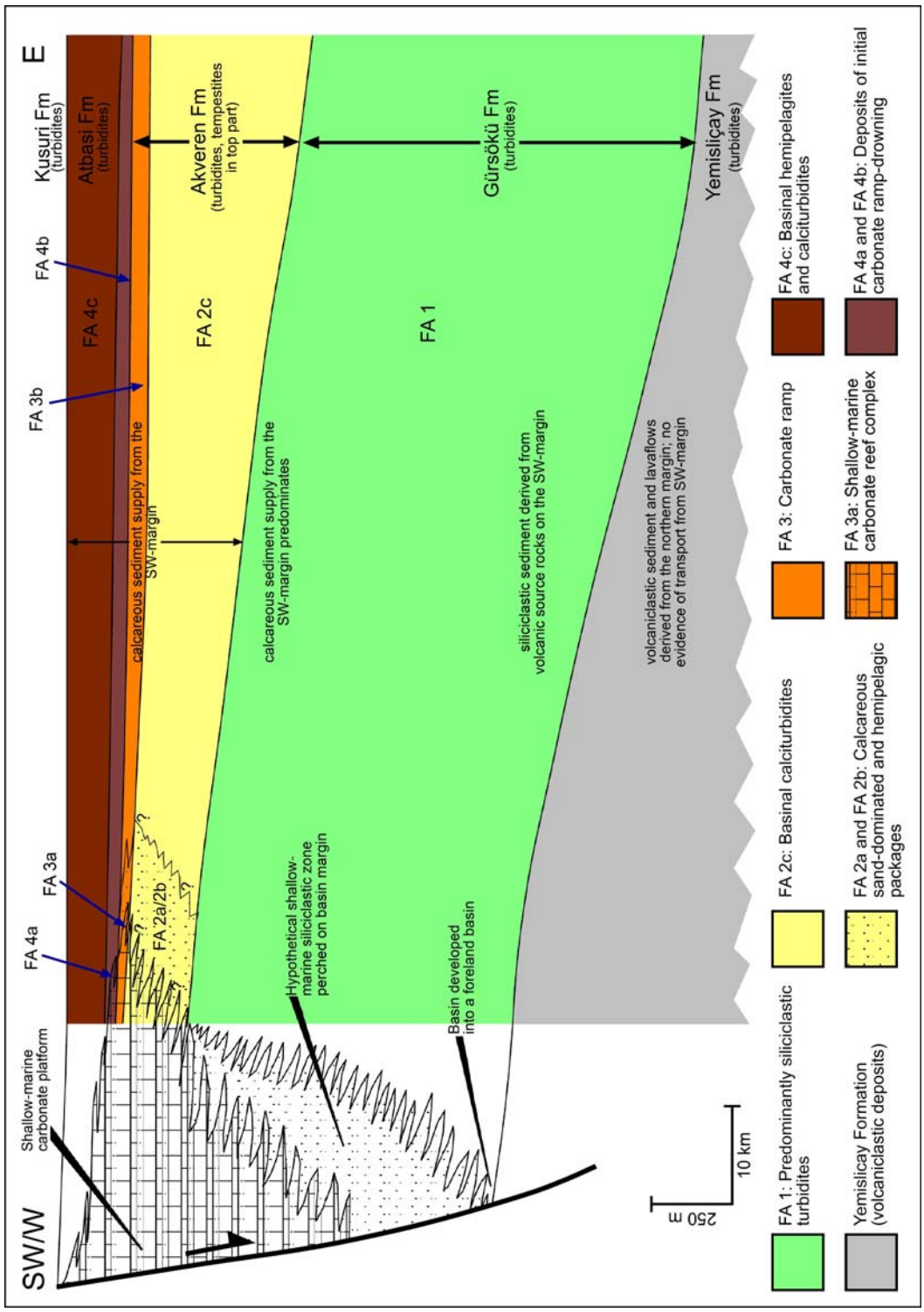

Figure 5.1. Summary of the Upper Cretaceous to Lower Eocene succession in the Sinop-Boyabat Basin with hypothetical source areas; the schematic vertical cross-section is approximately parallel to the basin axis. The different colours represent the main facies associations distinguished in the present study (cf. Fig. 4.1).

The Gürsökü Formation (Campanian-Maastrichtian) – The Gürsökü Formation overlies conformably, with a transitional boundary, the volcaniclastic Yemişliçay Formation of Coniacian to early Campanian age (Fig. 2.4). The Gürsökü Formation is up to 1200 m thick and consists of siliciclastic turbidites (facies F2a and F5a) alternating with marlstones (facies F7) and calcareous mudstones (facies F8a). This formation lacks volcaniclastic facies (Aydın *et al.*, 1995a), and although it was probably still sourced partly from the northern (hangingwall) margin – it only shows evidence of sourcing from the south-western (footwall) margin. It shows also clear evidence of the activation and increasing supply of sediment from a contemporaneous reefal platform, inferred to have formed in the western part of the basin and gradually expanded along the southern (footwall) margin. The palaeocurrent directions are towards the N, NE and E/SE, with main sediment dispersal towards the east (Fig. 4.5), and the sandstone beds show an increase in calcareous bioclastic content upwards in the formation. The formation is thicker towards the east (SE) (Fig. 5.1), which indicates that the basin floor was inclined and broader in that direction.

The deposits of the Gürsökü Formation, distinguished as facies association FA 1, are interpreted to represent the medial to distal part of a basin-wide, deep-marine turbiditic system that was dominated by unconfined turbidity currents of low to high density (facies subassociation FA 1a), but probably included channels in the proximal part. One such isolated palaeochannel, with evidence of lateral accretion (facies subassociation FA 1b), has been recognized in the lower part of the formation (Fig. 4.9). The stratigraphic position of this solitary palaeochannel at the base of the formation and the lack of palaeochannels at higher levels are attributed to an overall back-stepping of the turbiditic system, which was apparently dominated by aggradation, while the basin-floor subsidence driven by tectonic extension made the head part of the system retreat, rather than prograde. This notion is supported by the great thickness of the succession and its overall upward fining that reflects the gradual predominance of low-density and increasingly calcareous turbidity currents.

It is unclear whether the proximal part of the turbiditic systems had one or more perennial channels, which were shifting by avulsion and occasionally extending to the

medial zone; or whether it had channels that were formed only episodically, by the strongest and most voluminous currents. The basin-margin source area was of linear type, lacking major point sources, and the turbidity currents are thought to have been generated chiefly by storms and probably also earthquakes, which favoured wide, unconfined flows. However, the coalescence and hydrodynamic enhancement of turbidity currents along the basin axis apparently generated some robust sustained flows capable of forming sinuous channels, at least episodically and only in the proximal and lower part of the system.

The Sinop-Boyabat Basin at that stage is estimated to have been ca. 150 km wide and more than 350 km long, which allowed the vast majority of unconfined currents to spread widely and deposit sheet-like turbidites. The linear source provided an abundant sediment supply, because the impact of storms and earthquakes involved wide stretches of the shoreline – which was probably perched on the basin margin. Although the classical depositional pattern of channels and lobes is lacking in the case, it is possible the thick succession of sheet-like turbidites is a result of the amalgamation of some poorly defined and widely shifting depositional lobes (cf. Reading and Richards, 1994; Stow *et al.*, 1996). The predominantly eastward direction of turbidity currents was probably more due to the inclination of the basin floor, than to the basin confinement, although it is likely that some of the large currents were basin-wide (cf. Chan and Dott, 1983).

The Akveren Formation (Maastrichtian-Late Palaeocene) – The upward transition from the Gürsökü Formation to the Akveren Formation marks not only the predominance of calcareous sediment supply, but also the development of a depositional carbonate slope-arpon system (*sensu* Mullins and Cook, 1986) linked directly with the basin-margin reefal platform as a gently sloping, turbiditic fore-reef zone passing into the basin plain (Fig. 4.18). The composition of bioclastic sediment indicates consistent supply from a temperate, shallow-marine carbonate platform dominated by bryozoans and coralline red algea (cf. Lees and Buller, 1972). According to the palaeomagnetic data by Kissel *et al.* (2003), the region of Central Pontides was located around 20°N in the Late Cretaceous to Early Palaeocene times. This latitudinal position may be compatible with the palaeontological data acquired in the present study, because the definition of temperate carbonates is based

on both water temperature and salinity (Lees and Buller, 1972; Jones and Desrochers, 1992; James, 1997).

The Akveren Formation consists of calcarenites (facies F2b, F3, F4 and F5b) intercalated with marlstones (facies F7), calcareous mudstones (facies F8) and minor massive limestones (facies F6). The calcarenites in the lower and middle part of the formation (facies association FA 2) are turbidites, whereas those in the uppermost part (facies association FA 3) are chiefly tempestites, passing upwards into the reefal platform deposits (facies F6) in the western part of the basin and into a coeval package of amalgamated shoreface calcarenites (facies F3) in the central to eastern part (Fig. 5.1). The basin inclination is estimated to have decreased from more than 5^{o} (FA 2) to less than 0.1^{o} (FA 3) with time (Fig. 4.23). The decrease in slope gradient, combined with water shallowing, turned the turbidite-prone carbonate slope-apron into a carbonate ramp tempestite-prone shoreface and offshore transition zone.

The transitional lower boundary reflects a gradual transformation of the Gürsökü system (with a perched shoreline source, a bypass basin-margin slope and a basin-floor turbiditic depositional system) into the Akveren system of a reef-sourced, shore-attached calcareous turbiditic carbonate slope. The Akveren Formation is estimated to be up to 600 m thick and thinning towards towards the SW and W (Fig. 5.1), which supports the slope apron interpretation and indicates further major aggradation of the eastward-inclined basin floor. As a result of the aggradation and reduced rate of differential subsidence, the basin floor gradually became horizontal, while the sediment supply became limited to the southern (SW) margin, so that some of the turbidity currents tended to flow westwards, rather than towards the east. It is likely that the cessation of sediment supply from the western end of the basin and the levelling of the basin-floor topography were caused by an increased rifting in the basin's western part. Repetitive pulses of accelerated subsidence are indicated, indeed, by the episodic drowning of the reefal platform and decline in sand supply recorded by the calciturbiditic slope apron succession (Figs. 4.10 and 4.11). The progradation of the carbonate system and basin-floor aggradation, probably in combination with a pulse of compressional uplift, culminated in a late Maastrichtian-Early Palaeocene dramatic

shallowing of the basin recorded by the uppermost part of the Akveren Formation (FA 3; Fig. 5.1). In the Early Palaeocene, the basin floor reached the mean storm-wave base and further shallowing occurred, while the basin-margin reefal platform had expanded a few tens of kilometres basinwards.

The Atbaşı Formation (Late Palaeocene–Early Eocene) – The Atbaşı Formation overlies conformably the Akveren Formation, but its facies association (FA 4) represents another dramatic change in the basin's sedimentary environment: the relative sea level had rapidly increased, the reefal carbonate platform was drowned and deactivated, and a subneritic to bathyal environment was established, while the delivery of sand to the basin had declined and virtually ceased. The variegated calcareous mudstones (facies F8b) of the Atbaşı Formation, which is estimated to be ca. 200 m thick, indicate seafloor oxidation in a basin starved of sediment supply.

The thin calcarenitic interbeds in this formation are initially tempestites (facies F3), but these are replaced quickly by infrequent turbidites (facies F5b) upwards in the succession. Their deposition is attributed to rare strongest storms that were capable of sweeping sand from the inactive carbonate platform along the inundated basin margin. The bioclastic material and thin interbeds of marlstone (facies F7) and sporadic limestone (facies F6a) support this interpretation. This basal, fining-upward part of the formation, 20-25 m thick and composed of facies associations FA 4a-b, indicates rapid retreat of the reefal platform in response to a rising sea level (Fig. 4.29). The dramatic sea-level rise is attributed to rapid subsidence, apparently due to a strong pulse of rifting.

The Kusuri Formation (Early-Middle Eocene) – The overlying Kusuri Formation (ca. 1400 m thick) has a transitional lower boundary, but represents a major change in the basin configuration, with a siliciclastic (probably deltaic) source activated at the eastern end of the basin and with large, powerful, channelized turbidity currents flowing towards the west along the basin axis (Leren *et al.*, 2002; Janbu *et al*., 2003). The easternmost part of the basin was apparently uplifted by orogenic compression. The supply of calcareous sediment came to an end at this stage and the rate of sediment accumulation greatly increased, while the Sinop-Boyabat Basin had been split axially by a compressional pop-up ridge (combined

thrust-and-backthrust feature) into the northern Sinop Basin and the southern Boyabat Basin (Fig. 2.3). Despite continuing subsidence, the Sinop Basin had been rendered progressively narrower by tectonic compression, filled up to a shallow littoral level and eventually inverted by the end of Eocene (Okay and Şahintürk, 1997; Janbu *et al*., 2002).

5.2. Palaeogeographical reconstruction

The preceding interpretation of facies associations (sedimentary environments) has been the basis for a tentative palaeogeographical reconstruction of the basin and its tectonic development in the Late Cretaceous to Early Eocene time. The Sinop-Boyabat Basin formed and evolved in response to active tectonics, in an interference zone of the Western Black Sea rifting process and the process of Neotethys subduction under the Eurasian margin that culminated in the Pontide orogeny (Fig. 2.1; Okay *et al.,* 2001). The basin formed as an asymmetrical graben on the southern (SW) flank of the Western Back Sea Rift in Barremian time (Aydın *et al.*, 1995a; Tüysüz, 1999). The basin-floor subsidence driven by the rifting process persisted until the Eocene time and seems to have occurred in pulses, marked by the episodes of accelerated and broader subsidence, including the basin margins. As a result, the basin-fill succession reached an impressive thickness of possibly up to 7 km (Fig. 2.4). Superimposed on the subsidence process were pulses of orogenic compression, which cause “upsidence” (basin uplift) and both extra- and intra-basinal thrusting, progressively split the basin longitudinally into two parallel compartments and eventually inverted the whole basin by folding (Fig. 5.2).

Importantly, the orogenic deformation is generally considered to have been diachronous in the western, central and eastern segments of the Pontide mountain belt (Aydın *et al.*, 1995a; Tüysüz, 1999; Floyd *et al*., 2000; Göncüoğlu *et al*., 2000; Yılmaz *et al*., 2000; Okay *et al.,* 2001), and also the opening of the Western Black Sea Rift is thought to have occurred independently of the rifting in the Eastern Black Sea (Kazmin *et al.*, 2000; Meredith and Egan, 2002; Cloetingh *et al.*, 2003; Nikishin *et al.*, 2003). It is interesting,

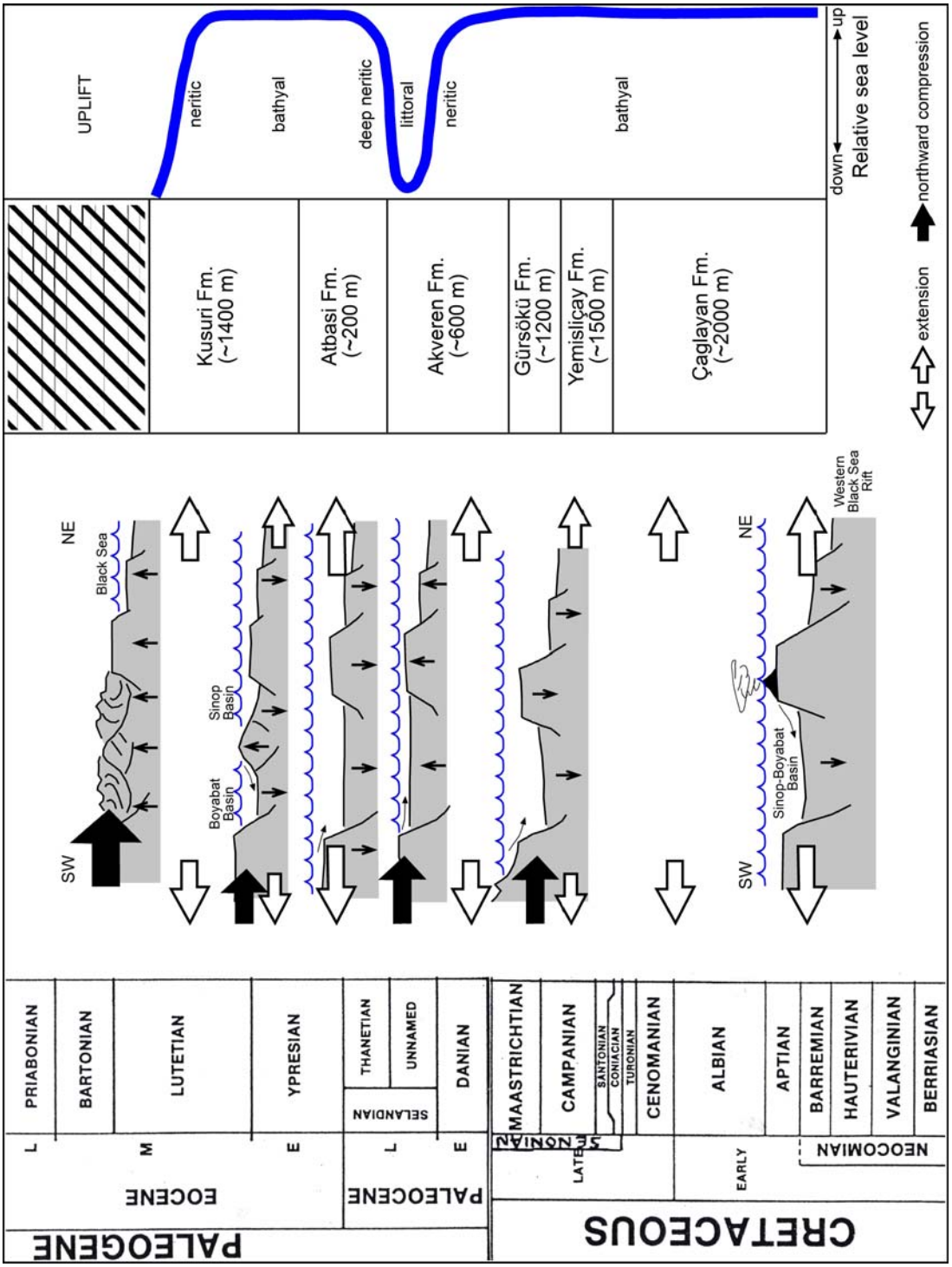

Figure 5.2. Sedimentation history of the Sinop-Boyabat Basin: schematic summary of the extension-driven subsidence, pulses of orogenic compression and relative sea-level changes in the basin.

therefore, to compare the sedimentation history of the Sinop-Boyabat Basin (Figs. 2.4 and 5.2) with the coeval sedimentary successions of the neighbouring basins in the Western and Eastern Pontides (Fig. 5.3), and attempt to distinguish between regional and subregional effects of the two interfering plate-tectonic processes. For the purpose of comparison, the Late Cretaceous-Early Eocene palaeogeographical history of the Sinop-Boyabat Basin has been divided into four time intervals: Coniacian to Early Campanian; Late Campanian to Early Maastrichtian; Late Maastrichtian to Early Palaeocene; and Late Palaeocene to Early Eocene (cf. Figs. 2.4 and 5.2).

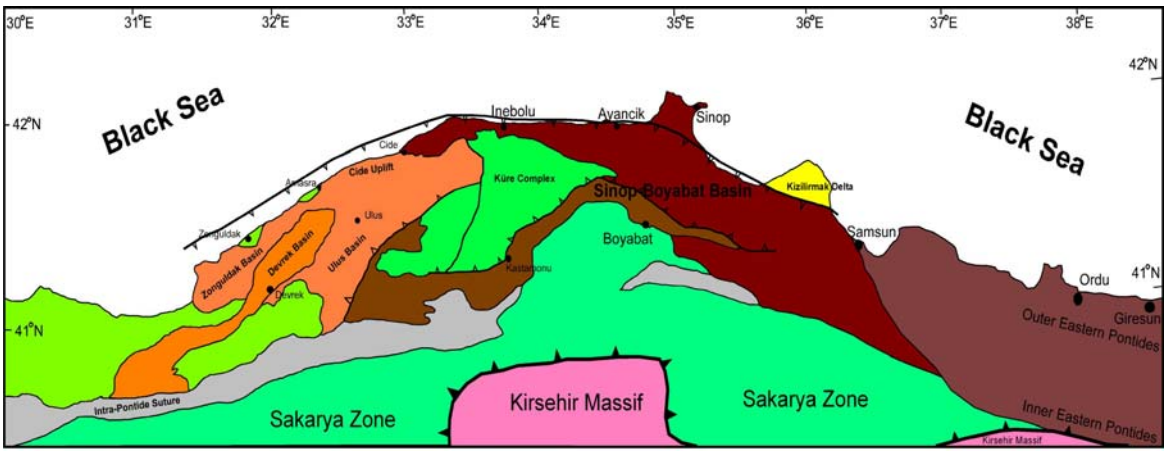

Figure 5.3. Main tectonic elements and sedimentary basins of the Pontides. The Central Pontides segment consists of the Sinop-Boyabat Basin and the metamorphic Küre Complex. The area to the west, including a larger part of the Küre Complex, is the Western Pontides and the area to the east is the Eastern Pontides. The Sakarya Zone and Kirşehir Massif are microcontinents accreted to the southern margin of Eurasia during the Pontide orogeny. Modified from Robinson et al. (1996), Tüysüz (1999), Okay et al. (2001) and Nikishin et al. (2003).

Coniacian-Early Campanian (Fig. 5.4) – The Yemisliçay Formation (Figs. 2.4 and 5.2) was deposited in a fault-bounded fore-arc trough, which formed as an extensional graben. The volcanic arc to the north acted as the principal source of sediment (predominantly volcaniclastic turbidity currents and lava-flows), before turning into the Western Balck Sea Rift and evolving into an incipient oceanic spreading zone (Kazmin *et al.*, 2000; Meredith and Egan, 2002; Cloetingh *et al.*, 2003; Nikishin *et al.*, 2003). The rifting process and development of volcanic arc commenced in the Cenomanian time, after

the accretion of the Sakarya microcontinent to the southern margin of Eurasia as a result of the northward subduction of Neotethys (Tüysüz, 1990; Okay *et al.*, 1994, 2001; Robinson *et al.*, 1995, 1996; Okay and Şahintürk, 1997; Ustaömer and Robertson, 1997; Yılmaz *et al.*, 1997; Tüysüz, 1999). The Sakarya block hosted an Early Cretaceous shallow-marine carbonate platform, and the volcaniclastic phase of sedimentation in the Sinop-Boyabat Basin was thus preceded by an early (pre-volcanic) phase when the incipient deep-water graben – formed in Barremian time – had collected products of carbonate resedimentation (calciturbidites and calcareous olistostromes; cf. Fig. 2.4).

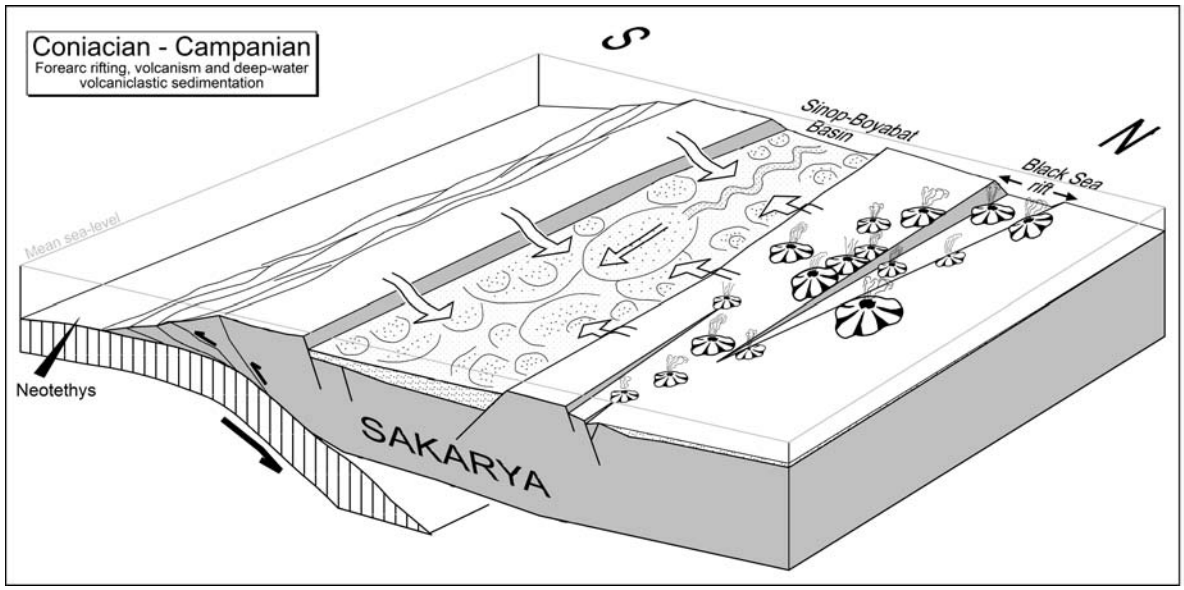

Figure 5.4. Schematic model for the tectonic and palaeogeographical setting of the Sinop-Boyabat Basin in Coniacian to Campanian time (Yemisliçay Fm.). The deep-water forearc basin was supplied with volcaniclastic sediment and lava-flows from the northern (NE) margin, but possibly also from the southern (SW) margin.

Late Campanian to Early Maastrichtian (Fig. 5.5) – The deposition of the turbiditic Gürsökü Formation in the Sinop-Boyabat Basin indicates a deep-water environment and an active supply of predominantly siliciclastic sediment from the southern (SW) and western margins, which were probably uplifted at that time. The abundant evidence of volcanic component in the sediment implies that the SW/W margin consisted of emerged submarine

volcanics and tephra, but it cannot be precluded that some of the sediment was derived also from the NE margin, before it collapsed and became negligible as a source area. The increasing supply of bioclastic calcareous sediment, more pronounced in the upper part of the Gürsökü Formation, indicates that a shallow-marine reefal platform began to develop at the SW/W margin, probably rimming the uplifted volcanic terrain. The episode of tectonic uplift is attributed to the accretion of the Kirşehir microcontinent to the Sakarya Zone of the Pontides (cf. Fig. 5.3). The collision commenced in Campanian time (Tüysüz *et al.*, 1995) and was probably completed in Maastrichtian (Okay and Tüysüz, 1999). The Gürsökü Formation is ca. 1200 m thick and shows no evidence of basin shallowing, which implies active subsidence – apparently driven by continued rifting. The backstepping of the turbiditic system towards the west indicates, in fact, that the rifting and basin-floor subsidence increased in that direction. The opening of the Western Black Sea Rift is thought to have been responsible also for the collapse of the basin's northern (NE) margin, which ceased to supply sediment (southward palaeocurrent directions are lacking).

Coeval deposits in the basins of Eastern and Western Pontides are predominantly volcanics and volcaniclastics (Robinson *et al.*, 1995; Okay and Şahintürk, 1997; Okay and Tüysüz, 1999; Tüysüz, 1999; Sunal and Tüysüz, 2002). However, Campanian deposits of mixed, bioclastic/siliciclastics composition, similar as in the Gürsökü Formation, occur in the Eastern Pontides, where they have been similarly attributed to the formation of a shallow-marine carbonate platform at the rims of volcanic terrain (Robinson *et al.*, 1995). The Gürsökü Formation contains no volcanics or tephra, which indicates that the volcanic activity in the Central Pontides ceased by the Late Campanian time, although it persisted until the end of Campanian in the Western Pontides (Tüysüz, 1999; Sunal and Tüysüz, 2002) and until the Early Palaeocene in the Eastern Pontides (Okay and Şahintürk, 1997; Okay and Tüysüz, 1999).

The accretion of the Kirşehir Massif to the Sakarya Zone caused the subduction zone to shift south of the former crystalline massif and hence away from the central part of the Pontide orogenic belt (cf. Fig. 5.3). This change might explain the cessation of volcanic activity and continued tectonic extension in the Central Pontides. As pointed out by Okay *et*

al. (2001), the cessation of subduction-related volcanism is probably the most reliable criterion for the dating of continental collisions. The collision and first pulse of compression are thought to have turned the Sinop-Boyabat fore-arc trough into a foreland basin.

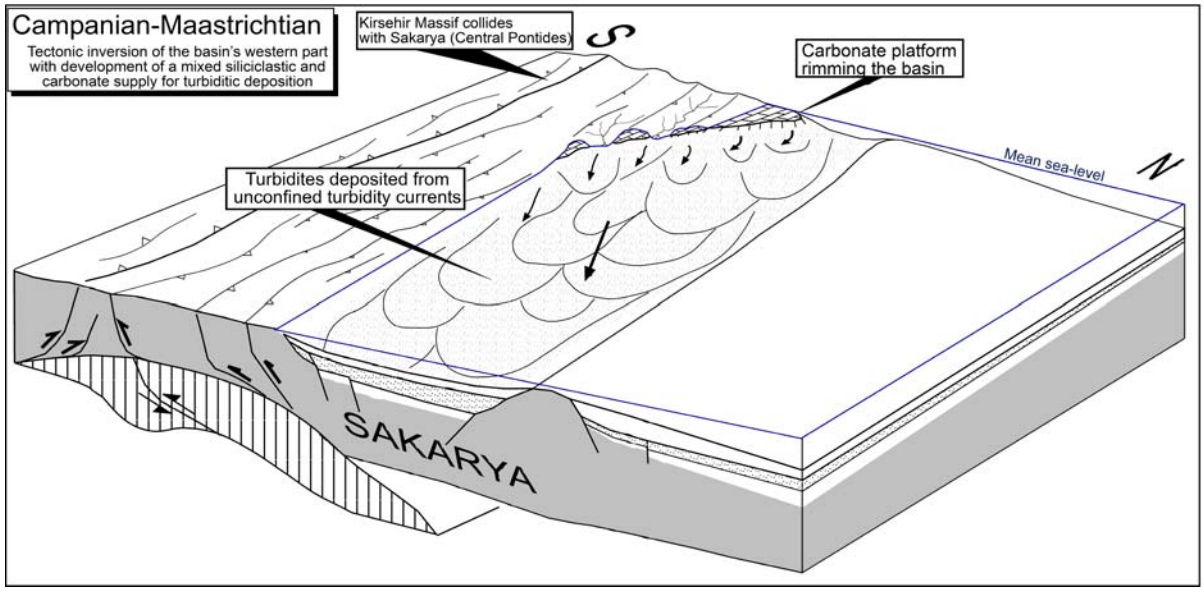

Figure 5.5. Schematic model of the tectonic and palaeogeographical setting of the Sinop-Boyabat Basin in Campanian to Maastrichtian time. The collision of Kirşehir Massif with Sakarya Zone in the western part of Central Pontides (cf. Fig. 5.3) elevated the basin's south-western margin and western neighbourhood, which supplied abundant siliciclastic sediment – dispersed eastwards by turbidity currents (Gürsökü Fm.); a shallow-marine reefal platform began to develop, perched on the basin margin and shedding calcareous sediment during storms.

Notably, the Cide Uplift in the adjacent Western Pontides (Fig. 5.3) is considered to have been was uplifted by the end of Campanian and submerged again in Maastrichtian time (Tüysüz, 1999), which mirrors the tectonic development in the Central Pontides. It is possible that some of the siliciclastic sediment of the Gürsökü Formation in the Sinop-Boyabat Basin was derived from the Cide Uplift, through a long fluvial system. However, the more adjacent Araç-Daday Belt, Daday-Devrekani Massif and Küre Complex of the Western Pontides (Fig. 5.3), also uplifted due to the Kirşehir-Sakarya collision, are more likely as a possible source area contributing to the sediment supply from the basin's

southern (SW) margin. Except for a small area between the southern Küre Complex and the Daday-Devrekani Massif, no Late Cretaceous or younger deposits have been found to the west of the Sinop-Boyabat Basin (Aydın *et al.*, 1995b), which may suggest exposure and denudation at that time.

Late Maastrichtian to Early Palaeocene (Fig. 5.6) – The deposition of the calcareous Akveren Formation in the Sinop-Boyabat Basin indicates an abundant sediment supply chiefly from the reefal platform (Fig. 5.1) that probably expanded along the basin's south-western margin. The calciturbiditic depositional system aggraded and is thought to have evolved from a carbonate slope apron (*sensu* Mullins and Cook, 1986) into a subhorizontal carbonate ramp linked directly with the reefal platform and its shoreline, with the turbidity currents generated by storms and earthquakes. The thickness of Akveren Formation (up to 600 m) represents more aggradation than progradation, which implies active subsidence, and hence continued tectonic extension. However, the rapid shallowing of the basin and the basinward expansion of the reefal platform recorded in the uppermost part (ca. 15 m) of the formation indicate a marked decline in the subsidence rate and possibly a pulse of mild compression (Fig. 5.2). As a result, the turbidite-prone carbonate slope apron turned into a carbonate ramp with a tempestites-prone offshore transition zone and storm-dominated littoral shoreface. The inferred pulse of compression might correspond with the end-Cretaceous development along the western segment of the subduction zone south of the Kirşehir Massif (Tauride-Anatolide Zone, Fig. 2.1), where trench-margin collision occurred at that time and ophiolites were emplaced southwards onto the Tauride microcontinent margin (Fig. 2.1), resulting in foundering of the Anamas-Akseki carbonate platform (Hayward, 1984; Collins and Robertson, 1998; Andrew and Robertson, 2002).

The compression was recorded in the Western Pontides (Okay and Tüysüz, 1999; Gürer and Aldanmaz, 2002), and hence was likely to affect also the Central Pontides. The Akveren Formation is correlative with a succession of micritic limestones, calciturbidites, carbonate olistromes and pelagic marlstones referred to by the same formation name in the Zonguldak and Devrek basins of the Western Pontides (Fig. 5.3) (Aydın *et al.*, 1995b; Görür, 1997; Tüysüz, 1999; Sunal and Tüysüz, 2002). Both the Central and Western

Pontide were thus dominated by bioclastic carbonate sedimentation at that time. The upper part of the Akveren Formation in the Western Pontides was interpreted to have recorded an uplift related to the onset of Tauride collision (Sunal and Tüysüz, 2002). No coeval deposits occur in the outer parts of the Eastern Pontides, but a thick succession of Palaeocene to Early Eocene calcareous deposits in the inner Eastern Pontides has been interpreted to bear a record of the collision (Okay and Tüysüz, 1999).

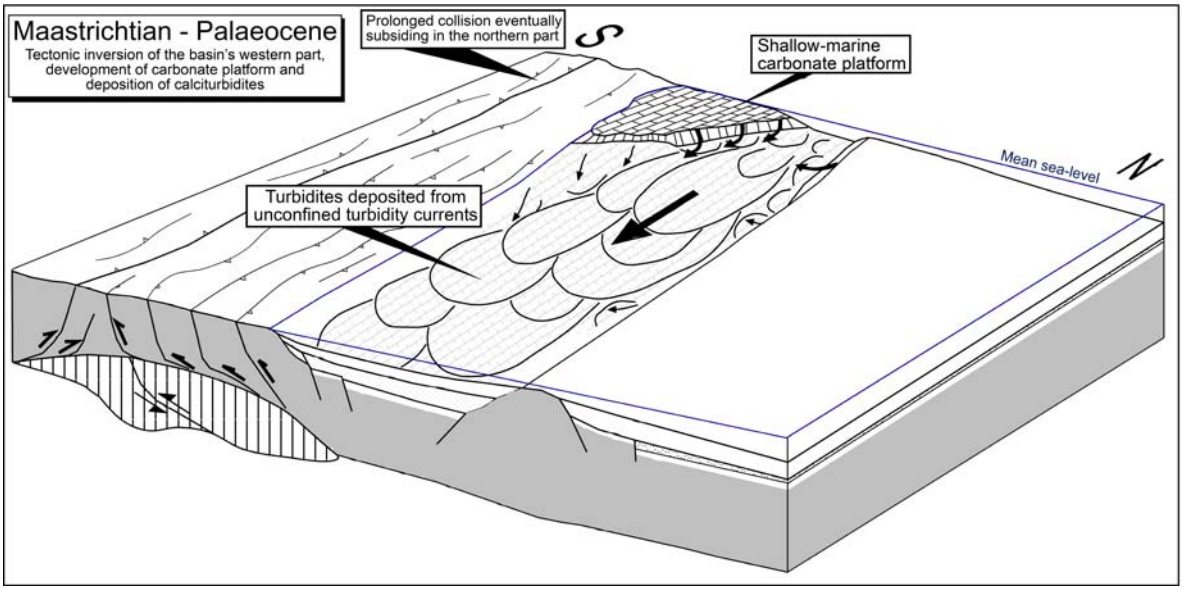

Figure 5.6. Schematic model for the tectonic and palaeogeographical setting of the Sinop-Boyabat Basin in Maastrichtian to Palaeocene time (Akveren Fm.). Calcareous sediment supplied from an extensive reefal platform, hosted by the basin's SW margin, was dispersed towards the east by storm-generated, non-channelized turbidity currents via a slope apron that aggraded and evolved into a shallowing-upward carbonate ramp. The reefal platform eventually expanded basinwards.

Late Palaeocene-Early Eocene (Fig. 5.7) – The deposition of the muddy, variegated Atbaşı Formation in the Sinop-Boyabat Basin indicates a rapid increase in the relative sea level, with the bathymetric change from littoral to deep neritic or subneritic accompanied by a cessation of sand supply, decreased sedimentation rate and an intense seafloor-oxidation. The reefal platform was drowned and the shoreline had shifted away from the basin. Although a climatic change might have, theoretically, terminated the growth of the reefal platform, this factor alone would not explain the simultaneous termination of sand

delivery to the basin (arguably, no climatic change might possibly render a large marine basin nearly stormless for a period of 10 Myrs). The mudstone succession is interspersed with thin calcitempestites passing upwards into thin calciturbidites, which are interpreted to be the distal products of some of the strongest storms reworking the inactive carbonate platform along a far-displaced shoreline (Fig. 5.1).

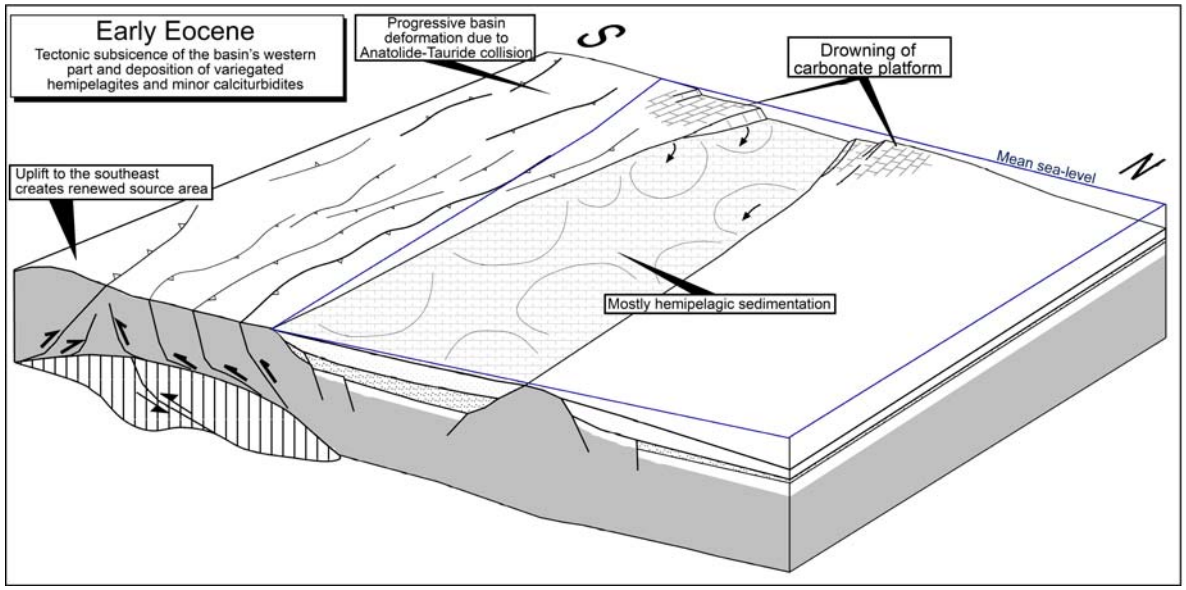

Figure 5.7. Schematic model for the tectonic and palaeogeographical setting of the Sinop-Boyabat Basin in Late Palaeocene to Early Eocene time (Atbaşı Fm.). A strong rifting pulse caused rapid increase in the relative sea level, and the bathymetric change from littoral to deep neritic or subneritic was accompanied by a cessation of sand supply, decreased sedimentation rate and an intense seafloor-oxidation resulting in sediment-starved conditions.

The drowning and deactivation of the littoral carbonate platform and the establishing of a sediment-starved deep-water environment is attributed to a strong pulse of rifting, which caused rapid subsidence of not only the basin floor (hangingwall block), but also the basin's southern margin (footwall block). The rifting event is thought to have been more pronounced in the western part of the basin, where the increased subsidence probably caused westward inclination of the basin floor. The overlying Kusuri Formation shows a complete reversal of the sediment transport direction along the basin axis, towards the west (Leren *et al*., 2002; Janbu *et al*., 2003).

Reddish, calcareous pelagic mudstones correlative with the Atbaşı Formation occur in the basins of Western Pontides, where they are referred to by the same formation name (Tüysüz, 1999). It is uncertain if similar deposits occur also in the inner Eastern Pontides, where a thick succession of Early Eocene deposits has been reported by Okay and Tüysüz (1999), without a detailed description.

The Atbaşı Formation is overlain by the siliciclastic turbidites of the Kusuri Formation, deposited in the latest Early Eocene to Middle Eocene time. Its siliciclastic composition, channelized turbiditic system and westward palaeocurrent directions (Leren *et al*., 2002; Janbu *et al.*, 2003) indicate a major restructuring of the basin configuration. The collision of the last Africa-derived microcontinents with the Sakarya-Kirşehir margin along the Tauride-Anatolide Zone (Fig. 2.1) was diachronous, and its onset – by trench closer – occurred in the latest Palaeocene time in eastern Turkey (Okay and Tüysüz, 1999; Gürer and Aldanmaz, 2002). In the Early Eocene, continental suturing along the entire Tauride-Anatolide Zone commenced, with the Hoyran-Beysehir-Hadim nappes beginning to be emplaced southwards (Andrew and Robertson, 2002) and also the Lycian nappes beginning to form in the west – as indicated by their Eocene Yavus foreland basin (Collins and Robertson, 1998, 1999). The resulting pulse of tectonic compression is thought to have closed and uplifted the easternmost part of the Sinop-Boyabat Basin, thus activating the eastern siliciclastic source area, while simultaneously splitting the basin axially into two parallel troughs: the northern Sinop Basin and the southern Boyabat Basin. The intrabasinal pop-up ridge was formed by a southward thrust coupled with northward backthrust (see the Ekinveren Thrust Zone and Erikli Fault in Fig. 2.2).

The closure of the whole Sinop-Boybat foreland basin by tectonic inversion (Leren *et al.,* 2002; Janbu *et al.*, 2003) is attributed to the main phase of emplacement of the Hoyran-Beysehir-Hadim and Lycian nappes (i.e., the climax of the Tuaride-Anatolide orogeny), which culminated in the Late Eocene, followed by gravitational last movements in the Early to Middle Oligocene time (Özgül, 1976; Collins and Robertson, 1998, 1999; Andrew and Robertson, 2002).

CHAPTER 6:
CONCLUSIONS

- The Late Cretaceous-Early Palaeogene sedimentary succession of the Sinop-Boyabat Basin in the Sakarya Zone of Central Pontides, northern Turkey, is nearly 7 km thick and provides a legible record of the basin's complex tectonic and palaeogeographical history. The present study of the Campanian-Early Eocene part of the basin-fill succession employed the sedimentological method of facies analysis, based on a detailed logging of outcrop sections and petrographical analysis of thin sections, supported with micropalaeontological and ichnological data.

- The Sinop-Boyabat Basin commenced its development in Barremian time, after the accretion of Sakarya microcontinent to the southern margin of Eurasia. The basin formed as a forearc graben associated with the volcanic arc created by the continuing northward subduction of the Neotethys oceanic plate – bearing a series of Africa-derived microcontinents. As the volcanic arc turned into the Western Black Sea Rift, the Sinop-Boyabat Basin – "hanging" on the rift's southern flank as an asymmetrical graben – continued to be controlled by tectonic extension, while becoming increasingly influenced by the orogenic compression resulting from the accretion of the successive microcontinents to the Sakarya margin. The encroaching Pontide orogeny, followed directly by the Tauride-Anatolide orogeny farther to the south, turned the extensional forearc graben into a rifting-controlled, compression-influenced foreland basin. The Sinop-Boyabat Basin is thus an unusual case of an active continental rift overtaken progressively by orogenic deformation.

- The alternating pulses of tectonic extension and compression, recognizable in the basin-fill succession and correlative with regional plate-tectonic events, culminated in the folding and tectonic inversion of the basin – coeval with the Late Eocene to Early Oligocene climax of the Tauride-Anatolide orogeny. This final pulse of strong northward compression marked the end of the formative process for the "Turkish Alps".

- The present study was focused on the Late Cretaceous to Early Eocene succession in the Sinop-Boyabat Basin, which is up to 2 km thick and comprises three formations (Gürsökü Fm., Akveren Fm. and Atbaşı Fm.). The deposits were described and their depositional processes interpreted in terms of eight component sedimentary facies, which were further recognized to form four major facies associations – stacked upon one another in the basin-fill succession.

- The Late Campanian-Early Maastrichtian Gürsökü Formation consists of alternating siliciclastic sandstones, calcareous mudstones and marlstones. These deposits are interpreted to represent the medial to distal reaches of an eastward-directed turbiditic system supplied with second-cycle volcanic detritus and increasingly more abundant bioclastic sediment from the basin's south-western margin. The sheet-like turbidites indicate unconfined currents of low to high density, but the system involved at least one isolated channel at the early stage. The system was subjected to a gradual retreat by backstepping, and it cannot be precluded that its proximal part included channels – whether perennial and shifting, or formed episodically by the largest currents. The activation of the southern (SW/W) siliciclastic source, where a contemporaneous reefal platform soon began to form, indicate an uplift that is attributed to the accretion of the Kirşehir microcontinent to the Sakarya margin in Campanian time.

- The Late Maastrichtian-Palaeocene Akveren Formation consists of sheet-like calcarenitic turbidites interbedded with marlstones, calcareous mudstones and subordinate bioclastic limestones. These deposits represent a carbonate slope apron sourced with bioclastic sediment from a reefal platform that expanded along the basin south-western margin and acted as the principal source. The turbiditic system aggraded and turned into a shallowing-upward carbonate ramp, initially turbidite-prone, but subsequently tempestites-prone and overlain by the basinward-expanding reefal platform. This rapid shallowing of the basin, recorded by the uppermost part of the formation, is attributed to the decline in subsidence, probably combined with a mild pulse of compressional uplift. The event correlates with the onset of continental collision in the adjacent Tauride-Anatolide Zone to the south.

- The Late Palaeocene-Early Eocene Atbaşı Formation, deposited in a deep neritic or subneritic, sediment-starved environment, consists of variegated calcareous mudstones interspersed with thin calcarenitic tempestites and turbidites. The rise in relative sea level and the cessation of sand supply are attributed to a wholesale rapid subsidence caused by strong rifting pulse, apparently instigated the opening process of Western Black Sea Rift.

- The overlying, Early-Middle Eocene Kusuri Formation is a siliciclastic turbiditic succession recording the last stages of the basin development, until its closure by tectonic inversion during the climax of the Tauride-Anatolide orogeny. This part of the basin-fill succession is the subject of a separate parallel study (N.E. Janbu, in prep.).

REFERENCES

Adams, A.E., MacKenzie, W.S., and Guilford, C. (1984) *Atlas of Sedimentary Rocks under the Microscope*. Longman, Harlow, 104 pp.

Adams, A.E., and MacKenzie, W.S. (1998) *A Colour Atlas of Carbonate Sediments and Rocks Under the Microscope*. Manson Publishing Ltd, London, 108 pp.

Aigner, T., and Reineck, H.-E. (1982) Proximality trends in modern storm sands from the Helgoland Bight (North Sea) and their implications for basin analysis. *Senckenbergiana Maritima,* **14**, 183-215.

Allen, J.R.L. (1982) *Sedimentary Structures: Their Character and Physical Basis.* Developments in Sedimentology, **30A-B**. Elsevier, Amsterdam, 1256 pp.

Allen, J.R.L. (1991) The Bouma division A and the possible duration of turbidity currents. *Journal of Sedimentary Petrology*, **61**, 291-295.

Andrew, T. and Robertson, A.H.F. (2002) The Beysahir-Hoyran-Hadim Nappes: genesis and emplacement of Mesozoic marginal and oceanic units of the northern Neotethys in southern Turkey. *Journal of the Geological Society of London,* **159**, 529-543.

Aydın, M., Demır, O., Serdar, H.S., Özaydin, S., and Harput, B. (1995a) Tectono-sedimentary evolution and hydrocarbon potential of the Sinop-Boyabat Basin, North Turkey. In: *Geology of the Black Sea Region* (Ed. by A. Erler, E. Tuncay, E. Bingöl and S. Örçen), General Directorate of Mineral Research and Exploration (MTA), Ankara, pp. 254-263.

Aydın, M., Demır, O., Özçelik, Y., Terzioğlu, N., and Satir, M. (1995b) A geological revision of Inebolu, Devrekani, Ağlı and Küre Areas: New observations in Paleotethys-Neotethys sedimentary successions. In: *Geology of the Black Sea Region: Proceedings of the International Symposium on the Geology of the Black Sea Region* (Ed. by A. Erler, E. Tuncay, E. Bingöl and S. Örçen), General Directorate of Mineral Research and Exploration (MTA), Ankara, pp. 33-38.

Bádenas, B., and Aurell, M. (2001) Proximal-distal facies relationships and sedimentary processes in a storm dominated carbonate ramp (Kimmeridgian, northwest of the Iberian Ranges, Spain). *Sedimentary Geology,* **139**, 319-340.

Badgley, P.C. (1959) *Stratigraphy and Petroleum Possibilities of the Sinop Region*. Tidewater Oil Co. Report, Petrol Isleri Genel Müdürlüğü arsivi, Ankara, 38 pp.

Bagnold, R.A. (1954) Experiments on a gravity-free dispersion of large, solid spheres in a Newtonian fluid model shear. *Proceedings of the Royal Society of London*, **A225**, 49-63.

Barka, A., Sutcu, Y.F., Gedik, A., Tekin, T.F., Arel, E., Özdemir, M., and Erkal, T., (1985) *Final Report Of The Geological Investigation Of The Sinop Nuclear Power Plant*, General Directorate of Mineral Research and Exploration (MTA) Report No: 7963, Ankara.

Boggs, S.J. (1995) *Principles of Sedimentology and Stratigraphy*. Prentice Hall, Upper Saddle River, N.J., 774 pp.

Bouma, A. (1962) *Sedimentology of Some Flysch Deposits*, Elsevier, Amsterdam, 168 pp.

Bowen, A.J. and Inman, D.L. (1969) Rip currents, 2: Laboratory and field evidence. *Journal of Geophysical Research,* **74**, 5479-5490.

Braga, J.C., Marin, J.M., and Wood, J.L. (2001) Submarine lobes and feeder channels of redeposited, temperate carbonate and mixed siliciclastic-carbonate platform deposits (Vera Basin, Almeria, southern Spain). *Sedimentology,* **48**, 99-116.

Bryhni, I. (1999) GeoLeksi, Geologisk Museum, Oslo; http://www.toyen.uio.no/geomus/leksi/.

Burchette, T.P., and Wright, V.P. (1992) Carbonate ramp depositional systems. *Sedimentary Geology,* **79**, 3-57.

Calvet, F., and Tucker, M.E. (1988) Outer ramp cycles in the Upper Mushelkalk of the Catalan

Basin, northeast Spain. *Sedimentary Geology,* **57,** 185-198.

Campbell, C.S. (1989) Self-lubrication of long runout landslides. *Journal of Geology,* **97**, 653-665.

Chan, M.A., and Dott, R.H. Jr. (1983) Shelf and deep-sea sedimentation in Eocene forearc basin, western Oregon – fan or non-fan? *American Association of Petroleum Geologists Bulletin,* **67**, 2100-2116.

Cloetingh, S., Spadini, G., Van Wees, J.D., and Beekman, F. (2003) Thermo-mechanical modelling of Black Sea Basin (de)formation. *Sedimentary Geology,* **156**, 169-184.

Collins, A.C. and Robertson, A.H.F. (1998) Processes of Late Cretaceous to Late Miocene episodic thrust sheet translation in the Lycian Taurides, SW Turkey. *Journal of the Geological Society of London,* **155**, 759-772.

Collins, A.C. and Robertson, A.H.F. (1999) Evolution of the Lycian allochthon, western Turkey, as a north-facing late Palaeozoic to Mesozoic rift and passive continental margin. *Geological Journal*, **34**, 107-138.

Collinson, J.D. and Thompson, D.B. (1982) *Sedimentary Structures*. Allen and Unwin, London, 207 pp.

Coniglio, M., and Dix, G.R. (1992) Carbonate slopes. In: *Facies Models: Response to Sea Level Change* (Ed by R.G. Walker, and N.P. James), Geological Association of Canada, St. John's, pp. 349-373.

Crimes, T.P. and Harper, J.C. (1970) *Trace Fossils.* Seel House Press, Liverpool, 547 pp.

Dalrymple, R.A. (1975) A mechanism for rip current generation on an open coast. *Journal of Geophysical Research,* **80**, 3485-3487.

DeCelles, P.G., and Cavazza, W. (1992) Constraints on the formation of Pliocene hummocky cross stratification in Calabria (Southern Italy) from consideration of hydraulic and dispersive equivalence, grain-flow theory, and suspended-load fallout rate. *Journal of Sedimentary Petrology*, **62**, 555-568.

Drake, T.G. (1990) Structural features in granular flows. *Journal of Geophysical Research,* **B95**, 8681-868.

Drzewiecki, P.A., and Simó, J.A. (2002) Depositional processes, triggering mechanisms and sediment composition of carbonate gravity flow deposits: examples from the Late Cretaceous of the south-central Pyrenees, Spain. *Sedimentary Geology,* **146,** 155-189.

Duke, W.L. (1990) Geostrophic circulation or shallow marine turbidity currents? The dilemma of paleoflow in storm-influenced prograding shoreline systems. *Journal of Sedimentary Petrology,* **60**, 870-883.

Duke, W.L., Arnott, R.W.C., and Cheel, R.J. (1991) Shelf sandstones and hummocky cross-stratification: New insights on a stormy debate. *Geology*, **19**, 625-628.

Dunham, R. J. (1962) Classification of carbonate rocks according to depositional textures. In: *Classification of Carbonate Rocks* (Ed by W.E. Ham), *American Association of Petroleum Geologists Memoir*, **1,** 108-121.

Ernst, G., and Zander, J. (1993) Stratigraphy, facies development, and trace fossils of the Upper Cretaceous of Southern Tanzania (Kilwa District). In: *Geology and Mineral Resources of Somalia and Surrounding Regions* (Ed. by E. Abbate, M. Sagri and F.P. Sassi), Istituto Agronomico per l'Oltremare, Florence, pp.259-278.

Faugeres, J.-C., and Stow, D.A.V. (1993) Bottom-current-controlled sedimentation; a synthesis of the contourite problem. *Sedimentary Geology,* **82**, 287-297.

Floyd, P.A., Göncüolğu, M.C., Winchester, J.A., and Yalınız, M.K. (2000) Geochemical character and tectonic environment of Neotethyan ophiolitic fragments and metabasites in the Central Anatolian Crystalline Complex. In: *Tectonics and Magmatism in Turkey and the Surrounding Area* (Ed. By E. Bozkurt, J.A. Winchester, and J.D.A. Piper), *Geological Society Special Publications*, **173**, 183-202.

Frey, R.W. (1975) *The Study of Trace Fossils.* Springer-Verlag, Berlin, 562 pp.

Gedik, A., and Korkmaz, S. (1984) Sinop havszasinin jeolojisi ve petrol olanaklari. *Geological Engineering,* **19**, 53-79.

Gedik, A., Ercan, T., and Korkmaz, S. (1984) Orta Karadeniz (Samsun-Sinop) havzasinin jeolojiisi ve volkanik kayaçlarin petrolojisi. *General Directorate of Mineral Research and Exploration (MTA) Bulletin***, 99/100,** 33-50.

Ghibaudo, G. (1992) Subaqueous sediment gravity flow deposits: practical criteria for their field description and classification. *Sedimentology***, 39,** 423-454.

Gierlowski-Kordesh, E., and Ernst, G. (1987) A flysch trace fossil assemblage from the Upper Cretaceous shelf of Tanzania. In: *Current Research in African Earth Sciences* (Ed. by G. Mathesis and H. Schandelmeier), A.A. Balkerna, Rotterdam, pp. 217-221.

Göksu, E., Pamir, H. N., and Erentöz, C. (1974) Samsun 1:500 000 map. *General Directorate of Mineral Research and Exploration (MTA)*, Ankara.

Göncüoğlu, M.C., Turhan, N., Şentürk, K., Özcan, A., Uysal, Ş., and Yalınız, M.K. (2000) A geotraverse across northwestern Turkey: tectonic units of the Central Sakarya region and their tectonic evolution. In: *Tectonics and Magmatism in Turkey and the Surrounding Area* (Ed. By E. Bozkurt, J.A. Winchester, and J.D.A. Piper), *Geological Society Special Publications*, **173**, 139-161.

Görür, N. (1997) Cretaceous syn- to postrift sedimentation on the southern continental margin of the Western Black Sea Basin. In: *Regional and Petroleum Geology of the Black Sea and Surrounding Regions* (Ed. by A.G. Robinson), *American Association of Petroleum Geologists Memoir*, **68,** 227-240.

Görür, N., and Tüysüz, O. (1997) Petroleum geology of the southern continental margin of the Black Sea. In: *Regional and Petroleum Geology of the Black Sea and Surrounding Regions* (Ed. by A.G. Robinson), *American Association of Petroleum Geologists Memoir*, **68,** 241-254.

Gruszczyński, M., Rudowski, S., Semil, J., Skomiński, J. and Zrobek, J. (1993) Rip currents as a geological tool. *Sedimentology,* **40**, 217-236.

Gürer, Ö.F., and Aldanmaz, E. (2002) Origin of the Upper Cretaceous-Tertiary sedimentary basins within the Tauride-Anatolide platform in Turkey. *Geological Magazine,* **139**, 191-197.

Hamblin, A.P., and Walker R. G. (1979) Storm-dominated shallow marine deposits; the Fernie-Kootenay (Jurassic) transition, southern Rocky Mountains. *Canadian Journal of Earth Sciences,* **16**, 1673-1690.

Hampton, M.A. (1975) Competence of fine-grained debris flows. *Journal of Sedimentary Petrology,* **45**, 834-844.

Harms, J.C., Walker, R.G., and Spearing, D. (1975) *Depositional Environments as Interpreted from Primary Sedimentary Structures and Stratification Sequences*. Soc. Econ. Paleont. Mineral. Short Course Lecture Notes 2, Tulsa.

Harms, J.C., Southard, J.B., and Walker, R.G. (1982). *Structures and Sequences in Clastic Rocks.* Soc. Econ. Paleont. Mineral. Short Course Lecture Notes 9, Tulsa.

Harris, M.T. (1994) The foreslope and toe-of-slope facies of the Middle Triassic Latemar buildup (Dolomites, northern Italy). *Journal of Sedimentary Research*, **B64**, 132-145.

Hay, W.W., Sibuet, J.-C. *et al.* (1984) *Initial Reports of the Deep Sea Drilling Project*. U.S. Government Printing Office, Washington, D.C.

Hayward, A.B. (1984) Sedimentation and basin formation related to ophiolite nappe emplacement, Miocene, SW Turkey. *Sedimentary Geology,* **40**, 105-129.

Hesse, R. (1987) Selective and reversible carbonate-silica replacements in Lower Cretaceous carbonate-bearing turbidites of the Eastern Alps. *Sedimentology*, **34,** 1055-1077.

Hesse, R. (1989) "Drainage systems" associated with mid-ocean channels and submarine yazoos: Alternative to submarine fan depositional systems*. Geology,* **17**, 1148-1151.

Hesse, R., and Rakofsky, A. (1992) Deep-sea channel/submarine-yazoo system of the Labrador Sea: a new deep-water facies model. *American Association of Petroleum Geologists Bulletin,* **76**, 680-707.

Howard, J.D., Valentine, J.W. and Warme, J.E. (1971) *Recent Advances in Paleontology and Ichnology.* AGI Short Course Lecture Notes, American Geological Institute, Washington, 267 pp.

James, N.P., and Bone, Y. (1991) Origin of a cool-water, Oligo-Miocene deep shelf limestone, Eucla Platform, southern Australia. *Sedimentology*, **38**, 323-341.

James, N.P., and Bourque, P.-A. (1992) Reefs and mounds. In: *Facies Models: Response to Sea Level Changes* (Ed. by R.G. Walker and N.P. James), Geological Association of Canada, St. John's, pp. 323-347.

James, N.P. (1997) The cool-water carbonate depositional realm. In: *Cool-water Carbonates* (Ed. by N.P. James and J.A.D. Clarke), *Society of Economic Paleontologists and Mineralogists Special Publication,* **56**, 1-19.

Janbu, N.E., Leren, B.L.S., Kırman, E., and Nemec, W. (2003) The Late Cretaceous-Eocene turbiditic sedimentation in the Sinop Basin, North-Central Turkey: Response to tectonic changes in basin morphology. In: *Abstracts from the American Association of Petroleum Geologists Annual Meeting*, Salt Lake City, pp. A84.

Johnson, A.M. (1970) *Physical Processes in Geology.* Freeman, Cooper & Co., San Fancisco, 577 pp.

Johnson, H.D., and Baldwin, C.T. (1996) Shallow clastic seas. In: *Sedimentary Environments: Processes, Facies and Stratigraphy* (Ed. by H.G. Reading), Blackwell Science, Oxford, pp. 232-280.

Jones, B., and Desrochers, A. (1992) Shallow platform carbonates. In: *Facies Models: Response to Sea Level Change* (Ed. by R.G. Walker and N.P. James), Geological Association of Canada, St. John's, pp. 277-301.

Jopling, A.V. (1965) Hydraulic factors controlling the shape of laminae in laboratory deltas. *Journal of Sedimentary Petrology,* **35**, 777-791.

Kazmin, V.G., Schreider, A.A., and Bulychev, A.A. (2000) Early stages of evolution of the Black Sea. In: *Tectonics and Magmatism in Turkey and the Surrounding Area* (Ed. By E. Bozkurt, J.A. Winchester, and J.D.A. Piper), *Geological Society Special Publications*, **173**, 235-249.

Kearey, P. (1996) *The New Penguin Dictionary of Geology*. Penguin Group, London, 365 pp.

Ketin, I., and Gümüş, Ö. (1963) *Sinop-Ayancık arasindaki III*, Bölgeye dahil shalarin jeolojisi hakkinda rapor, 2. Kisim, Jura ve Kretase Formasyonlarinin etüdü: Türkiye Petrolleri company report 213-288, 118 pp.

Kissel, C., Laj, C., Poisson, A., and Görür, N. (2003) Paleomagnetic reconstruction of the Cenozoic evolution of the Eastern Mediterranean. *Tectonophysics,* **362,** 199-217.

Kneller, B., and Branney, M. J. (1995) Sustained high-density currents and the deposition of thick massive sands. *Sedimentology***, 42,** 607-616.

Kneller, B., and Buckee, C. (2000) The structure and fluid mechanics of turbidity currents: a review of some recent studies and their geological implications. *Sedimentology*, **47**, 62-94.

Kneller, B. (2002) *Gravity Current Processes*. Short Course Lecture Notes, Department of Earth Science, University of Bergen, Bergen.

Lapidus, D.F., and Winstanley, I. (1990) *Collins Dictionary of Geology*, HarperCollins Publishers, New York, 562 pp.

Leckie, D.A., and Walker, R.G. (1982) Storm- and tide-dominated shorelines in Cretaceous Moosebar-lower Gates interval; outcrop equivalents of Deep Basin gas trap in Western Canada. *American Association of Petroleum Geologists Bulletin*, **66**, 138-157.

Lees, A., and Buller, A.T. (1972) Modern temperate-water and warm-water shelf carbonate

sediments contrasted. *Marine Geology,* **13**, 67-73.

Leren, B.L.S., Janbu, N.E., Kırman, E., and Nemec, W. (2002) The Late Cretaceous-Eocene turbiditic succession in the Sinop Basin, Turkey: Sedimentation in an evolving continental-margin rift closed by inversion. In: *16th International Sedimentological Congress Abstract Volume* (Ed. By M. Knoper and B. Cairncross), Rand Afrikaans University, Johannesburg, pp. 221-222.

Lien, T., Walker, R.G., and Martinsen, O.J. (2003) Turbidites in the Upper Carboniferous Ross Formation, western Ireland: reconstruction of a channel and spillover system. *Sedimentology*, **50,** 113-148.

Lønøy, A. (1996) *Carbonate Grains, Texture, Cements and Porosity*. Internal Research Report, U&P Division, Norsk Hydro Research Centre, Bergen.

Lowe, D.R. (1976) Grain flow and grain flow deposits. *Journal of Sedimentary Petrology,* **46**, 188-199.

Lowe, D.R. (1979) Sediment gravity flows: their classification and some problems of application to natural flows and deposits. *Society of Economic Paleontologists and Mineralogists Special Publication,* **27,** 75-82.

Lowe, D.R. (1982) Sediment gravity flows: II. Depositional models with special reference to the deposits of high-density turbidity currents. *Journal of Sedimentary Petrology*, **52**, 279-297.

Lowe, D.R. (1988). Suspended-load fallout rate as an independent variable in the analysis of current structures. *Sedimentology,* **35,** 765-776.

Meredith, D.J., and Egan, S.S. (2002) The geological and geodynamic evolution of the eastern Black Sea basin; insights from 2-D and 3-D tectonic modelling. *Tectonophysics*, **135**, 157-179.

Middleton, G.V. (1970) Experimental studies related to problems of flysch sedimentation. In: *Flysch Sedimentology in North America* (Ed. by J. Lajoie). *Geological Association of Canada Special Paper,* **7**, 253-272.

Middleton, G.V. and Hampton, M.A. (1976) Subaqueous sediment transport and deposition by sediment gravity flows. In: *Marine Sediment Transport and Environmental Management* (Ed. by D.J. Stanley and D.J.P. Swift). John Wiley, New York, pp. 197-218.

Middleton, G.V. and Southard, J.B. (1984) *Mechanics of Sediment Transport.* Society of Economic Paleontologists and Mineralogists, Tulsa.

Molina, J.M., Ruiz-Ortiz, P.A., and Vera, J.A. (1997) Calcareous tempestites in pelagic facies (Jurassic, Betic Cordilleras, Southern Spain). *Sedimentary Geology,* **109,** 95-109.

Monaco, P. (1992) Hummocky cross-stratified deposits and turbidites in some sequences of the Umbria-Marche area (central Italy) during the Toarcian. *Sedimentary Geology* **77**, 123-142.

Mount, J. (1985) Mixed siliciclastic and carbonate sediments: a proposed first-order textural and compositional classification. *Sedimentology,* **32,** 435-442.

Mullins, H.T., and Cook, H.E. (1986) Carbonate apron models: Alternatives to the submarine fan model for paleoenvironmental analysis and hydrocarbon exploration. *Sedimentary Geology,* **48,** 37-79.

Mutti, E. (1992) *Turbidite Sandstones*, Agip & Instituto di Geologia, University of Parma, Parma, 275 pp.

Myrow, P.M., and Southard, J.B. (1996) Tempestite deposition. *Journal of Sedimentary Research,* **66**, 875-887.

Myrow, P.M., Fisher, W., and Goodge, J.W. (2002) Wave-modified turbidites; combined-flow shoreline and shelf deposits, Cambrian, Antarctica. *Journal of Sedimentary Research*, **72**, 641-656.

Nemec, W., and Steel, R.J. (1984) Alluvial and coastal conglomerates: their significant features and some comments on gravelly mass-flow deposits. In: *Sedimentology of Gravels and Conglomerates* (Ed by E.H. Koster and R.J. Steel), *Canadian Society of Petroleum Geologists*

Memoir, **10**, 1-31.

Nemec, W. (1990) Aspects of sediment movement on steep delta slopes. In: *Coarse-Grained Deltas* (Ed. by A. Colella and D.B. Prior). *International Association of Sedimentologists Special Publication*, **10**, 29-73.

Nemec, W. (1995) The dynamics of deltaic suspension plumes. In: *The Geology of Deltas* (Ed. by M.N. Oti and G. Postma), A.A. Balkema, Rotterdam, pp. 31-93.

Nikishin, A.M., Korotaev, M.V., Ershov, A.V., and Brunet, M.-F. (2003) The Black Sea Basin: tectonic history and Neogene-Quarternary rapid subsidence modelling. *Sedimentary Geology,* **156,** 149-168.

Nøttvedt, A., and Kreisa, R.D. (1987) Model for the combined-flow origin of hummocky cross-stratification. *Geology*, **15,** 357-361.

Okay, A.I., Şengör, A.M.I., and Görür, N. (1994) Kinematic history of the opening of the Black Sea and its effect on surrounding regions. *Geology,* **22,** 267-270.

Okay, A.I., and Şahintürk, Ö. (1997) Geology of the Eastern Pontides. In: *Regional and Petroleum Geology of the Black Sea and Surrounding Regions* (Ed. by A.G. Robinson), *American Association of Petroleum Geologists Memoir*, **68,** 29-311.

Okay, A.I., and Tüysüz, O. (1999) Tethyan sutures of northern Turkey. In: *The Mediterranean Basins: Tertiary Extension within the Alpine Orogen* (Ed. by B. Durand, L. Jolivet, F. Horvath and M. Seranne), *Geological Society of London Special Publication*, **156,** 475-515.

Okay, A.I., Tansel, İ., and Tüysüz, O. (2001) Obduction, subduction and collision as reflected in the Upper Cretaceous-Lower Eocene sedimentary record of western Turkey. *Geological Magazine*, **138**, 117-142.

Özgül, N. (1976) Torosların bazı temel jeoloji özellikleri. *Bulletin of the Geological Society of Turkey,* **19**, 65-78.

Parker, G. (1982) Conditions for the ignition of catastrophically erosive turbidity currents. *Marine Geology*, **46**, 307-327.

Peakall, J., McCaffrey, B., and Kneller, B. (2000) A process model for the evolution, morphology, and architecture of sinuous submarine channels. *Journal of Sedimentary Research,* **70**, 434-448.

Pemberton, S.G., MacEachern, J.A., and Frey, R.W. (1992) Trace fossil facies models: environmental and allostratigraphic significance. In: *Facies Models: Response to Sea Level Change* (Ed by R.G. Walker and N.P. James), Geological Association of Canada, St. John's, 47-72.

Pettijohn, F.J., Potter, P.E., and Siever, R. (1987) *Sand and Sandstones*, Springer Verlag, New York, 553 pp.

Pickering, K.T., and Hiscott, R.N. (1985) Contained (reflected) turbidity currents from the Middle Ordovician Cloridorme Formation, Quebec, Canada: an alternative to the antidune hypothesis. *Sedimentology*, **32,** 373-394.

Pickering, K.T., Stow, D., Watson, M., and Hiscott, R. (1986) Deep-Water Facies, Processes and Models: A Review and Classification Scheme for Modern and Ancient Sediments. *Earth-Science Reviews*, **23,** 75-174.

Postma, G., Nemec, W., and Kleinspehn, K. (1988) Large floating clasts in turbidites: a mechanism for their emplacement. *Sedimentary Geology,* **58,** 47-61.

Prave, A.R., and Duke, W.L. (1990) Small-scale hummocky cross-stratification in turbidites: a form of antidune stratification. *Sedimentology***, 37**, 531-539.

Rangin, C., Bader, A.G., Pascal, G., Ecevitoğlu, B., and Görür, N. (2002) Deep structure of the Mid Black Sea High (offshore Turkey) imaged by multi-channel seismic survey (BLACKSIS cruise). *Marine Geology,* **182,** 265-278.

Reading, H.G., and Richards, M. (1994) Turbidite Systems in Deep- Water Basin Margins

Classified by Grain Size and Feeder System. *American Association of Petroleum Geologists Bulletin,* **78**, 792-822.

Reading, H.G., and Levell, B.K. (1996) Controls on the sedimentary rock record. In: *Sedimentary Environments: Processes, Facies and Stratigraphy* (Ed. by H.G. Reading), Blackwell Science, Oxford, pp. 5-36.

Robinson, A.G., Banks, C.J., Rutherford, M.M., and Hirst, J.P.P. (1995) Stratigraphic and structural development of the Eastern Pontides, Turkey. *Journal of the Geological Society, London,* **152,** 861-872.

Robinson, A.G., Rudat, J.H., Banks, C.J. and Wiles, R.L.F. (1996) Petroleum geology of the Black Sea. *Marine and Petroleum Geology,* **13,** 195-223.

Seguret, M., Moussine-Pouchkine, A., Gabaglia, G.R., and Bouchette, F. (2001) Storm deposits and storm generated coarse carbonate breccias on a pelagic outer shelf (South-East Basin, France). *Sedimentology*, **48**, 231-254.

Sonel, N., Sarı, A., Coşkun, B., and Tozlu, E. (1989) Importance of Ekinveren Fault in oil exploration in the Boyabat (Sinop) Basin. *Geological Bulletin of Turkey,* **32,** 39-49 (In Turkish, with English abstract).

Southard, J.B., Lambie, J.M., Federico, D.C., Pile, H.T., and Weidman, C.R. (1990) Experiments on bed configurations in fine sands under bidirectional purely oscillatory flow, and the origin of hummocky cross-stratification. *Journal of Sedimentary Petrology,* **60**, 1-17.

Stow, D.A.V., and Shanmugam, G. (1980) Sequence of structures in fine-grained turbidites: comparison of recent deep-sea and ancient flysch sediments. *Sedimentary Geology,* **25,** 23-42.

Stow, D.A.V., Wezel, F.C., Savelli, D., Rainey, S.C.R., and Angell, G. (1984) Depositional model for calcilutites: Scaglia Rossa limestones, Umbro-Marchean Apennines. In: *Fine-Grained Sediments: Deep-Water Processes and Facies* (Ed. by D.A.V. Stow and D.J.W. Piper), *Geological Society of London Special Publication,* **15,** 223-241.

Stow, D.A.V., and Piper, D.J.W. (1984). Deep-water fine-grained sediments: facies models. In: *Fine-Grained Sediments: Deep-Water Processes and Facies* (Ed by D.A.V. Stow, and D.J.W Piper), *Geological Society of London Special Publication,* **15**, 611-646.

Stow, D.A.V. (1985) Deep-sea clastics: where are we and where are we going? In: *Sedimentology: Recent Developments and Applied Aspects* (Ed. by P.J. Brenchley and B.P.J. Williams), *Geological Society of London Special Publication,* **18,** 67-93.

Stow, D.A.V., Reading, H.G., and Collinson, J.D. (1996) Deep seas. In: *Sedimentary Environments: Processes, Facies and Stratigraphy* (Ed. by H.G. Reading), Blackwell Science, Oxford, 395-453.

Sunal, G., and Tüysüz, O. (2002) Palaeostress analysis of Tertiary post-collisional structures in the Western Pontides, northern Turkey. *Geological Magazine,* **139**, 343-359.

Thompson & Thompson (1993) *Rose 1.0*. North Kiner Pike, Bloomington.

Tucker, M. E. (2001) *Sedimentary Petrology - An Introduction to the Origin of Sedimentary Rocks*, Blackwell Science, Oxford, 262 pp.

Tüysüz, O. (1990) Tectonic evolution of a part of the Tethyside orogenic collage: The Kargı Massif, northern Turkey. *Tectonics,* **9**, 141-160.

Tüysüz, O., Dellaloğlu, A.A., and Terzioğlu, N. (1995) A magmatic belt within the Neo-Tethyan suture zone and its role in the tectonic evolution of northern Turkey. *Tectonophysics,* **243,** 173-191.

Tüysüz, O. (1999) Geology of the Cretaceous sedimentary basins of the Western Pontides. *Geological Journal,* **34,** 75-93.

Ustaömer, T., and Robertson, A. (1997) Tectonic-Sedimentary Evolution of the North Tethyian Margin in the Central Pontides of Northern Turkey. In: *Regional and Petroleum Geology of the Black Sea and Surrounding Regions* (Ed. by A.G. Robinson), *American Association of*

Petroleum Geologists Memoir, **68,** 255-290.

Vera, J. A., and Molina, J. M. (1998) Shallowing-upward cycles in pelagic troughs. *Sedimentary Geology,* **119,** 103-121.

Vrolijk, P.J. and Southard, J.B. (1997) Experiments on rapid deposition of sand from high-velocity flows. *Geoscience Canada,* **24**, 45-54.

Walker, R.G. (1992) Turbidites and submarine fans. In: *Facies Models: Response to Sea Level Change* (Ed. by R.G. Walker and N.P. James), Geological Association of Canada, St. John's, pp. 239-264.

Walker, R.G., and Plint, A.G. (1992) Wave- and storm-dominated shallow marine systems. In: *Facies models: Response to Sea Level Change* (Ed by R.G. Walker and N.P. James), Geological Association of Canada, St. John's, pp. 219-238.

Wray, J.L. (1978) Calcareous algae. In: *Introduction to Marine Micropaleontology* (Ed by B.U. Haq and A. Boersma), Elsevier, Amsterdam, pp. 171-187.

Wright, V.P., and Burchette, T.P. (1996) Shallow-water carbonate environments. In: *Sedimentary Environments: Processes, Facies and Stratigraphy* (Ed. by H.G. Reading), Blackwell Science, Oxford, pp. 325-394.

Yılmaz, A., Adamia, S., Chabukiani, A., Chkhotua, T., Erdoğan, K., Tuzcu, S., and Karabıyıkoğlu, M. (2000) Structural correlation of the southern Transcaucasus (Georgia)-eastern Pontides (Turkey). In: *Tectonics and Magmatism in Turkey and the Surrounding Area* (Ed. By E. Bozkurt, J.A. Winchester, and J.D.A. Piper), *Geological Society Special Publications*, **173**, 171-182.

Yılmaz, Y., Tüysüz, O., Yiğitbaş, E., Genç, Ş.C., and Şengör, A.M.C. (1997) Geology and Tectonic Evolution of the Pontides. In: *Regional and Petroleum Geology of the Black Sea and Surrounding Regions* (Ed. by A.G. Robinson), *American Association of Petroleum Geologists Memoir*, **68,**183-226.

Yokokawa, M., Masuda, F. and Endo, N. (1995) Sand particle movement on migrating combined-flow ripples. *Journal of Sedimentary Research*, **A65**, 40-44.

APPENDIX

Appendix 1

Sedimentological logs 1 to 20

Appendix 2

Thin-section analyses

Appendix 1

Sedimentological logs 1 to 20

Log number	Location	Formation part	Facies association
1a	10 km S of Ayancik	Lower Gürsökü	FA 1a
1b	10 km S of Ayancik	Lower Gürsökü	FA 1b
2	400 m S of Çakıldak	Middle Gürsökü	FA 1a
3	Çakıldak village	Upper Gürsökü	FA 1a
4	300 m N of Çakıldak	Upper Gürsökü	FA 1a
5	1 km S of Tingir	Lower Akveren	FA 2c
6	Tangal	Lower-middle Akveren	FA 2c
7	Tangal	Middle Akveren	FA 2c
8	Sarnıç river valley	Middle Akveren	FA 2c
9	Sarnıç river valley	Middle Akveren	FA 2c
10	5 km E of Gerze	Middle Akveren	FA 2c
11	Kuğuköy	Middle-upper Akveren	FA 2a-2b
12	Kuğuköy	Middle-upper Akveren	FA 2a-2b
13	Kuğuköy	Middle-upper Akveren	FA 2a-2b
14	Kuğuköy	Upper Akveren	FA 2a-2b and FA 3a
15	5 km E of Gerze	Upper Akveren	FA 3b
16	Gerze pier	Upper Akveren	FA 3b
17	Yenikonak, E of river	Upper Akveren	FA 3b
18	Kuğuköy	Lower Atbaşı	FA 4a
19	Yenikonak, W of river	Lower Atbaşı	FA 4b
20	Tangal	Middle Atbaşı	FA 4c

Lithologies

Massive limestone

Massive sandstone

Marlstone

Calcareous mudstone

Clayey calcareous mudstone

Clasts, grains and fragments

Sandstone clasts

Marlstone clasts

Limestone clasts

Mud-clasts

Volcanic tuff-clasts

Other clast lithologies

Granules

Bioclasts

Plant detritus

Silica nodules

Structures

Erosive base

Loaded base

Sand injection-structures

Dish structures

Convoluted stratification and water escape structures

Planar parallel stratification

Graded planar parallelstratification

Scour and fill with sigmoidal cross stratification

Undulating stratification

Hummocky cross stratification

Trough cross stratification

Low-angled cross stratification

Current-ripple cross-lamination

Wave- and combined-flow ripple cross-lamination

Thin planar lamination

Bioturbation

Palaeocurrent direction

Sedimentary facies and subfacies

F1: Calcrudites of granule to pebble grade
- F1a: Clast-supported pebble calcrudite
- F1b: Clast- to matrix-supported, bioclastic granule calcrudites

F2: Thick- to medium-bedded siliciclastic sandstones and calcarenites with planar parallelstratification and/or current-ripple cross-lamination
- F2a: Very coarse- to very fine-grained siliciclastic sandstones
- F2b: Fine-grained to silty calcarenites

F3: Stratified calcarenites with wave-formed and combined-flow sedimentary stuctures

F4: Massive calcarenites

F5: Thin-bedded siliciclastic sandstones and calcarenites with mainly current-ripple cross-lamination
- F5a: Very coarse- to very fine-grained or silty siliciclastic sandstones
- F5b: Very fine-grained to silty calcarenites

F6: Massive bioclastic limestones
- F6a: Bedded limestones
- F6b: Non-bedded limestone

F7: Marlstones

F8: Calcareous mudstones
- F8a: Grey to greenish-grey calcareous mudstones
- F8b: Variegated calcareous mudstones

Facies associations and subassociations

FA 1: Predominantly siliciclastic turbidites
- FA 1a: Sheet-like turbidites with mud/marlcappings
- FA 1b: Isolated turbiditic palaeochannel

FA 2: Calcareous turbidites
- FA 2a: Packages of sand-dominated turbidites with chutes
- FA 2b: Packages of hemipelagites with thin sandy turbidites
- FA 2c: Basin-plain assemblage of alternating sheet-like turbidites and hemipelagites

FA 3: Carbonate ramp deposits
- FA 3a: Shallow-marine reef/alcomplex
- FA 3b: Storm-influenced offshore transition to wave-dominated shoreface deposits

FA 4: Carbonate ramp-drowning deposits
- FA 4a: Hemipelagites with tempestites/turbidites and massive limestones
- FA 4b: Basinal hemipelagites and tempestites
- FA 4c: Basinal hemipelagites and thin turbidites

Figure A1.1. Legend for logs 1a and 1b to 20 and figures containing logs.

LOG 1a

Location: 10 km S of Ayancik
Formation: Lower Gürsökü
Facies association: FA 1a
Facies content: F2a, F5a, F7, F8a

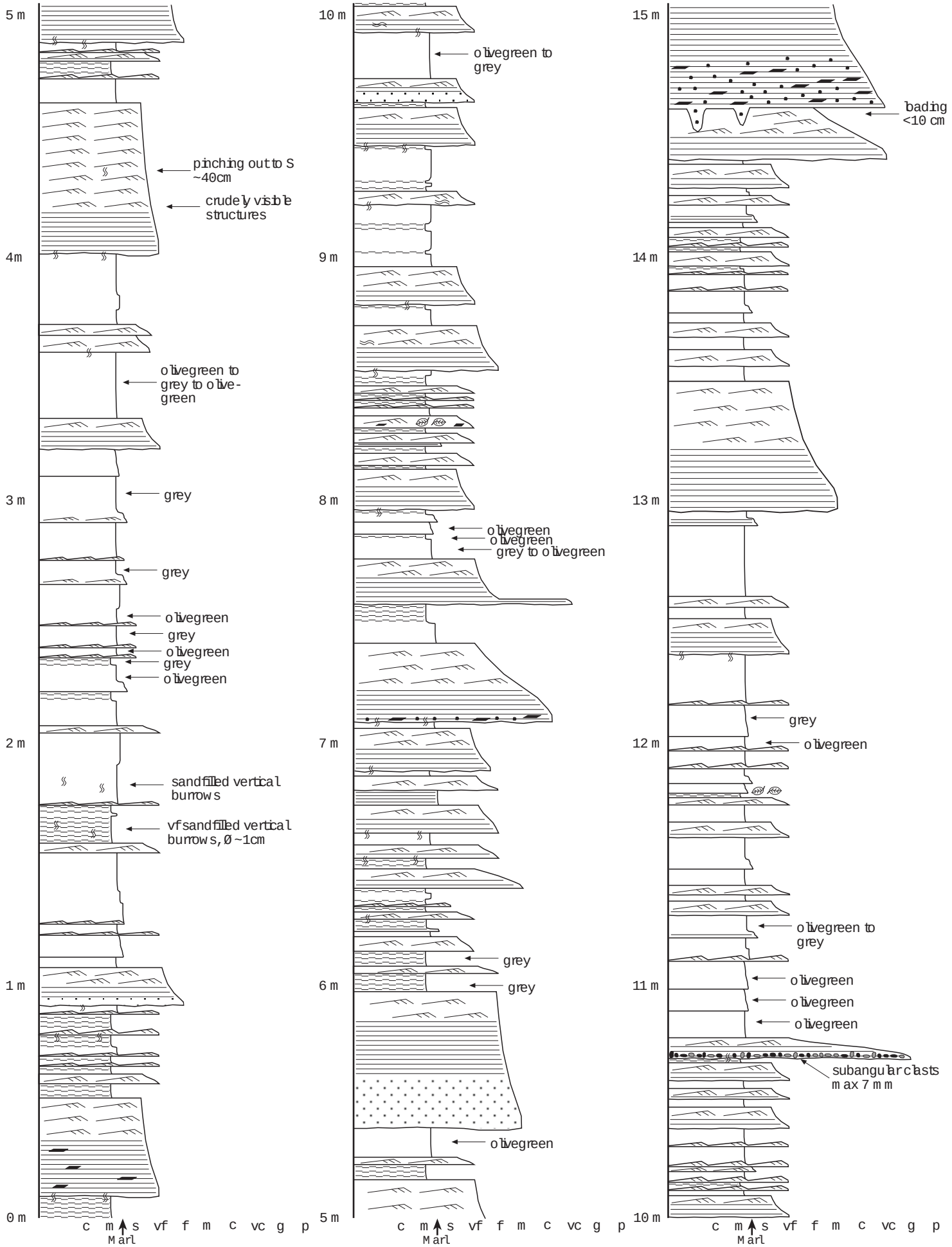

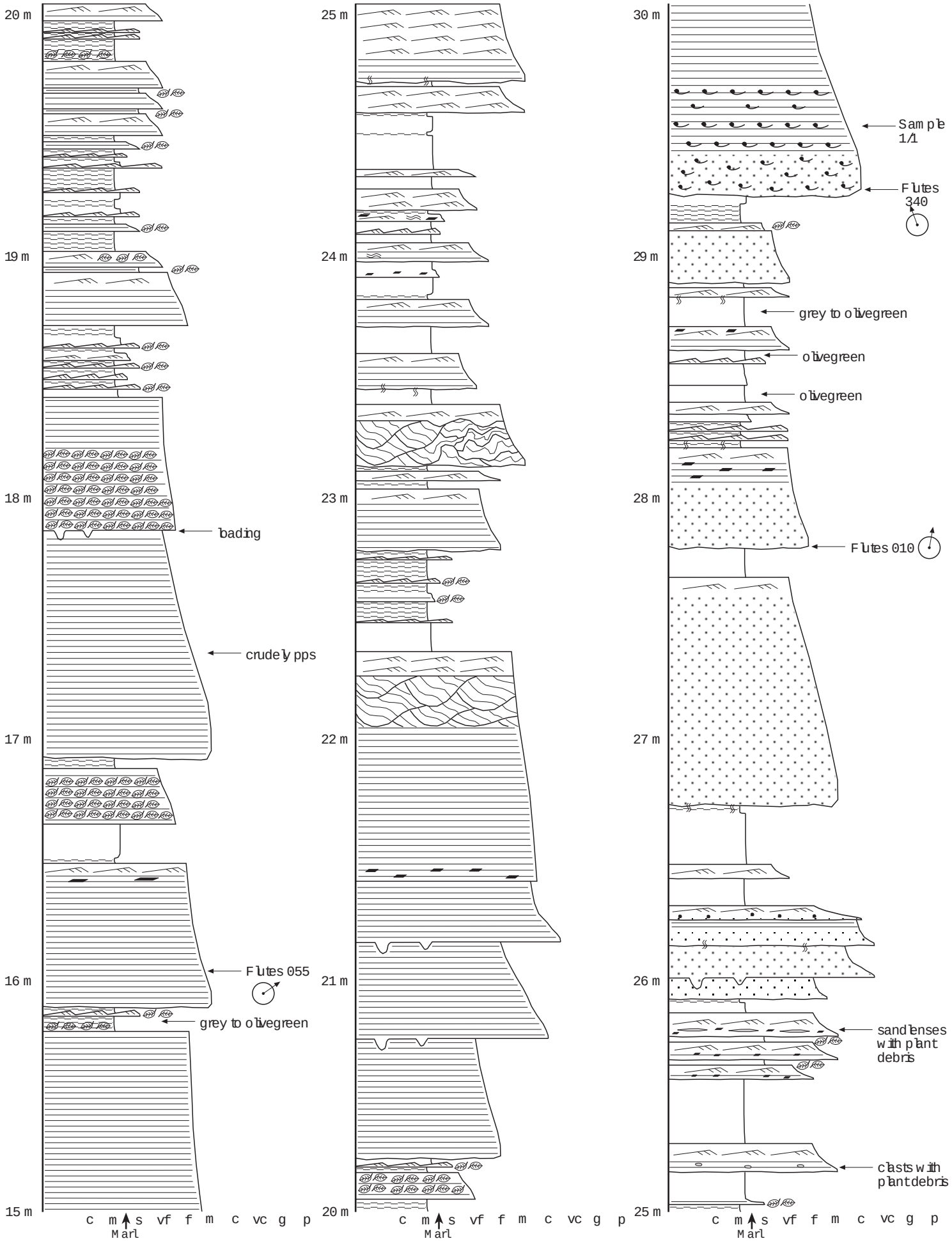
20 m
19 m
18 m
17 m
16 m
15 m
bading
crudely pps
Flutes 055
grey to olivegreen
c m s vf f m c vc g p
Marl
25 m
24 m
23 m
22 m
21 m
20 m
c m s vf f m c vc g p
Marl
30 m
29 m
28 m
27 m
26 m
25 m
Sample 1/1
Flutes 340
grey to olivegreen
olivegreen
olivegreen
Flutes 010
sand lenses with plant debris
clasts with plant debris
c m s vf f m c vc g p
Marl

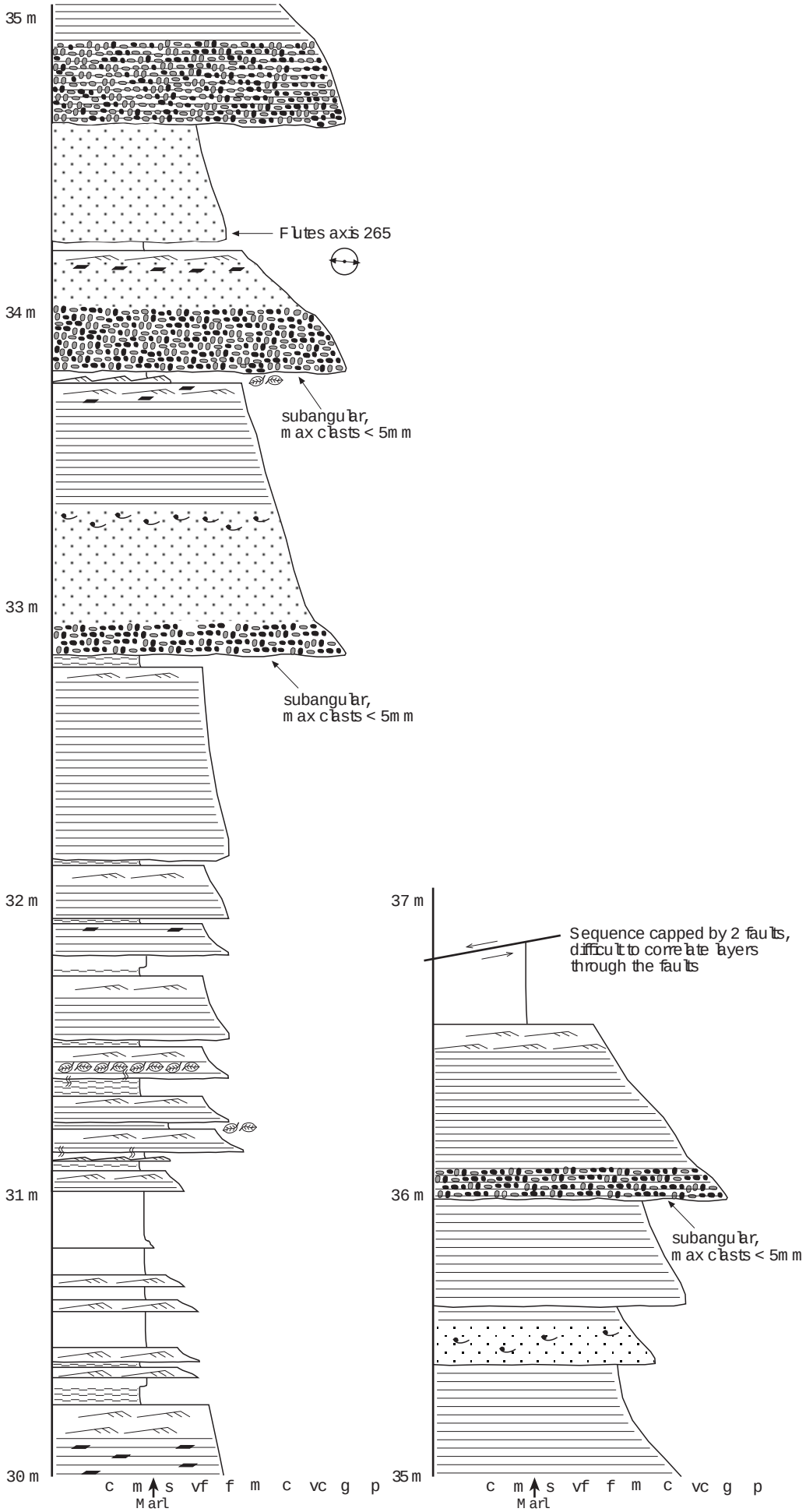
35 m
Flutes axis 265
34 m
subangular,
max clasts < 5mm
33 m
subangular,
max clasts < 5mm
32 m
31 m
30 m
c m s vf f m c vc g p
Marl
37 m
Sequence capped by 2 faults,
difficult to correlate layers
through the faults
36 m
subangular,
max clasts < 5mm
35 m
c m s vf f m c vc g p
Marl

LOG 1b

Location: 10 km S of Ayancik
Formation: Lower Gürsökü
Facies association: FA1b
Facies content: F2a, F5a, F7, F8a

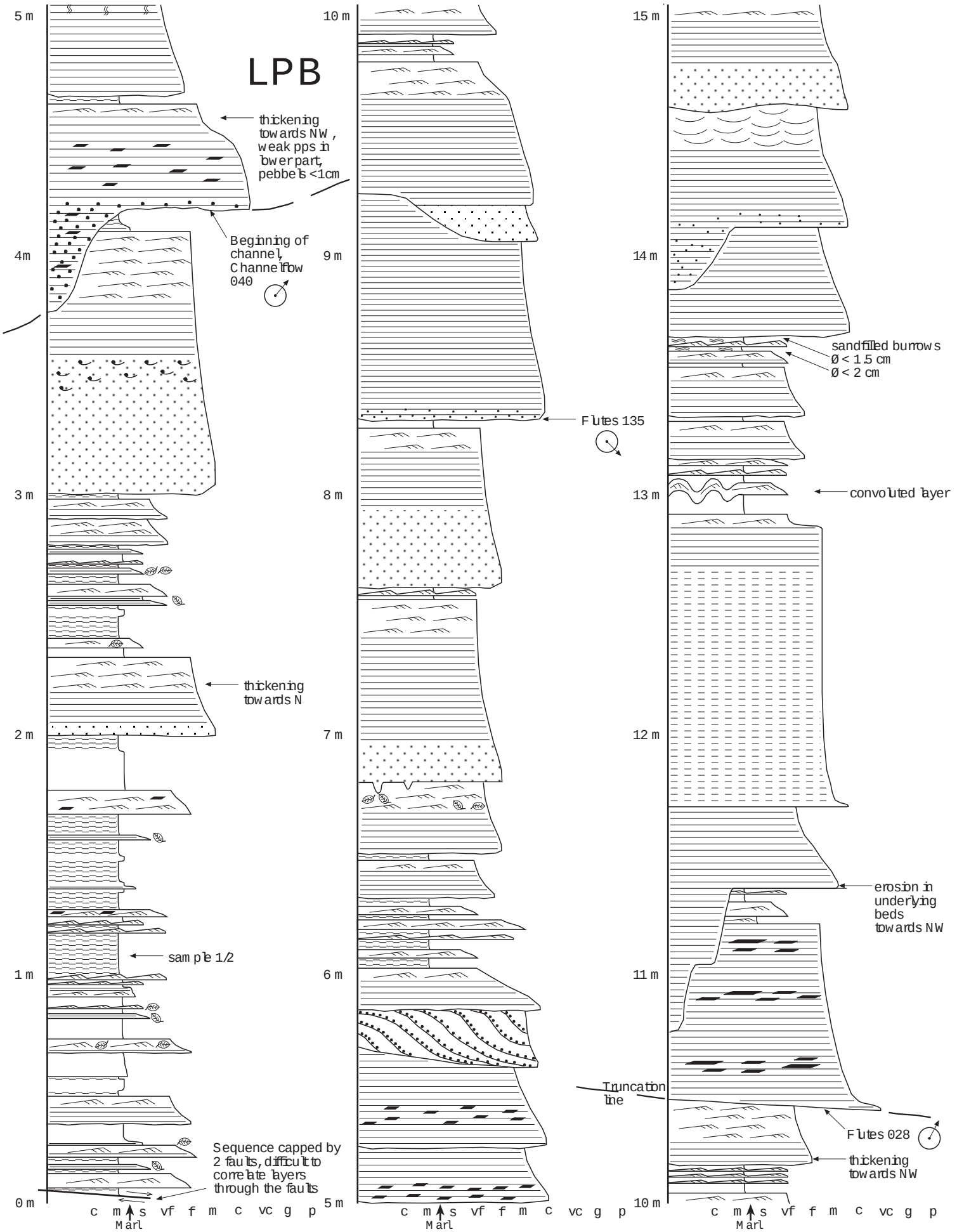

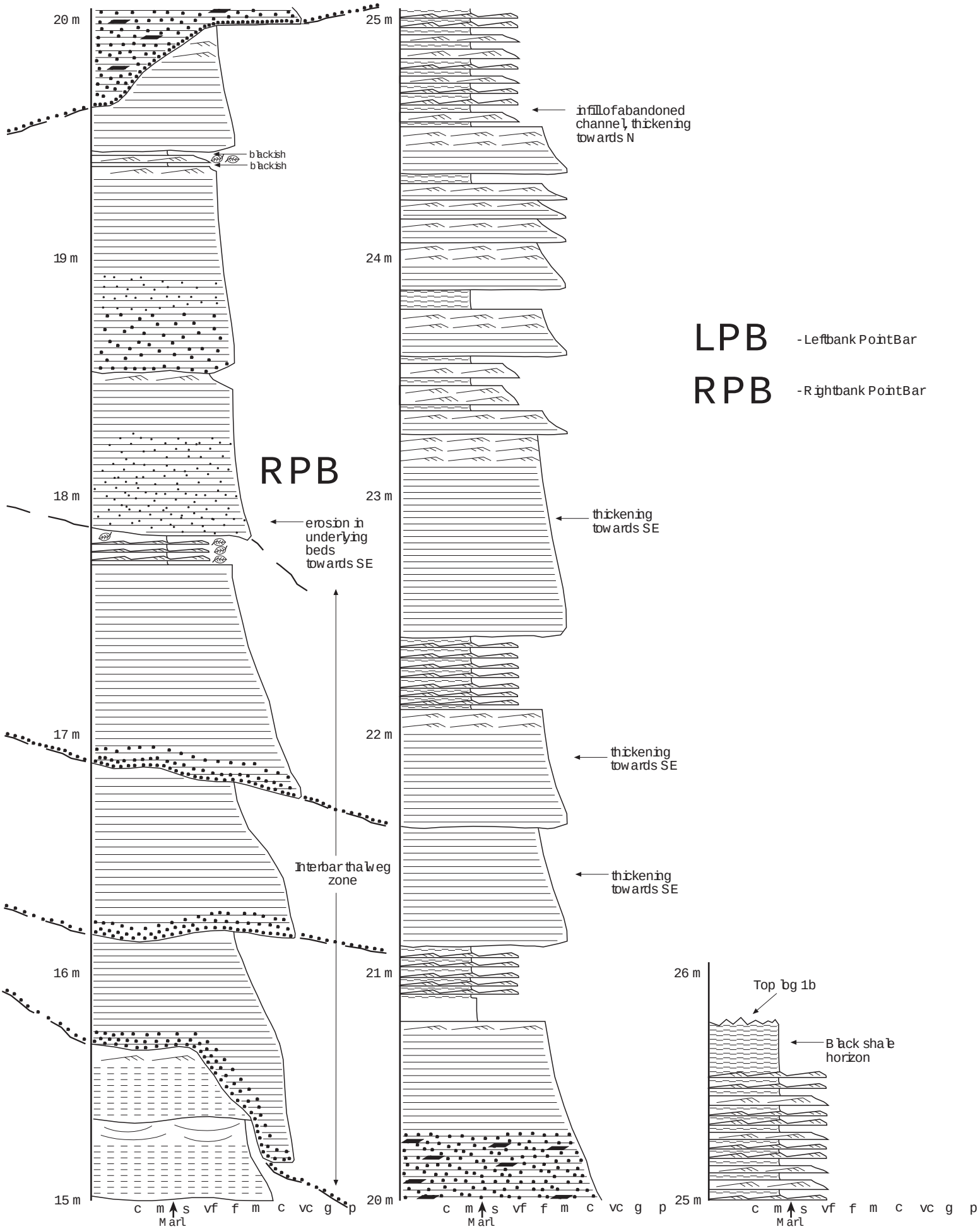
20 m
19 m
18 m
17 m
16 m
15 m
blackish
blackish
RPB
erosion in underlying beds towards SE
Interbar thalweg zone
c m s vf f m c vc g p
Marl
25 m
24 m
23 m
22 m
21 m
20 m
infill of abandoned channel, thickening towards N
thickening towards SE
thickening towards SE
thickening towards SE
c m s vf f m c vc g p
Marl
LPB - Leftbank Point Bar
RPB - Rightbank Point Bar
26 m
25 m
Top bg 1b
Black shale horizon
c m s vf f m c vc g p
Marl

LOG 2

Location: 400 m S of Çakýldak
Formation: middle Gürsökü
Facies association: FA 1a
Facies content: F2a, F5a, F7, F8a

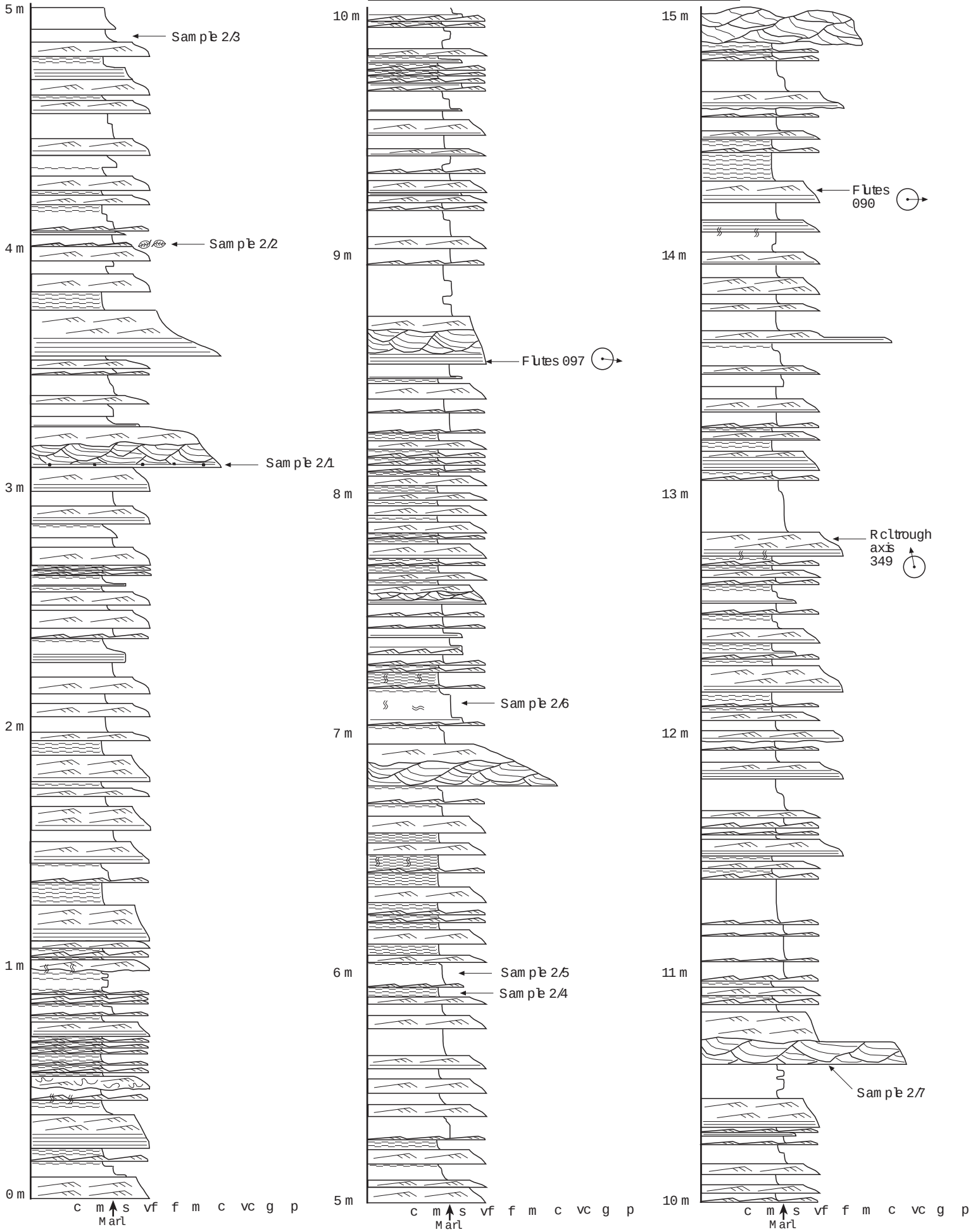

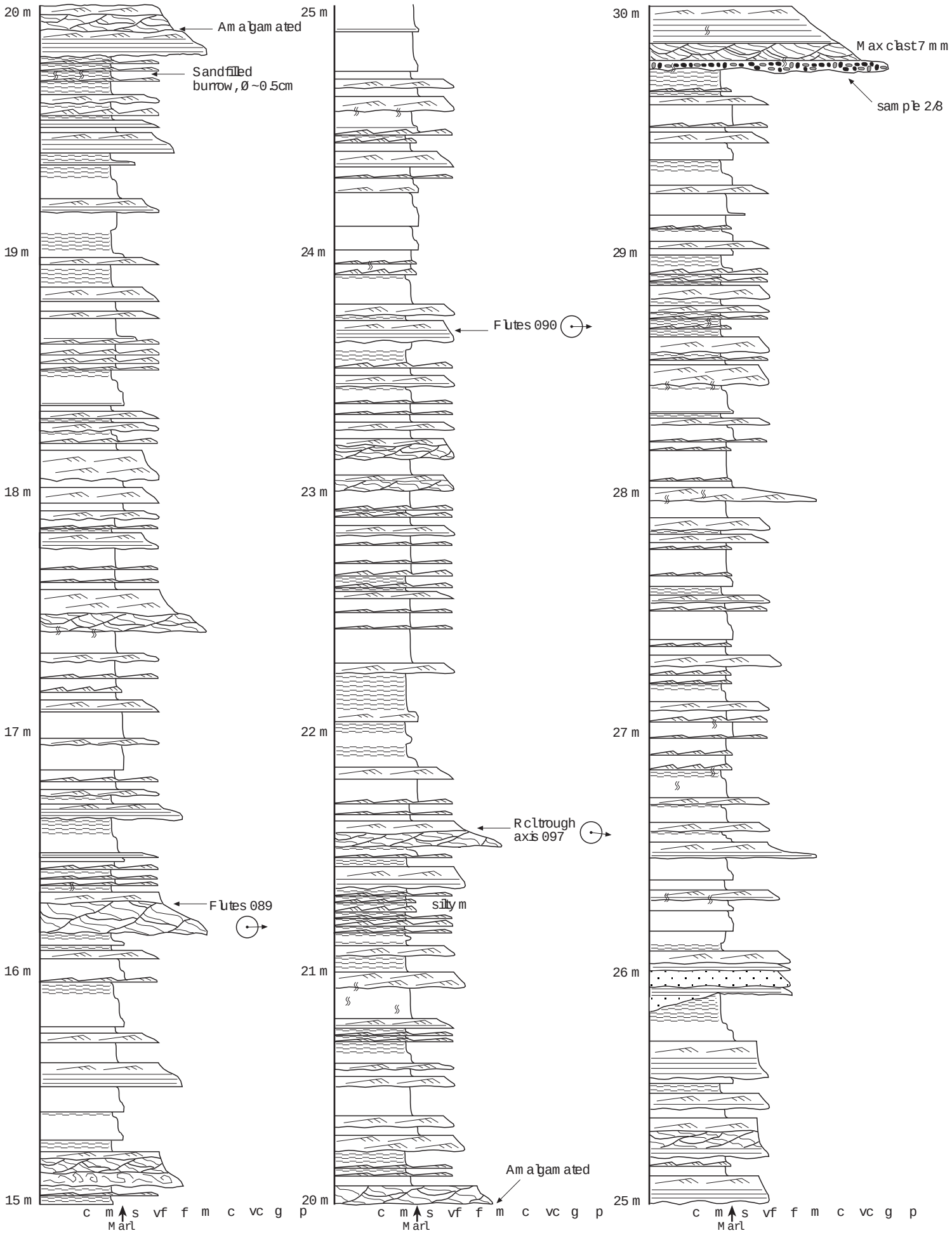
20 m
Amalgamated
Sandfilled burrow, Ø ~0.5cm
19 m
18 m
17 m
Flutes 089
16 m
15 m
c m s vf f m c vc g p
Marl
25 m
24 m
Flutes 090
23 m
22 m
Rcl trough axis 097
silty m
21 m
Amalgamated
20 m
c m s vf f m c vc g p
Marl
30 m
Max clast 7 mm
sample 2/8
29 m
28 m
27 m
26 m
25 m
c m s vf f m c vc g p
Marl

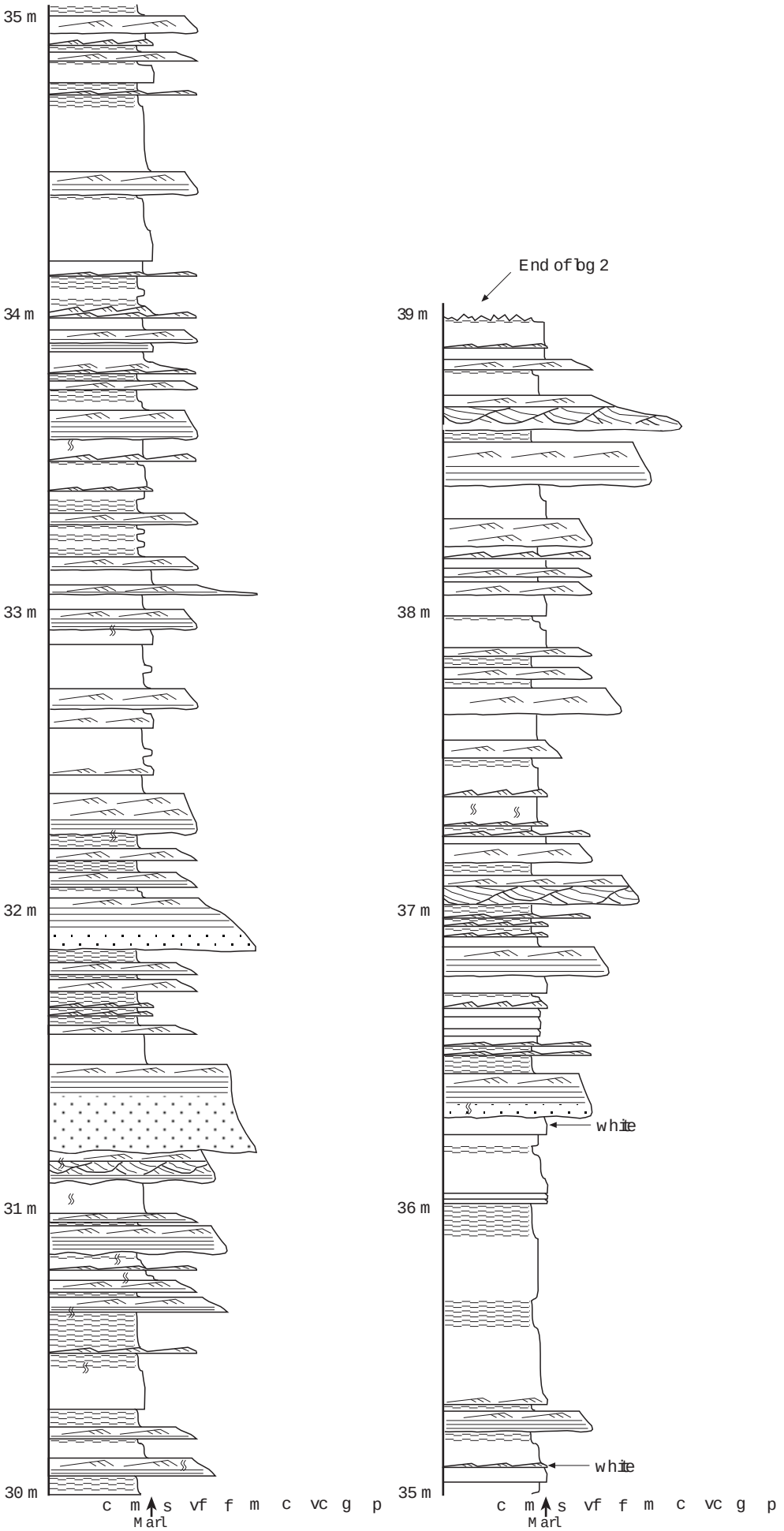
35 m
34 m
33 m
32 m
31 m
30 m
c m s vf f m c vc g p
Marl
End of log 2
39 m
38 m
37 m
36 m
35 m
white
white
c m s vf f m c vc g p
Marl

LOG 3

Location: Cakýdak village
Formation: middle Gürsöku
Facies association: FA 1a
Facies content: F2a, F5a, F7, F8a

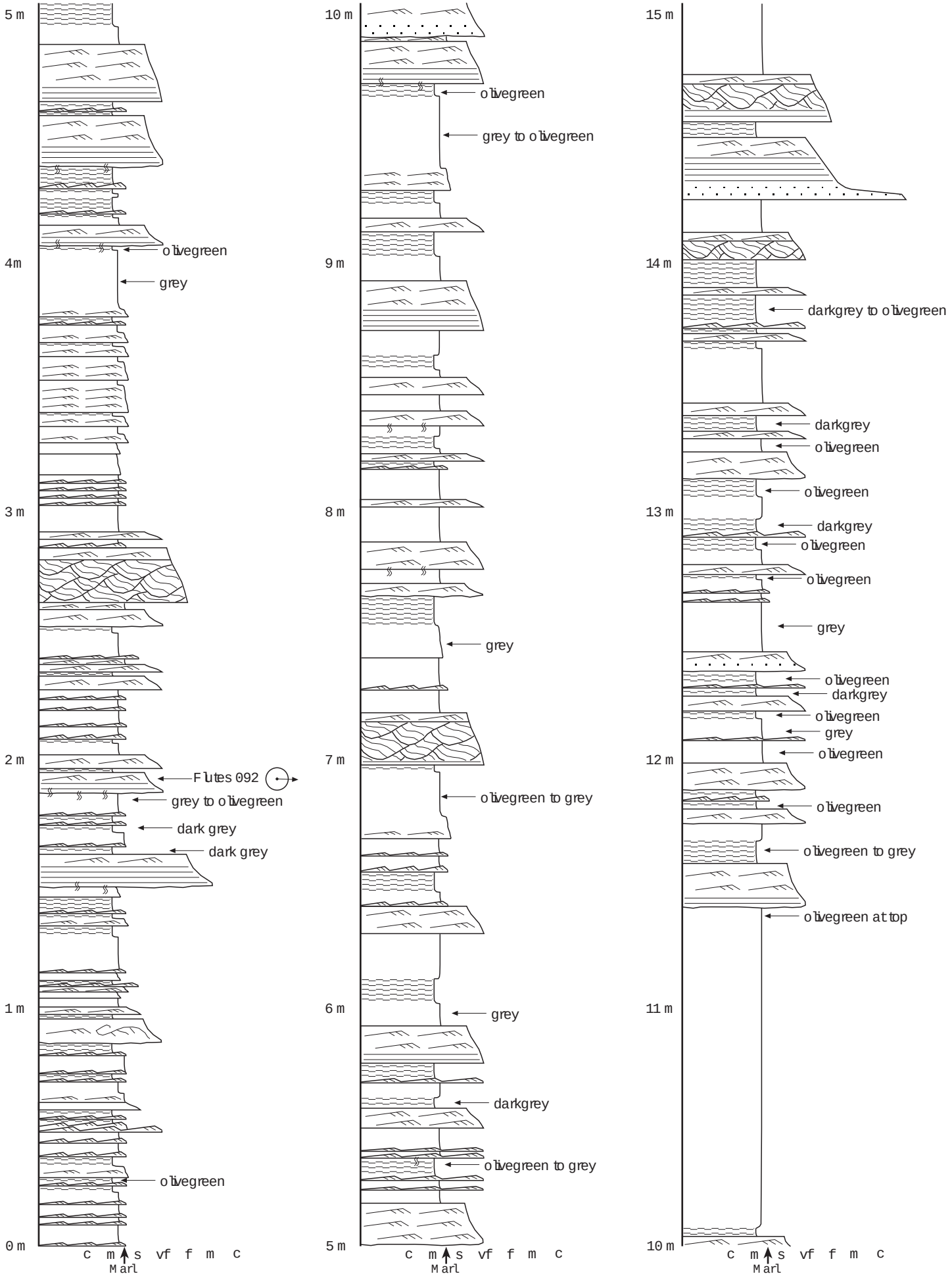

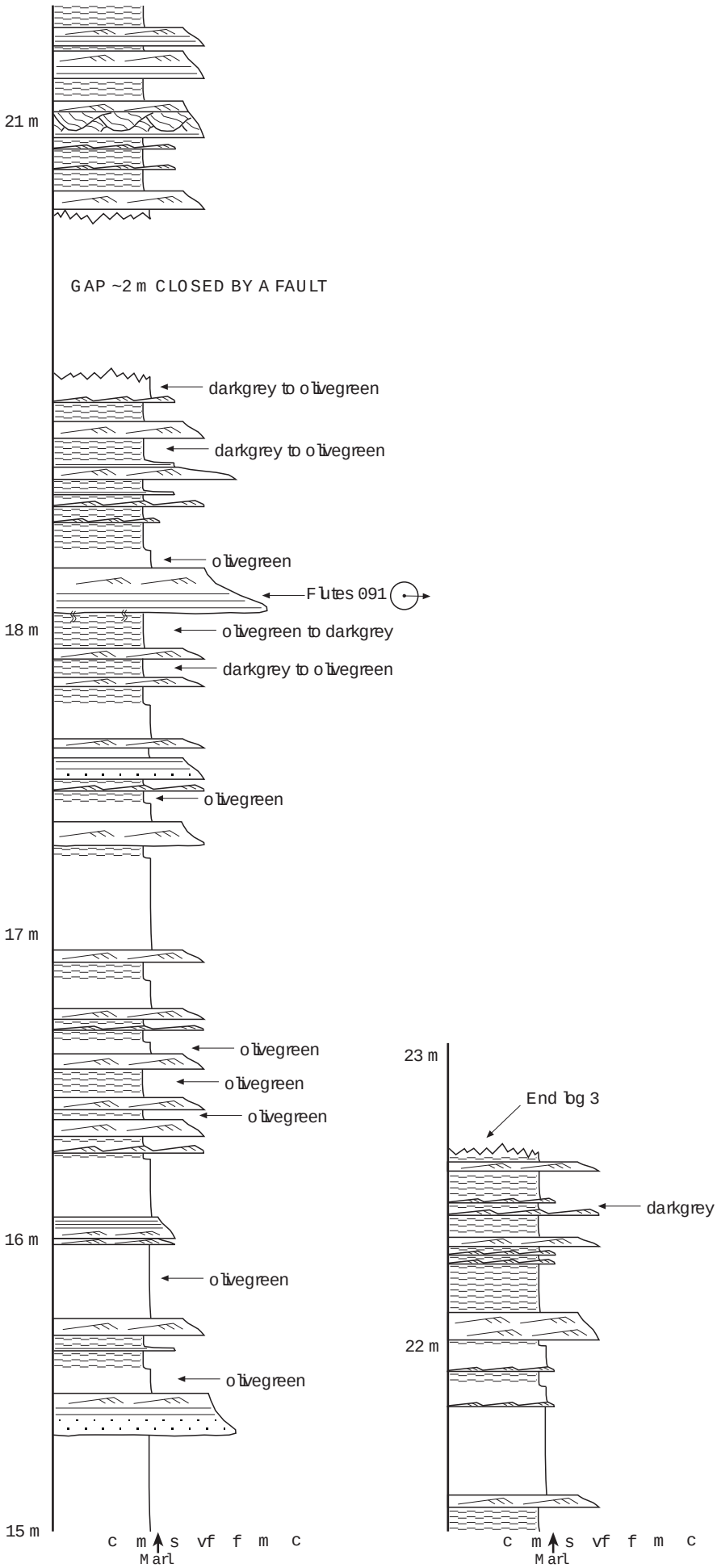
21 m
GAP ~2 m CLOSED BY A FAULT
dark grey to olive green
dark grey to olive green
olive green
Flutes 091
18 m
olive green to dark grey
dark grey to olive green
olive green
17 m
olive green
olive green
olive green
16 m
olive green
olive green
15 m
c m s vf f m c
Marl
23 m
End log 3
dark grey
22 m
c m s vf f m c
Marl

LOG 4

Location: 300 m N of Cakýldak
Formation: middle Gürsökü
Facies association: FA 1a
Facies content: F2a, F5a, F7, F8a

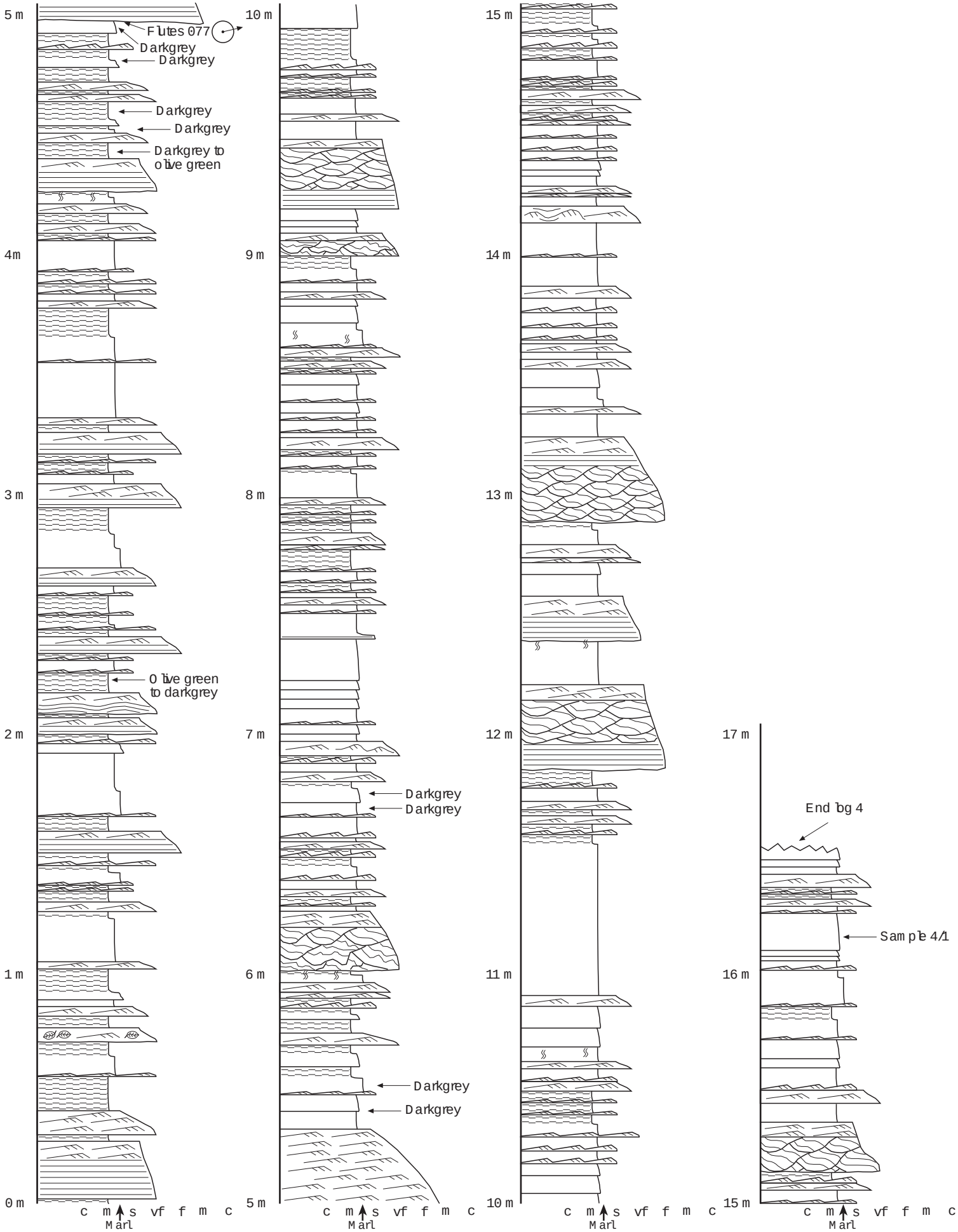

LOG 5

Location: 1 km S of Tingir
Formation: lower Akveren
Facies association: FA 2c
Facies content: F2b, F5b, F7, F8a

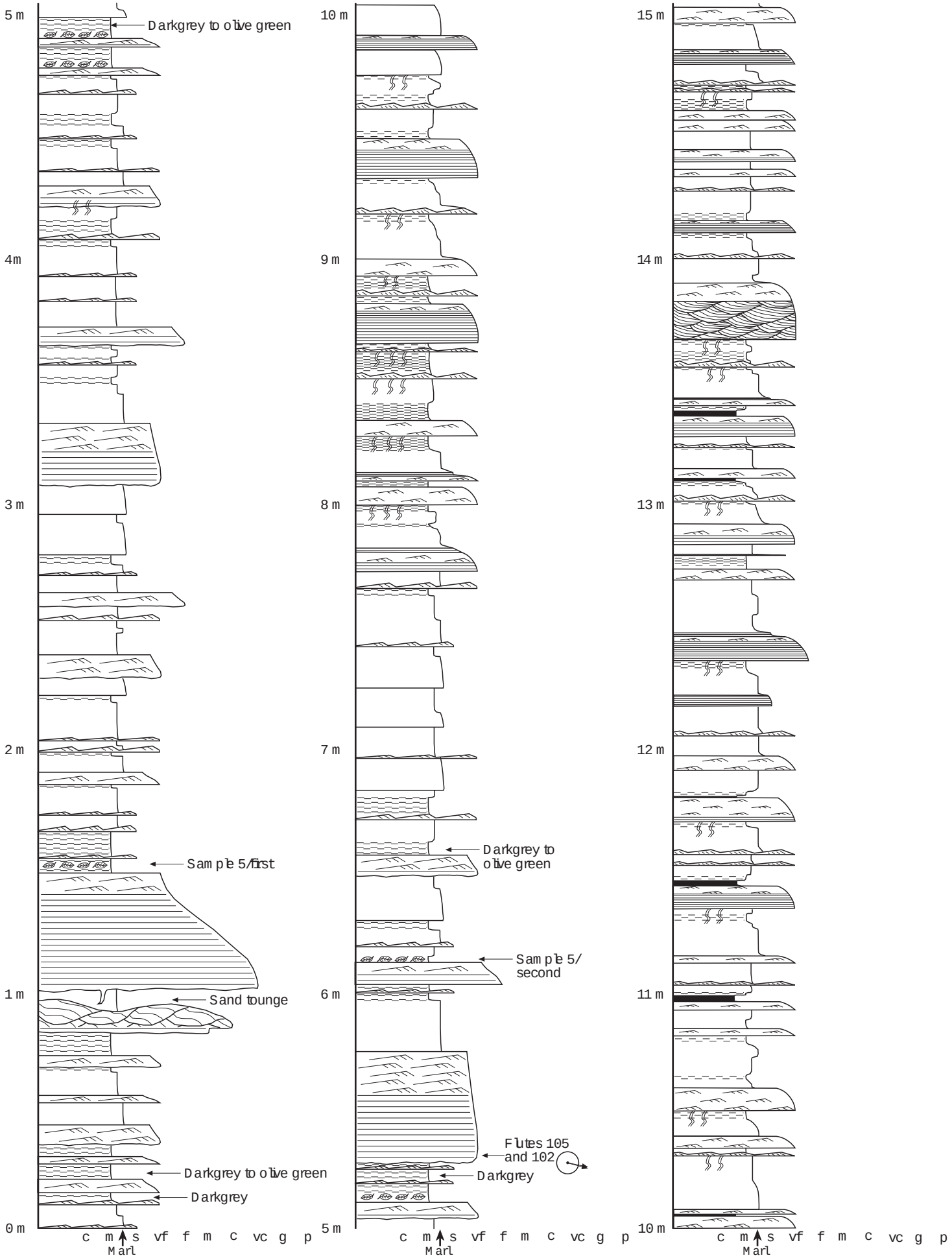

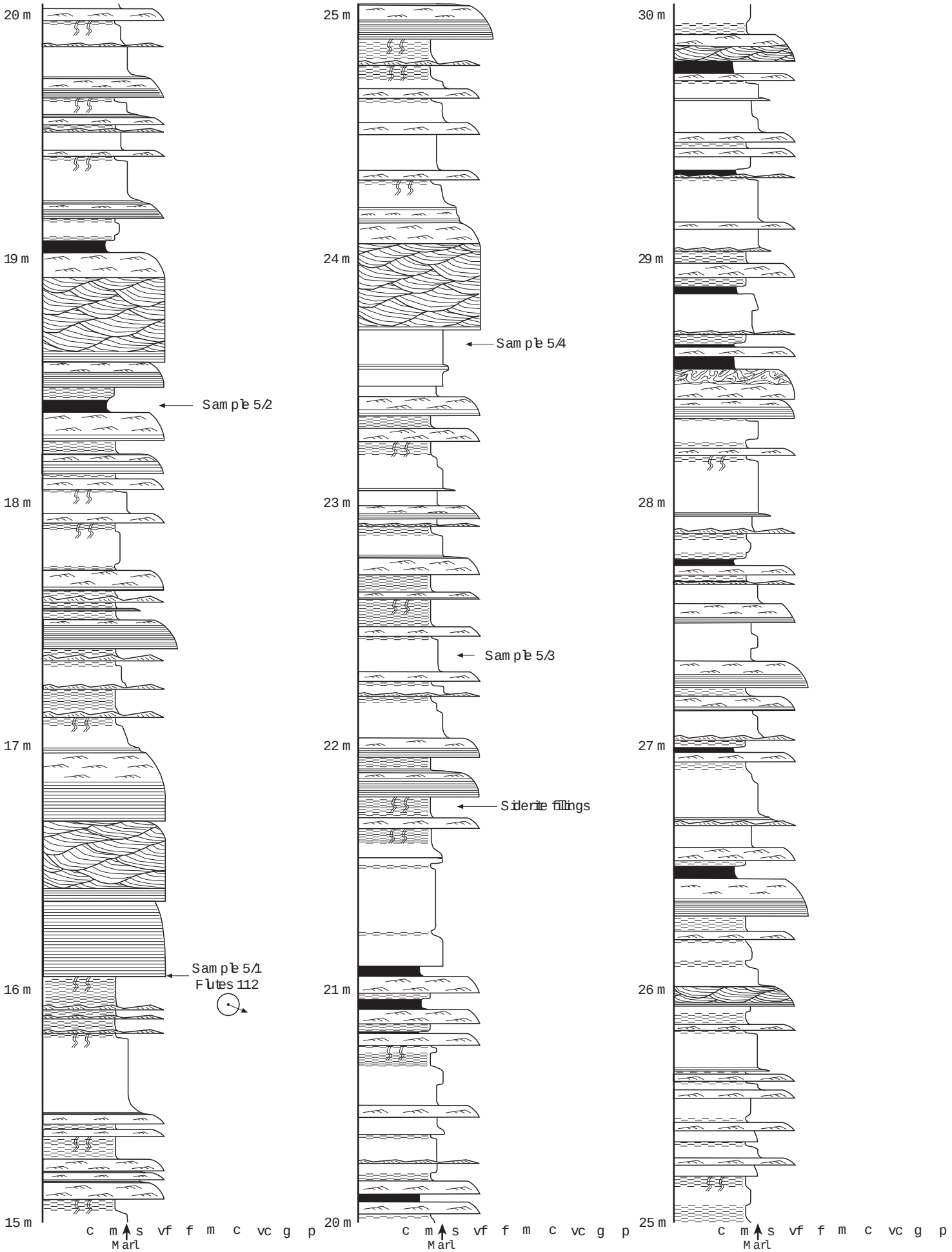
20 m
19 m
18 m
17 m
16 m
15 m
Sample 5/2
Sample 5/1
Flutes 112
c m s vf f m c vc g p
Marl
25 m
24 m
23 m
22 m
21 m
20 m
Sample 5/4
Sample 5/3
Siderite fillings
c m s vf f m c vc g p
Marl
30 m
29 m
28 m
27 m
26 m
25 m
c m s vf f m c vc g p
Marl

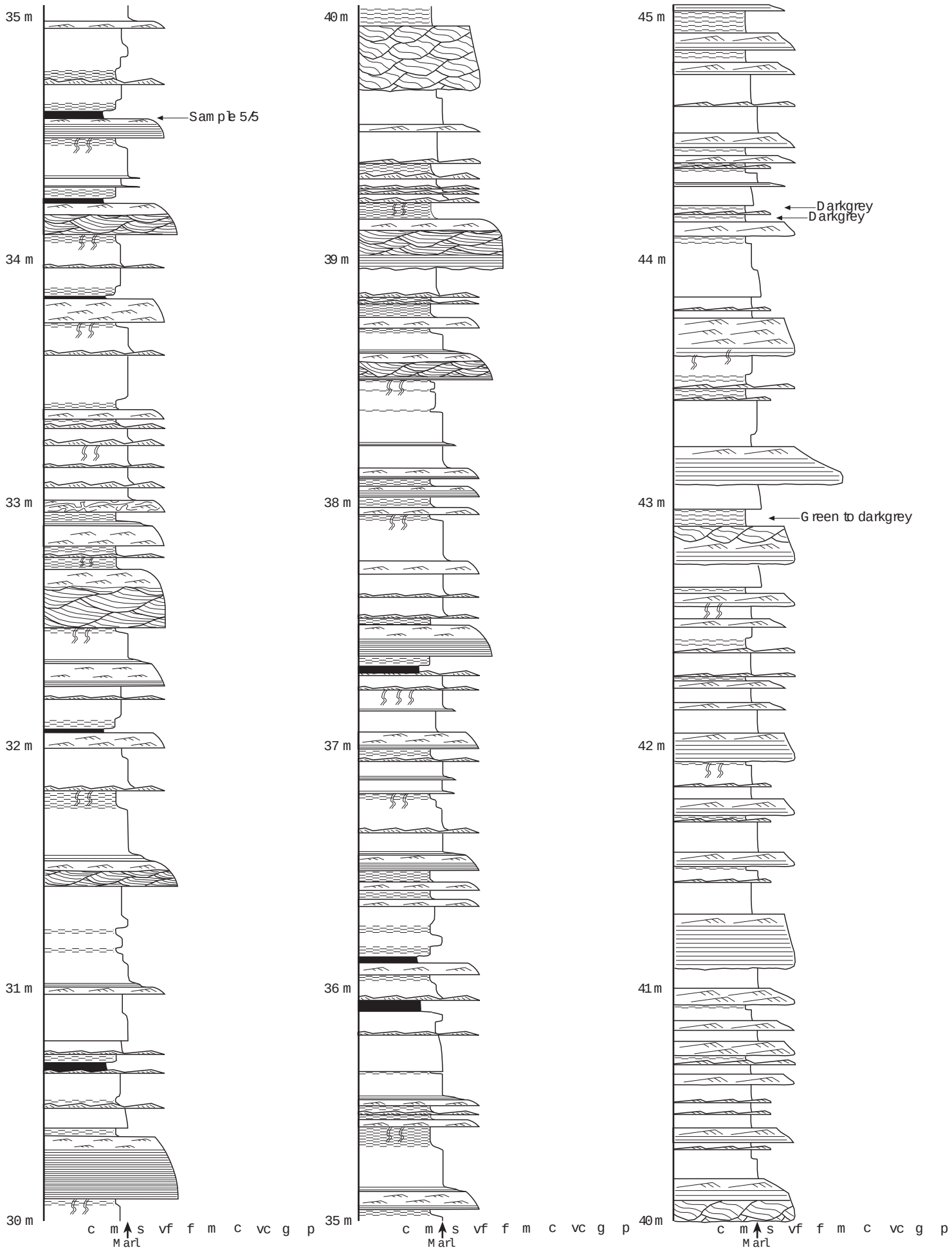
35 m
Sample 5/5
34 m
33 m
32 m
31 m
30 m
c m s vf f m c vc g p
Marl
40 m
39 m
38 m
37 m
36 m
35 m
c m s vf f m c vc g p
Marl
45 m
Darkgrey
Darkgrey
44 m
43 m
Green to darkgrey
42 m
41 m
40 m
c m s vf f m c vc g p
Marl

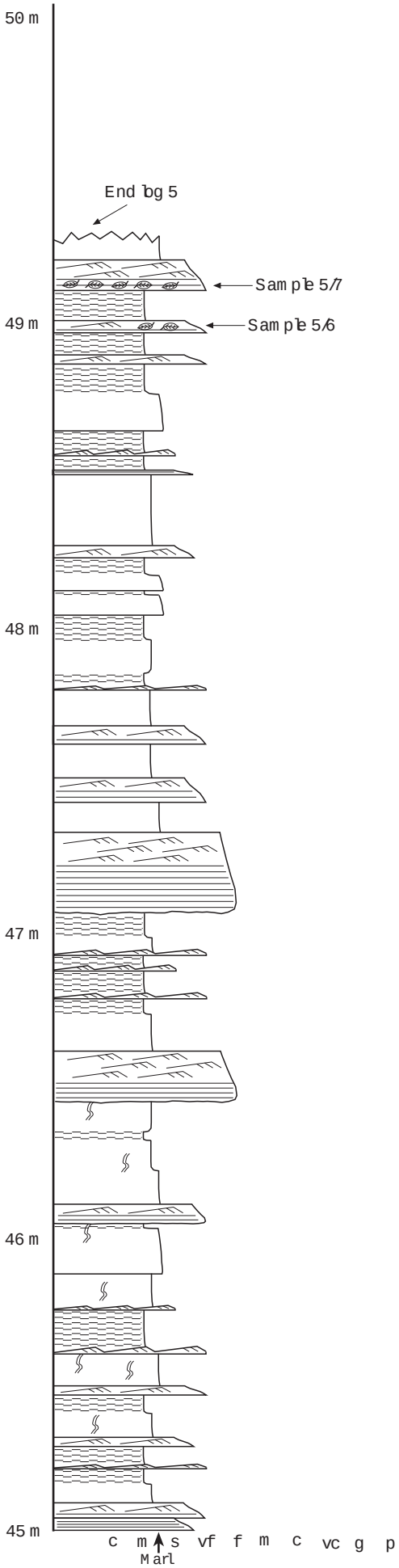
50 m
End log 5
Sample 5/7
49 m
Sample 5/6
48 m
47 m
46 m
45 m
c m s vf f m c vc g p
Marl

LOG 6

Location: Tangal
Formation: lower Akveren
Facies association: FA 2c
Facies content: F2b, F5b, F7, F8a

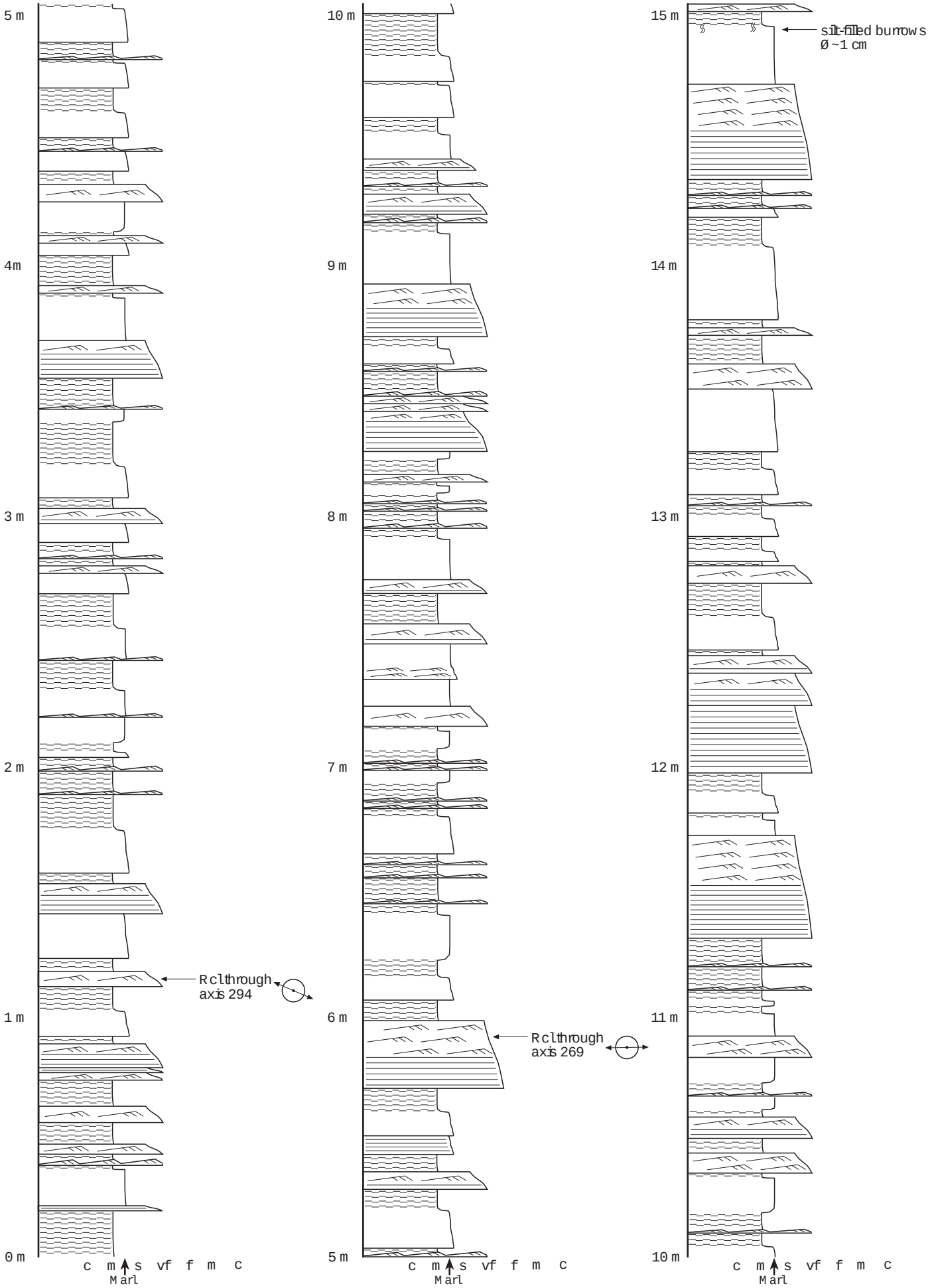

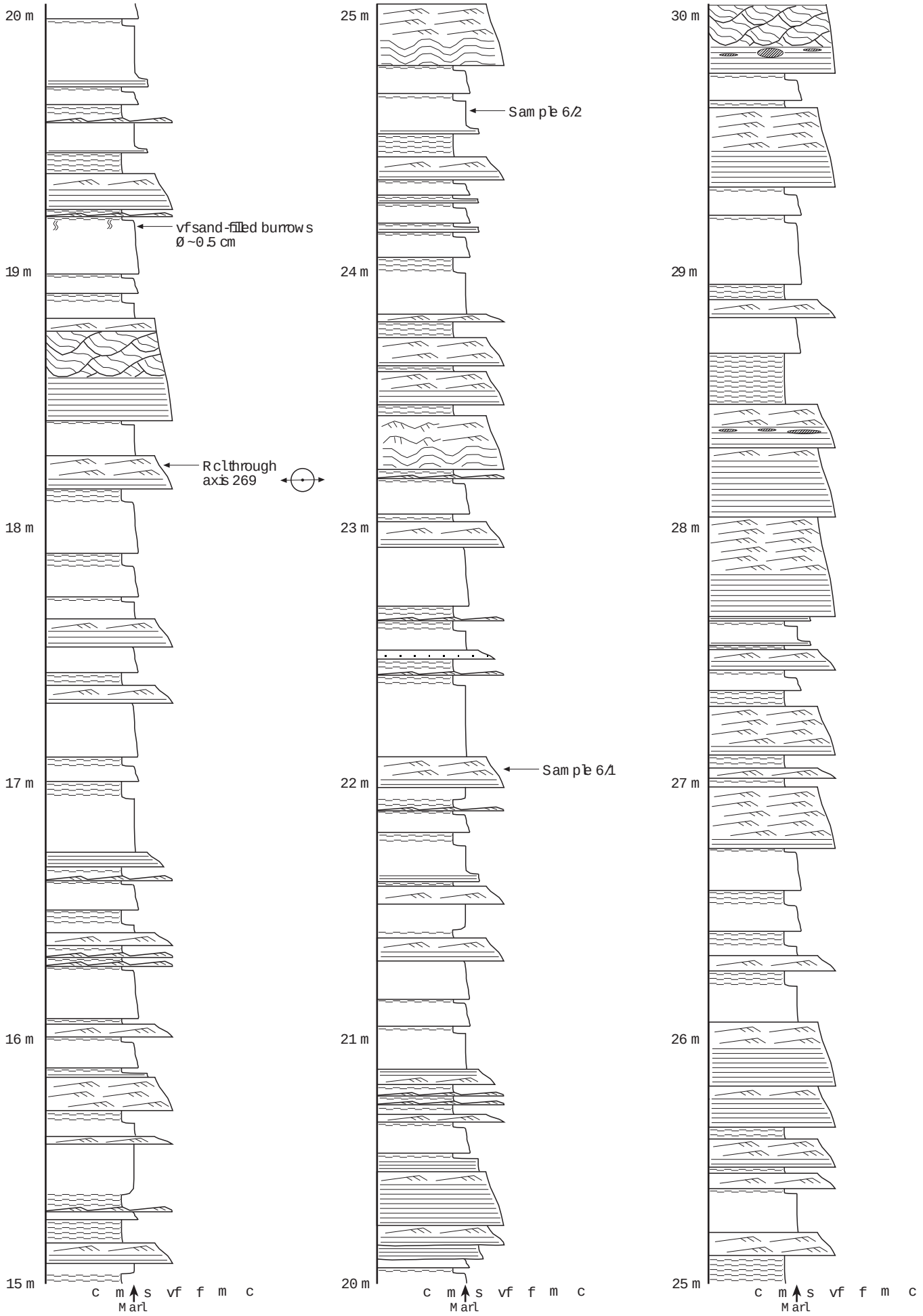
20 m
19 m
18 m
17 m
16 m
15 m
vf sand-filled burrows
Ø ~0.5 cm
R clt through
axis 269
25 m
24 m
23 m
22 m
21 m
20 m
Sample 6/2
Sample 6/1
30 m
29 m
28 m
27 m
26 m
25 m
c m s vf f m c
Marl


35 m
34 m
33 m
32 m
31 m
30 m
c m s vf f m c
Marl
40 m
39 m
38 m
37 m
36 m
35 m
c m s vf f m c
Marl
45 m
44 m
43 m
42 m
41 m
40 m
c m s vf f m c
Marl

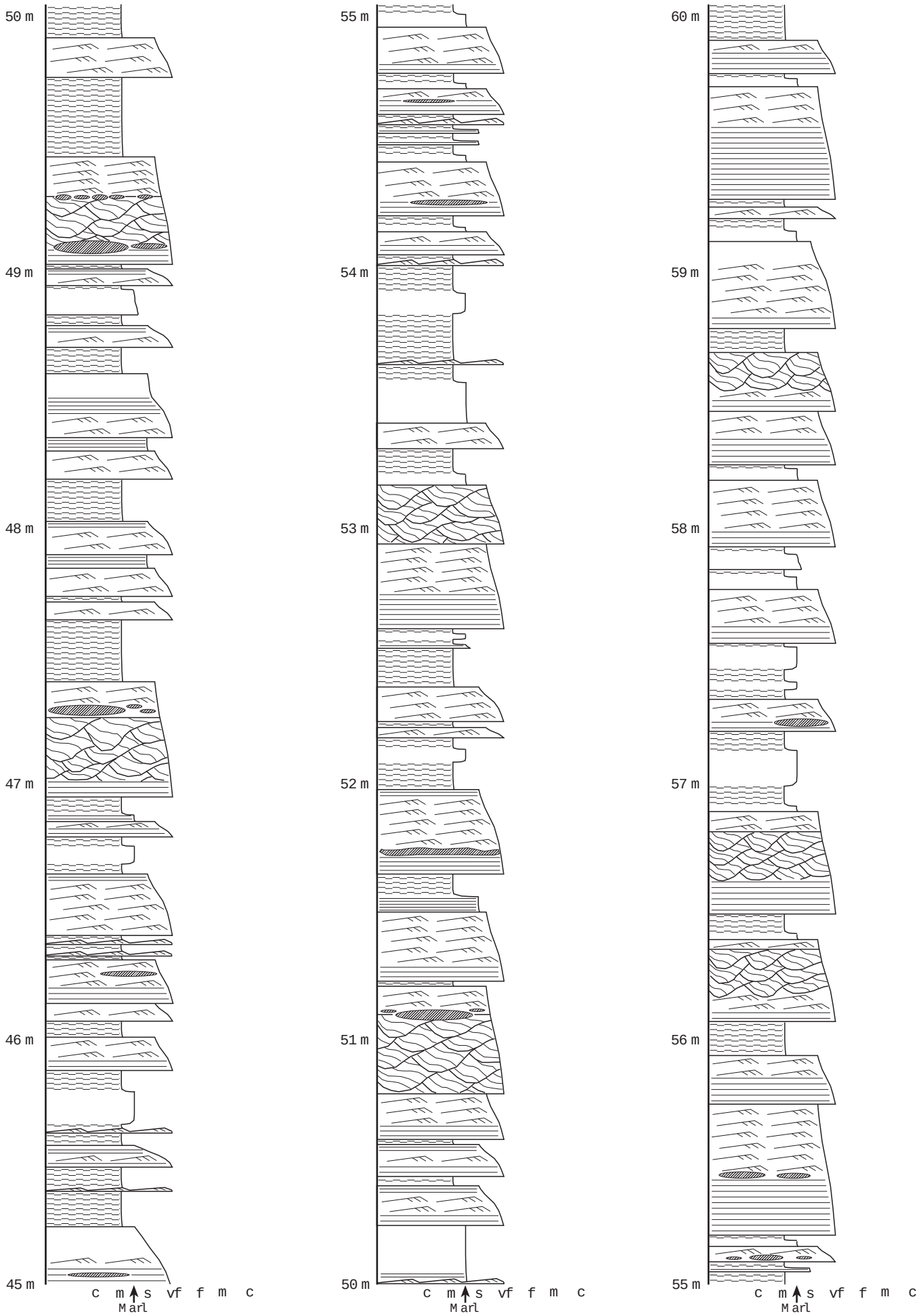
50 m
49 m
48 m
47 m
46 m
45 m
55 m
54 m
53 m
52 m
51 m
50 m
60 m
59 m
58 m
57 m
56 m
55 m
c m s vf f m c
Marl

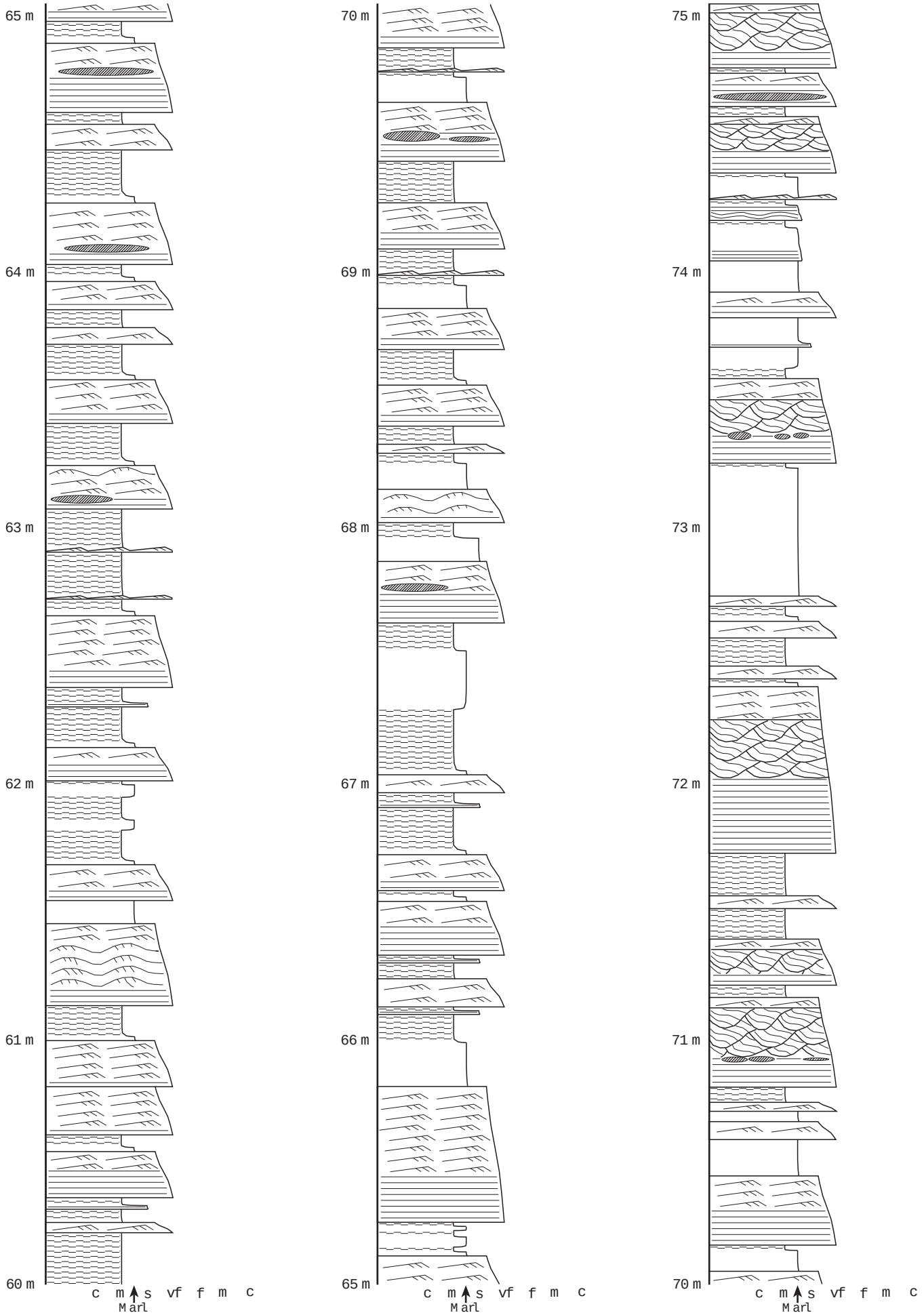
65 m
64 m
63 m
62 m
61 m
60 m
c m s vf f m c
Marl
70 m
69 m
68 m
67 m
66 m
65 m
c m s vf f m c
Marl
75 m
74 m
73 m
72 m
71 m
70 m
c m s vf f m c
Marl

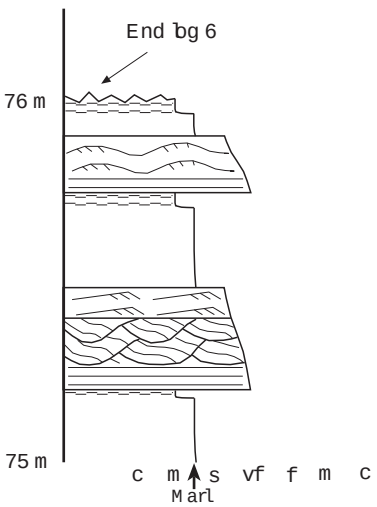
End log 6
76 m
75 m
c m s vf f m c
Marl

LOG 7

Location: Tangal
Formation: lower Akveren
Facies association: FA 2c
Facies content: F2b, F5b, F7, F8a

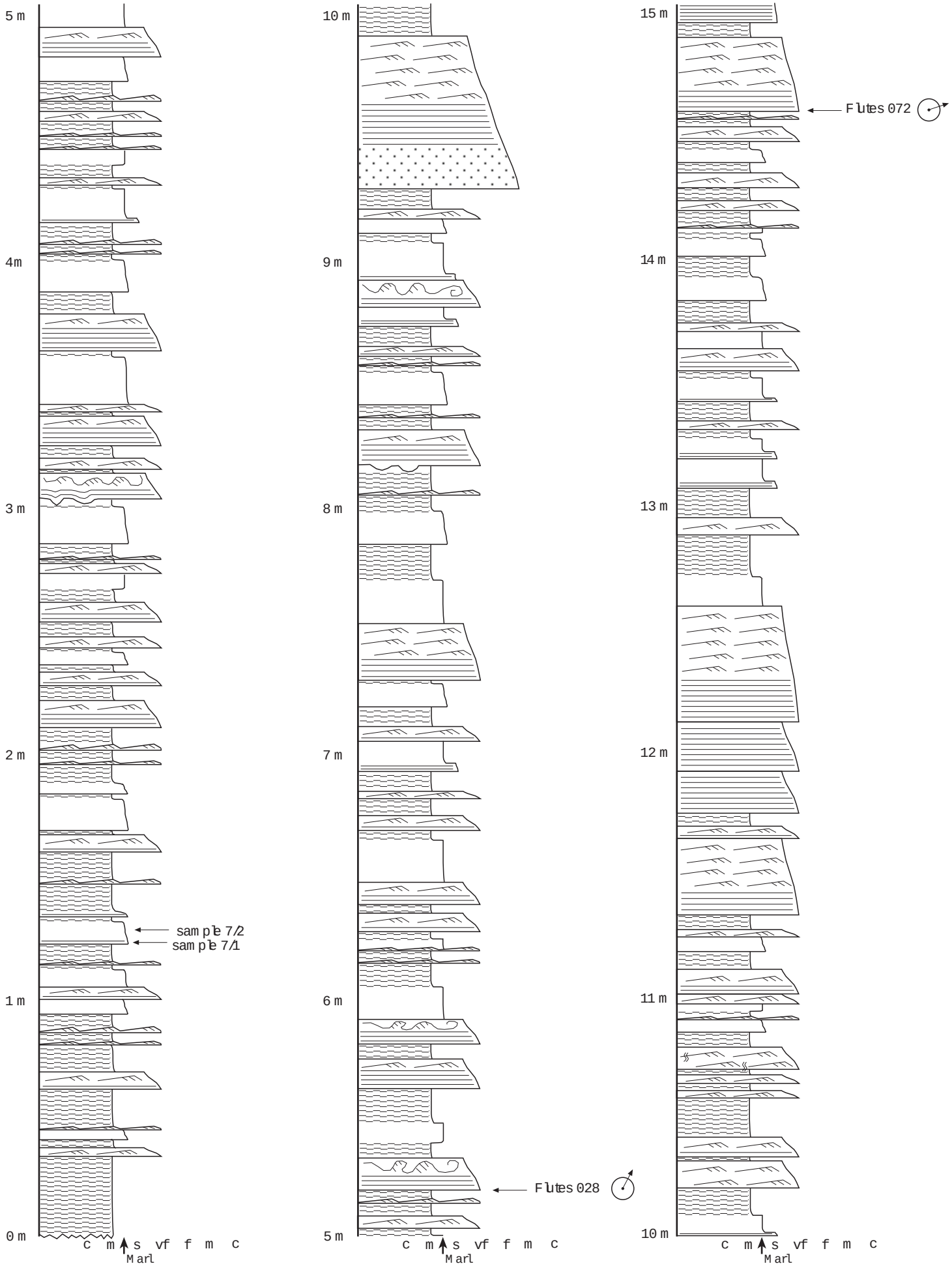

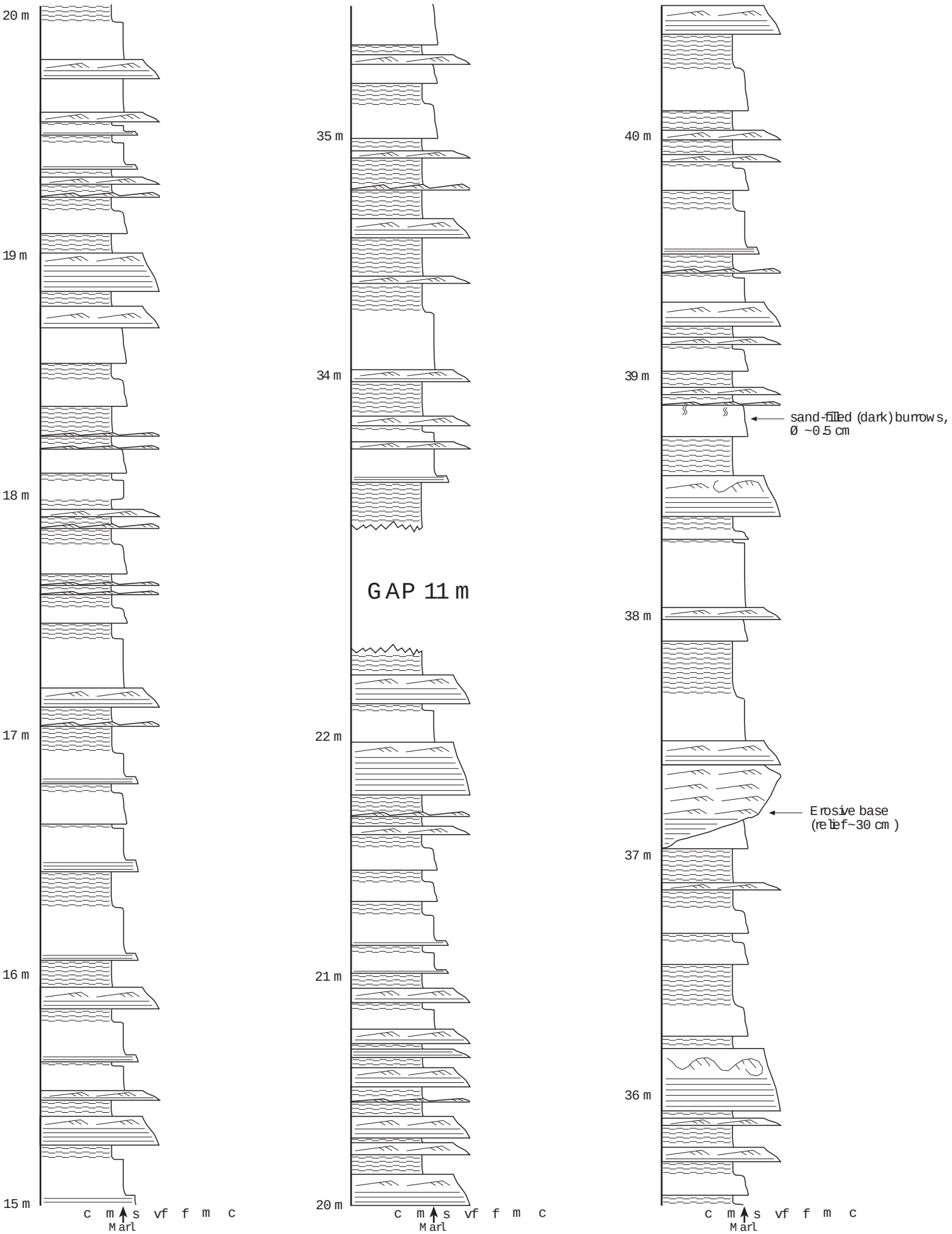
20 m
19 m
18 m
17 m
16 m
15 m
c m s vf f m c
Marl
35 m
34 m
GAP 11 m
22 m
21 m
20 m
c m s vf f m c
Marl
40 m
39 m
sand-filled (dark) burrows,
Ø ~0.5 cm
38 m
Erosive base
(relief~30 cm)
37 m
36 m
c m s vf f m c
Marl

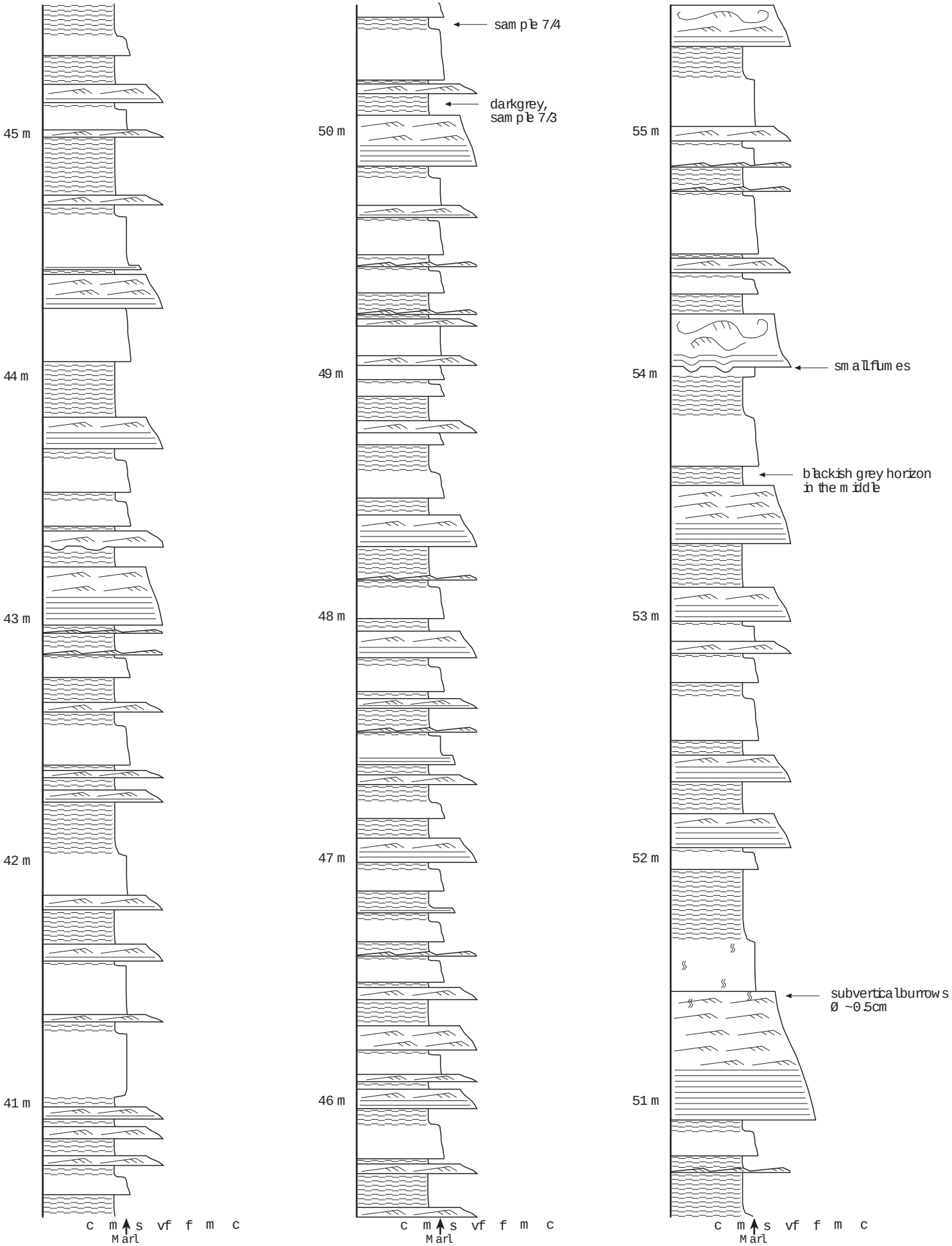
45 m
44 m
43 m
42 m
41 m
50 m
49 m
48 m
47 m
46 m
55 m
54 m
53 m
52 m
51 m
sample 7/4
dark grey, sample 7/3
small flumes
blackish grey horizon in the middle
subvertical burrows Ø ~0.5cm
c m s vf f m c
Marl


60 m
59 m
58 m
blackish grey
57 m
56 m
c m s vf f m c
Marl
Stop log 7
61 m
c m s vf f m c
Marl

LOG 8

Location: Samýç river valley
Formation: middle Akveren
Facies association: FA 2c
Facies content: F2b, F5b, F7, F8a

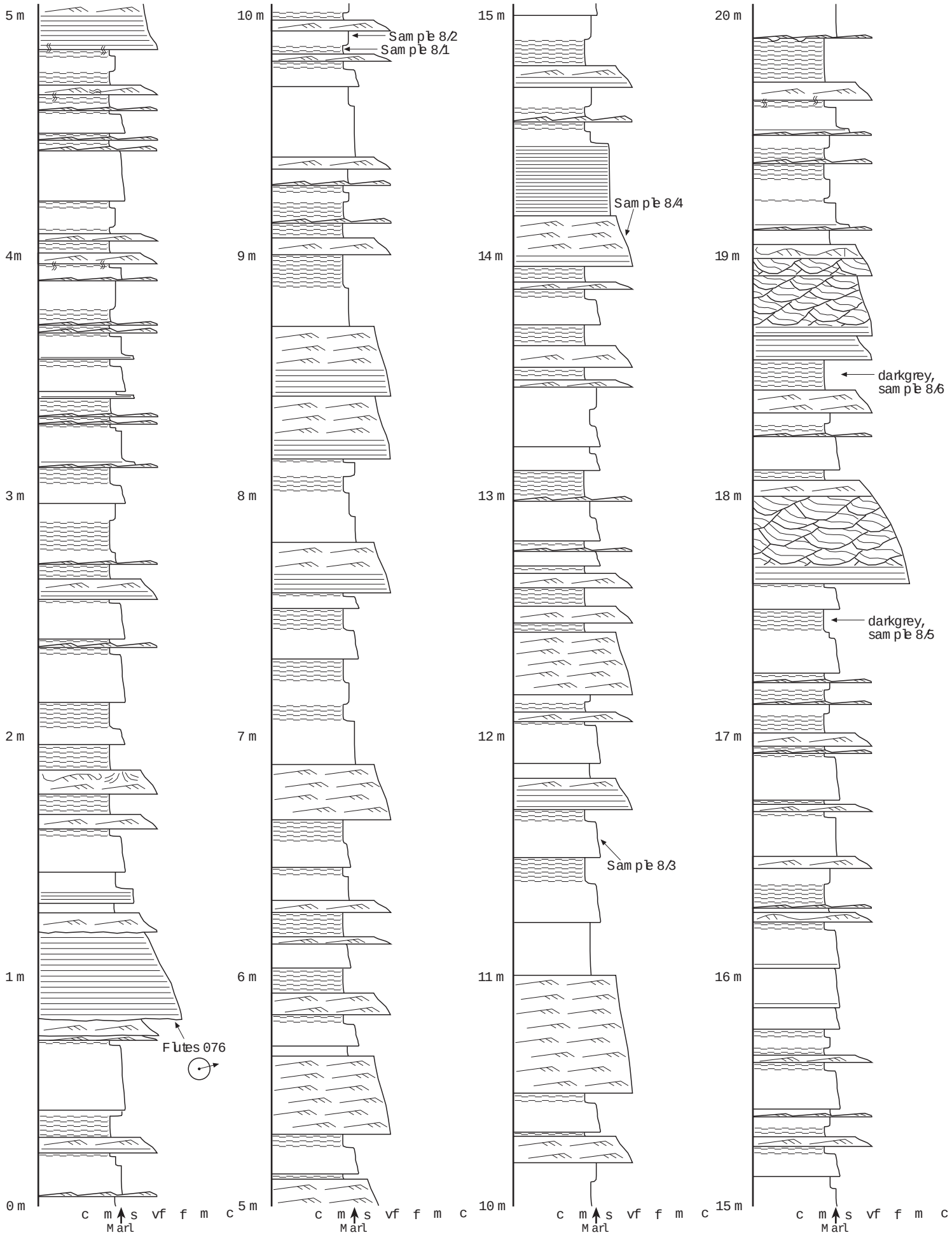

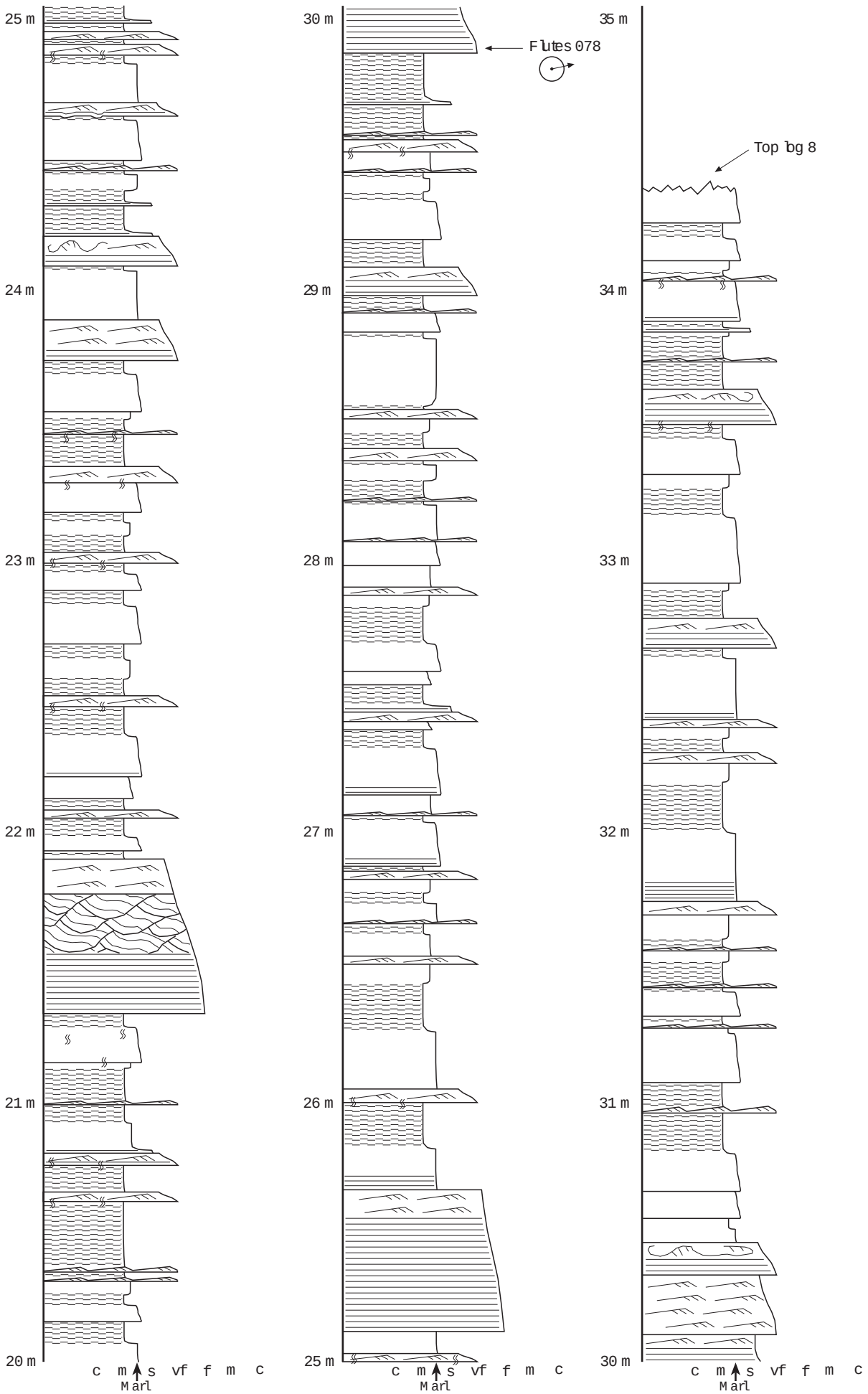
25 m
24 m
23 m
22 m
21 m
20 m
c m s vf f m c
Marl
30 m
29 m
28 m
27 m
26 m
25 m
Flutes 078
c m s vf f m c
Marl
35 m
34 m
33 m
32 m
31 m
30 m
Top bg 8
c m s vf f m c
Marl

LOG 9

Location: Samýç river valley
Formation: middle Akveren
Facies association: FA 2c
Facies content: F2b, F5b, F7, F8a

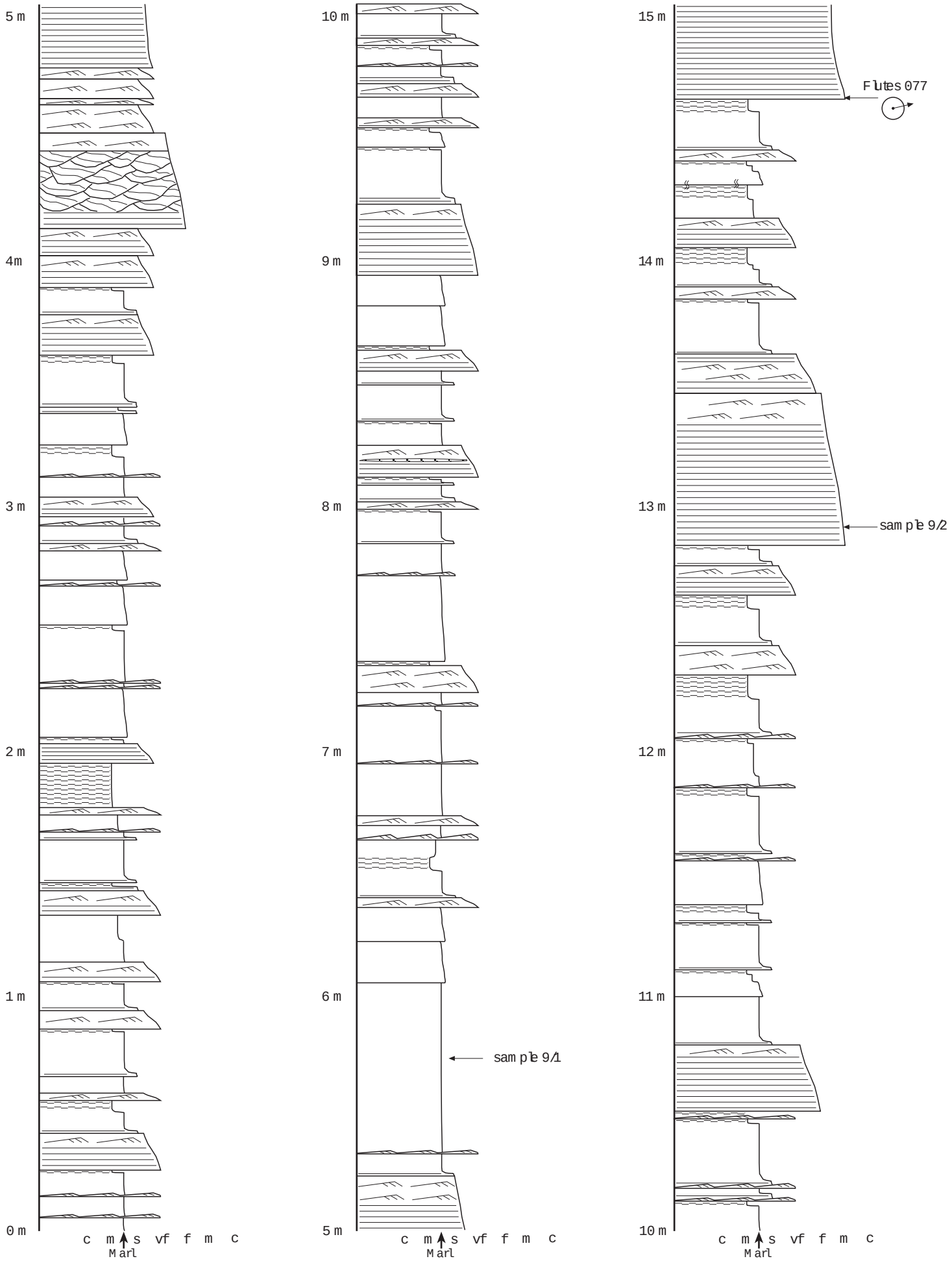

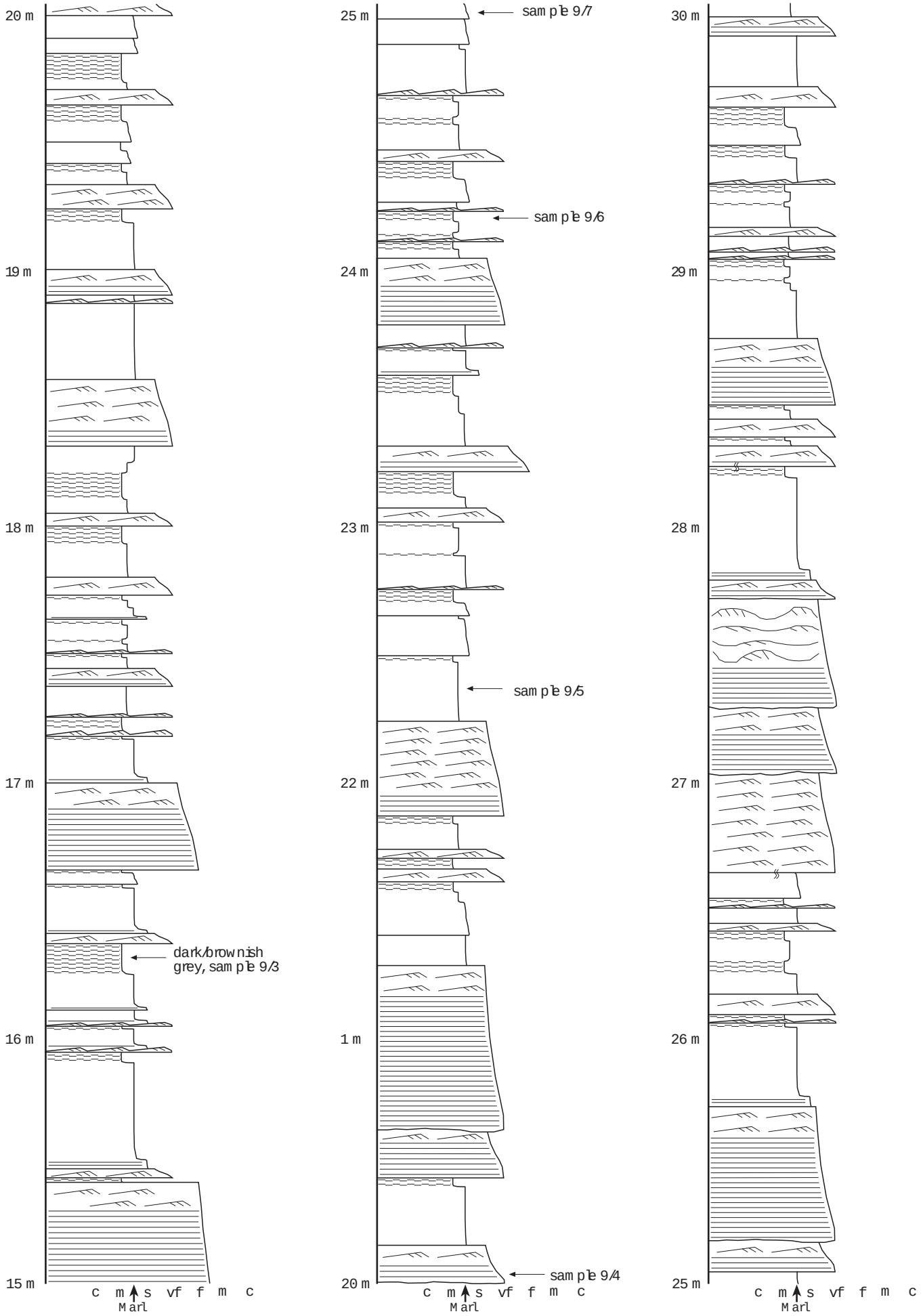
20 m
19 m
18 m
17 m
16 m
15 m
dark/brownish grey, sample 9/3
c m s vf f m c
Marl
25 m
24 m
23 m
22 m
1 m
20 m
sample 9/7
sample 9/6
sample 9/5
sample 9/4
c m s vf f m c
Marl
30 m
29 m
28 m
27 m
26 m
25 m
c m s vf f m c
Marl

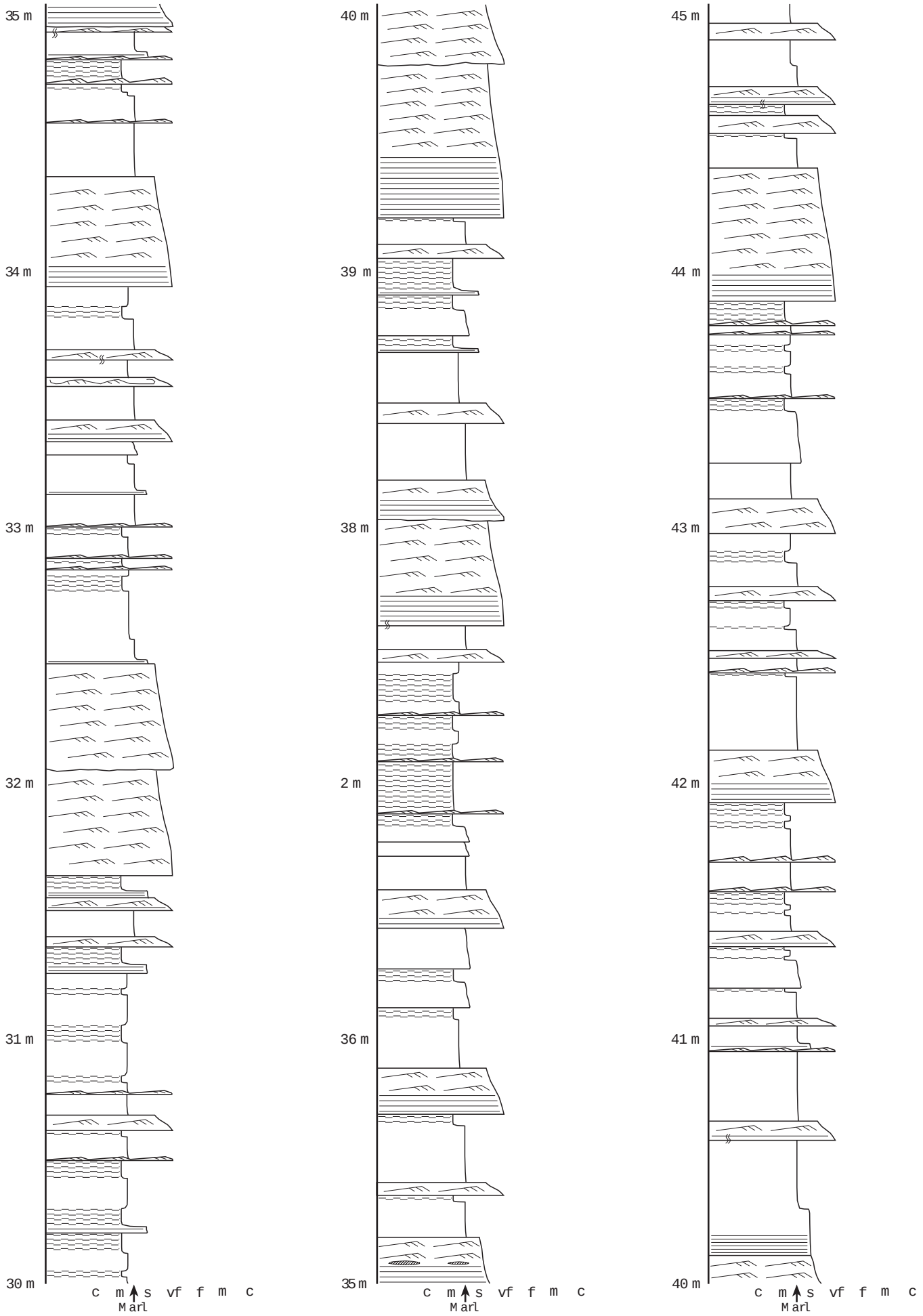
35 m
34 m
33 m
32 m
31 m
30 m
c m s vf f m c
Marl
40 m
39 m
38 m
2 m
36 m
35 m
c m s vf f m c
Marl
45 m
44 m
43 m
42 m
41 m
40 m
c m s vf f m c
Marl

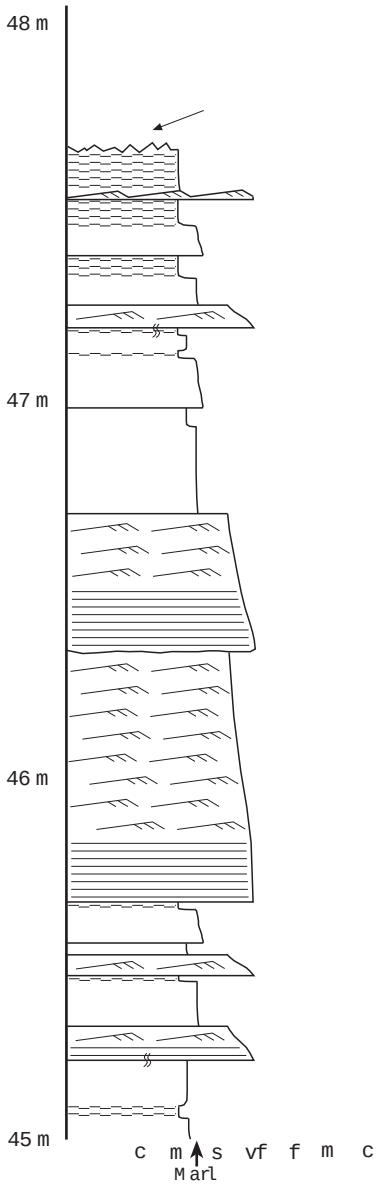
48 m
47 m
46 m
45 m
c m s vf f m c
Marl

LOG 10

Location: 5 km E of Gerze
Formation: middle Akveren
Facies association: FA 2c
Facies content: F2b, F5b, F7, F8a

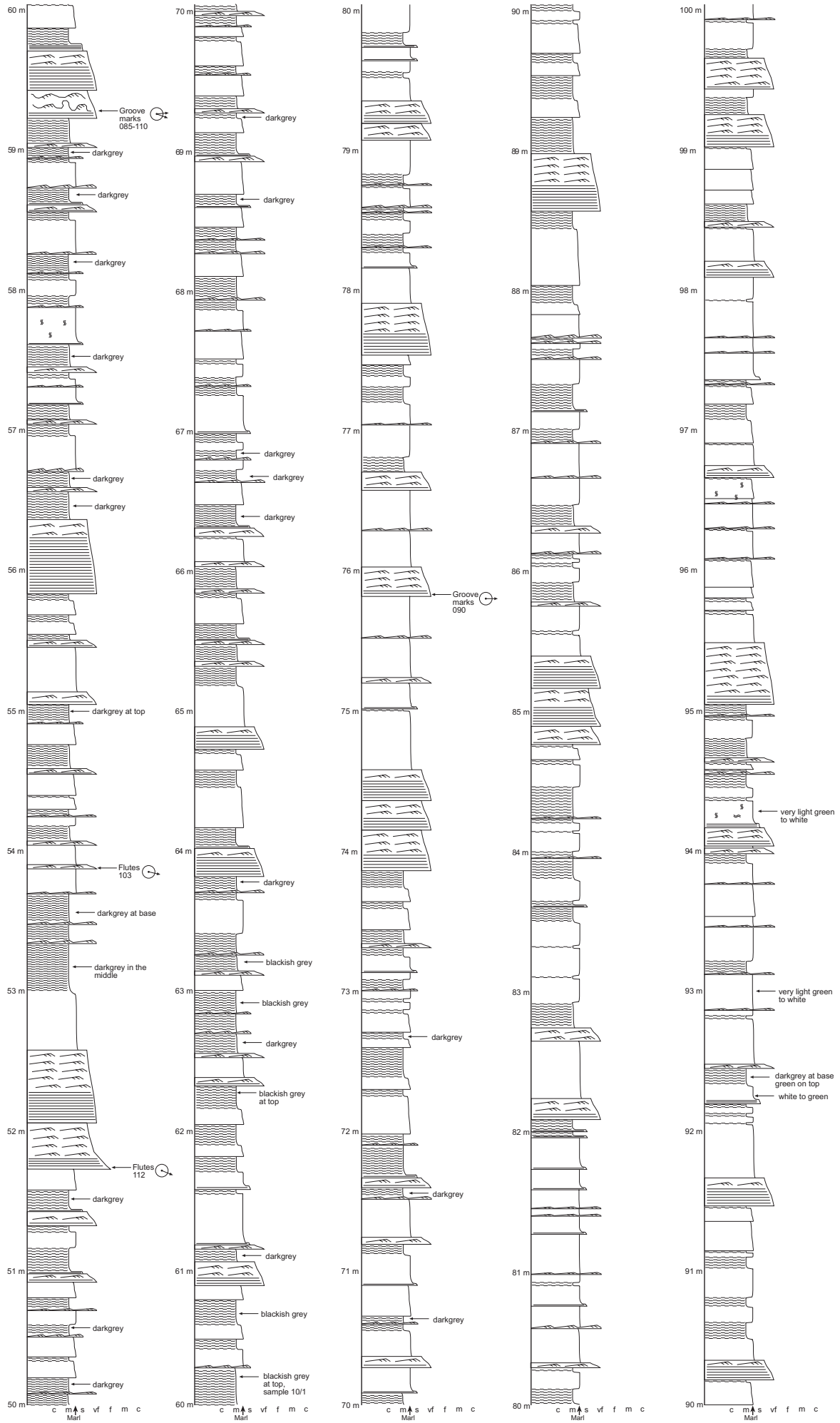
60 m
59 m
58 m
57 m
56 m
55 m
54 m
53 m
52 m
51 m
50 m
Groove marks 085-110
darkgrey
darkgrey
darkgrey
darkgrey
darkgrey
darkgrey
darkgrey
darkgrey at top
Flutes 103
darkgrey at base
darkgrey in the middle
Flutes 112
darkgrey
darkgrey
darkgrey
c m s vf f m c
Marl
70 m
69 m
68 m
67 m
66 m
65 m
64 m
63 m
62 m
61 m
60 m
darkgrey
darkgrey
darkgrey
darkgrey
darkgrey
darkgrey
blackish grey
blackish grey
darkgrey
blackish grey at top
darkgrey
blackish grey
blackish grey at top, sample 10/1
c m s vf f m c
Marl
80 m
79 m
78 m
77 m
76 m
75 m
74 m
73 m
72 m
71 m
70 m
Groove marks 090
darkgrey
darkgrey
darkgrey
c m s vf f m c
Marl
90 m
89 m
88 m
87 m
86 m
85 m
84 m
83 m
82 m
81 m
80 m
c m s vf f m c
Marl
100 m
99 m
98 m
97 m
96 m
95 m
94 m
93 m
92 m
91 m
90 m
very light green to white
very light green to white
darkgrey at base green on top
white to green
c m s vf f m c
Marl


110 m
109 m
108 m
107 m
106 m
105 m
104 m
103 m
102 m
101 m
100 m
grey
c m s vf f m c
Marl
120 m
119 m
118 m
117 m
116 m
115 m
114 m
113 m
112 m
111 m
110 m
c m s vf f m c
Marl
130 m
129 m
128 m
127 m
126 m
125 m
124 m
123 m
122 m
121 m
120 m
Flutes
094
darkgrey base
green top
green/grey at base
darkgrey at top
green
darkgrey
c m s vf f m c
Marl
140 m
139m
138 m
137 m
136 m
135 m
134m
133 m
132 m
131 m
130 m
Flutes
098
c m s vf f m c
Marl
150 m
149 m
148 m
147 m
146 m
145 m
144 m
143 m
142 m
141 m
140 m
c m s vf f m c
Marl
155 m
154 m
153 m
152 m
151 m
150 m
End log 10
Flutes
080
sample 10/2
c m s vf f m c
Marl

LOG 11

Location: Kuðuköy
Formation: middle-upper Akveren
Facies association: FA 2a and FA 2b
Facies content: F1b, F4, F7, F6a, F8a

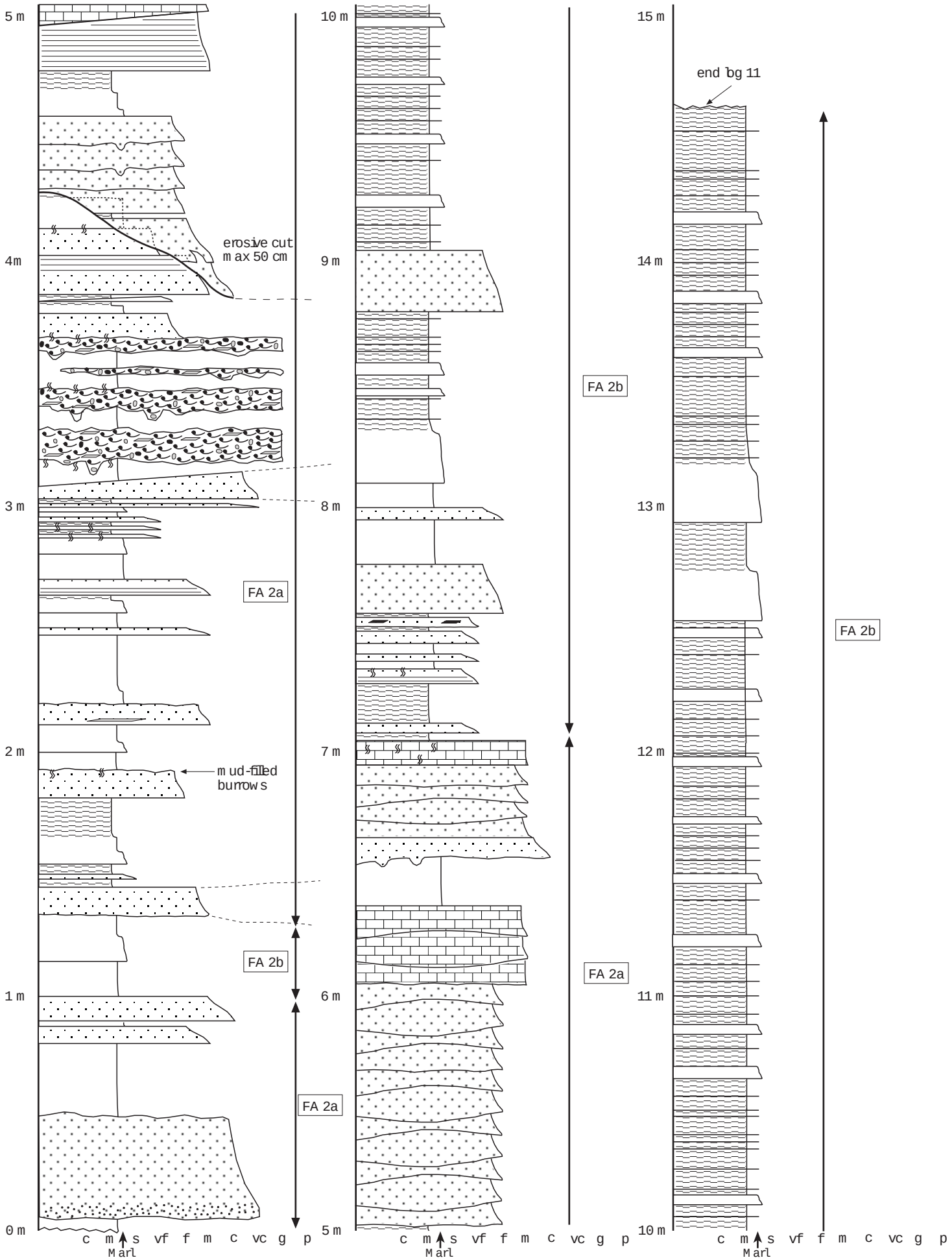

LOG 12

Location: Kuðuköy
Formation: middle-upper Akveren
Facies association: FA 2a and FA 2b
Facies content: F4, F7, F8a

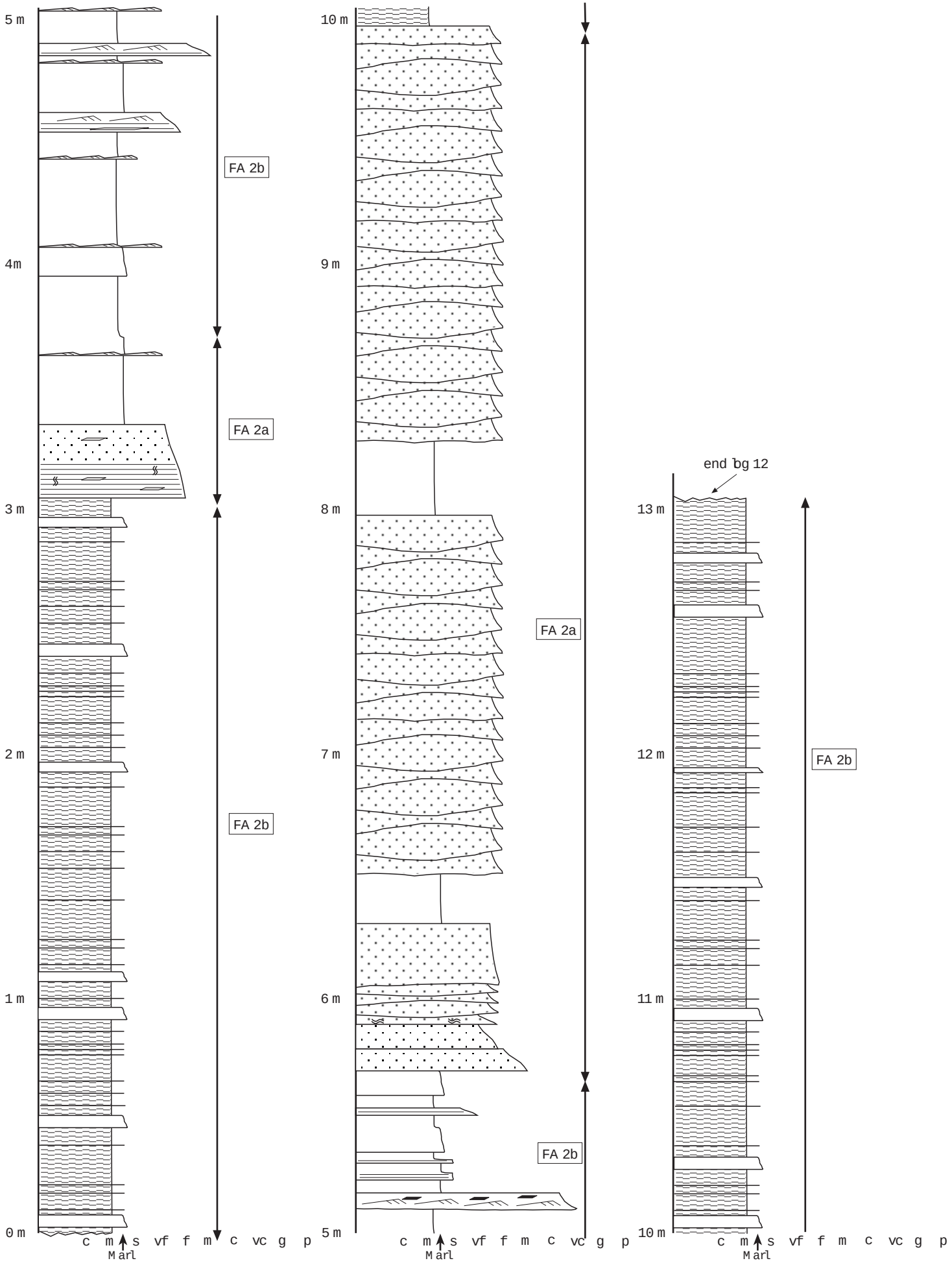

LOG 13

Location: Kuðuköy
Formation: middle-upper Akveren
Facies association: FA 2a and FA 2b
Facies content: F4, F7, F8a

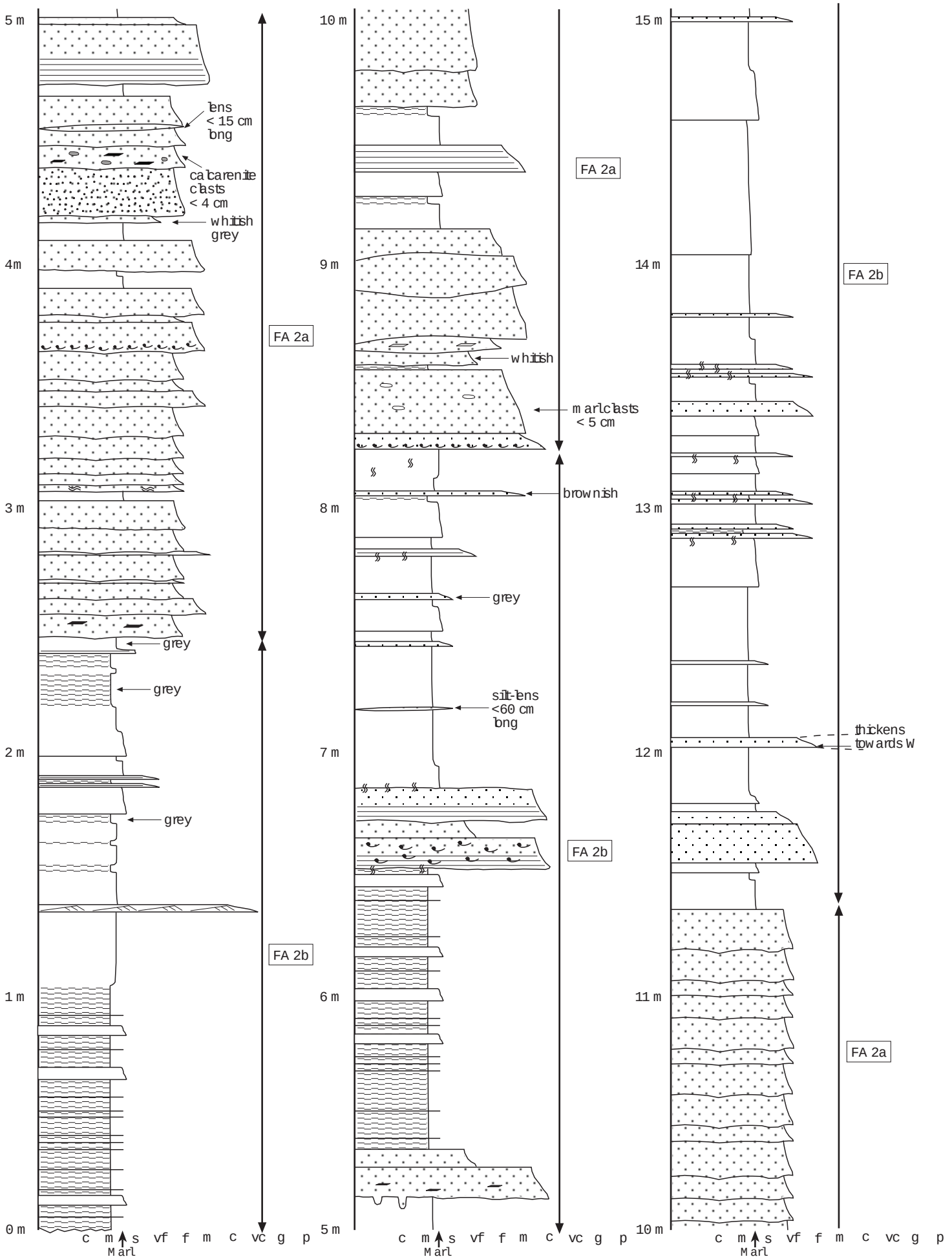

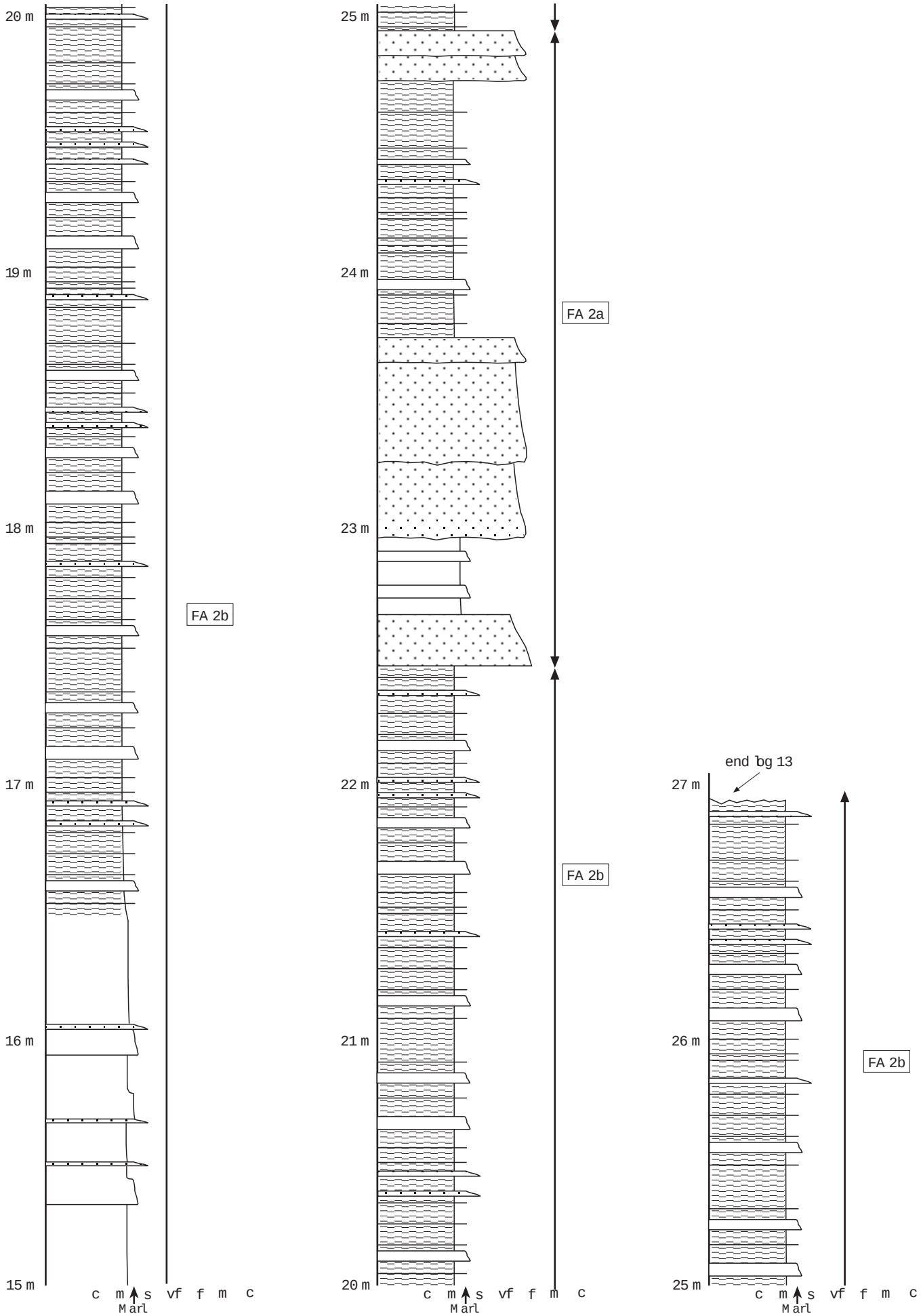
20 m
19 m
18 m
17 m
16 m
15 m
FA 2b
c m s vf f m c
Marl
25 m
24 m
23 m
22 m
21 m
20 m
FA 2a
FA 2b
c m s vf f m c
Marl
end bg 13
27 m
26 m
25 m
FA 2b
c m s vf f m c
Marl

LOG 14

Location: Kuðuköy
Formation: upper Akveren
Facies association: FA 2a/2b and FA 3a
Facies content: F4, F7, F6a, F6b, F8a

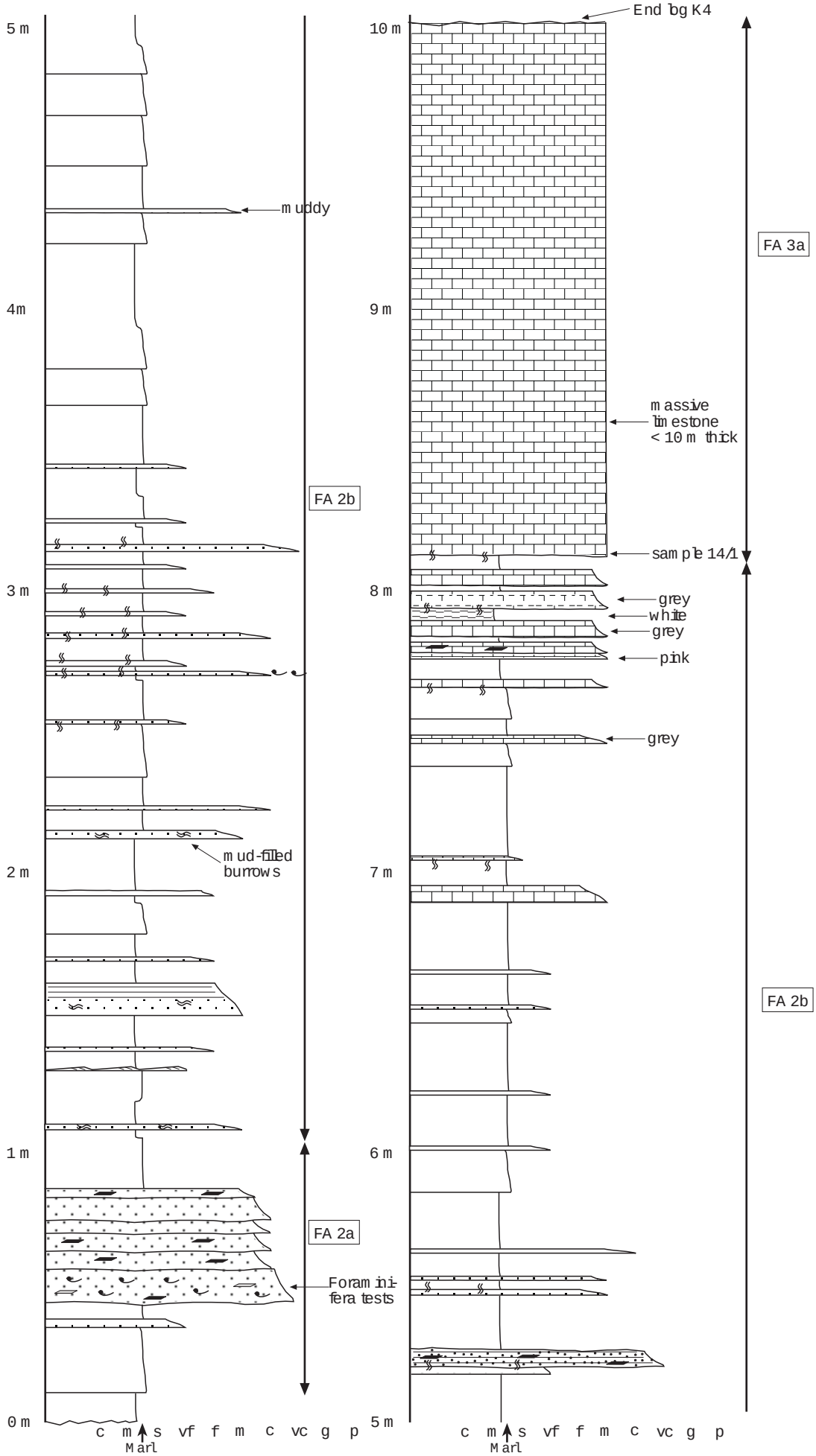

LOG 15

Location: 5 km E of Gerze
Formation: upper Akveren
Facies association: FA 3b
Facies content: F2b, F3, F5b, F7, F8b

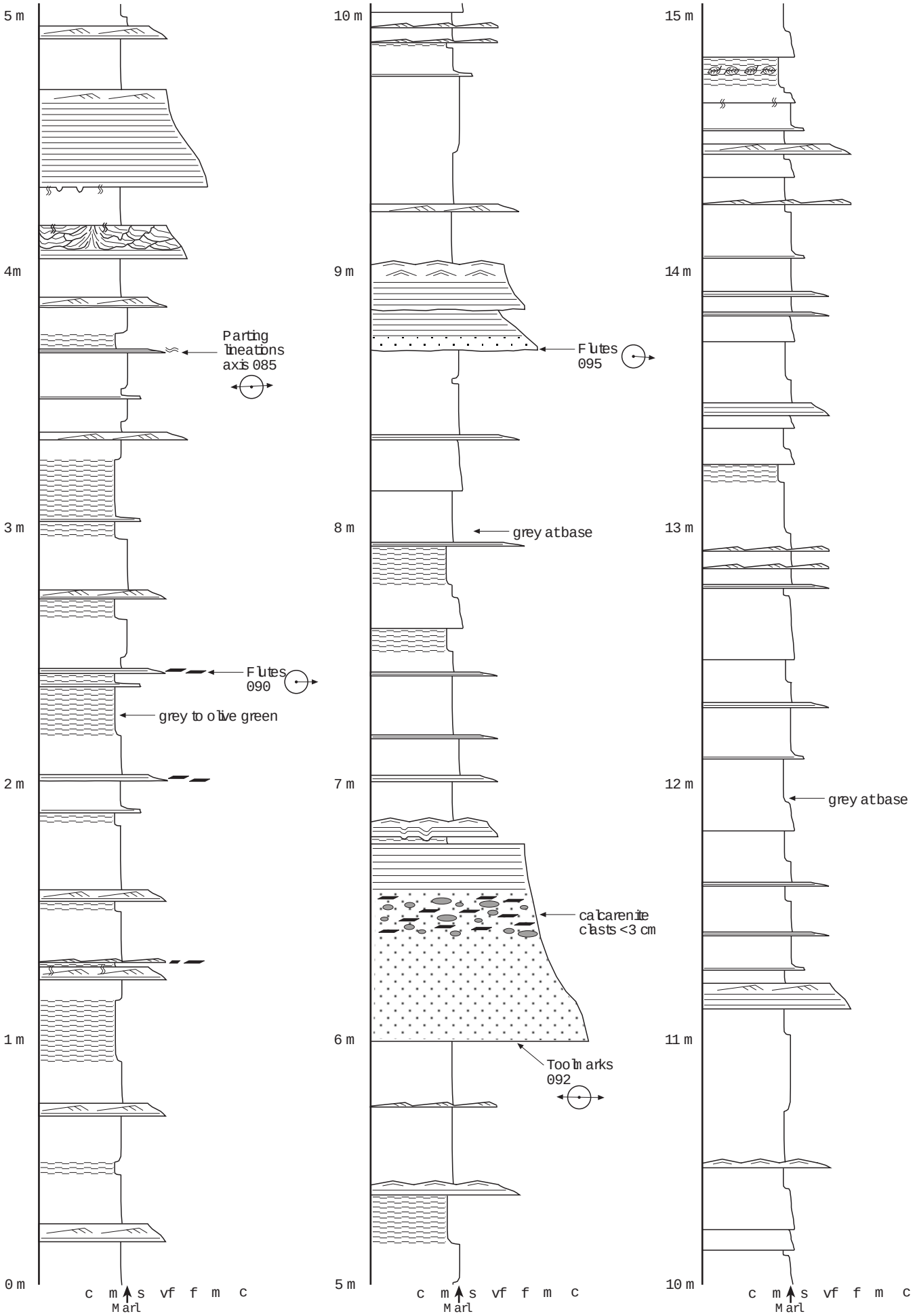

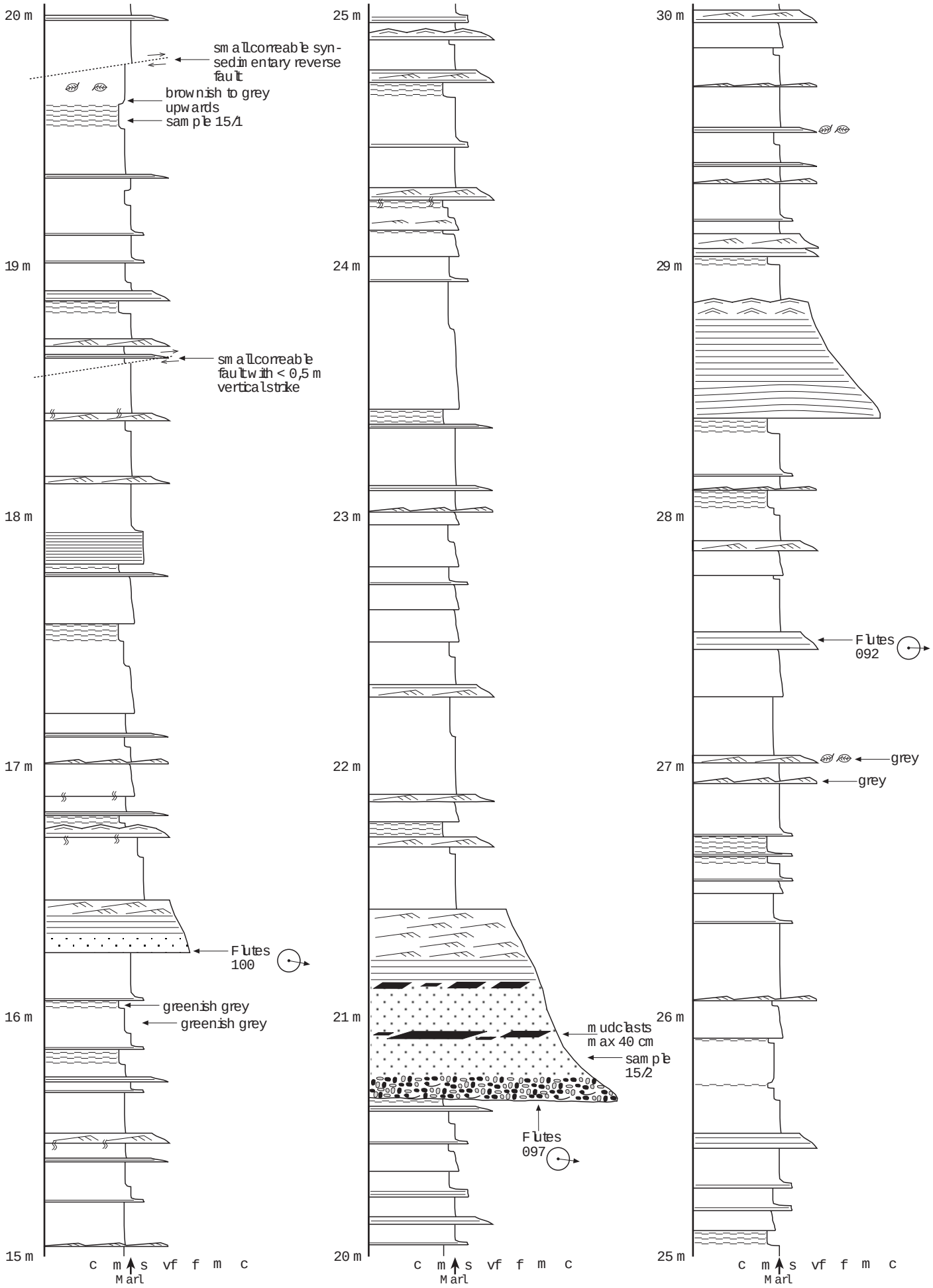
20 m
19 m
18 m
17 m
16 m
15 m
small correable syn-sedimentary reverse fault
brownish to grey upwards
sample 15/1
small correable fault with < 0,5 m vertical strike
Flutes 100
greenish grey
greenish grey
c m s vf f m c
Marl
25 m
24 m
23 m
22 m
21 m
20 m
mudclasts max 40 cm
sample 15/2
Flutes 097
c m s vf f m c
Marl
30 m
29 m
28 m
27 m
26 m
25 m
Flutes 092
grey
grey
c m s vf f m c
Marl

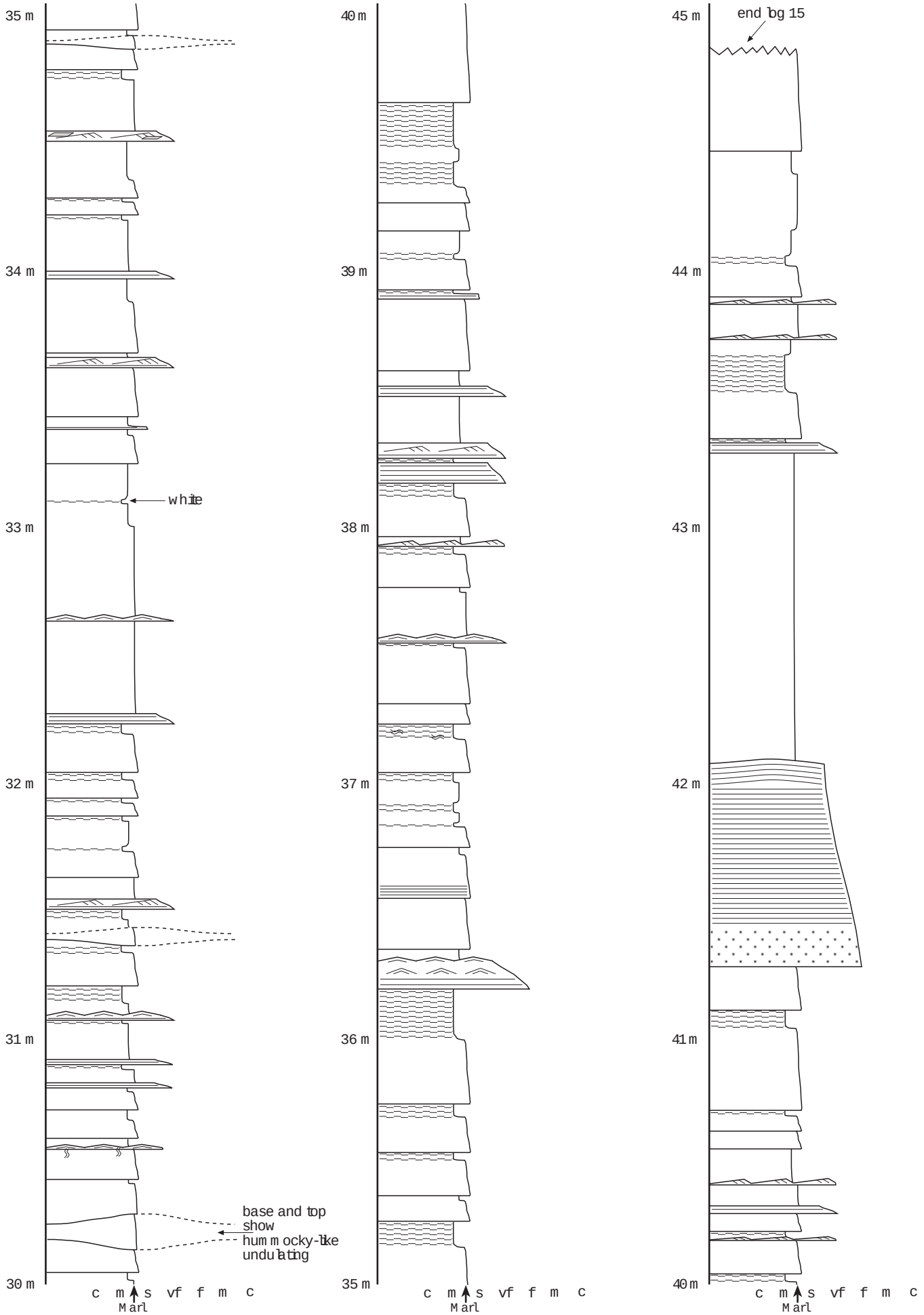
35 m
34 m
33 m
32 m
31 m
30 m
white
base and top show hummocky-like undulating
c m s vf f m c
Marl
40 m
39 m
38 m
37 m
36 m
35 m
c m s vf f m c
Marl
45 m
end log 15
44 m
43 m
42 m
41 m
40 m
c m s vf f m c
Marl

LOG 16

Location: Gerze pier
Formation: upper Akveren
Facies association: FA 3b
Facies content: F3, F7, F8a

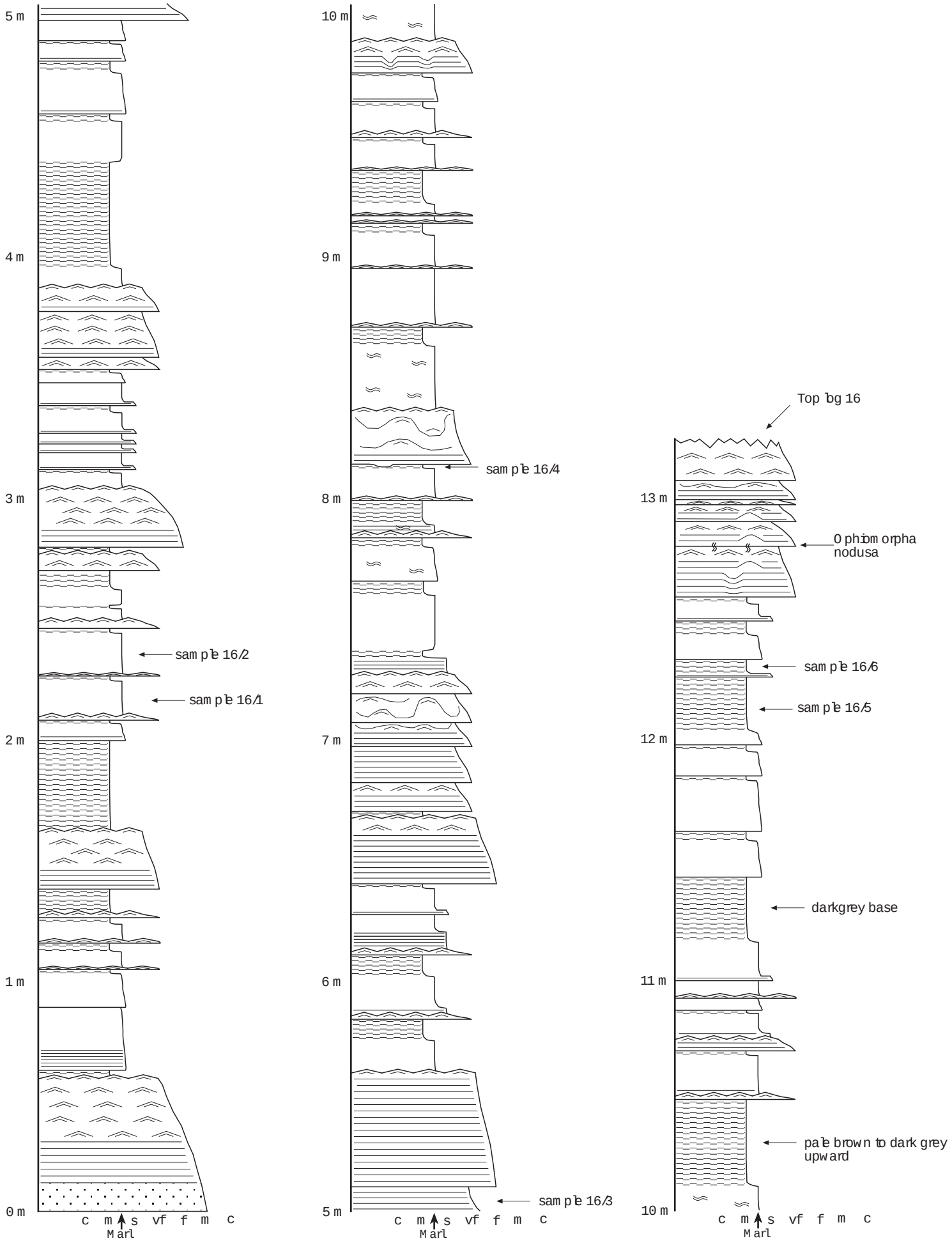

LOG 17

Location: Yenikonak, E of river
Formation: upper Akveren
Facies association: FA 3b
Facies content: F1a, F3, F7, F8

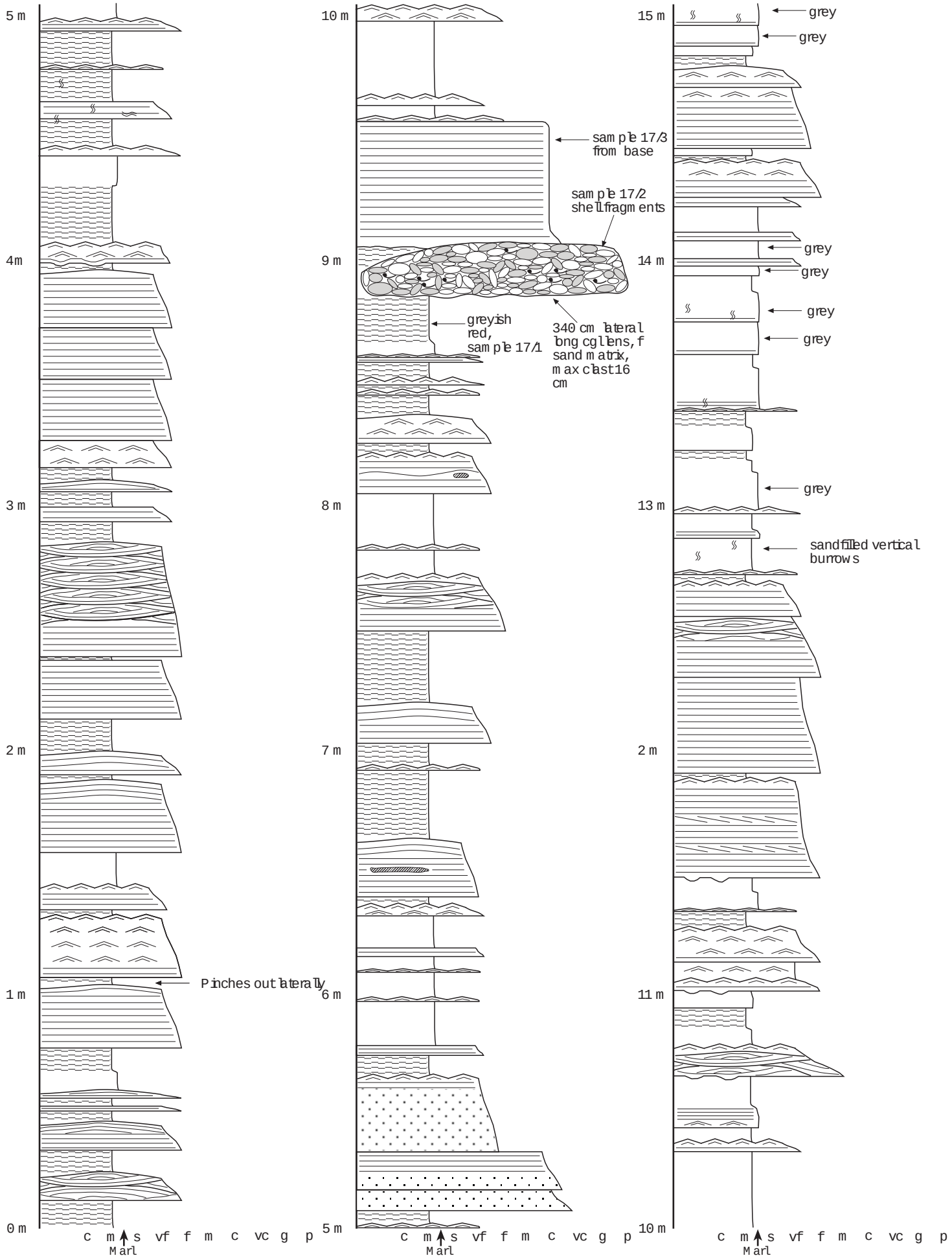

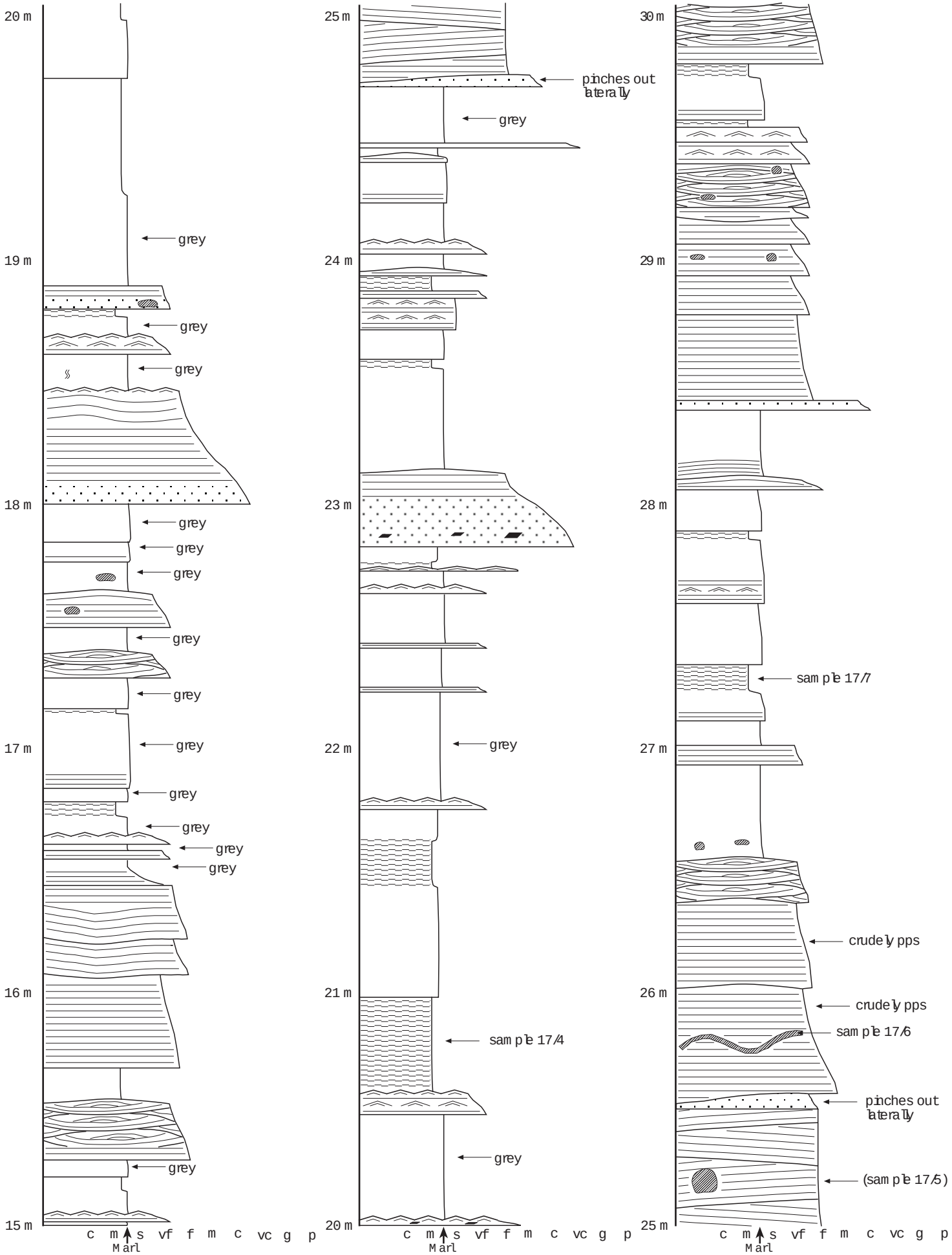
20 m
19 m
18 m
17 m
16 m
15 m
grey
grey
grey
grey
grey
grey
grey
grey
grey
grey
grey
grey
grey
grey
c m s vf f m c vc g p
Marl
25 m
24 m
23 m
22 m
21 m
20 m
pinches out laterally
grey
grey
sample 17/4
grey
c m s vf f m c vc g p
Marl
30 m
29 m
28 m
27 m
26 m
25 m
sample 17/7
crudely pps
crudely pps
sample 17/6
pinches out laterally
(sample 17/5)
c m s vf f m c vc g p
Marl

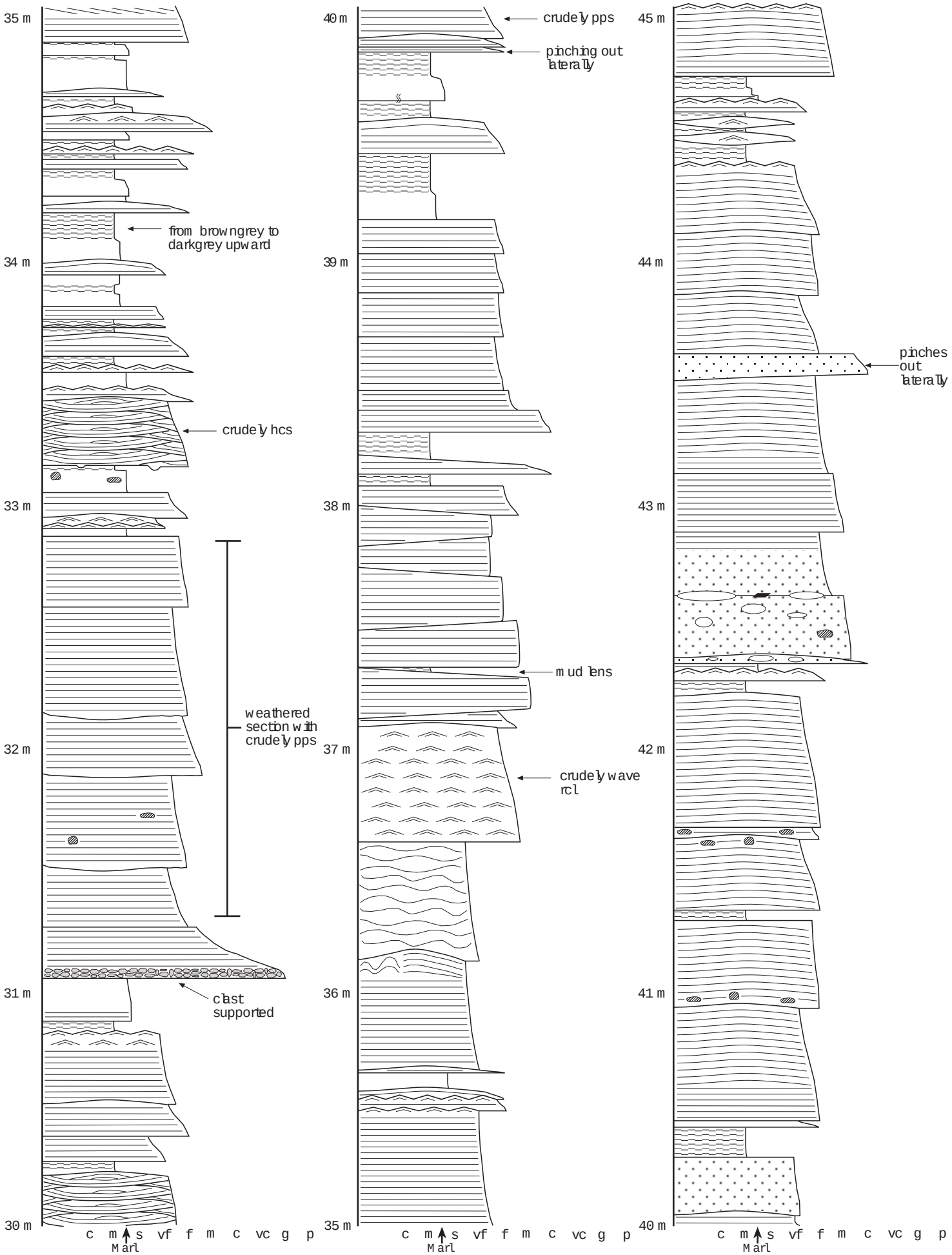
35 m
34 m
33 m
32 m
31 m
30 m
from brown grey to dark grey upward
crudely hcs
weathered section with crudely pps
clast supported
c m s vf f m c vc g p
Marl
40 m
39 m
38 m
37 m
36 m
35 m
crudely pps
pinching out laterally
mud lens
crudely wave rcl
c m s vf f m c vc g p
Marl
45 m
44 m
43 m
42 m
41 m
40 m
pinches out laterally
c m s vf f m c vc g p
Marl

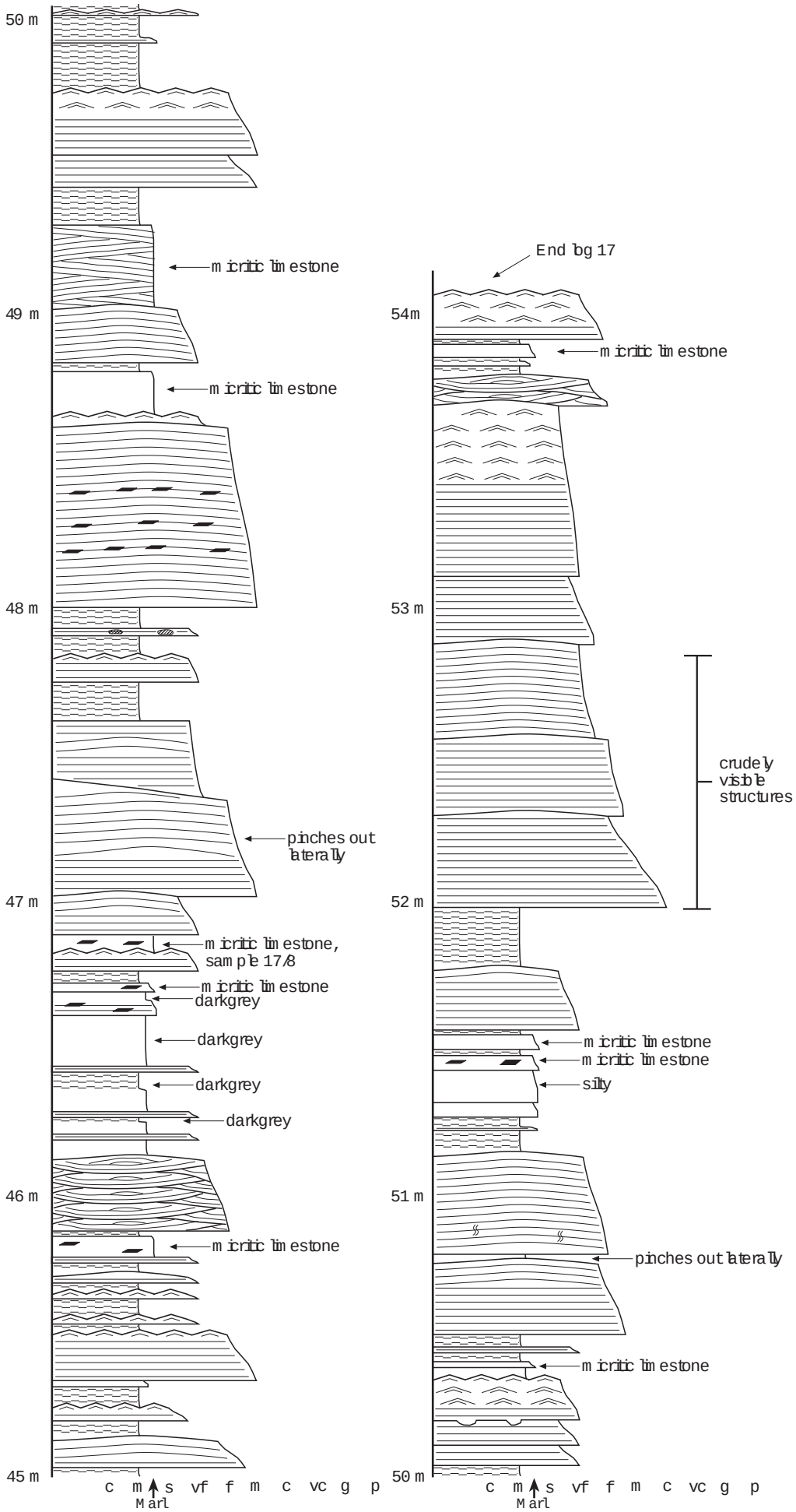
50 m
micritic limestone
49 m
micritic limestone
48 m
pinches out laterally
47 m
micritic limestone, sample 17/8
micritic limestone
darkgrey
darkgrey
darkgrey
darkgrey
46 m
micritic limestone
45 m
c m s vf f m c vc g p
Marl
End log 17
54m
micritic limestone
53 m
crudely visible structures
52 m
micritic limestone
micritic limestone
silty
51 m
pinches out laterally
micritic limestone
50 m
c m s vf f m c vc g p
Marl

LOG 18

Location: Kuðuköy
Formation: upper Akveren - lower Atbasi
Facies association: FA 4a
Facies content: F4, F6a, F7, F8

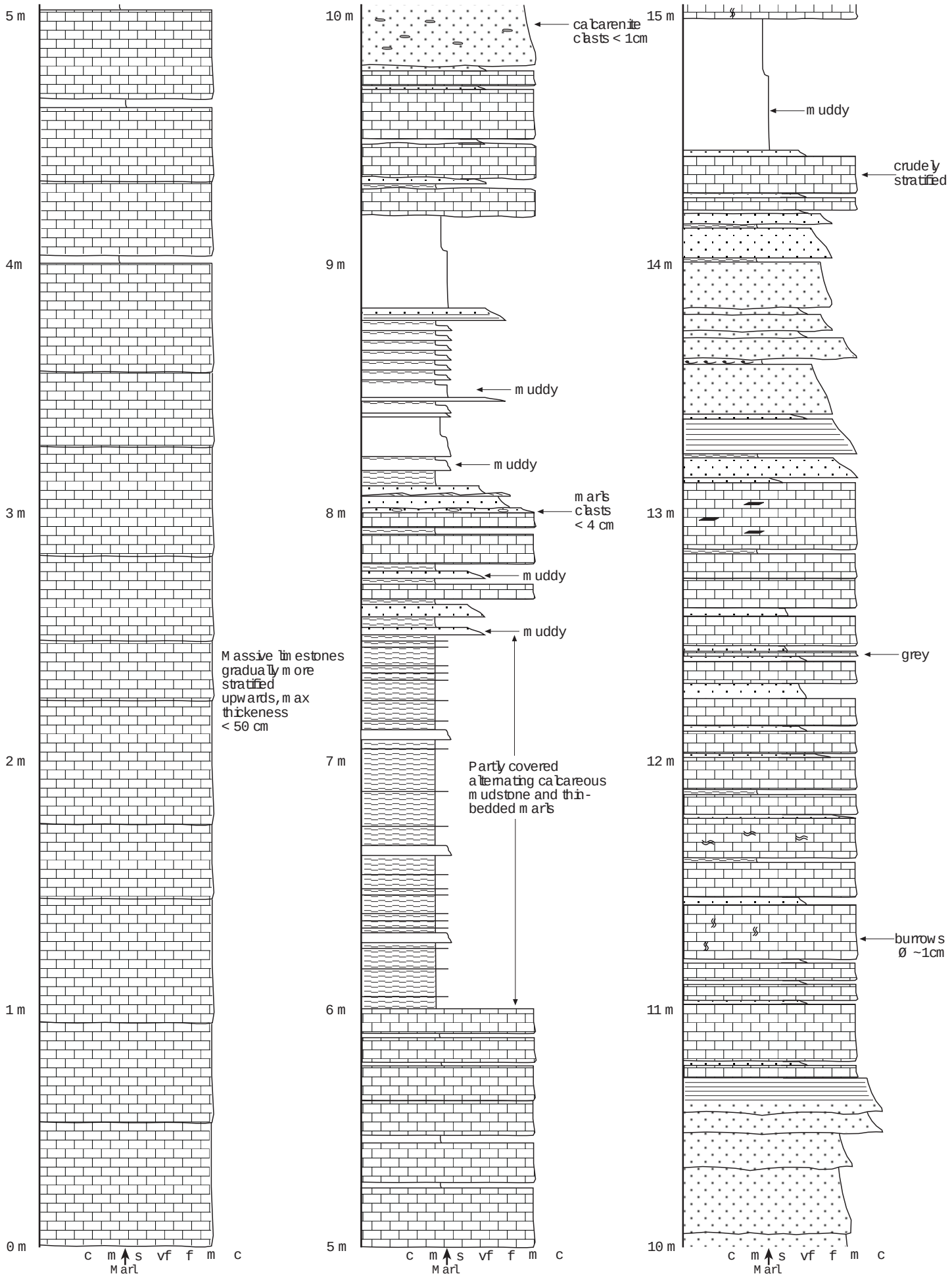

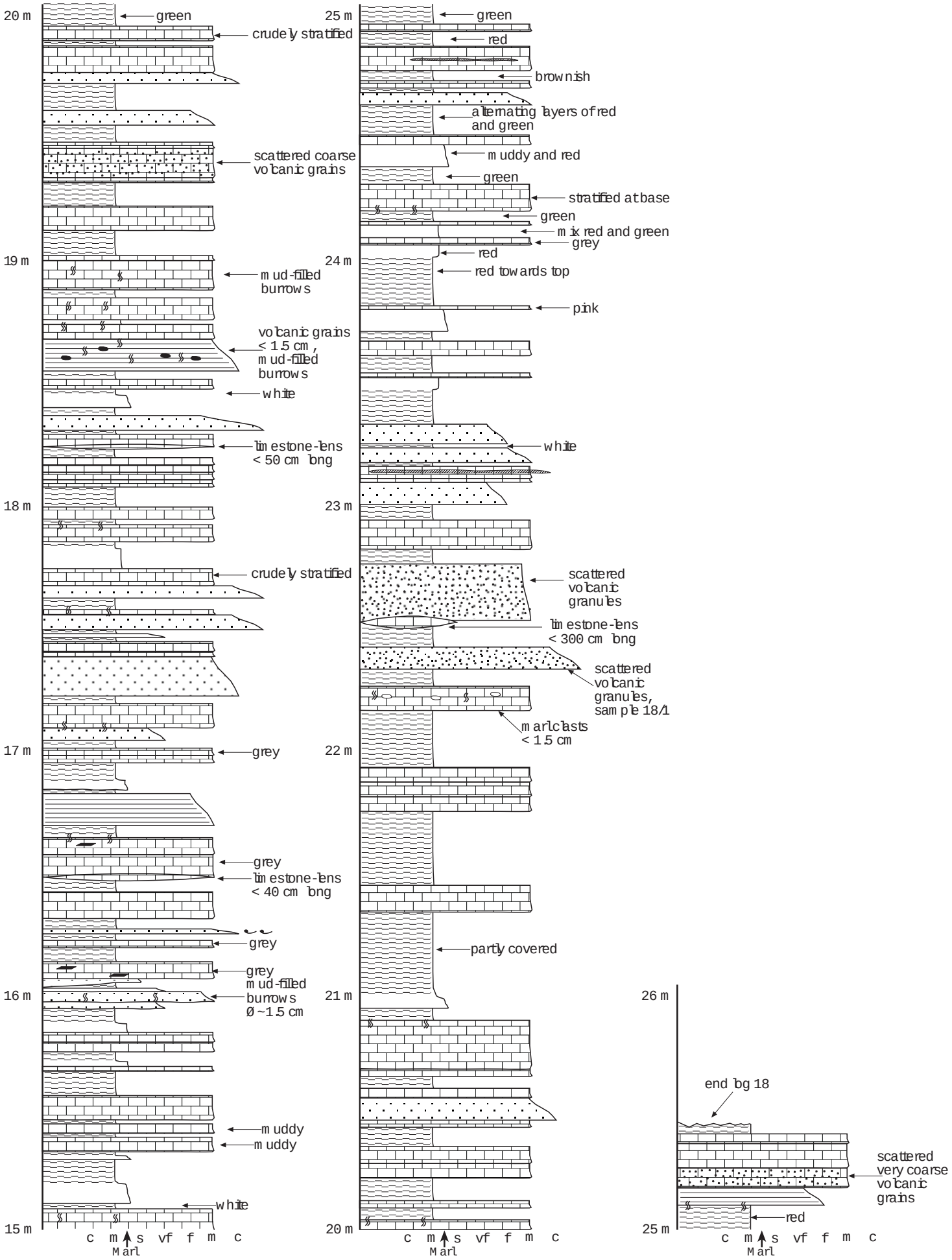
20 m
green
crudely stratified
scattered coarse volcanic grains
19 m
mud-filled burrows
volcanic grains < 1.5 cm, mud-filled burrows
white
limestone-lens < 50 cm long
18 m
crudely stratified
17 m
grey
grey
limestone-lens < 40 cm long
grey
grey
mud-filled burrows Ø ~1.5 cm
16 m
muddy
muddy
white
15 m
c m s vf f m c
Marl
25 m
green
red
brownish
alternating layers of red and green
muddy and red
green
stratified at base
green
mix red and green
grey
24 m
red
red towards top
pink
white
23 m
scattered volcanic granules
limestone-lens < 300 cm long
scattered volcanic granules, sample 18/1
marlclasts < 1.5 cm
22 m
partly covered
21 m
20 m
c m s vf f m c
Marl
26 m
end log 18
scattered very coarse volcanic grains
red
25 m
c m s vf f m c
Marl

LOG 19

Location: Yenikonak, W of river
Formation: lower Atbasi
Facies association: FA 4b
Facies content: F3, F7, F8b

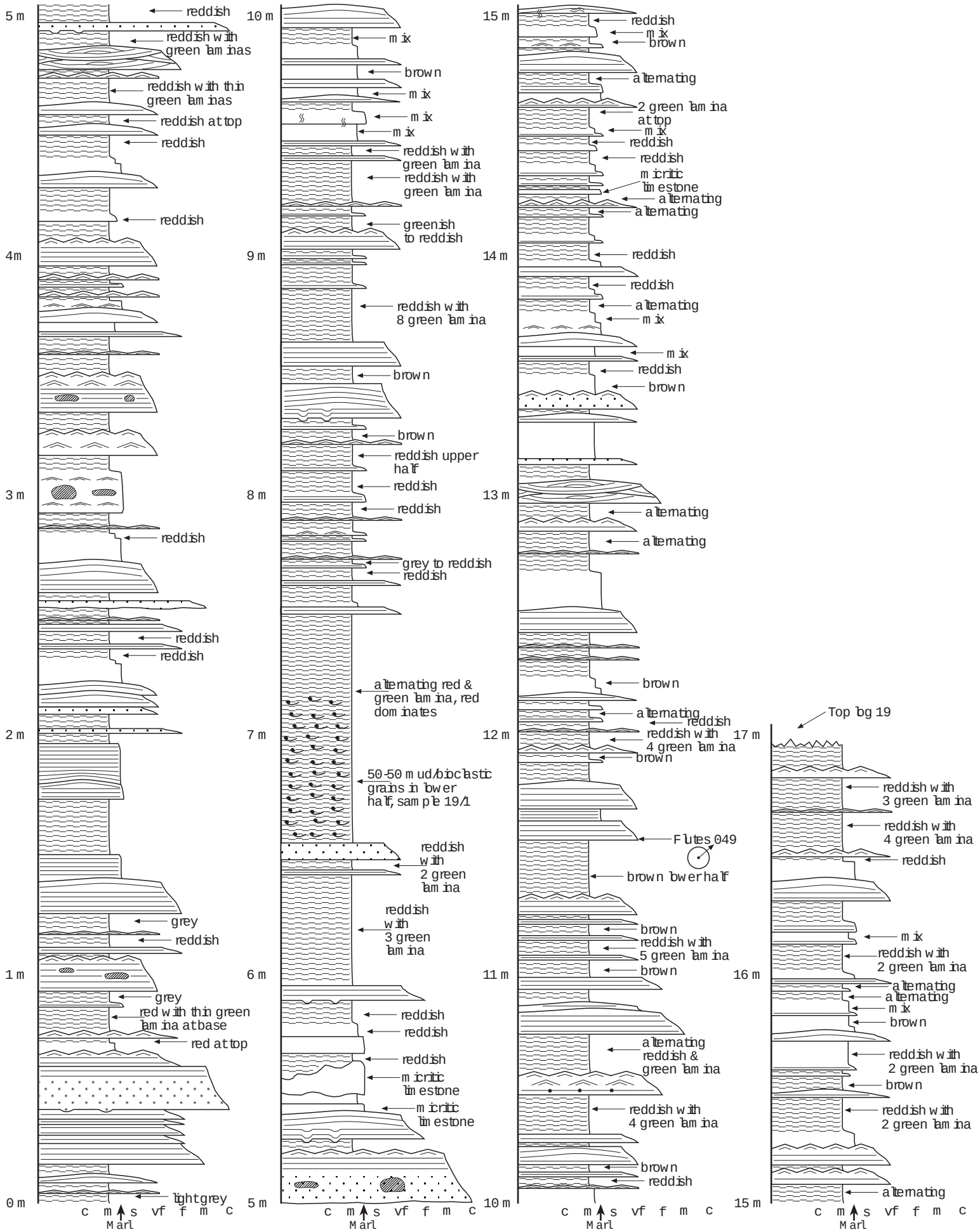

LOG 20

Location: Tangal
Formation: Atbasi
Facies association: FA 4c
Facies content: F2b, F5b, F7, F8b

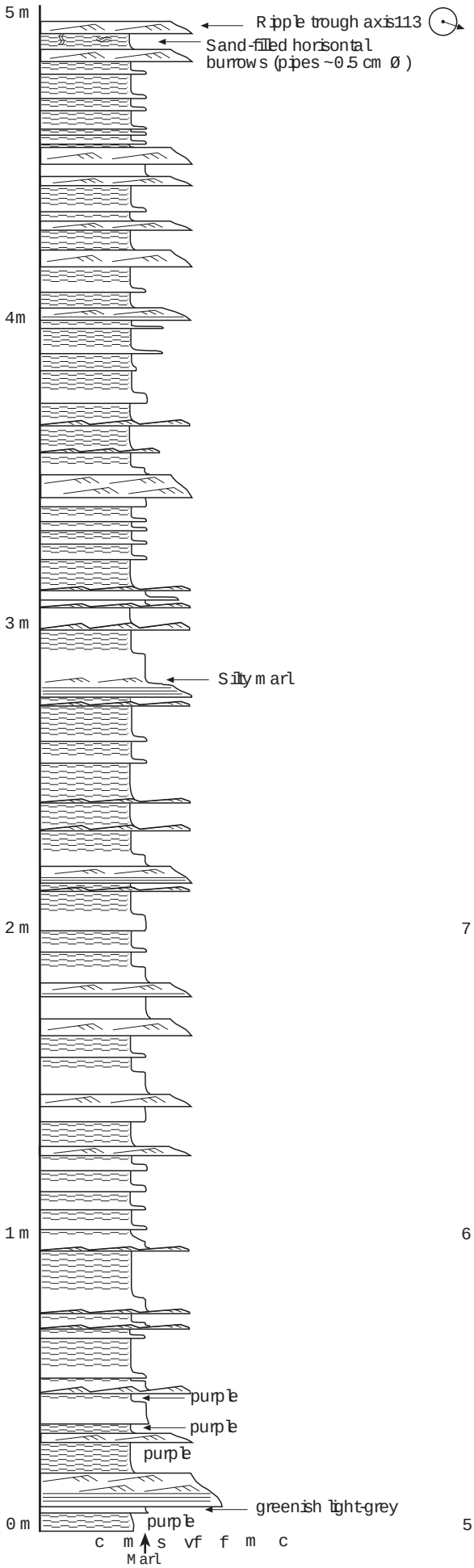

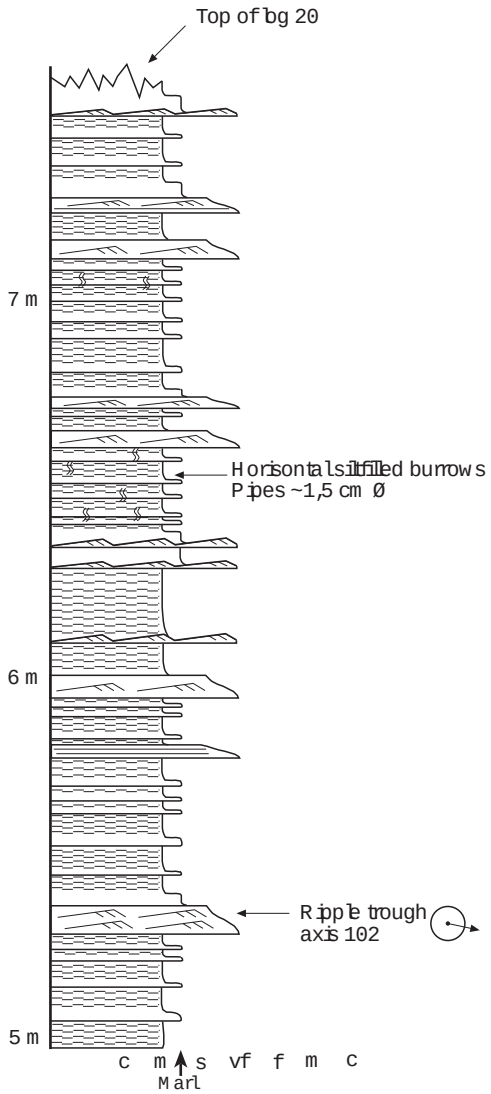

Appendix 2

Thin-section analyses

Table	Formation part	Log numbers
Table A2.1	Gürsökü	1, 2
Table A2.2	Lower and middle Akveren	5, 6, 7
Table A2.3	Lower and middle Akveren	8, 9, 10
Table A2.4	Uppermost Akveren and lower Atbaşı	14, 16, 17, 18, 20

Table A2.1. Thin-sections of samples taken from the sedimentological Logs 1 and 2 from outcrops of the Gürsökü Formation. Letter symbols: RF- Rock Fragments.

Sample	***1/1***	***2/1***	***2/6***	***2/7***	***2/8***
Hand specimen	Coarse- to very fine/fine-grained sandstone with scattered shell fragments	Coarse-grained sandstone with scattered granules	Marl	Very coarse-grained sandstone	Gravely coarse-grained sandstone
Facies	F2a	F2a	F7	F2a	F2a
Grains	50 vol.% Quartz 5 vol.% Plagioclase 30 vol.% RF (fine-grained volcanics and sandstone) 15 vol.% Mica Angular to subangular	40 vol.% Quartz 50 vol.% RF (volcanics) 10 vol.% Dark minerals, plagioclase and mica Angular to subangular	Micrite, zones with scattered quartz-grains representing burrows, no distinct siliciclastic clay/mud observed	20 vol.% Quartz 65 vol.% RF (volcanics) 15 vol.% Dark minerals, feldspars and mica Angular to subangular	90 vol.% RF (fine-grained volcanics) 7 vol.% Quartz 3 vol.% Plagioclase Subrounded to subangular
Bioclasts	<5 vol.% fragmented Foraminifera and bryozoans, brachiopods, echinoderms, remineralized, voids filled with sparite	None observed	10-15 vol.% scattered small fossil fragments	None observed	None observed
Cement	Micrite ~15 vol.%	Micrite ~10 vol.%	Micrite	Micrite <5 vol.%	Mostly micrite <5 vol.%, equant sparite rare
Classification	Litharenite (Fig. 3.3A)	Litharenite	Wackestone	Litharenite	Litharenite (Fig. 3.3B)

Table A2.2. Thin- sections of samples taken from lower and middle Akveren Formation (Logs 5, 6 and 7). Letter symbols: RF- Rock Fragments.

Sample	***5/1***	***5/4***	***6/1***	***6/2***	***7/1***	***7/2***	***7/4***
Hand specimen	Very fine-grained calcarenite	Marl	Very fine-grained calcarenite	Marl	Parallel laminated silty marl	Marl	Marl
Facies	F2b	F7	F2b	F7	F7	F7	F7
Siliciclastic grains	5 vol.% of subangular quartz and some volcanic RF	Micrite, no distinct siliciclastic clay/mud observed	5 vol.% angular quartz-grains, some volcanic RF (greenish opaque)	Micrite, no distinct siliciclastic clay/mud observed	Micrite, light grey "silt" grained micritic lamina alternating with brownish micritic lamina, no distinct siliciclastic clay/mud observed	Micrite, no distinct siliciclastic clay/mud observed	Micrite, some plant fragments, no distinct siliciclastic clay/mud observed
Bioclasts	Fragmented Foraminifera, molluscs, blurry appearance, remineralized and micritic envelopes	<10 vol.% of scattered fossil fragments floating in micrite matrix, some Foraminifera	95 vol.% of mostly Foraminifera, some echinoderm plates, molluscs, fragmented corals and bryozoans, remineralized to sparite, including voids	<10 vol.% of scattered floating fossil fragments	10-15 vol.% of scattered fossil fragments	<10 vol.% of scattered floating fossil fragments	10-15 vol.% scattered fossil fragments, Foraminifera, remineralized to sparite, including voids
Cement	Micrite	Micrite	Micrite	Micrite	Micrite	Micrite	Micrite
Classification	Grainstone	Mudstone	Grainstone	Mudstone	Wackestone	Mudstone	Wackestone

Table A2.3. Thin- section samples taken from lower and middle Akveren Formation (Logs 8, 9 and 10). Letter symbols: RF- Rock Fragments.

Sample	***8/3***	***8/4***	***9/1***	***9/2***	***9/4***	***9/7***	***10/2***
Hand specimen	Marl	Very fine-grained to silty calcarenite	Marl	Medium- to fine - grained calcarenite	Very fine-grained to silty calcarenite	Marl	Silty marl
Facies	F7	F2b	F7	F2b	F2b	F7	F7
Siliciclastic grains	Micrite, no distinct siliciclastic clay/mud observed	90 vol.% quartz 10 vol.% mica and volcanic RF Subangular	Micrite, no distinct siliciclastic clay/mud observed	No siliciclastic grains observed	No siliciclastic grains observed	Micrite, no distinct siliciclastic clay/mud observed, 1 fine-grained volcanic RF (greenish opaque)	Micrite, no distinct siliciclastic clay/mud observed
Bioclasts	10-15 vol.% of scattered fossil fragments, burrow filled with bioclasts, voids filled with sparite	Few recognizable, maybe some fragmented	<10 vol.% of scattered fossil fragments	Red coralline algae (*Corallinaceae Melobesieae*), bryozoan fragments, Foraminifera , some micritization	Coral fragments, molluscs, Foraminifera, thick micritic envelopes, remineralized, voids filled with sparite	<10 vol.% of scattered floating fossil fragments	>15 vol.% of scattered fossil fragments, some Foraminifera, remineralized to sparite, including voids
Cement	Micrite	Micrite ~15 vol.%	Micrite	Micrite <5 vol.%	Micrite	Micrite	Micrite
Classification	Wackestone	Sublitharenite	Mudstone	Grainstone (Fig. 3.9)	Grainstone	Mudstone	Wackestone

Table A2.4. Thin- section samples taken from uppermost Akveren Formation and lower Atbaşı Formation (Logs 14, 16, 17,18 and 20). Letter symbols: RF- Rock Fragments.

Sample	***14/1***	***16/1***	***16/3***	***17/3***	***17/8***	***18/1***	***20/2***
Hand specimen	Base of monotonous limestone	Marl	Fine to very fine-grained calcarenite	Very coarse to coarse-grained calcarenite	Marl (micritic limestone)	Very coarse to medium-grained calcarenite	Very fine-grained to silty calcarenite
Facies	F6b	F7	F3	F3	F7	F4	F5b
Siliciclastic grains	< 2 vol.% subangular to rounded, quartz, microcline, plagioclase, and volcanic tuff/glass	Micrite, no distinct siliciclastic clay/mud observed	No siliciclastic grains observed	<1 vol.% of angular Q-grains and volcanic RF (greenish opaque)	Micrite, no distinct siliciclastic clay/mud observed	< 5 vol.% angular to subrounded, plagioclase, quartz, volcanic glass, and fine-grained volcanic tuff	< 10 vol.% angular Q-grains
Bioclasts	Mean grain-size: fine-grained. Remineralized, fragmented bivalves, brachiopods, delicate branching cyclostome bryozoans, echinoderm plates, red coralline algae (*Corallinaceae Melobesieae*), Foraminifera, a few marl clasts. Thin micritic envelopes.	>15 vol.% of scattered fossil fragments, none identified	Remineralized and blurry, thick micritic envelopes (some completely micritized), molluscs fragments (bivalves), Foraminifera, fragmented spines, coralline red algae, fragmented coral (bryozoan)	Thick micritic envelopes (some completely micritized), Foraminifera, fragmented corals, bryozoans, brachiopods and echinoderm spines/plates, red coralline algae (*Corallinaceae Melobesieae*)	10-15 vol.% fragmented bioclasts. Strongly bioturbated, burrows filled with fragmented bioclasts	Remineralized, thick micritic envelopes common, fragmented bryozoans, brachiopods, bivalves, red coralline algae (*Corallinaceae Melobesieae*), Foraminifera, echinoderm plates and few marl clasts.	Heavily fragmented, the majority consists of Foraminifera test, sporadic echinoid spines and bivalve
Cement	Micro- to macrocrystalline sparite, local micrite, syntaxial overgrowths on rare echinoderm plates	Micrite	Micrite	Micrite dominates, some syntaxial overgrowths, microcrystalline sparite	Micrite	Micrite	Micrite, local grains with hematite coatings
Classification	Grainstone with a local crystalline zones (Fig. 3.24)	Wackestone	Grainstone	Grainstone (Fig. 3.16)	Wackestone	Grainstone (Fig. 3.19)	Grainstone